Impacts of Climate Change on UK Coastal and Estuarine Habitats: A Critical Evaluation of the Sea Level Affecting Marshes Model (SLAMM)

Aikaterini Pylarinou

Coastal and Estuarine Research Unit

Department of Geography

University College London

A thesis submitted for the degree of

Doctor of Philosophy

September 2014

To N. & D. K.

Declaration

I, Aikaterini Pylarinou confirm that this thesis entitled *Impacts of Climate Change on UK Coastal and Estuarine Habitats: A Critical Evaluation of the Sea Level Affecting Marshes Model (SLAMM)* is the result of my own research. Where information has been derived from other sources, I confirm that this has been indicated in the thesis.

Signature _____
Name _____
Date _____

Acknowledgements

Firstly, I would like to thank my supervisor Professor Jon French for his helpful supervision and support. He was always willing to discuss any difficulties with great patience. I would also like to thank my second supervisor Dr Helene Burningham for her advice and contribution over the last four years. Thanks also to my colleagues in the Department of Geography at University College London, especially Darryl, Miriam and Mandy for our discussions and their encouragement. A special thanks to my wonderful husband for his support and encouragement during these years. Finally, I acknowledge the Environment Agency for the provided airborne LiDAR datasets and the UK Permanent Service for Mean Sea Level for the provided sea-level data. This work was also benefitted from support from the NERC Integrating COAstal Sediment SysTems (iCOASST) project (NE/J005541/1).

Abstract

From an increasing awareness of the risks posed by climate change emerge the need to model potential impacts on coasts at a high spatial resolution, broad spatial scales, and time scales that correspond to the widely used IPCC sea-level rise scenarios. Little previous work has been carried out at this scale in the UK. This thesis investigates the potential of 'reduced complexity' models as a tool to represent mesoscale impacts of sea-level rise on UK estuarine environments. The starting point for this work is the Sea Level Affecting Marshes Model (SLAMM), which has been widely used in the USA. The SLAMM source code is first modified to accommodate the different tidal sedimentary environments and habitats found in the UK, and evaluated in a pilot study of the Newtown estuary, Isle of Wight. The modified SLAMM is then applied to the more complex environments of the Suffolk estuaries and the Norfolk barrier coast in order to evaluate its ability to produce meaningful projections of intertidal habitat change under the UKCP09 scenarios. Validation is also attempted against limited known historic changes, while a comparison of the SLAMM outputs to a GIS-based approach is also undertaken. Given sufficient sedimentation data, this approach produces robust projections in landform and habitat change at a whole estuary scale, with visually powerful outputs to convey possible future changes to stakeholders and policy makers. Although the nature of the SLAMM outputs is more sophisticated than the GIS-based approach, SLAMM is shown to have some limitations. The most serious of them lies in the empirical nature of the various sub-models of intertidal deposition and erosion. Whilst these can be calibrated to give meaningful results for saltmarsh, the lack of a robust formulation for tidal flats means that SLAMM is unable to resolve key landform and habitat transition in estuaries.

Table of Contents

List of Figures

List of Tables

1 INTRODUCTION

1.1 Overall study aim

There is an increasing need to investigate the coastal and estuarine behaviour at time-scales measured at decades and centuries. This is challenging though because much of our understanding is rooted in fine-scale processes and on the other hand we have very idealised theoretical models that apply to longer geological time-scales (French and Burningham, 2013; Nicholls et al., 2015). This thesis focuses on the problem of sea-level rise in UK estuarine environments and the potential of reduced complexity models that are explicitly designed to work at high spatial resolution, broad spatial scales, and time scales that correspond to the widely used IPCC sea-level rise scenarios (French et al., 2015). Little previous work has been carried out at this scale in the UK. The starting point for this work is the Sea Level Affecting Marshes Model (SLAMM), which has been widely used in the USA (e.g. Linhoss et al., 2013, 2015), Australia (e.g. Akumu et al., 2010) and China (e.g. Wang et al., 2014). By critically evaluating this model, after modifying it to suit the tidal sedimentary environments typically found in the UK, the appropriateness of reduced complexity models as a tool to represent the meso-scale impacts of sea-level rise on UK coastal and estuarine habitats is explored.

1.2 Climate Change at the Coast

According to the latest Reports of the Intergovernmental Panel on Climate Change (IPCC), there are many signs that the Earth's climate at the start of the 21st century is different from that of the 19th century, and that important changes happened in the 20th century (IPCC, 2007, 2013). These changes in climate, globally, are attributed a combination of human and natural causes. Natural causes include ocean and atmosphere interactions, the Earth's orbital changes and the fluctuations in energy that the Earth receives from sun and volcanic eruptions (Hulme et al., 2002; Jenkins et al., 2009). On the other hand, the human-induced changes stem largely from emissions of greenhouse gases (Hulme et al., 2002).

The indicator most widely used for climate change is the global-mean, annual-average, near-surface air temperature, typically referred to as simply global temperature (Jenkins et al., 2008). Observation records show an increase of 0.8ºC (0.76ºC ± 0.19ºC), from the

late 19th century until the first years of the 21st century (Brochier and Ramieri, 2001; Jenkins et al., 2008), with the greatest warming in the period between 1910 and 1940 and since the mid-1970s (Brochier and Ramieri, 2001). Since 1850, the more recent years, especially 1998 and 2005, have been the warmest (IPCC, 2013). Crucially, the warming trend for the last 50 years is twice as rapid as that for the last 100 years and IPCC (2007) assessment concluded that "*it is extremely unlikely that global climate change of the past 50 years can be explained without external forcing, and very likely that it is not due to known natural causes alone*". Thus, it is very likely that the main cause of the observed temperature rise is man-made greenhouse gas emissions (Hulme et al., 2002; IPCC, 2007; Jenkins et al, 2008). This conclusion in echoed by the recently released IPCC AR5 assessment, which notes that the evidence for human influence as the dominant cause of the observed warming has grown since the AR4 (IPCC, 2013).

The main consequence at the coast of increasing global temperature is sea-level rise, primarly due to the warming of the ocean and the melting of land ice (valley glaciers, ice caps and the major ice sheets) (Milliman and Haq, 1996; IPCC, 2001) (Table 1.1, IPCC, 2007). Many studies have estimated the rate of sea-level rise over the last century by combining trends at tidal stations around the world (see Table 1.2 for a summary). It might be argued that, despite the different sampling strategies and techniques in processing the data in these studies, the agreement between these rates is fortuitous and reflects the use of an essentially common dataset (Gornitz et al., 1995). However, the authoritative IPCC analyses (IPCC, 2013) report a high confidence that sea level has risen by 0.19 [0.17 to 0.21] m over the period 1901 to 2010. In particular, the average rate of sea-level rise globally for the same period is estimated to be 1.7 [1.5 to 1.9] mm yr^{-1}, with a faster rate during the last two decades of about 3.2 [2.8 to 3.6] mm yr^{-1}.

Table 1.1: Observed rate of recent historical sea-level rise and estimated contribution from different sources (IPCC, 2013).

Source of sea level rise	***Rate of sea-level rise (mm yr^{-1})***	
	1971-2010	**1993-2010**
Thermal expansion	0.8 [0.5 to 1.1]	1.1 [0.8 to 1.4]
Glaciers except Greenland and Antarctica[a]	0.62 [0.25 to 0.99]	0.76 [0.39 to 1.13]
Glaciers in Greenland[b]	0.06 [0.03 to 0.09]	0.10 [0.07 to 0.13]
Greenland ice sheet	-	0.33 [0.25 to 0.41]
Antarctic ice sheet	-	0.27 [0.16 to 0.38]
Land water storage	0.12 [0.03 to 0.22]	0.38 [0.26 to 049]
Total of contributions	-	2.8 [2.3 to 3.4]
Observed total sea-level rise	2.0 [1.7 to 2.3]	3.2 [2.8 to 3.6]

a: Data for all glaciers extend to 2009, not 2010, b: This contribution is not included in the total because is included in the observational assessment of the Greenland ice sheet.

Table 1.2: Synthesis of various estimates of historical global sea-level rise (from Pirazzoli 1989; Gornitz 1995; Brochier and Ramieri, 2001; FitzGerald et al., 2008).

Author(s)	***Comments***		***Rate (mm yr^{-1})***
Gutenberg (1941)	69 stations,	1807-1937	1.1±0.8
Valentin (1952)	253 stations,	1807-1947	1.1
Poli (1952)	110 stations,	1871-1940	1.1
Cailleux (1952)	76 stations,	1885-1951	1.3
Lisitzin (1958) (in Lisitzin, 1974)	6 stations,	1807-1943	1.1± 0.4
Fairbridge and Krebs (1962)	Selected stations,	1900-1950	1.2
Kalinin and Klige (1978)	126 stations,	1900-1964	1.5
Emery (1980)	247 stations,	1935-1975	3
Gornitz et al. (1982)	195 stations, 14 reg,	1880-1980	1.2±0.1
Klige (1982)	Many stations,	1900-1975	1.5
Barnett (1983)	Selected stations,	1903-1969	1.5±0.15
Barnett (1984)	152 stations,	1881-1980	1.4±0.14
Gornitz and Lebedeff (1987)	130 stations,	1880-1982	1.2±0.3
	130 stations, 11 reg	1880-1982	1.0±0.1
Barnett (1988)	155 stations,	1880-1986	1.15
Pirazzoli (1989)	58 stations, Europe,	1881-1986	0.9±1.2
Peltier and Tushingham (1989, 1991)	40 stations,	1920-1970	2.4±0.9
Trupin and Wahr (1990)	84 stations,	1900-1986	1.75±0.13
Wahr and Trupin (1990)	69 stations,	1900-1986	1.67±0.33
Douglas (1991)	21 stations,	1880-1980	1.8 ±0.1
Nakiboglu and Lambeck (1991)	655 stations, (10^0x 10^0 blocks)	1807-1990	1.15±0.38
Emery and Aubrey (1991)	517 stations,	1807-1996	Not determined
Peltier and Tushingham (1991)		1920-1970	2.4 ± 0.9
Shennan and Woodworth (1992)	33 stations, UK & North Sea	1901-1988	1.0±0.15
Groger and Plag (1993)	854 stations,	1807-1992	Not determined
Gornitz (1995)	Eastern USA		1.5
Unal YS and Ghil M(1995)		1807-1988	1.62±0.38
Douglas BC(1997)			1.8±0.1
Holgate and Woodworth (2004)	177 stations	1948-2002	1.7±0.9
Cazenave and Nerem (2004); Leuliette et al. (2004)		1993-2003	3.1±0.7
Miller and Douglas (2004)			1.5 -2
Church and White (2011)		1880-2009	1.7±0.2
		1961-2009	1.9±0.4

Although climate affects the sea level globally, regional changes that include both climate effects and those due to geological factors are also important (Titus et al., 1991; Douglas, 1992; Lambeck, 2002; Church et al., 2004). Thus, a distinction is made between eustatic and relative sea-level change. Eustatic changes are the changes in the global mean sea level and result from changes in the ocean water volume and are

mainly associated with glacial/interglacial cycles. On the other hand, relative sea-level changes are controlled by isostatic effects (Clark et al., 1978; Vellinga and Leatherman, 1989; Warrick and Oerlemans, 1990; Nicholls and Leatherman, 1996). These are strongly influenced by regional and local factors (Nicholls and Leatherman, 1996; Nicholls, 2002) and by mechanisms that vary greatly on spatial and temporal scales (Table 1.3; French and Spencer, 2001; Douglas and Peltier, 2002). Local relative sea-level changes are recorded by land-based tide gauges (Cazenave and Nerem, 2004; see also Figure 1.1). The interactions of the eustatic and isostatic effects can be generalised at a regional scale to give different characteristics of relative sea-level signatures (Clark et al., 1978; Figure 1.2). These differences provide a crucial backdrop for future coastal vulnerabilities (Slaymaker et al., 2009).

Table 1.3: Major processes resulting in secular trend and interannual variability in Mean Sea Level (French and Spencer, 2001).

PROCESS		
SECULAR TRENDS	***Rate (mm yr^{-1})***	***Timescale (yr)***
Eustasy		
Tectono-eustasy	±0.001-0.1	10^3-10^8
Glacio-eustasy	±1-10	10^3-10^5
Regional (100-1000km) land movements		
Glacio-isostasy	±1-10	10^4
Lithospheric cooling and sediment loading	0.03	10^7-10^8
Local (<100km) land movements		
Neotectonic uplift/subsidence	±1-10	10^2-10^4
Shelf sedimentation; delta plains	1-5	10-10^4
Anthropogenic processes		
Water impoundment (reservoirs)	-0.5-0.75	<100
Groundwater extraction (via river runoff)	0.4-0.7	<100
Deforestation and wetland loss	0.2	<100
Subsidence due to water, hydrocarbon, mineral extraction (very local)	1-5+	<100
INTERANNUAL VARIABILITY	**Amplitude(cm)**	**Period (yr)**
Geostrophic currents	1-100	1-10
Low-frequency atmospheric forcing	1-4	1-10
El Nino	10-50	1-3

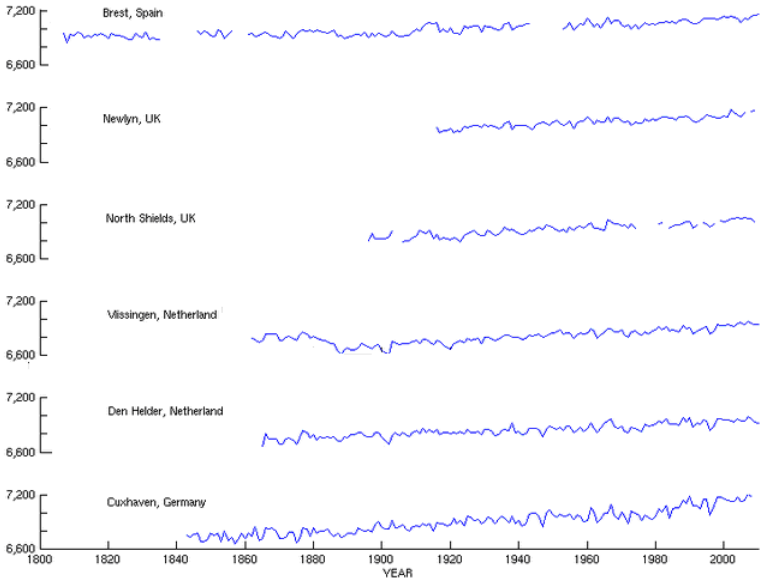

Figure 1.1: Time series of relative sea level for selected stations in Northern Europe (data from PSMSL, 2012).

Figure 1.2: Regionalized Holocene sea-level curves resulting from contrasting deglaciation histories (Clark et al., 1978).

Apart from the interest of scientists in observed sea-level rise and the processes that force it, much effort is being devoted to the prediction of future changes. The time horizon for these studies is generally 2100 (although later IPCC reports include longer time frames) and the magnitude of change over this period varies considerably since the earliest studies of the 1980s. There has been a general tendency towards lower rates of rise (with better estimation of the uncertainty) in recent years (Figure 1.3), with the latest IPCC report of 2013 projecting a warming of 0.3ºC to 4.8 ºC and a sea-level rise of 0.26 to 0.98 m by 2100, depending on the chosen scenario.

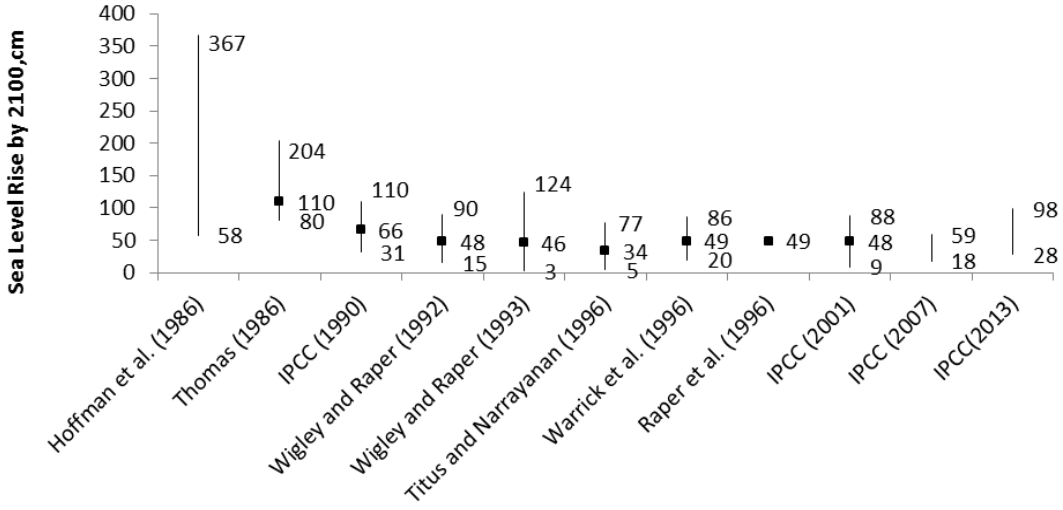

Figure 1.3: Changing estimates of the range of potential sea-level rise to 2100. Vertical bars indicate range, with best estimate also shown where available.

However, it is clear from Figure 1.3 that, against this longer-term thread, the IPCC Fifth Assessment predictions of 2013 has increased the expected rate of sea-level rise. This revision is founded on improved the climate models and also incorporating the effects of changes in the large ice sheets that cover Greenland and Antarctica. This limitation of the 4th Assessment report was firstly pointed out by Rahmstorf (2007), who, in order to address it, developed a new semi-empirical approach for estimating sea-level rise, based on the idea that the rate is proportional to the amount of global warming. Later studies have followed Rahmstorf's (2007) semi-empirical approach (Horton et al., 2008; Grinsted et al., 2009; Jevrejeva et al., 2010; Vermeer and Rahmstorf, 2010). This methodology results in a predicted rise for the 21st century that is much higher than the IPCC projections, potentially exceeding 1m by 2100 if the emissions of greenhouse gas continue to escalate (Figure 1.4, Rahmstorf, 2010).

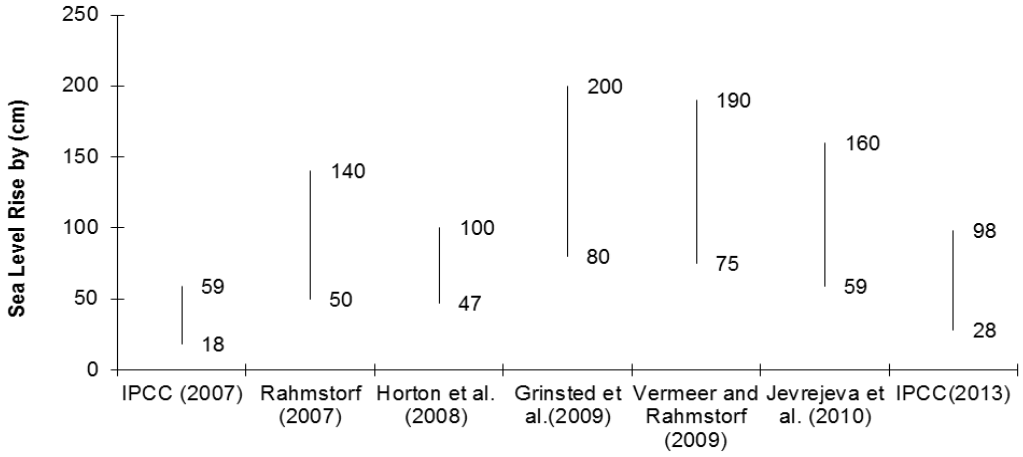

Figure 1.4: Estimates for twenty-first century global sea-level rise from semi-empirical models as compared to the latest IPCC Reports. (modified after Rahmstorf, 2010).

If greenhouse-gas emissions were to stabilise, global mean temperature would stabilize relatively quickly, neglecting fluctuations due to natural factors, but sea level would continue to rise with stabilization occurring over a much longer timescale (Figure 1.5; Wigley, 1995; Mitchell et al., 2000). This results from the so-called 'commitment to sea-level rise', which includes the slow penetration of heat into the deeper ocean (Nicholls, 2003). Thus, the rise of sea level due to thermal expansion will take centuries or even millennia to reach equilibrium (Wigley and Raper, 1993; IPCC, 2001, 2007), whereas the rise of sea level due to ice melting will take several millennia (IPCC, 2001, 2007). Of course, it is very difficult to stabilize the carbon dioxide concentrations, because of the very long effective lifetime of CO_2 in the atmosphere (of the order of 100 years). This would require a reduction of 60 to 70% relative to 2002 values (Hulme et al., 2002).

Although the prospect of large sea-level rises over hundreds of years has clear implications for the sustainability of major coastal cities (eg. Nicholls, 1995; WWF, 2009; Weiss et al., 2011), the rise in global mean and local sea levels that is expected to happen over the 21st centrury is of most pressing significance for coastal managers. Even the relatively modest global rises envisaged by the latest IPCC reports frequently translate into larger relative changes on account of geological factors. Such changes clearly have the potential to drive major changes in both coastal morphology (eg. French G.T. et al., 1995; Han et al., 1995; Selivanov, 1996; Crooks, 2004; Garcin et al., 2011) and ecosystems and habitats (Gornitz, 1991; Hoozemans et al., 1993; Bijilsma et al., 1996; Mclean et al., 2001; Pethick, 2001; Reed et al., 2009).

The areas that will be affected the most from global warming are low-lying coastal and estuarine margins (Boorman et al., 1989, Vellinga and Leatherman, 1989; Tooley and Jelgersma, 1992; Galbraith et al., 2005; Nicholls et al., 2007; FitzGerald et al., 2008; Poulos et al., 2009; Snoussi et al., 2009), where inundation will be the main result (Gornitz, 1991; Gesch et al., 2009). Inundation-related changes are likely to be manifest in a variety of ways, including coastal flooding, either in deltaic regions (eg. Day et al., 1995; El-Raey, 1997; Nguen et al., 2007; Mah et al., 2011) or urban centres (eg. Han et al., 1995; Gornitz et al., 2001; Dasgupta et al., 2009) , raised water tables and saltwater incursion into regional coastal areas (eg. Marshall Islands, Tuvalu, etc; Roy and Connell, 1991, Nunn and Mimura, 1997). More generally, there is also likely to be a tendency towards more rapid and more widespread coastal erosion (Schwartz, 1965; Gornitz, 1991; Leatherman et al., 2000; Peizen et al., 2001). All these can be expected to impact on coastal therefore cause the ecosystem to lose area and important services related to their wetlands (Barth and Titus, 1984 in Titus et al. 1991; Pascual and Rodriguez-Lazaro, 2006; Gardiner et al., 2007; FitzGerald et al., 2008; Larsen et al., 2010).

While sea-level rise is usually considered to be the main threat posed by climate change to the coastal zone, there are other climate change aspects that will have implications for these areas (Nicholls, 2002). A major concern is that global warming will also result in an increase in the intensity and frequency of extreme storms (Nicholls, 2003; Wolf et al., 2009). Storm–driven inundation and erosion may be of greater immediate concern that a progressive rise in sea level (e.g. Henderson-Sellers et al., 1998; Nicholls, 2003). During storms, strong winds cause high waves (USAGE, 1984) and, combined with low atmospheric pressure, create storm surges (Hadley, 2009), which increase the water level, and expose higher parts of the beach to wave attack (USAGE, 1984). The situation is exacerbated when storm surges are superimposed on a progressive increase in sea level (USAGE, 1984; FitzGerald et al., 2008; Storch and Woth, 2008). Storm surges can be the major cause of damage to settlements and infrastructure (USAGE, 1984; Lowe and Gregory, 2005) and have been also implicated in the degradation of coastal wetlands (Guntenspergen et al., 1995; Cahoon et al., 1995b; Nyman et al., 1995; Cahoon, 2006, Fagherazzi and Priestas, 2010) and broader ecosystem changes that impact on productivity and biodiversity (Day et al., 1995; Hayden et al., 1995; Christian et al., 2000; Day et al 2008). In the longer term, changes in the intensity, distribution, frequency and timing of storms can alter the composition of wetland species and

important ecosystem process rates (Twilley et al. 1999; Sherman et al. 2000; Baldwin et al., 2001 cited in Day et al., 2008).

In light of the above observations, it is clear that estuarine and coastal landforms and habitats are potentially vulnerable to multiple aspects of climate change in the 21st century, including sea-level rise, changes in the intensity and frequency of storms as well as the direct effects of increased air temperatures. These effects are evident at local, regional and global scales (Akumu et al., 2010) and are both complicated and exacaberated by human acivities (e.g. Pont et al., 2002; Chust et al., 2009; Restrepo, 2012).

1.3 Climate Change in the UK

The effects of climate change are already visible in the UK (Cassar, 2005). Average temperatures have increased between 1961 and 2006 in all regions (Jenkins et al., 2008). The Central England Temperature (CET) record, which is the longest continuous surface air temperature record in the world, and also temperature series for Northern Ireland, Scotland and Wales show an increase of almost 1°C since 1970s, after a period of relative stability during the 20th century (Jenkins et al., 2009; UKMMAS, 2010). The air temperature over the southern North Sea shows the most rapid increase of around 0.6°C per decade. Increases in the sea surface temperature of 0.5-1°C are also evident for the period 1870-2007 (UKMMAS, 2010), with the largest changes being in the eastern English Channel and the Southern North Sea (MCCIP, 2011). Projections indicate that the UK climate will become warmer, with an increase in annual temperature across the UK of 2°C to 3.5°C by the 2080s. Warming will be greatest in the south and east (Hulme et al., 2002; Zsamboky et al., 2011) and in summer and autumn rather than in winter and spring (Hulme et al., 2002).

Changes in precipitation are more variable, although in some areas of the UK, an increase can be observed in the annual total precipitation (Zsamboky et al., 2011). The biggest change in winter precipitation has been in the western areas of UK with an increase of 33%; the Scottish highlands show a decline of a few % (Jenkins et al., 2009; Zsamboky et al., 2011). On the other hand, summer became drier in most areas and the precipitation at this time of year has decreased since 1914, especially in London and Southeast England. Indeed, in southern England summer precipitation reduced by about

40%, when the changes at northern Scotland were close to zero (Jenkins et al., 2009; Zsamboky et al., 2011). Projections indicate that the winter precipitation is expected to continue increasing by up to 23% by 2080, with a decrease in summer precipitation of up to 28% over the same period (Zsamboky et al., 2011).

At the coast, the UK is already experiencing a rise in mean sea-level (Jenkins et al., 2009; Zsamboky et al., 2011) with an increase in eustatic sea level of around 1mm yr^{-1} during the 20th century, although the rate of rise was higher in 1990s and 2000s (Jenkins et al., 2009; UKMMAS, 2010). However, these average trends obscure important regional variability, mainly due to vertical land movements, which are typically between -10 and +10 cm over a century (Jenkins et al., 2009). Notably, the trends in Scotland are lower because of land uplift effects due to the post-glacial isostatic adjustment (Figure 1.5; Zsamboky et al., 2011; Wahl et al., 2013). While northern Britain is rising at 0.5 to 1 mm yr^{-1}, southern Britain is subsiding at around 1 to 1.5 mm yr^{-1} (Hulme et al., 2009). The eustatic sea level around the UK is projected to increase by 12-76 cm for the period 1990-2095, with slightly larger projections for the southern part, and somewhat lower increases in relative sea level rise for the north due to land movements (Figure 1.6; Jenkins et al., 2009).

To the effects of sea-level rise must be added the predicted increase in windiness and storm activity, especially in winter (Hadley et al., 2009). An increase in mean wind speed of up to 8% has been projected for northern Europe, especially during winter and spring (Zsamboky et al., 2011). This may lead to greater coastal wave heights and higher storm surges (Hadley et al., 2009; Zsamboky et al., 2011). Since the 1960s, strong south and southwesterly winds occur more often in the southern UK (Pye, 2000; Hadley, 2009). The intensity and frequency of easterly winds increased from 1973 to 1997, although the following decade saw a decrease (Van der Wal and Pye, 2004). Although there is little evidence of secular changes in wave and storm climate in the North Sea and most of the northeast Atlantic in the 20th century, decadal-scale variability is significant and there is some evidence for a more energetic wave climate in recent decades (WASA Group, 1998). Although similar reports have been published (Gulev and Hasse, 1999; Gulev and Grigorieva, 2004), it is not clear whether this apparent trend is due to climate change or whether it lies within the envelope of natural variability (Hadley, 2009). In general, the number of severe storms has increased since

the 1950s in the UK, but again this may lie within natural long-term variability (Alexander et al., 2005).

Figure 1.5: Mean sea-level trends (in mm yr^{-1}) from tidal stations with more than 15 years of records for the UK (Zsamboky et al., 2011).

Figure 1.6: Relative sea-level rise projections relative to 1990 for four sample locations around the UK and the three emissions scenarios. Thick lines represent the central estimate values and the thin lines the 5^{th} and 95^{th} percentile limits of the uncertainty range (Zsamboky et al., 2011).

Storm surge heights are also predicted to increase (Hulme et al., 2002; Lowe and Gregory, 2005) due to sea-level rise and the increased storminess, along most of the UK coast (Lowe and Gregory, 2005). The largest relative increase is expected to be in southeast England (Hadley 2009). The UKCIP (Hulme et al., 2002) investigated this relationship between sea-level change and storminess and predicted that the current 1:50 year storm surge events will become 1:10 year events by the end of 21st century under low-estimate sea-level rise scenarios and will occur more than once per year under the high-estimate scenarios. Lozano et al. (2004) suggest that, for the area west of the British Isles under doubled CO_2 concentration, the number of storms will not be appreciably greater, but some of them will be more intense.

In conclusion, climate change driven sea-level rise is likely to be significant around many parts of the UK, exacerbated by land movement in subsiding areas and increased wave heights (Hadley et al., 2009; Lowe et al., 2009; Zamboky et al., 2011). While erosion and storm inundation has long been an issue facing many coastal cities (Shennan, 1993; Cassar, 2005), the present situation will clearly be made worse by the anticipated changes in regional climate (Cassar, 2005). Projections of these coastal impacts of climate change are thus very important for effective mitigation of flood and erosion risk and management of habitats.

1.4 Projecting the impacts of climate change and sea-level rise

1.4.1 Need for projection at the meso or regional scale

Numerous attempts have been made to conceptualise and model the influence of rising sea level on coastal morphodynamics (French and Spencer, 2001; FitzGerald et al., 2008 for review). Both Dearing et al. (2006) and French and Burningham (2011) have characterised this need as a major challenge in environmental science. However, there are no universally applicable methodologies to relate coastal morphodynamic responses to sea-level rise based on first principles of hydrodynamics and sediment transport (List et al., 1997). Accordingly, much emphasis is placed on various forms of modelling, both empirical and physically-based. Despite their limitations (Cooper and Pilkey, 2004), at least some of them are useful in understanding and predicting the coastal behaviour (Murray, 2007).

Much of the difficulty in modelling the impacts of sea-level rise on coasts stems from the variety of factors that determine coastal behaviour and also the range of the scales at which these operate (French and Spencer, 2001; FitzGerald et al., 2008). There are many alternative conceptualisations of the spatial and temporal scales relevant to the understanding of coastal morphodynamic behaviour, reflecting the problems and objectives that scientists have addressed in different scientific disciplines (Carter, 1988; Kraus et al., 1991; Stive et al., 1991; Pethick and Leggett, 1993; Cowell and Thom, 1994; Pye and Blott, 2008; Whitehouse et al., 2009). All emphasise the correlation between space and time scales, but differ in the terminology and the groupings of scales identified. Kraus et al. (1991) defined these scales from a coastal engineering perspective, according to which, processes like turbulence, individual waves, wind, individual grains, beach profile change and bed or/and shoreface occur within micro time periods (seconds to minutes) covering a micro (mm to cm) to meso (m to km) spatial scale. Sediment pathways, tides and shoreline changes cover longer time scales, from macro (months to years) up to mega (decade to centuries), while in term of space range from 1 to 10 km. Finally, sub-regional and regional (mega spatial scale >10km) occur within macro to mega time scales.

In contrast, Cowell and Thom (1994) proposed a conceptual scheme from a geomorphological perspective, in which four distinct time scales, associated with characteristic length scales, were identified (Figure 1.7):

i) *'Instantaneous'* time scales: involve the morphological evolution during a single cycle of the forces that drive morphological change, like waves and tides.

ii) '*Event'* time scales: are concerned with coastal evolution in response to processes occuring in time periods that range from that of an individual event, like a storm, through to seasonal variations in driving forces.

iii) '*Engineering' (*or historical) time scales: involve composite evolution over many fluctuations in boundary conditions, each of which entails many cycles in the fundamental processes responsible for sediment transport.

iv) '*Geological'* time scales: evolution takes place due to changes in environmental conditions.

From a coastal management perspective, probably the most appropriate timescale is decades to centuries (Figure 1.8), because these scales are more relevant to livelihoods

and human life and they correspond to the scale of IPCC-type scenarios (Slaymaker et al., 2009; French and Burningham, 2011). Since sea-level rise effects on coasts vary spatially (Gornitz, 1991), and vary with individual landform type, it is necessary to analyze and downscale these changes down to more local scales (Dean, 1987; Fenster and Dolan, 1993; Pilkey et al., 1993; Cooper and Pilkey, 2004). The range of relevant spatial scales is thus quite broad, perhaps from 1 to 100 km.

Figure 1.7: Spatial and temporal scales involved in coastal evolution (Cowell and Thom, 1994).

Figure 1.8: Spatial and temporal scales from a coastal management perspective (Slaymaker et al., 2009).

Of critical importance here is the separation of variability (i.e. high order processes) from progressive change (low order processes). The 'coastal tract' concept was proposed by Cowell et al. (2003) to provide a framework for this. The tract is presented as "a spatially contiguous set of morphological units representative of a sediment sharing coastal cell" (Figure 1.9). A hierarchy of morphologies and processes can be identified, in which the coastal tract constitutes the lowest order. Within the tract, meso-scale coastal landforms and landform complexes exhibit morphological behavior constrained by the residual effects of higher-order processes, as well as the lower-order controls exerted by the coastal shelf and the Quaternary geology (Cowell et al., 2003).

Figure 1.9: Physical morphology encompassed by the coastal tract. The upper shoreface may include (A) dune, washovers, flood-tide deltas, lagoonal basins and tidal flats, (B) mainland beaches, and (C) fluvial deltas (Cowell et al., 2003).

1.4.2 Mesoscale coastal responses to climate change

Climate affects the distribution, form, functioning and dimensions of coastal and estuarine landforms and their associated ecosystems (Woodroffe, 1993; Douglas, 2001; Pethick, 2001; Scavia et al., 2002; Day, 2008). Morphodynamic responses to a rise in sea level are determined by the balance between erosive forces, sediment supply and sumbergence (Reed, 1995; Allen, 2000; French and Burningham, 2003; FitzGerald et al., 2008) and also mediated by the influence of climate on biotic processes (Reed, 1995; McKee et al., 2007).

The natural long-term response of shorelines to the sea-level rise is to retreat landwards in order to maintain their relative position (Titus, 1991; Pethick, 2001; Blott and Pye, 2004; Defeo et al., 2009), unless obstructed by cliffs or where there is sufficient sediment supply to maintain seaward propagation (Titus, 1991; Valentin, 1952). Typical rates of shoreline retreat along coastal plain coasts are 0.3 to 1 m per year (Pilkey and Cooper, 2004). Conceptually, Bruun (1962) proposed that while sea level rises, erosion of the upper part of the beach is taking place and is deposited offshore restoring the beach profile's shape with respect to sea level. However, the shoreline retreat due to a sea-level rise is not continuous but episodic (SCOR Working Group 89, 1991) and also not just a simple inundation, but a more complex reorganisation (Pilkey and Cooper, 2004).

Slow global average sea-level rise has been been associated within more-or-less manageable coastline retreat in many areas (Ranasinghe and Stive, 2009). The accelerated rates of rise predicted for the twenty-first century (Leuliette et al., 2004; Beckley et al., 2007) can be expected to lead to more rapid and also more widespread erosion and retreat (Bird, 1985; National Research Council, 1990; Leatherman, 2001), especially on low gradient and predominantly sandy coasts (Defeo et al., 2009). An acceleration in coastal erosion is driven by storm events superimposed upon a background trend of rising sea level (SCOR Working Group 89, 1991). Allan and Komar (2006) argued that increased erosion along the west coast of US since 1970s had been associated with bigger wave heights because of sea-level rise and as well as more intense storms. More specifically, storm surges cause large waves that can pass over the beach without breaking, but when they finally break, the surf zone's remaining width is not enough to dissipate their energy (USAGE, 1984). On coastal barrier islands, this wave erosion may transport sand landward as 'overwash', forcing the barrier island to migrate and therefore to keep pace with the sea-level rise (Figure 1.10; Titus, 1990).

Changes in sea level and coastal wave climate will also influence rates of cliff erosion (Bray and Hooke, 1997). Hard rock coasts may remain more-or-less stable as sea level rises (National Research Council, 1987; Forbes et al., 1989), on account of their naturally slow rates of erosion (Allison, 1989). On the other hand, soft-rock cliffs are prone to erosion (Howe, 2002) making them much more sensitive to climate changes and sea-level rise. Higher cliffs typically retreat more rapidly (Richards and Lorriman, 1987) and produce more sediment per unit of retreat (Dalrymple et al., 1986; Bray and

Hooke, 1997). More rapid erosion will increase the sediment supply (Bird, 1993) and the eroded material will be transported in large quantities elsewhere (USAGE, 1984; Bird, 1993), balancing the land losses that would otherwise happen through erosion and submergence (Bird, 1993).

Figure 1.10: Overwash: natural response of undeveloped barrier islands to sea-level rise (Titus, 1990).

Although sea-level rise has been considered as the major factor driving open coastal erosion (Pilkey and Cooper, 2004; Stive et al., 2009), other factors may be more important (Titus, 1990; French and Spencer, 2001). Sediment starvation, for example, can cause coastal erosion even if the sea level is stable, while sufficient sediment supply can cause the coastline to grow seaward even if the sea level is rising (Figure 1.11; Marchand, 2010). Sediment delivery rates are often dominated by anthropogenic changes (Komar, 1999; Kirwan and Murray 2007). For example, an analysis of erosion problems at Sandy Hook (New Jersey, USA) showed that only 1% of the erosion since 1953 is due to sea-level rise, while the rest is caused by sediment starvation downdrift of a major groyne installation, combined with an increase in the frequency and magnitude of major storms over the period of observation (Allen, 1981).

Figure 1.11: Coastal evolution through a combination of sea-level changes and sediment availability (after Valentin, 1952).

As sea-level rises, estuaries also try to maintain their relative position within the tidal and wave energy frame by the process of transgression. This process was first suggested by Allen (1990a) and is mainly caused due to the redistribution of sediment within the estuarine system itself. The deeper due to the sea-level rise water in the outer estuary increases the waves propagating in from the sea, resulting in erosion and therefore retreat of the mudflat-saltmarsh boundary. The eroded material are moved landward and re-deposited on the upper intertidal zone of the inner estuary, increasing the elevation of the marshes and tidal flats. This results in a potential transgression of the landward edge of the marsh, while the tidal flat – saltmarsh boundary continues to erode due to increased fetch-driven waves. That means that the estuary channel moves landward as a unit while sea-level rises (Pethick, 2001).

The vulnerability of the estuaries to the sea-level rise depends on the wetland types they contain, on constraints on plant productivity, and also the abundance of external sediment supply (Figure 1.12; Allen, 2000; Schwimmer and Pizzuto, 2000; French and Spencer, 2001; Environment Agency, 2007; FitzGerald et al., 2008; Wolanski et al., 2009). Saltmarshes for example, may respond to sea-level rise with areal reduction, stability or even expansion, depending on the concurrent changes in sediment availability (Philips, 1986). Increasing inundation of the saltmarsh surface translates

into more accommodation space available for infilling (French, 2006), which may in turn drive both vertical and lateral accretion (Redfield, 1972; McCaffery and Thomson, 1980; Pethick, 1981; Shaw and Ceman, 1999). Under constant sea-level forcing, vertical accretion may be sufficient to ultimately restore the marsh to a new equilibrium position in the tidal frame (French, 1993).

Figure 1.12: Major factors that affect marsh elevation (FitzGerald et al., 2008).

Many studies have determined salt marsh vertical accretion rates and investigated the feedback between sea-level rise and accretion (for British studies, see French, 1993; French and Spencer, 1993; Allen and Duffy, 1998; for the Mississippi delta, see DeLaune et al., 1983; Hatton et al., 1983; Copnner and Day 1991; Cahoon et al., 1995a,b; for the Mediterranean, see Stanley 1988; Sestini 1992; Bondesan et al., 1995; Ibanez et al 1997, 2010; Day et al., 1999, 2011; Pont et al., 2002). The higher the rate of sedimentation, the bigger the rate of relative sea-level rise that can be tolerated with no wetland loss (Day et al., 2008). In areas where the rate of sedimentation exceeds sea-level rise, saltmarshes tend to prograde seaward (Reed, 1990; Doody, 2001). However, vertical accretion rates of the marshes are usually limited (Baumman et al., 1984; Walker et al., 1987; Kearny and Stevenson, 1991; Temmerman et al., 2003; FitzGerald et al., 2008), resulting in erosion and therefore wetland loss when rates of relative sea-

level rise are high (Phillips, 1986; Hackney and Cleary, 1987; Kearny and Stevenson, 1991; Britsch and Dunbar, 1993; Boomans and Day, 1993; Reed and Foote, 1997; Van der Wal and Pye, 2004).

In many saltmarshes, the production and incorporation of organic material is the principal factor that determines the maximum rate of vertical accretion (Nyman and Delaune, 1995; Reed, 1995; Callaway et al., 1997). Halophytic plants thus exert an important role on the long-term sustainability of these ecosystems, because they control their habitat elevation through the production of above- and below- ground biomass (Morris et al., 2002). In addition to its contribution to marsh soil volume (see Figure 1.12), vegetation also creates conditions conducive for deposition (Allen and Pye, 1992; Bartholdy, 2012) by reducing the velocity of water flow (Boorman, 1998) and attenuating wave energy (Moller et al., 1999). However, many other systems, especially in northwest Europe, are primarily dependent upon an external supply of inorganic mineral sediments whether from marine or fluvial sources (French, 2006).

Tidal exchange of water and sediment occurs preferentially via channel systems (French and Stoddart, 1992; D'Alpaos et al., 2006). The proximity to the creek network have been also suggested in many studies as the main factor that controls the sediment deposition rates (French and Spencer, 1993; French et al., 1995), whereas the small creeks have a less important influence (Stoddart et al., 1989; Bartholdy et al., 2010a, 2012). As the proximity to the primary creek increases, the sediment deposition decreases (Letzch and Frey, 1980; Carling, 1982; Reed, 1988; Stoddart et al., 1989; French and Spencer, 1993; French et al., 1995; Bartholdy, 1997; Reed et al., 1999; Bartholdy, 2010a). Deposition primarly takes place close to the creek margin of the marsh edge, while it will be a minimum deposition at some distances away from the source (Bartholdy, 2012).

Despite the effectiveness of vegetation in trapping and binding sediment (Cahoon and Reed, 1995; Adam, 2002), wind waves also exert an important control on marsh stability (Redfield, 1972; Pethick and Reed 1987; Allen 1989, 1997; Schwimmer, 2001). Saltmarshes typically exist in fetch-limited settings (Coward et al., 2011) in which wave height is determined by the interplay of the wind forcing (wind speed and duration), fetch distance and the water depth (Jackson and Nordstrom, 1992; Jackson et al., 2002; Nordstrom and Jackson, 2012). Many estuarine and backbarrier environments

are effectively depth-limiting such that an increase in wind speed does not significantly increase wave height (Jackson et al., 2002). However, the bottom depth increases when sea level rises, resulting in larger waves that erode the upper intertidal flats, and induce retreat of the outer salt marsh edge (Gardiner et al., 1992; Nicholls et al., 1999, 2004; Gardiner and Porter 2001; Pethick, 2001; Simas et al., 2001; Davidson–Arnott et al., 2002; Syvitski et al., 2005; Cahoon et al., 2006; Moller, 2006; Reed et al., 2009).

The eroded sediments will be redistributed within the marshes and the tidal flats by the waves and may aid the vertical adjustment of the marshes, thereby aiding their landward migration (Gardiner et al., 1992; Nicholls et al., 1999, 2004; Gardiner and Porter 2001; Pethick, 2001; Simas et al., 2001; Davidson–Arnott et al., 2002; Syvitski et al., 2005; Cahoon et al., 2006; Reed et al., 2009). When the inland migration is not possible, due either to steep terrain or, often, the presence of embankments and dykes that protect the area from the sea, ‘coastal squeeze’ can occur (Figure 1.13; Titus, 1986; Bijlsma et al., 1996; French, 1997; Pontee, 2013).

Figure 1.13: Coastal squeeze (a) before sea wall construction; (b) after construction of a sea wall; (c) constrained by steep terrain (Pontee, 2013).

Finally, sea-level rise is also associated with saltwater intrusion into rivers, coastal aquifers and estuaries (Titus, 1990; Gornitz, 1991; Nile Delta Aquifer and Madras Aquifer, Sherif and Singh, 1999; Douglas, 2001; Bobba, 2002; Nicholls et al., 2007; Shellenbarger Jones et al., 2009; Werner and Simmons, 2009; Wiedenman, 2010). A theoretical analysis of the saltwater intrusion indicates that a free water table of 1m above the mean sea level supports 40m of freshwater below the sea level (Ghyben-Herzberg equation). Thus, a rise in sea level of 0.5 m will cause a reduction in the freshwater thickness of 20m (Figure 1.14; Sherif and Singh, 1999). This relationship is based on assumptions that do not apply in all situations and is typically true away from the sea boundary. In these areas, the water tables are more affected by pumping and recharge activities rather than any change in sea level (Hull and Titus, 1986; Sherif and Singh, 1999; Werner and Simmons, 2009; Ferguson and Gleeson. 2012). Higher salinity levels will clearly affect the functioning of estuarine ecosystems and the distribution of their habitas and species (Berry et al., 2003). In Chesapeake Bay, for example, some islands have become so contaminated by salt that logging and farming activities are no longer possible (Kearney and Stevenson, 1991). However, if there is space for migration and the rate of sea-level rise is not too rapid then the animal and plant communities may be able to adapt (Nicholls et al., 2007).

Figure 1.14: Sharp interface and sea-level rise, based on the Ghyben – Herzberg relationship (Ghyben, 1888; Herzberg, 1901) (Sherif and Singg, 1999).

Concluding, it can be said that coastal systems adjust dynamically to a rise in sea level and maintain a characteristic geometry, unique to each coast (FitzGerald et al., 2008). The structure and functioning of most coastal ecosystems is closely linked to sea level;

if sea level increases at a rate that the ecosystem can not keep pace with, the state of the coast will fundamentally change (Anderson et al., 2009). Given that most of the interactions between climate change and landform and ecological responses to it are non-linear, the effect is not just a simple innundation but a complex spatially-distributed set of morphological and associated ecological changes. This requires appropriate models if such changes are to be predicted with any confidence.

1.4.3 UK Coastal and Estuarine Environments and their Likely Vulnerability to Climate Change

The coastline of the UK is naturally dynamic along much of its length on account of a predominantly meso and macro tidal regime together with an energetic storm wave climate (May and Hansom, 2003). Tidal ranges are very variable as a result of well-developed amphidromic tidal systems and the indented nature of the coast (Pugh, 1987). Western coasts are exposed to an energetic wind climate, which together with the North Atlantic swell, results in high energy waves. On the other hand, the North Sea is characterised by lower wind speeds and shallower waters, producing lower energy waves along the east coast (Laurence, 1980; May and Hansom, 2003).

The UK coast can be subcategorised into low-lying soft coasts, which are often protected by sea walls, and more resistant coasts, typically dominated by hard rock cliffs (Boorman et al., 1989; Figure 1.15). This variation in the geology combined with the sea-level history influences both erosion rates and the nature of the eroded material. Much of Scotland and some parts of the Welsh coast are highly resistant and predominantly source coarse gravel and boulders to local beaches (May and Hansom, 2003). Much of the contemporary beach sediment in these areas has derived from glaciogenic sources (May and Hansom, 2003). On the other hand, much of eastern and southern England are very prone to erosion because they consist of less resistant sedimentary rocks or glacial sediments and of offshore sediment reworked during the Holocene marine transgression (Boorman et al., 1989; Clayton and Shamoon, 1998; May and Hansom, 2003; Zsamboky et al., 2011).

Studies show that 67% of the coast of eastern England has retreated landward over the last century (Evans et al., 2004; Taylor et al., 2004). More generally, around 3000 km (about 17%) of the total UK coastline is currently eroding (EUROSION, 2004). Within

this bigger picture, 30% of England's coastline; 20% in Northern Ireland; 23% in Wales; and 12% in Scotland shows active erosion (MCCIP, 2011). Continuing coastal erosion contributes an important contemporary sediment sources that are important in maintaining local beaches and more distant muddy intertidal environments (Boorman et al., 1989). But these sediment feeds are reduced by coastal protection. In particular, in UK almost 2300 km of the total coastline is artificially protected, the largest proportion in Europe (EUROSION, 2004). This amounts to 46% of England's coastline; 20% of Northern Island's; 28% Wales' and 7% of Scotland's (MCCIP, 2011).

Figure 1.15: Relative resistance of rocks of the UK (after May and Hansom, 2003).

A notable feature of the UK coast is its degree of indentation, where numerous valleys and embayments are occupied by estuaries. These not only increase the shoreline length but they also contain significant areas of settlement and agriculture located on land reclaimed from the sea since medieval times (Austin et al., 2001). Such land is highly vulnerable to inundation if the extensive flood defence infrastructure is not maintained and upgraded to cope with higher sea level. This is especially true of southeast England, which has some of the most extensively reclaimed estuaries (Gray, 1977; Austin et al., 2001) and is also subject to the highest rates of relative sea-level rise (Woodworth et al., 1999; Hulme et al., 2009; Jenkins et al., 2009, Wahl et al., 2013).

UK estuaries contain a large proportion of the tidal wetland habitats in northwest Europe, many of which are designated as "Special Areas of Conservation" (SAC) under the EC Habitats Directive (Council Directive 92/43/EEC of 21 May 1992). Saltmarsh is especially well developed, primarly in meso and macro tidal areas (Allen, 2000), and occur in four main settings; open coast, back-barrier environments, embayments and estuaries.

Most of the saltmarshes that are actively formed today in Great Britain are characterized as allochthonous in terms that they are formed primarily through the introduction of externally derived clastic sediments. In general, little is known about the budgets and the sources of British saltmarsh sediments (see, for example, French, 2006). Possible sources of mineral matter include coastal and estuarine cliffs, offshore mud deposits and river catchments. Mud can travel long distances from a source, and it can also be mixed with other materials before arriving at its new deposition site (Allen and Pye, 1992). Many studies (Eisma and Kalf, 1987; McCave, 1987; Kirby, 1987) show that small amounts of sediment are provided by the rivers that drain into the Irish and the North Sea, and most of the suspended mud in tidal waters is provided by eroded unconsolidated Pleistocene glacial sediments exposed in retreating coastal cliffs.

Saltmarsh degradation and loss has been evident over the last century or so, especially in southeast England (Boorman et al., 1989; Pye, 2000). Vertical accretion rates appear to be sufficient to cope with relative sea-level rise, in both open coast (e.g. Dengie peninsula, Essex; Reed, 1988) and estuarine marshes (e.g. those of the Greater Thames; Van der Wal and Pye, 2004). However, marsh area has declined significantly over the last few decades (Pye, 2000), with losses of 10 to 44% from 1973 to 1985/1988 (Burd,

1992; Cooper et al., 2001). A variety of different mechanisms of saltmarsh degradation have been identified and it is likely the observed changes are the results of some combination of these rather than one mechanism alone. Although increased storminess due to sea-level rise has been reported as a cause of increased saltmarsh erosion (Doody, 1992; Pethick, 1992), the pattern of marsh-edge erosion in south-east England cannot support an explanation based only on the wave action (Burd, 1992; Hughes and Paramor, 2004). Losses of subtidal seagrass (*Zostera sp.)* in this area have increased vulnerability to wave action and erosion of the marsh edge, but cannot explain the loss of marsh in sheltered locations (Hughes and Paramor, 2004).

Coastal squeeze has also been reported as a cause of saltmarsh losses that is especially applicable to southeast England (Shennan, 1989; Burd 1992; English Nature 1992; Covey and Laffoley, 2002; Taylor et al., 2004). Here too, the evidence is patchy. Although there is a scarcity of plant species on the upper marshes on southeast England, as expected under the process of coastal squeeze, this may also be a consequence of the long history of enclosure that removed the upper marsh from the influence of the tide (Hughes and Paramor, 2004). Covey and Laffoley (2002) argue that only 5% of recent marsh loss is due to land claim and the constructions of flood defences.

Although many areas of the UK coastline are under threat from sea-level rise and other aspects of climate change (Dearing et al., 2006), the vulnerability of coastal and estuarine wetlands is of particular concern given their already high rates of loss and the extent to which their natural response is constrained by reclamation and flood defence structures (Wolters et al., 2005). Although hard defences still feature prominently in coastal management and flood protection planning (DEFRA, 2002; Pethick, 2002), a new strategy of managed realignment has become progressively favoured since the 1990s (English Nature, 1992; Doody, 2012). This approach is reflected in the Shoreline Management Plans (SMPs) for England and Wales, which aim to set out policies to manage coastal erosion and flood risk (Zsamboky et al., 2011; Doody, 2012). It is also adopted by many agencies and organizations, not only in the UK but elsewhere too (Hughes and Paramor, 2004; Morris et al., 2004) and contributes to the rationale for improving our modelling capability, by improving our understanding on the processes involved (Garbutt et al., 2006).

1.5 Modelling Approaches

From an awareness of the risks posed by climate change, emerges the need to create robust models to provide a scientific basis for understanding, predicting and managing the potential impacts on coasts (FitzGerald et al., 2008). This leads to the challenge of predicting these impacts at the crucial mesoscale of 10 to 10^2 km and a time horizon of 10 to 10^2 or 10^3 years, corresponding to the 'engineering' scale of Cowell and Thom (1994). A major problem with such a mesoscale is that it is situated between the small scale processes of sediment transport, which are relatively well understood and broader coastal evolution, which is informed by the record of Holocene stratigraphy (Figure 1.16; French and Burningham, 2009).

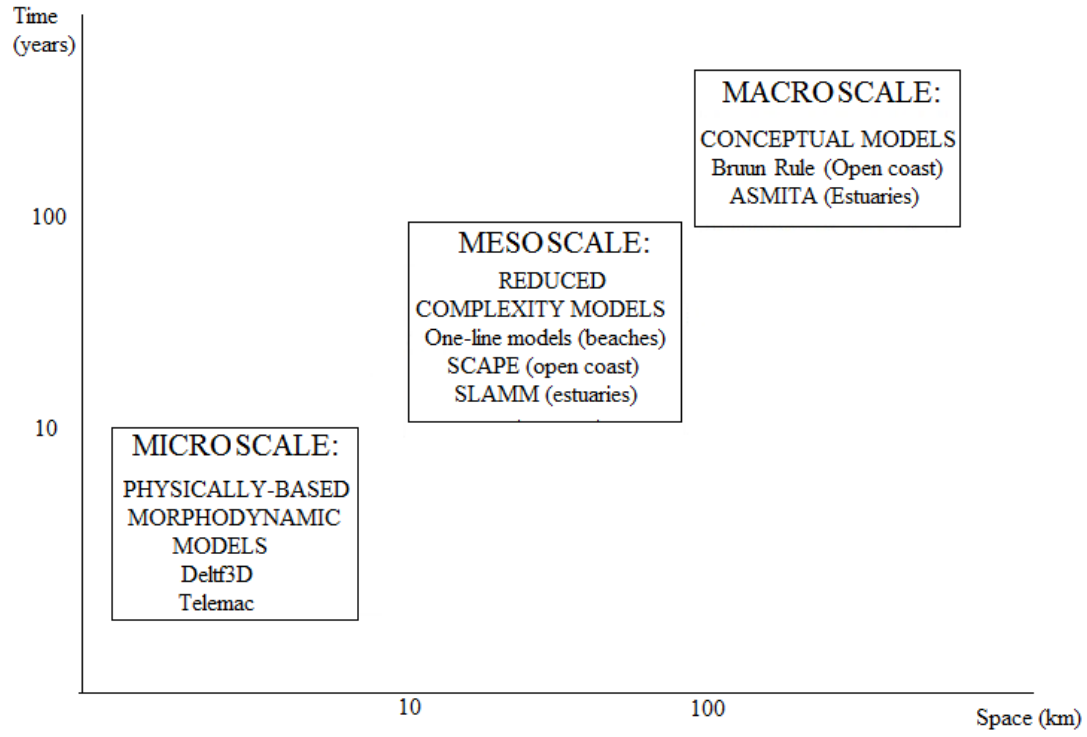

Figure 1.16: Modelling approaches applicable to different scales (after French and Burningham, 2009).

An approach that has been very popular in coastal management and planning is to estimate future shoreline retreat by extrapolating past rates of change, assuming that the observed coastal behaviour encompasses the kind of behaviour that can be expected in the future (National Research Council, 1990; Fenster et al., 1993; Hooke and Bray, 1996). Historical Trend Analysis (National Research Council, 1987; Leatherman, 1990) has been used by many studies (for future shoreline position projections see: NRC 1990, Fenster et al., 1993, Douglas et al., 1998; Futurecoast study (Defra, 2002); Pye and Blott, 2008 and for sea-level rise effects on wetlands see: Orson et al., 1985; Vanderzee,

1988; Parkinson et al., 1994). It is preferred because it is site-specific and uses data that can be acquired relatively easily. Its main assumption is that sea-level rise is the dominant influence on recession while other parameters remain constant (Bray and Hooke, 1997; Whitehouse et al., 2009). This assumption might be valid with rapid rates of relative sea-level rise but is a significant limitation when other factors are important (Bray and Hooke, 1997). Also, this method can predict behaviour only under well represented in the historic record conditions (e.g.: Dolan et al., 1991; Hall et al., 2002; Walkden and Hall, 2005), otherwise the reported rates will be inconsistent (Addo et al., 2008).

Microscale processes lead to nonlinear dynamic coastal responses to environmental change, which can be captured over short timescales by morphodynamic models based on hydrodynamic and sediment transport principles (de Vriend et al., 1993a; Wang et al., 1995; Nicholson et al., 1997; Cayocca , 2001; Lesser et al., 2004; Sutherland et al., 2004; Dearing et al., 2006; Gardiner et al., 2007; Scott and Mason, 2007). Such models are becoming increasingly sophisticated (Lesser et al., 2004) and typically incorporate multiple modules that interact with each other to represent the hydrodynamics, residual sediment transport patterns, and also the evolution of the bed morphology (eg. ECOMSed (Hydroqual, 2002), ROMS (Warner et al., 2008), Delft3D (Lesser et al., 2004), MIKE21 (Warren and Bach, 1992) (van Rijn et al., 2003; Villaret et al., 2012). The increasing use of unstructured finite element and finite volume computational meshes (e.g. TELEMAC) means that such models are able to handle complex geometries, including estuaries, inlets and open coasts (Villaret et al., 2012).

However, morphodynamic models usually perform poorly in detail (de Vriend et al., 1993a; Nicholson et al., 1997; Sutherland et al., 2004) because much of the behaviour modelled is incompletely understood (Roelvnik and Broker, 1993). Crucially, most of the relevant physics included in these models relates to the hydrodynamics, meaning that they operate in time scales that are much shorter than the changes in morphology (DeVriend et al., 1993b; Hanson et al., 2003; van Rijn et al., 2003; Scott and Mason, 2007). These short-term hydrodynamic and sediment transport problems also require a lot of computer power (Roelvnik and Broker, 1993; Whitehouse et al., 2009) making them unsuitable for modelling on a timescale of a century (DeVriend et al., 1993b; Hanson et al., 2003). Even if the computer power is enough to run these small scales for a long period of time, this may be not the best way (DeVriend et al., 1993b).

On the timescale of a century, the basis for most models of coastal evolution is the Equilibrium Shoreface Profile (Larson, 1991; Pilkey et al., 1993; Thieler et al., 2000; Kaiser and Frihy, 2009). In a two-dimensional sense, the shoreface profile refers to a hypothetical long-term average profile achieved under a given wave climate and in a particular set of materials (Schwartz, 1982). Many scientists have doubted its existence due to its restrictive assumptions (Wright et al., 1991; Pilkey et al., 1993; Carter and Woodroffe, 1994; Thieler et al., 1995, 2000). It has also been argued that it is a purely theoretical morphology that is rarely if ever attained in practise, given that beach morphology is always adjusting to, and lags behind, changes in wave conditions (Moore, 1982; Kriebel et al., 1991; Pilkey et al., 1993; Wright, 1995). However it is very useful to examine the behaviour of sandy beaches and dunes when longshore transport gradients can be ignored (Roelvink and Broker, 1993).

Bruun (1954) was the first to describe the geometry of such an equilibrium profile providing the basis for the so-called 'Bruun Rule' (Schwarts, 1967). The Bruun Rule is a two dimensional mathematical principle founded on mass conservation that is used to predict shoreline erosion (and therefore coastal recession) due to sea-level rise (Bruun 1962, 1983; Ranasinghe and Stive, 2009). It assumes that the shoreface profile is developed entirely in sand, and as sea level rises, moves up and back, maintaining its shape. The amount of sand that is removed from the upper part of the profile is equal to the amount of deposited sand on the lower profile (Figure 1.17; Brunn, 1962). Due the restrictive nature of these assumptions, the Bruun rule performs well only under specific environmental circumstances (Bruun 1983, 1988; French and Spencer, 2001; Cooper and Pilkey, 2004).

Figure 1.17: The Bruun Rule of shoreline retreat (Bruun, 1962).

A key limitation of the Bruun Rule comes from the the inclusion of a 'closure depth' in the model. The choice of this depth is to some extent arbitary; while Bruun (1962) assumed a depth of 18m, other studies used a depth of around 9 m (Pilkey et al. 1993). Bruun (1988) suggested that field identification could be based on sedimentological boundaries, while Nicholls et al. (1998) estimated closure depth based on nearshore wave statistics. The Bruun Rule can be applied successfully in restricted fetch settings where the depth of closure is limited (French and Spencer, 2001) and may hold for estuarine beaches (e.g.. Rosen, 1978, Hands, 1983, Kaplin and Selivanon, 1995). Many modifications have been proposed (Dubois, 1977; Weggel., 1979; Dean and Maurmeyer, 1983; Hands, 1983; Dean, 1991; Davidson- Arnott, 2005) in order to address these limitations and also many attempts have been made to test its predictive capability (Schwartz, 1967, 1987; Rosen, 1978; Pilkey and Davis, 1987; Bruun 1988; List et al., 1997). The results have been mixed. On one hand, fundamental objections have been raised over the use of equilibrium profiles as a basis for shoreline change modelling because there are more geological factors and numerous hydrodynamic influences that condition actual profiles than the Bruun model considers (Dubois, 1992, Pilkey et al., 1993). Many studies (Kaplin and Selivanov, 1995; List et al., 1997; Pilkey et al., 2000; Sallenger et al., 2000; Thieler et al., 2000) have shown that the Bruun Rule is an inadequate model of shoreline retreat (Cooper and Pilkey, 2004) and that even under ideal conditions, the rule has never given accurate predictions (SCOR Working Group 89,1991; List et al., 1997; Pilkey and Cooper, 2004). Thus, Cooper and Pilkey (2004) conclude that the Bruun Rule, whilst was a useful tool for its time, has outlasted its usefulness and it should be abandoned and replaced by other models.

On the other hand, the Bruun rule remains the most widely used contemporary method because it is simple, it does not require field study, it can be applied by scientists with no critical appraisal and finally due to the lack of an alternative model (Pilkey and Cooper, 2004; Ranassinghe and Stive, 2009). Thus, it is often embedded in more complex numerical modelling systems to represent cross-shore adjustments of the beach. Its main assumption, for example, that the profile shape remains constant, is also used in the 'one-line' GENEralized Model for Simulating Shoreline Change (GENESIS) (Hanson and Kraus,1989) and the SBEACH numerical model (Larson and Kraus, 1989). The first of these is empirically based and mainly used to analyse the shoreline response to the longshore sediment transport rate and also to develop sediment budgets in a regional scale (Kaiser and Frihy, 2009). The second examines the change

of the shoreline caused by the cross-shore sediment transport (Kaiser and Frihy, 2009) and is used to predict the beach and dune erosion caused by storms (Thieler et al., 2000). A combination of these two and CASCADE planning model (Larson et al., 2002) emerged in a new model suitable for mesoscale prediction, the GENCADE model (Hanson et al., 2011). The longshore sediment transport in both GENESIS and GENCADE is calculated by using the CERC Formula (Nielsen, 1992).

More sophisticated process-based models are often preferred because they incorporate much greater mechanistic understanding (Costanza et al., 1990; Roelvnik and Broker, 1993). In order to characterise the behaviour of the 'whole' system at large spatial and temporal scales so-called 'reduced complexity models' have been developed, commonly used in geomorphology (Murray and Paola, 1994; Coulthard et al., 2002). These incorporate simplified parameterisations of the fine-scale processes that can be considered to be 'sub-grid' at a mesoscale, and focus on the key linkages and feedbacks between the major morphological components (Dickson et al., 2007). A good example of this type of model on coastal landforms is the SCAPE (Soft Cliff and Platform Erosion) model, which simulates the sensitivity of shore profile response, including cliff recession rates over timescales of decades to centuries (Walkden and Hall, 2005; Dickson et al., 2007; Addo et al., 2008; Walkden and Dickson, 2008; Walkden and Hall, 2011). It was used initially on a specific site, the Naze Peninsula, in Essex, southern England (Walkden and Hall, 2005) but extended later to be a general representative of soft-rock shores overlain by a sparse beach (Figure 1.18; Dickson et al., 2007). It can also be characterised as a hybrid model because it includes several modules in order to describe all the different processes (wave tranformation, platform erosion and a beach) (Figure 1.19) but also includes two feedback processes between and within the modules that regulates their behaviour (Dickson et al., 2005; Walkden and Hall, 2011):

- Cliff retreat results in beach formation, which results in greater protection and ultimately in a reduced rate of to cliff retreat.
- More rapid cliff retreat also results in a flatter shore platform profile, which results in greater wave dissipation, thus, less platform downwearing and therefore a reduction in the rate of cliff retreat. (Whitehouse et al., 2009).

Figure 1.18: Schematic representation of a typical SCAPE model profile (Walkden and Dickson, 2008).

Figure 1.19: Processes represented in SCAPE (Walkden and Dickson, 2008).

A comparison between the predictions of SCAPE and those made using the modified Bruun rule showed that SCAPE predicts more complex responses and lower sensitivity of soft rock shores to sea-level rise (Dickson et al.. 2007). However, it can not be used in all situations or where historical sea-level rise data are not available (Walkden and Dickson, 2008). Thus, it must be used in conjuction with other predictive models (see, for example, Addo et al., 2008).

When more spatially extensive low-gradient environments are considered, vertical changes are often as important as the horizontal shifts in a shore profile or a cliff, and these adjustments are usually highly non-linear (Nicholls et al., 1999; Nicholls, 2004). This is particularly true of estuarine margins dominated by extensive tidal wetlands. As sea level increases, vertical accretion on the surface of the wetland is also increased due to the increased organic matter (ΔS_{org}) and sediment input (ΔS_{sed}) and is calculated as the sum of these inputs (Bartholdy, 2012). However, in order to simulate the final vertical growth (ΔE) of marsh platforms due to sea-level change for long time periods (50 to 10^3 years), the deposit thickness due to autocompaction (ΔP) and the possible isostatic and eustatic changes (ΔM) must also be included. Various researchers have investigated the interplay between these factors using a zero-dimensional approach (equation 1.1; Krone, 1987; Allen, 1990, 1991; French, 1993, 1994; Temmerman et al., 2003; French, 2006; Bartholdy, 2012).

$$\Delta E=\Delta S_{sed}+\Delta S_{org}-\Delta M-\Delta P, \qquad (1.1)$$

This essentially a spatial formulation is justified given that the topography of the marsh platform is nearly horizontal (Temmerman et al., 2003). The terms ΔM and ΔP are given and the ΔS_{org} is often ignored in predominantly allochthonous systems, where it is relatively small. So, the challenge is to simulate the ΔS_{sed} (Bartholdy, 2012). Krone (1987) was the first to develop a zero-dimensional mass model to calculate ΔS_{sed} and used it to simulate how tidal marshes in San Francisco Bay respond to historical sea-level change. He proposed an equation to calculate the time-dependent sedimentation on a salt marsh unit area, which is integrated over a tidal period and then over all the tidal periods in a year. Dividing mass deposition per unit area per year by the bulk dry density of the material deposited yields ΔS_{sed}. Latter, Allen (1990) used this approach to simulate the long-term vertical growth of salt marshes in the Severn estuary. Similar approaches have been developed by French (1993, 2004, 2006) and Allen (1995, 1997). More recent work has shown that this type of model can better simulate observed long-term historical marsh growth by incorporating a relationship between suspended sediment concentration (C_0) and inundation depth. If this relationship is not included, the observed historical growth will be underestimated, resulting to rather conservative under-predictions of vertical marsh growth under sea-level rise scenarios (Temmerman et al., 2003).

In some systems, especially those with less significant mineral sediment inputs, vegetation growth and decomposition must also be taken into account (Friedrichs and Perry, 2001). Morris et al. (2002) included the alterations in biological productivity with varying levels of tidal inundation in order to show how long-term vertical accretion rates are almost equal to sea-level rise rates on a vegetated marsh platform. In his model, the biomass density enhance the deposition rates, reinforcing the ability of the marsh platform adjust towards an elevation or inundation depth at which the rate of deposition and the rate of sea-level rise will be equal. This equilibrium elevation depends on the rate of sea-level rise, vegetation type, and also the suspended inorganic sediment concentration.

For even more realistic results, the autocompation term (Allen, 1999) should ideally be included. French (2006) incorporated an autocompaction term in his zero-dimensional mass-balance model (French, 1993, 1994), although unlike the Temmerman et al. (2003) model, this still assumes that C_0 and w_s (settling velocity) remain constant. French (2006) also advocates consideration of vertical marsh adjustment in the context of sediment supply and not solely the determination of net elevation balance.

A different approach was used more recently by Bartholdy et al. (2004, 2010a) to determine the average deposition ΔS_{sed} (kg m^{-2} tidal $period^{-1}$) in specific time at a specific site, by taking into account the elevation of the saltmarsh (E(t)) and the concentration of sediment available for deposition ($\Delta C_{(HWL)}$). Although the last term is location-specific, it depends on the high tide level relative to the mean high water level (MHWL) (equation 1.2; Bartholdy, 2012).

$$\Delta S_{sed} = \Delta C_{(HWL)} * [HWL - E(t)], \qquad (1.2)$$

In order to include the autocompaction, the calculated ΔS_{sed} must be added to the mass depth (kg m^{-2}) of the saltmarsh from the surface to the lower boundary of the salt marsh deposits, at the particular location. The result will be introduced in the mass depth equation (equation 1.3, Bartholdy et al., 2010b, 2012) and by solving it for z, the required salt marsh level will be given.

$$MSD_z = A * z\ln(z) + z(B-A), \qquad (1.3)$$

where, A and B are two empirical constants.

Based on mean accretion measurements across the Skallingen backbarrier saltmarshes, in western Denmark (Nielsen, 1935; Jakobsen, 1953; Bartholdy et al., 2004, 2010a), and after their correction for autocompaction, the correlation of the calculated by the equation 1.3 saltmarsh level to the sea level seems to depend on the distance to marsh edge and to distance to creeks. This produces a pattern of more rapid accretion in the outer part of the backbarrier and also along the major creeks (Bartholdy, 2012), enhancing the importance of the spatial variations in the rate of sedimentation at all time scales (French and Spencer, 1993; French et al., 1995; Leonard, 1997). In order for these factors (elevation, distance to creeks and distance to marsh edge) to be modelled, a two-dimensional approach is clearly necessary.

In order to model whole estuary evolution under different climate change scenarios, broad-scale interactions between the tidal basin and the adjacent coastal environment need to be included (Stive et al., 1998). Behaviour-oriented modelling (de Vriend et al., 1993b) has been extensively used to study the evolution of tidal inlets (Van Goor et al., 2003). These are typically based on "empirical-equilibrium assumptions" created by applying "data-knowledge" (Dissanayake et al., 2011), meaning that this approach uses real data to map the system behaviour onto a simple mathematical model (de Vriend et al., 1993b). The processes considered are based on elementary physics but these are applied to a highly idealised set of morphological sub-systems under simplified hydrodynamic forcing (Hibma et al., 2004). Although this modelling approach has been used in various models (Di Silvio, 1989; van Dongeren and de Vriend, 1994), the most well known is the ASMITA (Aggregated Scale Morphological Interaction between Tidal basin and the Adjacent coast) model (Stive et al., 1998).

In its basic form, ASMITA represents an estuary using a simple three-element schematisation (Figure 1.20), each one of which has a tendency towards a morphological equilibrium, when the hydrodynamic forcing is constant (van Goor et al., 2003). These elements and their interactions are characterised by mathematical expressions (Whitehouse et al., 2009), while the volume and area of each equilibrium can be defined by using empirical relationships (Stive et al., 1998) and more particular by a linear relationship with the tidal prism. That means that when the tidal prism changes, the volume and area of each element equilibrium also change forcing the elements to reach a new equilibrium by exchanging sediment (Whitehouse et al., 2009).

These empirical relationships are based on available data, and are thus different for each estuary (Rossington and Nicholls, 2007).

Figure 1.20: Estuary three-element schematisation used in ASMITA (Whitehouse et al., 2009).

Models such as ASMITA are limited not only by their lack of spatial detail (they are effectively aspatial box models) but also by their assumption of equilibrium tendencies. This limits their ability to resolve the subtleties of climate change impacts, especially ecological changes within key landform types. In this respect, some promising developments have occurred within the field of spatial landscape modelling. While earlier ecological models concentrate on temporal changes with no or little spatial articulation, a different generation of models can project cumulative impacts at many spatial and temporal scales (Risser et al., 1984; Sklar et al. 1985; Reyes, 2009). A typical spatial landscape model discretises the study region into a raster of cells. Each cell contains a dynamic ecosystem simulation model, which in the case of coastal and estuarine wetlands includes water flow and levels, tidal and river inputs, sedimentation, subsidence and salinity, and is connected to the adjacent ones by the exchanges of the water and suspended materials. The physical and ecological dynamics are calculated in every cell, and any habitat change determining using a logical decision tree (Sklar et al., 1985).

This approach is exemplified by the Coastal Ecological Landscape Spatial Simulation (CELSS) Model (Costanza et al. 1988; Sklar et al., 1989; Costanza et al., 1990) which was developed using 2479 cells, each representing 1 km^2, to simulate large-scale ecological habitat transitions in Atchafalaya/Terrebonne marsh/estuarine complex in south Louisiana. Later versions of this model have taken advantages in computing

capability to increase the spatial resolution, making it suitable for more localised change prediction studies at the estuary scale (e.g. Sklar et al., 1994).

The use of GIS has emerged parallel with such spatial models and is clearly a very useful tool for coastal vulnerability assessment (McLeod et al., 2010), whether coupled with a dynamic simulation model or not (Green and King, 2003; Rodriquez et al., 2009). Based on an elevation analysis only, GIS can provide a crude indication of potential inundation of coastal lowland following a rise in sea level (eg. Brooks et al., 2006; Snoussi et al., 2009; Chust et al., 2010; Tian et al., 2010). However, GIS is more useful when coupled with an essentially mechanistic model of some kind, and can provide vital spatial analyses in support of the modelling (Lyon and McCarthy, 1995; Green and King, 2003) as well as powerful visualisation tools (Green and King, 2003). Attempts have been made to develop global databases for the coastal regions of the world (e.g. LOICZ (Maxwell and Buddemeier, 2002), EUROSION (http://www.eurosion.org), CoastBase (http://www.coastbase.org)). With the exception of EUROSION, however, most of these databases have not been originally developed for coastal applications. Accordingly, their use in coastal modelling and analyses is limited (Vafeidis et al., 2008). A new global coastal database has been developed specifically for vulnerability and impact analysis due to sea-level rise at regional to global scales in the DINAS-COAST project (Dynamic and Interactive Assessment of National, Regional and Global Vulnerability of Coastal Zones to Climate Change and Sea-Level Rise) (DINAS-COAST Consortium, 2006). This was created in a GIS framework (Vafeidis et al., 2008) and can be used in conjunction with the linked DIVA model to evaluate sea-level scenarios at both regional and global scales (Hinkel, 2005; Hinkel and Klein, 2007, 2009).

The DIVA tool neglects many of the processes that occur in conjuction with sea level changes, such as changes in the frequency and intensity of storms, accretion and subsidence induced by humans (Mcleod et al., 2010). However, it has been used by many projects, notably the BRANCH project in the UK (BRANCH partnership, 2007) to examine the impacts of climate change, and particularly sea-level rise, on coastal habitats at a European Union - scale. BRANCH uses a set of sea-level rise scenarios (no sea-level rise and IPCC low and high sea-level rise) and three time slices (2020s, 2050s, 2080s) compared to the baseline year of 2000. It also includes estimations for land uplift and subsidence, so the initial global scenarios are converted to scenarios of relative sea-

level rise for each impact analysis. Finally, using its 'impact algorithm', losses of these habitats are estimated. A major limitation is that the DIVA model includes only two types of coastal habitats relevant to Europe; saltmarsh and low unvegetated wetlands (i.e. tidal flats).

Crucially, none of these approaches take account of dynamic feedbacks between processes and coastal morphology – such as the ability of the saltmarsh to respond to sea-level rise by increased accretion and/or the landward migration. That is why, the DIVA software has been criticised as a basis for informing goverments and coastal managers about adaptation, migration and also policy development (Green and King, 2003; McLeod et al., 2010). These limitations are at least partially addressed in the Sea Level Affecting Marshes Model (SLAMM) (Park et al., 1986), providing this way a more dynamic basis for evaluations of sea-level rise impacts at local to regional scales (Mcleod et al., 2010).

SLAMM is a rule-based spatial model that simulates the dominant processes involved in shoreline modifications and wetland conversions due to sea-level rise (Park et al. 1989), and the extent to which sea water inundation contributes to the conversion of one habitat to another (based on elevation, habitat type, slope, sedimentation and accretion and erosion rate), and also the extent to which the affected area is protected by existing sea walls. The processes modelled include inundation, erosion and accretion, overwash, and salinity (Clough et al., 2010). The appropriate spatial scale to use varies from local to regional (e.g. 1 km^2- 100.000 km^2), while the temporal scale also varies from a time-step of 5 to 25 years depending on the chosen sea–level rise scenarios (McLeod et al., 2010). Over the last 20 years it has been widely used in North America in decision-making processes in coastal research for environmental protection and also economic development (Park, 1991; Craft et al., 2009).

In conclusion, it is clear that models such as SLAMM, combined with the increasing availability of high-resolution terrain datasets and GIS tools to manage both data and model, provide a basis for a more mechanistic understanding of climate change impacts on coastal and estuarine environments. However, much more work needs to be done to better integrate existing models with our understanding of the dominant physical and ecological processes in a wider range of geographical contexts.

1.6 Aims and Objectives

Within the context of the preceding review, the overarching aim of this thesis is to evaluate the potential of reduced complexity, spatial landscape models to represent mesoscale impacts of sea-level rise on estuary environments in the UK. Specifically, the following objectives are addressed:

1. To adapt the Sea Level Affecting Marshes Model (SLAMM) for application to the tidal sedimentary environments and habitats found in the UK, with particular reference to eastern and southern England.
2. To undertake a sensitivity analysis of the modified SLAMM code using as a 'testbed', a small estuarine system on the south coast of England (Newtown estuary, Isle of Wight).
3. To apply and critically evaluate the modified SLAMM to more complex estuary and coastal barrier systems of eastern England, for which boundary condition and validation data are available.
4. To critically evaluate SLAMM predictions against alternative approaches to predicting sea-level rise impacts (e.g. the BRANCH model).

It is hoped that this study will serve to demonstrate the potential of reduced complexity approaches as a computationally efficient yet robust means of projecting broad-scale changes in coastal and estuarine morphology and habitat characteristics. Also, it is envisaged that such modelling tools may also have an important role in the visualization and communication of coastal change and alternative coastal futures to wider, non-specialist audiences. More specifically, by applying for the first time in the UK a spatial landscape modelling approach for projecting the estuarine responses to sea-level rise, there is the potential for UK estuary management policy to be informed more effectively such that management strategies relating to the intertidal zone may be fundamentally changed.

2 RESEARCH DESIGN

2.1 Overview

The Sea Level Affecting Marshes Model (SLAMM) is used in this thesis as a modelling platform with which to evaluate the meso-scale impacts of sea-level rise in the kind of estuarine and backbarrier settings that are found in the UK. SLAMM is free and open source software, which after 20 years of development, has been characterised as an important forecast and simulation model in coastal research (Liao et al., 2011). It has been used at a wide range of scales, in North America (see examples at http://www.fws.gov/refuges/planning/seaLevelRise.html), Australia (e.g. Akumu et al., 2010) and China (e.g. Wang et al., 2014) in order to inform decision-making processes not only for environmental protection but for economic development too (Liao et al., 2011).

SLAMM was first developed in 1986, funded by the United States Environmental Protection Agency (EPA) (Park et al., 1986). Since then, six versions of the model have been released (SLAMM2: Park et al., 1989; Park, 1991; Titus et al., 1991, SLAMM3: Lee et al., 1991; Park et al., 1991, 1993; Lee et al., 1992, SLAMM4: Galbraith et al., 2002; Galbraith et al., 2003, SLAMM4.1: NWF, 2006, SLAMM5: Craft et al., 2009, SLAMM6: used by many consultancy projects made by Warren Pinnacle Consulting on behalf the U.S. Fish and Wildlife Service, National Wildlife Refuge System; Geselbracht et al., 2011; Glick et al., 2013; Linhoss et al., 2013, 2015; Chu et al., 2014; Wang et al., 2014). An upgrade of the latest major version will be released soon (SLAMM 7).

SLAMM is a rule-based spatial model, which represents a domain as an array of discrete cells, the size of which depends on data availability and the characteristics of the study site but typically ranges from 5 to 30 m. The only required data to specify the initial condition are the elevation, slope and land classification raster layers. These are provided in a standard ASCII grid format, which can be generated by most GIS packages. A complex but flexible decision tree, which consists of qualitative and geometric relationships, is then used to determine how the habitat class within each cell will be affected and converted to another one, given specific site parameters and rate of sea-level rise (Figure 2.1; Clough et al., 2010).

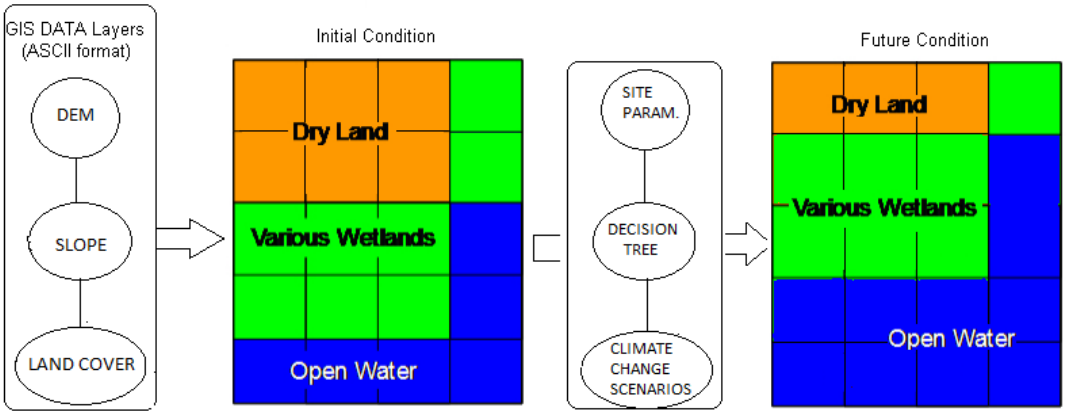

Figure 2.1: Basic structure of SLAMM (based on version 6.0.1).

A key component of the present study is the adaptation of this model to suit the tidal sedimentary environments and habitats encountered in the UK. The modified SLAMM is then used to evaluate its potential, and that of a raster-based modelling approach in general, as a basis for projecting the impacts of sea-level rise on key intertidal landforms and habitats.

Initial evaluation and adaptation of SLAMM was accomplished using Newtown estuary on the Isle of Wight, southern England as a pilot study. This site was selected on account of its small size and computational tractability, which allowed a sensitivity analysis of the basic processes included in the model. A more crucial factor, though, was the availability of high resolution altimetry data at no cost via the Channel Coastal Observatory. Following evaluation at this test site, the modified SLAMM code is applied to contrasting case study systems in eastern England, in order to critically evaluate its ability to produce meaningful projections of intertidal habitat change under a set of UKCP09 scenarios. These sites include the Deben and Blyth estuaries in Suffolk, and the spit and backbarrier saltmarsh complex at Blakeney Point, Norfolk. These case studies were chosen to take advantage of Environment Agency Lidar datasets that became available as the project progressed via the NERC Integrating Coastal Sediment Systems (iCOASST) project (Nicholls et al., 2012). Also, the availability of previous studies of recent sedimentation facilitates parameterisation of the various sub-models in SLAMM. Validation is attempted against limited known historic changes and a sensitivity analysis is undertaken in order to better understand the nature of sea-level rise effects. Finally, results from SLAMM are compared with those from empirical models, and more specifically the currently used one in the UK BRANCH model.

2.2 Processes modelled in SLAMM

Six primary processes are modelled within SLAMM in order to project the fate of the habitat distribution under different sea-level rise scenarios: inundation, accretion, erosion, overwash, saturation and salinity (Figure 2.2). The simulations are usually executed with a time-step of 25 years by 2100, in order to correspond to the time scales used within the IPCC sea-level rise scenarios. However, any other time-step or even specific time-series of years can be executed. A simulation for the 'current' year can also be executed in cases where the land classification layer does not match the SLAMM conceptual model, and therefore it must be 'corrected' based on the DEM. Prior to a simulation, SLAMM checks if the dates of the land cover map and that of the digital elevation model (DEM) are the same. If they are not, then the elevations used in the model can be adjusted to account for the effects of relative sea-level rise in the intervening period, as specified in equation 2.1. In each time-step, the land elevation is adjusted such that the Mean Tide Level (MTL) remains zero; this is the internal datum within SLAMM (Clough et al., 2010).

$$Elev_{NWIDate} = Elev_{DEMdate} - \frac{(Year_{NWIDate} - Year_{DEMDate})(HistSLR_{Local} - HistSLR_{Global})}{1000} \quad (2.1)$$

where, $Elev_{Date}$ = Elevation at given date (m)

NWI = US National Wetland Inventory

$Year_{Date}$ = Year number for given date

$HistSLR_{Local}$ = Site specific historic trend of sea level rise (mm yr^{-1})

$HistSLR_{Global}$ = Global historic trend (IPCC, 2007)

1000 = unit conversion constant (mm yr^{-1})

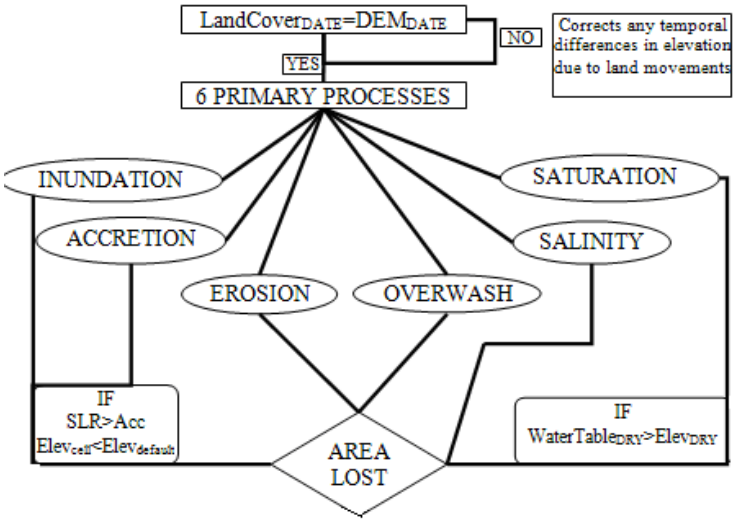

Figure 2.2: Processes modelled in SLAMM.

2.2.1 Inundation

The response of each wetland category to sea-level rise depends on its ability to maintain its relative elevation within the tidal frame (Reed, 1990). In that direction, the minimum elevation of each wetland category is recalculated within SLAMM in each time-step (equation 2.2). This is then compared to the minimum elevation of the specific wetland category in order to determine the fate of the cell habitat under the sea-level rise scenario being modelled (Clough et al., 2010).

$$MinElev_{Category,t} = MinElev_{Category,t-1} + DT * Accr_{category} - SLR \quad (2.2)$$

where $MinElev_{category}$ = Minimum elevation of the relevant category (m)

DT = Time step (yr)

Accr = Accretion or sedimentation rate (m yr^{-1}), which is assumed to be zero if the land is protected by a flood defence

SLR = Predicted local sea-level rise during time step (m)

If this elevation is lower than the minimum elevation for the existing wetland type and the sea-level rise is greater than the accretion, inundation is assumed. In that case, the habitat will undergo a transition. The fraction transformed is then computed for each time step as a function of the minimum elevation, the lower elevation boundary of that wetland and also the slope of the cell (equation 2.3) (Clough et al., 2010).

$$FracLost_{Cat} = \frac{\left(\frac{LowBound - MinElev_{Cat,t}}{\tan Slope}\right)}{Width_{Cat}} \quad (2.3)$$

where $FracLost_{Cat}$ = Fraction of wetland that is lost in time step (untless)

LowBound = Lower elevation boundary of the wetland class (m)

$MinElev_{cat,t}$ = Minimum elevation of the wetland class at time t before the conversion (m)

Slope = Slope of the cell (degrees)

Width t_{Cat} = Width of the cell (m)

The sea level is calculated at any time in the future by adding the 'local' sea level trend to the global projections of sea-level rise. In order the 'local' trend to be isolated, the global historic sea-level rise is subtracted from the local historic trend (equation 2.4) (Clough et al., 2010).

$$SLR_{TModel} = GlobalSLR_{TModel} + \frac{(Year_{TModel} - Year_{T0})(HistSLR_{Local} - HistSLR_{Global})}{1000} \quad (2.4)$$

where, SLR_{TModel} = Projected local sea level rise at current model year (m)

$GlobalSLR_{TModel}$ = Global average slr predicted in current model year (m)

$Year_{TModel}$ = Current model year

$Year_{T0}$ = Date when model started

$HistoricSLR_{Local}$ = Site specific historic trend of sea level rise (mm yr^{-1})

$HistoricSLR_{Global}$ = Global historic trend (IPCC, 2007)

1000 = unit conversion constant (mm m^{-1})

Also, the model can take into account spatially explicit land movements, if a spatial uplift or subsidence map is available (equation 2.5). In this approach the historic sea-level rise parameter is ignored (Clough et al., 2010).

$$SLR_{TModel} = GlobalSLR_{TModel} - \frac{(Year_{TModel} - Year_{T0})(Uplift_{cell})}{100} \quad (2.5)$$

where $Uplift_{cell}$ = Spatial map of land uplift (cm yr^{-1}).

SLAMM uses 1990 as a base year for all simulations, following the lead of IPCC sea-level rise scenarios. If the SLAMM start date is before 1990 then the local historic trend must be added to projected sea level rise:

$$SLR_{TModel} = SLR_{TModel} + \frac{(1990 - Year_{T0})(HistoricSLR_{Local})}{1000} \quad (2.6)$$

If the start date is after 1990 then the projected sea level rise from 1990 to the model start date must be subtracted from the projected global sea level rise:

$$SLR_{TModel} = SLR_{TModel} - GlobalSLR_{T0} \quad (2.7)$$

Finally, the relative sea-level rise is calculated from one time step to another using the following equation (Clough et al., 2010):

$$SLR = SLR_{TCurrent} - SLR_{TPrevious} \quad (2.8)$$

where SLR = Sea level rise since previous time step (m)

$SLR_{TCurrent}$ = Sea level rise projected at current model year (m)

$SLR_{TPrevious}$ = Sea level rise projected at previous time-step (m)

2.2.2 Accretion

Accretion process is a fundamental component of marsh stability under sea-level rise, since it can restore the marsh to a new equilibrium position in the tidal frame (French, 1993). SLAMM simulates the effect of sediment accretion within various classes of intertidal wetland. The simplest option allows the user to specify constant accretion rates for each wetland category. However, the accretion rate can also be allowed to vary as a function of other factors, such as elevation or the distance to channel (Letzch and Frey, 1980; Carling, 1982; Reed, 1988; Stoddart et al., 1989; French and Spencer, 1993; French et al., 1995; Bartholdy, 1997; Reed et al., 1999; Bartholdy, 2010a; 2012). In this case, accretion becomes a time-varying function of cell elevation, distance to channel and salinity, described by the equation 2.9. This equation can be specified individually for the dfferent wetland type.

$$A_{cell} = A_{elev} * (D * S) \quad (2.9)$$

where A_{cell} = predicted accretion rate for a cell (mm yr^{-1})

A_{elev} = accretion rate for a cell as a function of elevation

D = factor representing distance to river or tidal channel

S = salinity factor representing salinity effects (when accretion rates cannot be described based on the elevation and distance to channel)

2.2.3 Erosion

While marshes typically experience at least some degree of inundation due to sea-level rise, the marsh edges may also be eroded due to exposure to wave action, resulting to additional marsh loss (Pethick, 2001; Schwimmer, 2001; Moller, 2006). SLAMM includes the process of lateral erosion by assuming that it depends on the maximum

fetch, which is calculated at the beginning of each time-step on a cell-by-cell basis, and the proximity of the wetland to open ocean or estuarine water. A simple thresholding of erosion rates is used, informed by the work of Knutson et al. (1981). It is assumed that marsh edge erosion occurs when the maximum fetch exceeds 9 km, while erosion of the tidal/ocean flat is assumed to occur at all times (Table 2.1). This process applies only to cells adjacent to open water. The actual erosion rates are specified by the user as constant values, except in the case of the ocean beach for which it is calculated based on the Bruun Rule (equations 2.10, 2.11). The additional fraction lost due to erosion is determined according to equation 2.12 (Clough et al., 2010).

Table 2.1: Erosion based on the maximum fetch (Clough et al., 2010).

Max Fetch (km)	**Erosion**
<9	None
9-20	Heavy
>20	Severe (cell is exposed to open ocean)

$$Erosion_{category} = Recession - Distance \quad (2.10)$$

$$Recession = 100 * SLR \quad (2.11)$$

$$FracLost_{Cat} = \Delta T \left(\frac{Erosion_{category}}{Width_{Category}}\right) \quad (2.12)$$

where, $Erosion_{category}$ = Erosion in the current cell (m yr^{-1} or m for the ocean beach)

Recession = width of the lost beach during the specific time step (m)

Distance = Distance from the cell's front edge to open ocean (m)

$FracLost_{cat}$ = Additional fraction of wetland lost due to erosion (unitless)

$Width_{category}$ = Class width in the specific cell (m yr^{-1})

2.2.4 Overwash

The process of overwash is only simulated for beaches on an open coast. SLAMM suggests that this occurs on barrier beaches less than 500 m in width due to storms occurring on a frequency of 25 years. Based on observations in the USA, SLAMM suggests that 50% of the adjacent to the beach transitional marsh and salt marsh (and 25% of any mangrove) are converted to undeveloped dryland and beach respectively (Leatherman and Zaremba, 1986). Also it is suggested that estuarine beach within 500 m of the ocean beach migrates advancing by 60 m, while the ocean beach will recede by

30 m. However, the user may specify different values for each assumption. Any dryland adjacent to the ocean beach will convert to ocean beach (Clough et al., 2010).

2.2.5 Saturation

A rise in sea level forces a water table response at the coast, which may, in turn, cause freshwater wetlands to migrate onto adjacent uplands. If a dryland cell is within 6 km of the open ocean and if between them a 500 m width of freshwater wetland exists, SLAMM calculates the water table elevation for the dry land. If this is greater than the elevation of the dryland, saturation is assumed to take place and the dryland is converted to the nearest wetland type (Clough et al., 2010).

2.2.6 Salinity

In areas with significant freshwater flow, the type of the marsh is often more correlated to water salinity than elevation (Higinbotham et al., 2004), resulting in overlapping of their elevation ranges. Thus, SLAMM includes a simple salt wedge model to specify the wetland elevation ranges based on the water salinity, where the different fresh-water flows must be specified. SLAMM assumes that if fresh water wetlands and dry lands fall below the "salt boundary", they will be inundated by salt water. A connectivity model is also used in this point in order to determine the categories based on their connection to a saltwater source, and therefore their ability to be subjected to saline inundation (Clough et al., 2010).

2.2.7 Structures

Areas protected from inundation by flood defences may be defined via an input raster layer indicating the defended location and the area behind it as protected. When this layer is not available, these areas can be assigned as dryland into the initial land classification layer and assumed within SLAMM as protected by enabling the so-called 'Protection Scenario' (Figure 2.3a). Protected areas in both situations are not allowed to change during the course of a simulation.

Another approach can also be used if the defences are very well depicted into the DEM. In this case, the defences and the areas behind them are not assigned as protected, but they are subjected to inundation based on their connectivity to a saltwater source. This

connectivity is calculated by enabling the so-called connectivity algorithm (Figure 2.3b), and it can be used to also test the efficacy of the defences (Clough et al., 2010).

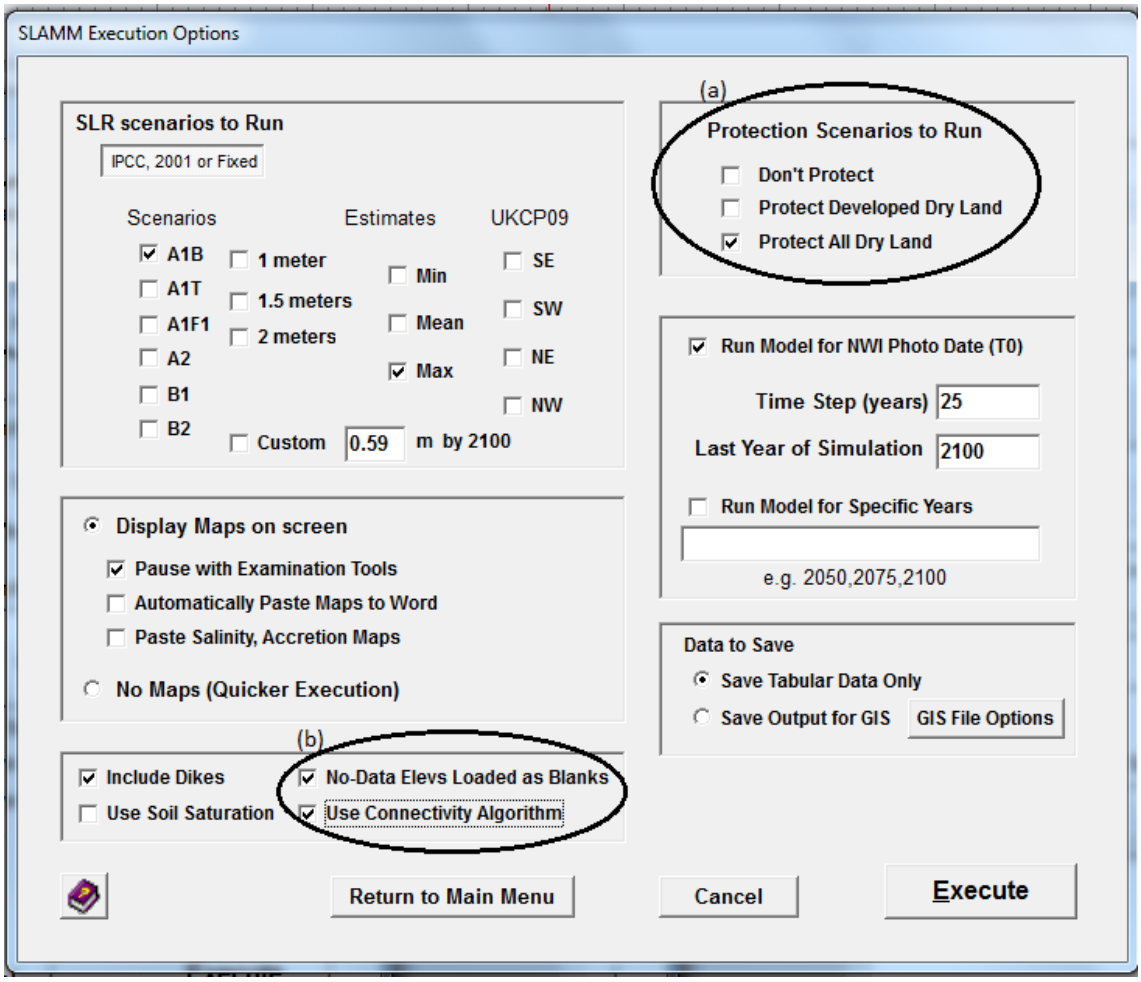

Figure 2.3: a) Protection scenarios and b) connectivity algorithm at the SLAMM execution table.

2.2.8 SLAMM data requirements and workflow

Arguably the most important data requirement is that of high vertical accuracy and high spatial resolution elevation data (Figure 2.4a). When only low-quality elevation data are available, a pre-processor can be used to 'correct' them by assigning elevations to each wetland category, based on known relationships between tidal ranges and wetland types, assuming that the wetland classification layer (e.g. Wetland maps as developed by the US National Wetlands Inventory (NWI); Figure 2.4b) is correct. Even where LiDAR data are used, an elevation analysis can optionally be run to determine if the DEM and classification layer are consistent with the rule base within SLAMM. If not, the wetland elevation range rules can be manually edited.

Although many LiDAR survey systems allow remote measurements of both topography and shallow bathymetry (e.g. SHOALS (Lillycrop and Banic, 1993; Lillycrop et al., 1993, 1994), LADS (Setter and Willlis, 1994; Nairn, 1994), Hawk eye (Koppari et al., 1994; Steinvall et al., 1994)), conventional topographic LiDAR systems cannot penetrate water bodies (Smart et al., 2009). In this case, the topographic DEM must be supplemented by separate bathymetric data to create a composite DEM with elevations expressed relative to MTL, as noted above. This DEM is then used to generate a slope map layer, used to calculate the fractional loss of a cell due to inundation, and a wetland classification layer, based on the elevation-dependence of habitat types as enclosed within SLAMM's rule base. Table 2.2 summarises the site specific parameters that must be defined by the user, either for the whole area or for specific sub-areas. Finally, the sea-level rise scenarios and the time-step must be specified (Figure 2.4).

Table 2.2: Site specific parameters used in SLAMM.

SITE-SPECIC PARAMETERS	
NWI Photo Date	(YYYY)
DEM Date	(YYYY)
Direction Offshore	[n,s,e,w]
Historic Trend	(mm y^{-1})
GT Great Diurnal Tide Range	(m)
Salt Elevation	(m above MTL)
Marsh Erosion	(m y^{-1})
Tidal Flat Erosion	(m y^{-1})
Regularly Flood Marsh Accrettion	(mm y^{-1})
Irregularly Flood Marsh Accrettion	(mm y^{-1})
Tidal Fresh Marsh Accrettion	(mm y^{-1})
Beach Sedimentation Rate	(mm y^{-1})
Use Elevation Pre-Processor	[TRUE, FALSE]

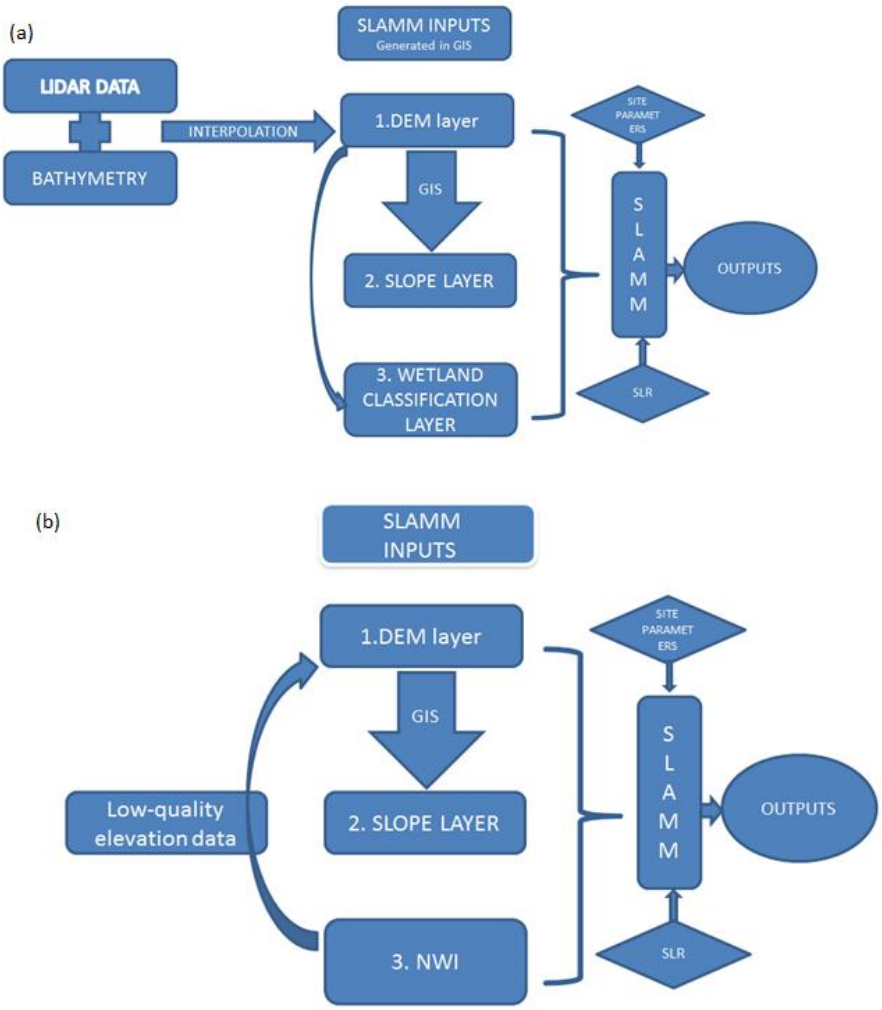

Figure 2.4: SLAMM workflow. a: where LiDAR data are available; b: where only low-quality elevation data and NWI wetland classification maps are available.

2.2.9 Climate Change Scenarios

SLAMM is pre-coded with the IPCC (2001) A1B, A1T, A1F1, A2, B1, B2, sea level scenarios, which are described in detail in the Special Report on Emissions Scenarios (Nakicenovic et al., 2000). More particularly, the minimum, mean or maximum estimate of each of the above scenarios can be used (Table 2.3; Clough et al., 2010). The A1 family is usually preferred because this assumes a rapid economic growth, a peak of global population in mid-century and a rapid introduction of new and more efficient technologies, and more specifically, A1B, which assumes that all sources will be balanced (Nakicenovic et al., 2000). SLAMM includes additional sea-level rise scenarios of total eustatic sea-level rise of 1, 1.5 or 2 m (Figure 2.5), produced by scaling up the A1B maximum scenario. Alternatively, other sea-level rise estimates for the 21st century can be specified by the user.

Table 2.3: Eustatic sea-level rise (mm) used as SLAMM inputs (Clough et al., 2010).

	A1B	A1T	A1F1	A2	B1	B2
Min						
2025	28	28	30	26	27	29
2050	63	66	64	58	52	56
2075	100	125	94	103	76	85
2100	129	182	111	155	92	114
Mean						
2025	76	82	76	75	76	79
2050	167	175	172	157	150	160
2075	279	278	323	277	233	255
2100	387	367	491	424	310	358
Max						
2025	128	128.5	137	127	128	134
2050	284	291	299	269	259	277
2075	485	553	491	478	413	451
2100	694	859	671	743	567	646

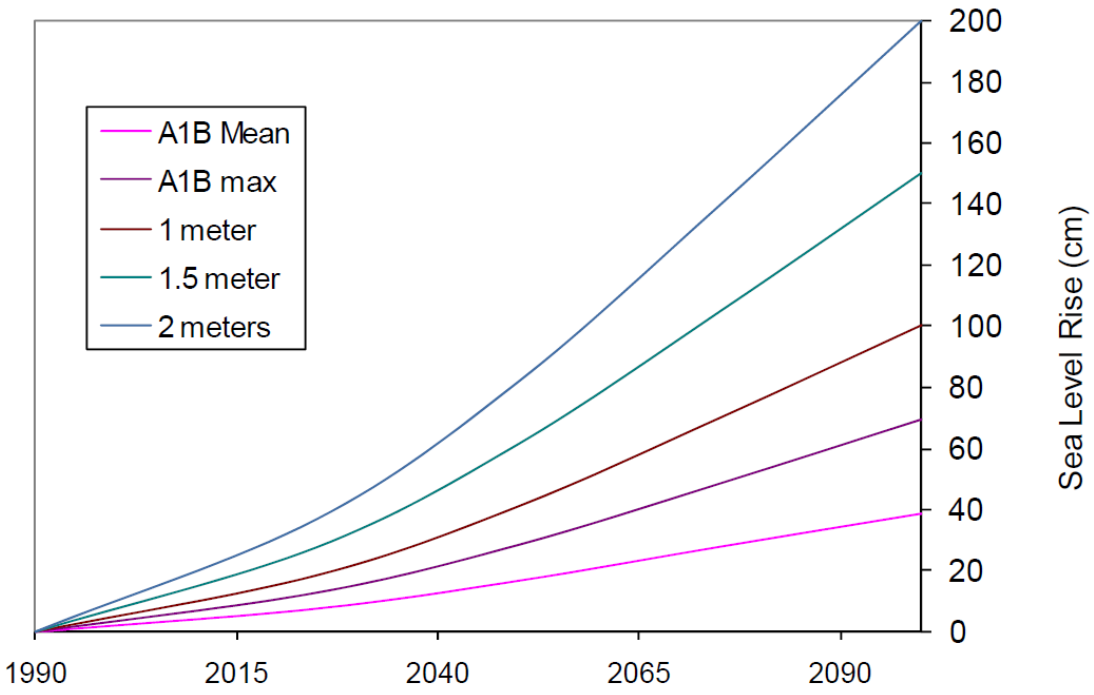

Figure 2.5: Scaling from A1B IPCC Scenario to the 1, 1.5 and 2 m scenarios (Clough et al., 2010).

2.3 SLAMM code modifications

2.3.1 Overview

SLAMM is written in Object Pascal and is open source software, distributed under a Common Public License. It is developed in Delphi 2007 and also requires the Delphi OpenGL libraries in order to be compiled. Its architecture is slightly unconventional in that the land cover classification is hard coded in accordance with the US National Wetland Inventory (NWI) scheme, which is not widely used elsewhere. Moreover, the forcing scenarios and various aspects of the sub-model parameterisations are also embedded in the source code rather than being read from external files. This means that source code alterations and re-compilation are required for application to sites outside North America. Accordingly, the first task undertaken in the present work is to modify the SLAMM source code to include a simplified land cover classification based on categories more suited to UK coastal and estuarine contexts. Also required, are a set of modified habitat transition rules and amended rules specifying their relation to the tidal frame. Support for UK-specific regional sea-level rise scenarios is also needed.

2.3.2 Implementation of a simplified habitat classification

SLAMM uses 25 wetland categories that follow the US National Wetland Inventory (NWI) but these are not readily transferable to the UK. Accordingly, this study is guided by a simple set of wetland categories defined by the INTERREG funded BRANCH project (BRANCH partnership, 2007) in the direction of promoting the use of spatial planning to help EU biodiversity to adapt to climate change. The "crosswalk" between these two classification systems is summarised in Table 2.4.

Table 2.4: Crosswalk between the UK and NWI wetland categories.

	SLAMM code	NWI Classes	UK Coastal Habitats (BRANCH, 2007)	Modified SLAMM Categories
Estuary Model	1	Dev. dry land	10. Land	1. Dry Land
	7	Trans.marsh	5.Transitional marsh	7. Trans.Marsh
	20	Irr. Fl. marsh	4. Upper marsh	20. Upper Marsh
	8	Reg.fl. marsh	3. Pioneer saltmarsh	8. Lower Marsh
	11	Tidal flat	2.Mudflat	11. Tidal Flat
	17	Estuarine water	1.Standing water	17. Est. subtidal
Coastal model	12	Ocean Beach		12. Ocean beach
	13	Ocean flat	Use of Leatherman	13. Ocean flat
	19	Open ocean	(2001) equation in GIS	19. Open ocean

2.3.3 Modification of habitat transition rules

Conversion of one wetland category to another occurs in response to either inundation or erosion. As described in section 2.2.3, erosion depends on the maximum fetch and the proximity of the wetland to the open ocean or the estuarine water, while the critical parameter that defines when a wetland category is inundated and therefore converted to another wetland category is its minimum elevation. The maximum elevation of each wetland category is only used when the Elevation Pre-Processor is utilised, in order to assign wetland elevation on the basis of wetland type, tide range and direction offshore, when LiDAR data are not available (Clough and Larson, 2010). All these transition rules are described on Table 2.5, and compared to the UK rules on Figure 2.6. In order to adapt the code to the UK, the decision tree is modified by assuming that the transitional marsh converts to upper marsh instead of lower marsh due to inundation, and the dryland to transitional marsh instead of estuarine beach when it is adjacent to the subtidal (Figure A-0.1 in Appendix).

Table 2.5: SLAMM decision tree (Clough et al., 2010).

Converting from	Inundation - Converts to	Erosion -Converts to
Dry Land	Transitional Marsh	Ignored
	Ocean Beach (if adj to ocean water)	
	Estuarine beach (if adj to water-erosion>heavy*)	
Trans.Marsh	Lower Marsh	Tidal Flat
Upper Marsh	Lower Marsh	Tidal Flat
Lower Marsh	Tidal Flat	Tidal Flat
Tidal Flat/Beach	Estuarine Subtidal	Est. Subtidal
Oc. Flat/Beach	Open Ocean	Open Ocean

*heavy erosion when maximum fetch > 9km (see table 2.1)

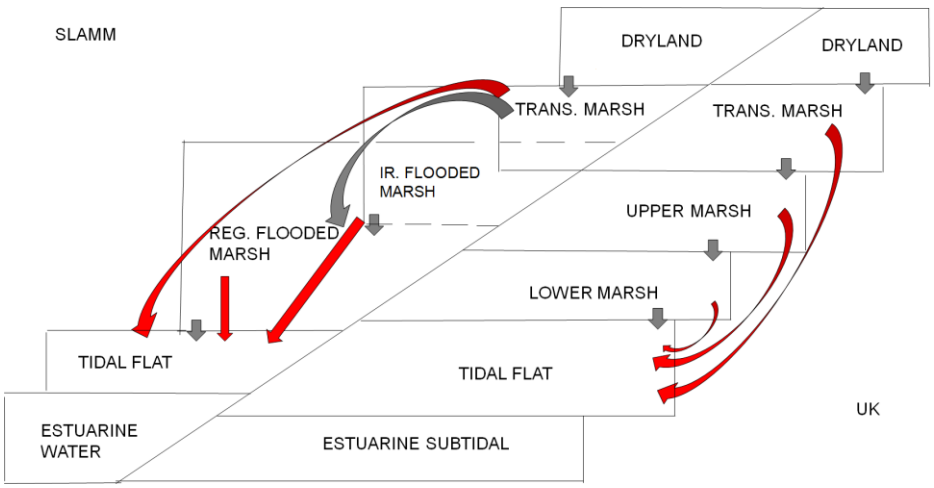

Figure 2.6: SLAMM decision tree modification (grey arrows: inundation; red arrows: erosion).

2.3.4 Adjustment of Habitat Elevation Ranges

In the original SLAMM code, the default elevation ranges of each wetland category are defined in the Elevation Inputs and Analysis Table as a function of the Salt Elevation, the Half Tide Unit (HTU) and the Mean Tide Level (MTL) (Table 2.6). The Salt elevation is that which is inundated by water once per month. This effectively defines the location where the dry land and the fresh water wetland begin. The Half Tide Unit (HTU) is defined from equation 2.13 (Clough and Larson, 2010), while the MTL is assumed to remain constant at zero. So, the HTU is equal to MHHW, which together with the MLLW are defined in the code from equations 2.14 and 2.15.

$$HTU = MHHW - MTL \quad (2.13)$$

$$MHHW = GtideRange / 2 \quad (2.14)$$

$$MLLW = MTL - GtideRange/2 \quad (2.15)$$

Table 2.6: SLAMM default elevation ranges.

SLAMM category No	Category Name	Default Min. Elev.	Default Max. Elev.
1	DryLand	1 Salt Elevation	
7	Transitional Marsh	1 HTU	1 Salt Elevation
20	Upper Marsh	0.5 HTU	1 Salt Elevation
8	Lower Marsh	0 HTU	1.2 HTU
11	Tidal Flat	-1 HTU	MTL
17	Estuarine Subtidal	0	0
12	Ocean Beach	-1 HTU	1 Salt Elevation
13	Ocean Flat	-1 HTU	MTL
19	Open Ocean	0	0

Although these could be useful for a secondary determination of tidal datum when primary data are not available (e.g. NOAA, 2000), they will likely vary from area to area. Thus, the modified code determines the position of each intertidal habitat according to their position in the tidal frame (Table 2.7; Figure 2.7), as used in the BRANCH project (after Chapman, 1960; Pye and French, 1993; Leggett and Dixon, 1994; Blott and Pye, 2004). Firstly, the tidal range parameters are added at the '*Site Parameter Table*' as required input values (see Figures A-0.2 to A-0.10 in Appendix) and their values are linked to the default wetland elevation boundaries at the '*Elevation Input and Analysis Table'* (see Figures A-0.11 to A-0.16 in Appendix). Thus, in each simulation the user defines the tidal range in the '*Site Parameter Table*', and SLAMM automatically updates the elevation of each wetland category at the '*Elevation Input and Analysis Table'*, adapting it to each specific area.

Table 2.7: UK default elevation ranges according to tidal ranges (BRANCH partnership, 2007).

	SLAMM category No	Category Name	Default Min. Elev.	Default Max. Elev.
Estuarine Habitats	1	DryLand	HAT	
	7	Transitional Marsh	MHWS	HAT
	20	Upper Marsh	MHW	MHWS
	8	Lower Marsh	MHWN	MHW
	11	Tidal Flat	LAT	MHWN
	17	Estuarine Subtidal		LAT
Open Ocean Habitats	12	Ocean Beach	LAT	HAT
	13	Ocean Flat	LAT	HAT
	19	Open Ocean		LAT

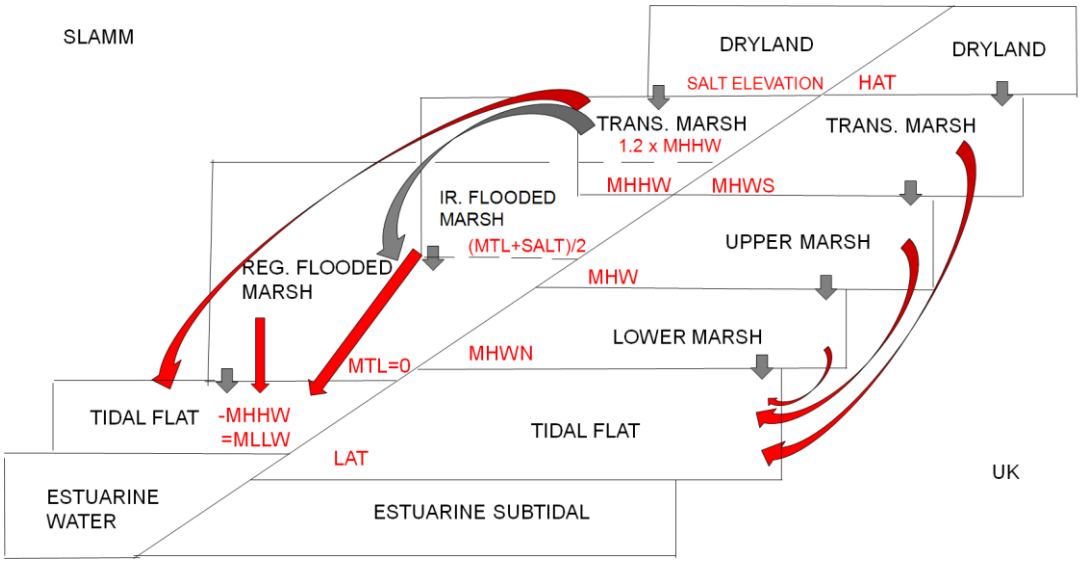

Figure 2.7: SLAMM decision tree modification, including tidal ranges (grey arrows: inundation; red arrows: erosion).

2.3.5 Addition of UK-specific sea level scenarios

The UKCP09 sea-level scenarios are incorporated into the modified SLAMM code (Table 2.8; Figure 2.8). These are based on the IPCC Fourth Assessment Report (IPCC, 2007), and assume that the rates of vertical land movement remain constant over the 21st century. Land movement uncertainty is neglected because this is likely to be small in comparison to the eustatic sea-level rise estimates (UKCP, 2009). These new scenario options were added to the SLAMM user interface (as illustrated in Figure 2.9). Accordingly, the mean sea-level trend is defined as required by the user parameter (1.7 mm yr^{-1} for the IPCC scenarios (IPCC, 2007), 1.4 mm yr^{-1} for the UK (Woodworth et al., 2009; Wahls et al., 2013)) (see Figures A-0.17 to A-0.26; update A-0.2 to A-0.4 and A-0.6 to A-0.10).

Table 2.8: SLAMM inputs based on UKCP09 sea-level rise scenarios (mm).

UKCP09 sea-level rise scenarios (mm)												
	LONDON (SE)			CARDIFF (SW)			EDINBURGH (NE)			BELFAST (NW)		
	H	M	L	H	M	L	H	M	L	H	M	L
2025	137.5	116	98	137	115.5	98	91	69.5	52	94.5	73	66
2050	258	218	184	259	218	184	180	139	105	186	145	111
2075	402.5	337.5	284	402	336.5	284	303.5	225	171.5	298.5	233.5	180.5
2100	565	472	396	565	472	396	419	326	250	430	338	262

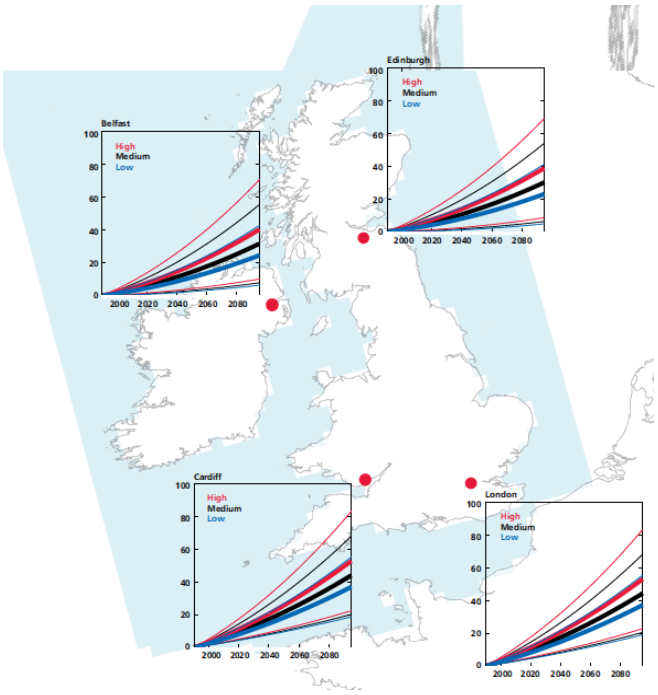

Figure 2.8: UKCP09 relative sea-level rise relative to 1990. Thick lines represent the central estimate values and thin lines the 5th and 95th percentile limits of the ranges of uncertainty.

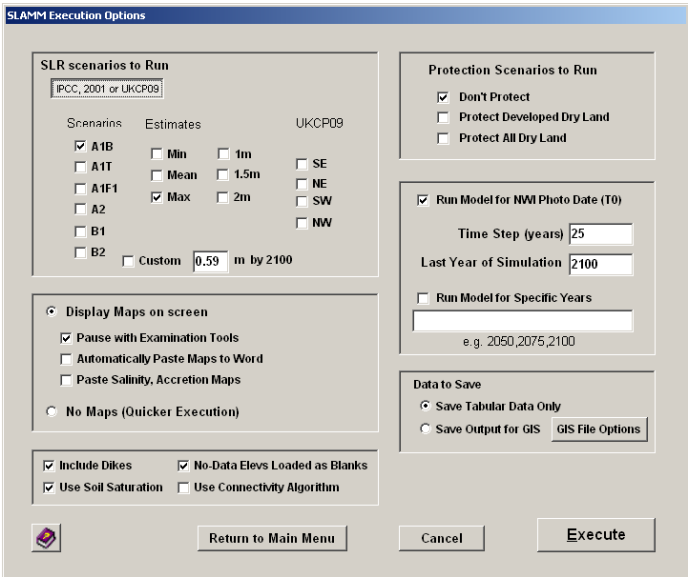

Figure 2.9: The execution dialogue in the modified code.

2.4 Benchmarking the modified code

In order to ensure that the code is not broken by the modifications made, and given that the code is too complicated to be logically tested, benchmarking is necessary. To this end, at each modification step of the code, the output was evaluated against that from the original code with reference to an idealised domain of simple geometry. An idealised coastal terrain created in MATLAB (Figure 2.10) was used to generate the required input DEM (Figure 2.11) and slope layers (as described in section 2.2.8); the slope layer is clearly constant here. The wetland classification layer (Figure 2.12 for the estuarine model, Figure 2.13 for the open ocean model), is based on the position of the wetlands into the tidal range (Table 2.9).

```
>> %Create idealised coastal terrain for testing of modified
SLAMM code
% Feb 2012
%output filename
demfile = 'test_elev1.txt';

%terrain dimensions
ncols = 824;
nrows = 633;
xllcorner = 440372.47353308;
yllcorner = 89784.80516105;
cellsize = 5;
NODATA_value = -9999;

%vertical frame
min_subtidal = -5;
dry_land = 5;

%make sloping profile for DEM
profile = linspace(min_subtidal,dry_land,nrows);

%write DEM file in SLAMM format
fid = fopen(demfile,'w');
fprintf(fid,['ncols         ' num2str(ncols) '\n']);
fprintf(fid,['nrows         ' num2str(nrows) '\n']);
fprintf(fid,['xllcorner     ' num2str(xllcorner) '\n']);
fprintf(fid,['yllcorner     ' num2str(yllcorner) '\n']);
fprintf(fid,['cellsize      ' num2str(cellsize) '\n']);
fprintf(fid,['NODATA_value  ' num2str(NODATA_value) '\n']);
for i = 1:nrows
 for j = 1:ncols
  fprintf(fid,'%8.5f  ',profile(i));
 end
 fprintf(fid,'\n');
end
fclose(fid);
```

Figure 2.10: MATLAB script to create an idealised coastal terrain in ASCII grid format.

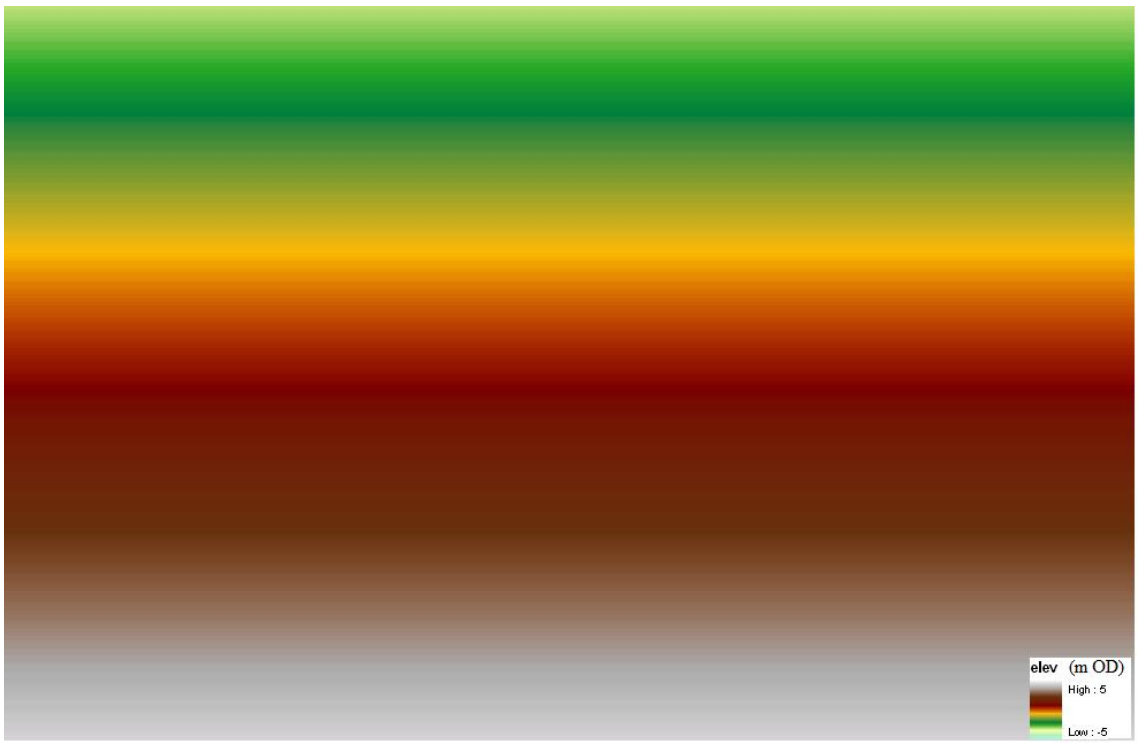

Figure 2.11: The elevation input layer of the idealised coastal terrain.

Table 2.9: Criteria for defining habitat position in the estuary and open ocean model (note that numerical values here are purely for illustrative purposes).

Coastal Habitats in the Estuary Model	**Coastal Habitats in the Open Ocean Model**	**Criteria for defining habitat position based on elevation and tidal level**	
Dry Land	DryLand	>HAT	>1.9
Transitional marsh		MHWS-HAT	1.5-1.9
Upper marsh	Ocean Beach	MHW-MHWS	1.15-1.5
Lower marsh	Ocean Flat	MHWN-MHW	0.8-1.15
Tidal Flat		LAT-MHWN	(-2.6)-0.8
Estuarine Subtidal	Open Ocean	<LAT	<(-2.6)

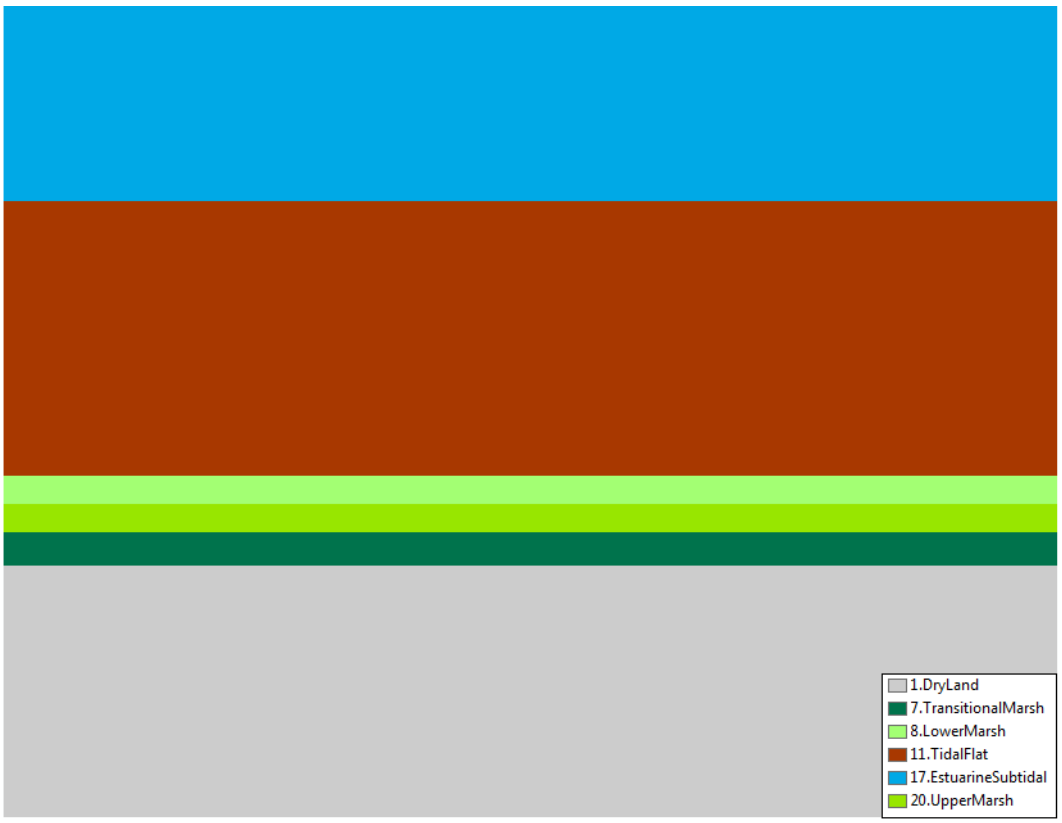

Figure 2.12: The estuarine model layer.

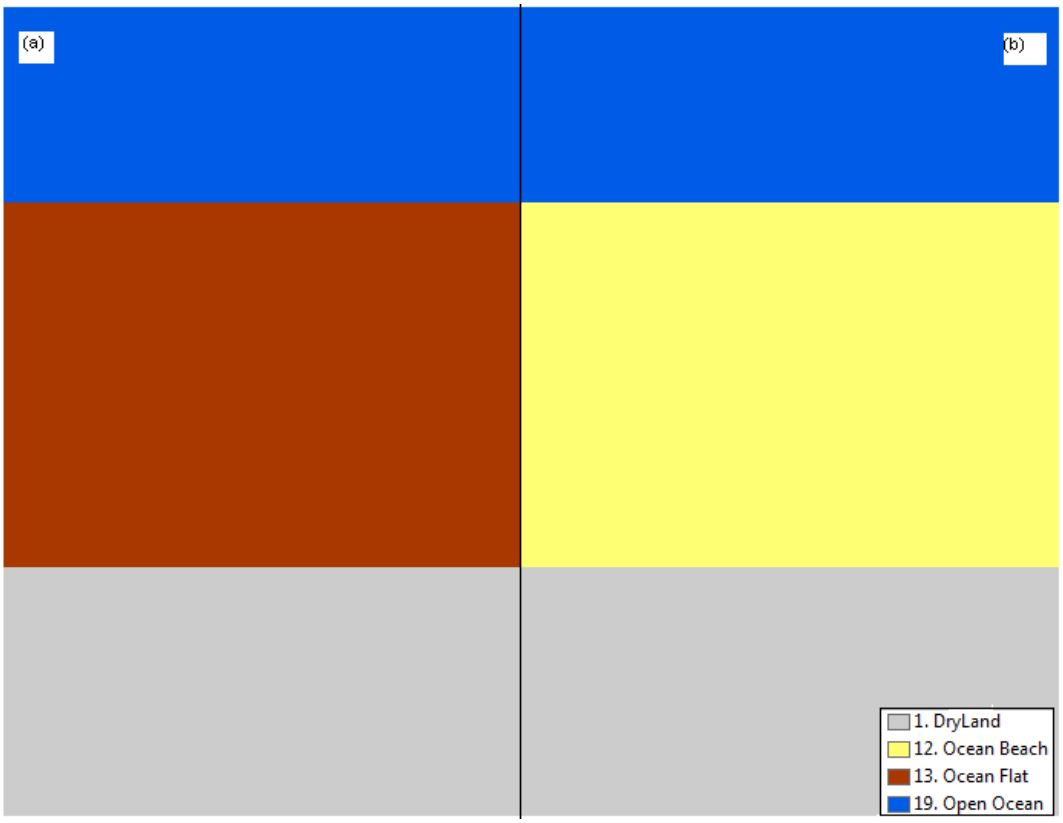

Figure 2.13: The Open Ocean model layer for (a) muddy and (b) sandy environments.

Before each simulation, the site parameters (Table 2.10) are defined, where more parameters are required in the modified code in order to describe an area, due to the third modification step. Accordingly, the wetland boundary conditions are automatically updated within the modified code, while they must be manually adjusted within the original code. The simulations are executed under the A1B max IPCC sea-level rise scenario within a time-step of 25 years.

Table 2.10: Site Parameters Table (note that numerical values are purely for illustrative purposes).

ORIGINAL SLAMM CODE	**MODIFIED SLAMM CODE**	
Historic Trend (mm yr^{-1})	Historic Trend (mm yr^{-1})	1.5
GT Great Diurnal Tide Range (m)	GT Great Diurnal Tide Range (m)	3.4
Salt Elevation (m above MTL)	Salt Elevation (m above MTL)	1.9
	HAT (m)	1.9
	MHWS (m)	1.5
	MHW (m)	1.15
	MHWN (m)	0.8
	LAT (m)	-2.6
Marsh Erosion (m yr^{-1})	Marsh Erosion (m yr^{-1})	0.25
T.Flat Erosion (m yr^{-1})	T.Flat Erosion (m yr^{-1})	0.2
Reg. Flood Marsh Accr (mm yr^{-1})	Lower Marsh Accr (mm yr^{-1})	2.0
Irreg. Flood Marsh Accr (mm yr^{-1})	Upper Marsh Accr (mm yr^{-1})	1.8
Tidal Fresh Marsh Accr(mm yr^{-1})	Tidal Fresh Marsh Accr(mm yr^{-1})	-
Beach Sed.Rate (mm yr^{-1})	Beach Sed.Rate (mm yr^{-1})	2.0

Firstly, the modified code is benchmarked within the estuarine environment. The first step ("TM1") simply adopts the UK-based wetland classification; the fact that no quantitative changes in overall intertidal areas are predicted confirms that this modification has no adverse effect on the model algorithm. Thus, this code is then used to benchmark the next step with the modified transition rules ("TM2"), where different projected areas are generated for the lower and upper marsh category without affecting the behaviour of the other ones (Table 2.11; Figure 2.14).

Table 2.11: Benchmarking the code for the estuarine sub-environments.

Simulation: "T0" (original)							
Date	**SLR**	**v. Dry La**	**Trans. M.**	**Reg. Fl. Marsh**	**Tidal Flat**	**Est. Op. W.**	**Irr. Fl M.**
0	0	356.3	51.9	43.8	428.2	280.7	43.9
2008	0	356.3	51.3	44.7	427.9	281.1	43.5
2025	0.06	349.7	54.3	48.6	427.9	284.2	40.0
2050	0.22	330.7	60.0	62.6	427.9	296.8	26.7
2075	0.42	306.1	65.6	82.2	428.0	315.1	7.8
2100	0.63	280.4	61.8	99.1	429.1	334.5	0.0
Simulation:"TM1" (1st step)							
Date	**SLR**	**Dry Land**	**Trans. M.**	**Lower Marsh**	**Tidal Flat**	**Est. Subtidal**	**Upper M.**
0	0	356.3	51.9	43.8	428.2	280.7	43.9
2008	0	356.3	51.3	44.7	427.9	281.1	43.5
2025	0.06	349.7	54.3	48.6	427.9	284.2	40.0
2050	0.22	330.7	60.0	62.6	427.9	296.8	26.7
2075	0.42	306.1	65.6	82.2	428.0	315.1	7.8
2100	0.63	280.4	61.8	99.1	429.1	334.5	0.0
Simulation: "TM2" (2nd step)							
Date	**SLR**	**Dry Land**	**Trans. M.**	**Lower Marsh**	**Tidal Flat**	**Est. Subtidal**	**Upper M.**
0	0	356.3	51.9	43.8	428.2	280.7	43.9
2008	0	356.3	51.3	44.1	427.9	281.1	44.1
2025	0.06	349.7	54.3	44.5	427.9	284.2	44.1
2050	0.22	330.7	60.0	45.1	427.9	296.8	44.1
2075	0.42	306.1	65.6	45.8	428.0	315.1	44.1
2100	0.63	280.4	61.8	45.4	429.1	334.5	53.7
compare "T0" to "TM1"							
TRUE	TRUE	TRUE	TRUE	TRUE	TRUE	TRUE	TRUE
TRUE	TRUE	TRUE	TRUE	TRUE	TRUE	TRUE	TRUE
TRUE	TRUE	TRUE	TRUE	TRUE	TRUE	TRUE	TRUE
TRUE	TRUE	TRUE	TRUE	TRUE	TRUE	TRUE	TRUE
TRUE	TRUE	TRUE	TRUE	TRUE	TRUE	TRUE	TRUE
TRUE	TRUE	TRUE	TRUE	TRUE	TRUE	TRUE	TRUE
compare "TM1" to "TM2"							
TRUE	TRUE	TRUE	TRUE	TRUE	TRUE	TRUE	TRUE
TRUE	TRUE	TRUE	TRUE	**FALSE**	TRUE	TRUE	**FALSE**
TRUE	TRUE	TRUE	TRUE	**FALSE**	TRUE	TRUE	**FALSE**
TRUE	TRUE	TRUE	TRUE	**FALSE**	TRUE	TRUE	**FALSE**
TRUE	TRUE	TRUE	TRUE	**FALSE**	TRUE	TRUE	**FALSE**
TRUE	TRUE	TRUE	TRUE	**FALSE**	TRUE	TRUE	**FALSE**

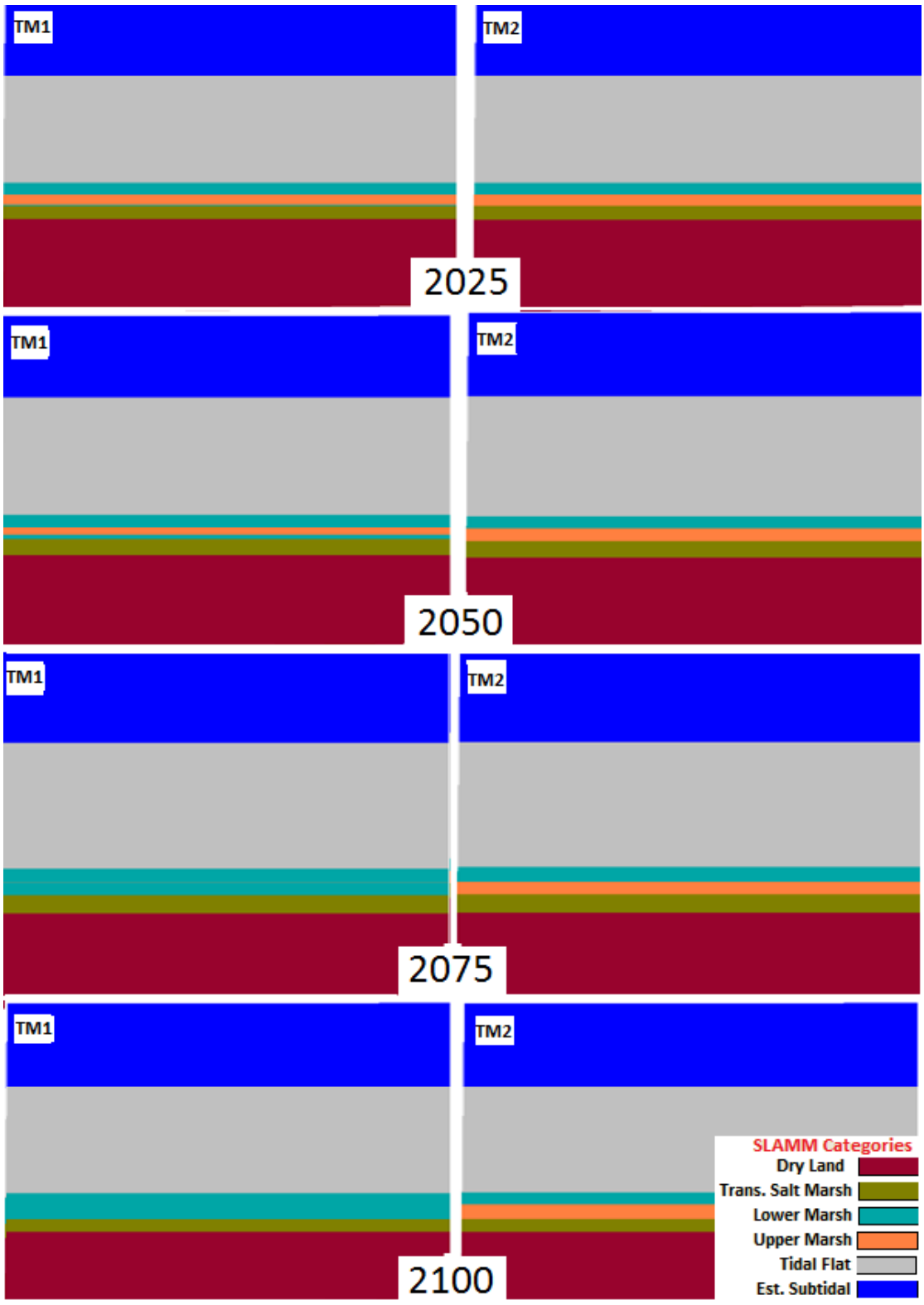

Figure 2.14: Benchmark the 2nd modification step (TM1: 1st step; TM2: 2nd step).

This change was expected, but further investigation is required in order to ensure that nothing else is affected. Table 2.12 summarises the habitat conversion rules in each time-step. Although, the conversion rule for the transitional marsh is modified and converted to upper marsh instead of lower marsh, the amount of area converted is not

affected, as desired. This modification results in a more dynamic behaviour of the upper marsh by assuming that this habitat also migrates upland to transitional marsh; in the original SLAMM code it is assumed that it only loses area to lower marsh, giving rise to a continual decrease in the area of this habitat. These changes means that, in the test case, 20ha of upper marsh are inundated at the last time-step when using the modified code while only 8ha according to the original one.

Table 2.12: Habitat conversion rules in each simulation (TM1: 1st step, TM2 :2nd step).

Simulation: "TM1"

	DRYLAND	TRANS.M.	UPPER	LOWER	TIDAL F.	ES.SUBTIDAL
0-2008	0	-0.60	-0.36	0.84	-0.24	0.36
		0.60	**0.96**	**0.12**	**0.36**	
2008-2025	-6.54	3.02	-3.52	3.95	0.01	3.08
	6.54	**3.52**	**7.04**	**3.09**	**3.08**	
2025-2050	-18.99	5.67	-13.32	13.96	0.02	12.66
	18.99	**13.32**	**26.64**	**12.67**	**12.66**	
2050-2075	-24.60	5.67	-18.93	19.59	0.02	18.25
	24.60	**18.93**	**37.86**	**18.28**	**18.25**	
2075-2100	-25.74	-3.86	-7.76	16.88	1.09	19.39
	25.74	**29.60**	**37.36**	**20.47**	**19.39**	

Simulation: "TM2"

	DRYLAND	TRANS.M.	UPPER	LOWER	TIDAL F.	ES.SUBTIDAL
0-2008	0	-0.60	0.24	0.24	-0.24	0.36
		0.60	0.36	0.12	0.36	
2008-2025	-6.54	3.02	0.00	0.43	0.01	3.08
	6.54	**3.52**	**3.52**	**3.09**	**3.08**	
2025-2050	-18.99	5.67	0.00	0.64	0.02	12.66
	18.99	**13.32**	**13.32**	**12.67**	**12.66**	
2050-2075	-24.60	5.67	0.00	0.66	0.02	18.25
	24.60	**18.93**	**18.93**	**18.28**	**18.25**	
2075-2100	-25.74	-3.86	9.53	-0.41	1.09	19.39
	25.74	**29.60**	**20.06**	**20.47**	**19.39**	

	DRYLAND	TRANS.M.	UPPER	LOWER	TIDAL F.	ES.SUBTIDAL
0-2008	TRUE	TRUE	**FALSE**	**FALSE**	TRUE	TRUE
	TRUE	TRUE	**FALSE**	TRUE	TRUE	
2008-2025	TRUE	TRUE	**FALSE**	**FALSE**	TRUE	TRUE
	TRUE	TRUE	**FALSE**	TRUE	TRUE	
2025-2050	TRUE	TRUE	**FALSE**	**FALSE**	TRUE	TRUE
	TRUE	TRUE	**FALSE**	TRUE	TRUE	
2050-2075	TRUE	TRUE	**FALSE**	**FALSE**	TRUE	TRUE
	TRUE	TRUE	**FALSE**	TRUE	TRUE	
2075-2100	TRUE	TRUE	**FALSE**	**FALSE**	TRUE	TRUE
	TRUE	TRUE	**FALSE**	TRUE	TRUE	

The modified code is also benchmarked for the open coast sub-environments that are presented in SLAMM. Since the first modification step does not affect directly the coastal model, its benchmarking is ignored but used to investigate the response of each coastal category to the sea-level rise, by recognising two different cases depending on the context of the shore; a sandy ("TM1o_beach") and a muddy ("TM1o_flat") shore (Table 2.13; Figure 2.15). The muddy tidal flat is more capable to cope with the sea-

level rise, while most of the sandy beach is lost to the ocean according to the Bruun rule. In addition, although the muddy environment presents the same transition rules to the estuarine one, a more complex behaviour is presented on the sandy environment, due to the different responses of the dryland to sea-level rise based on its proximity to the open ocean (see Table 2.5). Thus, at the beginning of the simulation, inundated dryland is converted to transitional marsh, since it is not close to the ocean, while most of the ocean beach is eroded. Thus, the area of the open ocean is dramatically increased considering the dryland adjacent to the ocean at the last time-steps. At these time-steps dryland is inundated to ocean beach. Finally, it is worth mentioning here that although the criteria for the procedure of erosion are not met (actual maximum fetch <9 km), transitional marsh is eroded to tidal flat at year 2075. This is explained by the fact that the fetch is assumed as infinite at locations where open water persists to the edge of the study area (SLAMM forum).

Table 2.13: Open coast sub-environment model behaviour (1st modification step for (a) sandy and (b) muddy shore).

(a) Simulation "TM1o_beach"

Date	SLR	DRYLAND	TRANS.	UPPER	LOWER	T. FLAT	ES. SUBT.	OC.BEACH	OC.FLAT	OP.OCEAN
0	0	356.3	0	0	0	0	0	567.8	0	280.7
2008	0	356.3	0	0	0	0	0	567.4	0	281.1
2025	0.0622	349.7	6.5	0	0	0	0	467.7	0	380.8
2050	0.2182	330.7	25.5	0	0	0	0	0.0	0	848.5
2075	0.4187	306.1	23.5	0	0	2.0	0	16.4	0	856.7
2100	0.6282	280.4	11.4	0	12.1	0.0	2.0	15.9	0	883.0
	0-2008	0	0	0	0	0	0	-0.4	0	0.4
	2008-2025	-6.5	6.5	0	0	0	0	-99.7	0	99.7
	2025-2050	-19.0	19.0	0	0	0	0	-467.7	0	467.7
	2050-2075	-24.6	-2.0	0	0	2	0	16.4	0	8.2
						24.6			8.2	
	2075-2100	-25.7	-12.1	0	12.1	-2	2	-0.6	0	26.3
						25.7			26.3	

(b) Simulation "TM1o_flat"

Date	SLR	DRYLAND	TRANS.	UPPER	LOWER	T. FLAT	ES. SUBT.	OC.BEACH	OC.FLAT	OP.OCEAN
0	0	356.3	0	0	0	0	0	0	567.8	280.7
2008	0	356.3	0	0	0	0	0	0	567.4	281.1
2025	0.0622	349.7	6.5	0	0	0	0	0	564.3	284.2
2050	0.2182	330.7	25.5	0	0	0	0	0	551.7	296.8
2075	0.4187	306.1	50.1	0	0	0	0	0	533.4	315.1
2100	0.6282	280.4	61.8	0	14.1	0	0	0	514.0	334.5
	0-2008	0	0	0	0	0	0	0	-0.4	0.4
	2008-2025	-6.5	6.5	0	0	0	0	0	-3.1	3.1
	2025-2050	-19.0	19.0	0	0	0	0	0	-12.7	12.7
	2050-2075	-24.6	24.6	0	0	0	0	0	-18.3	18.3
	2075-2100	-25.7	11.6	0	14.1	0	0	0	-19.4	19.4
			25.7		14.1					

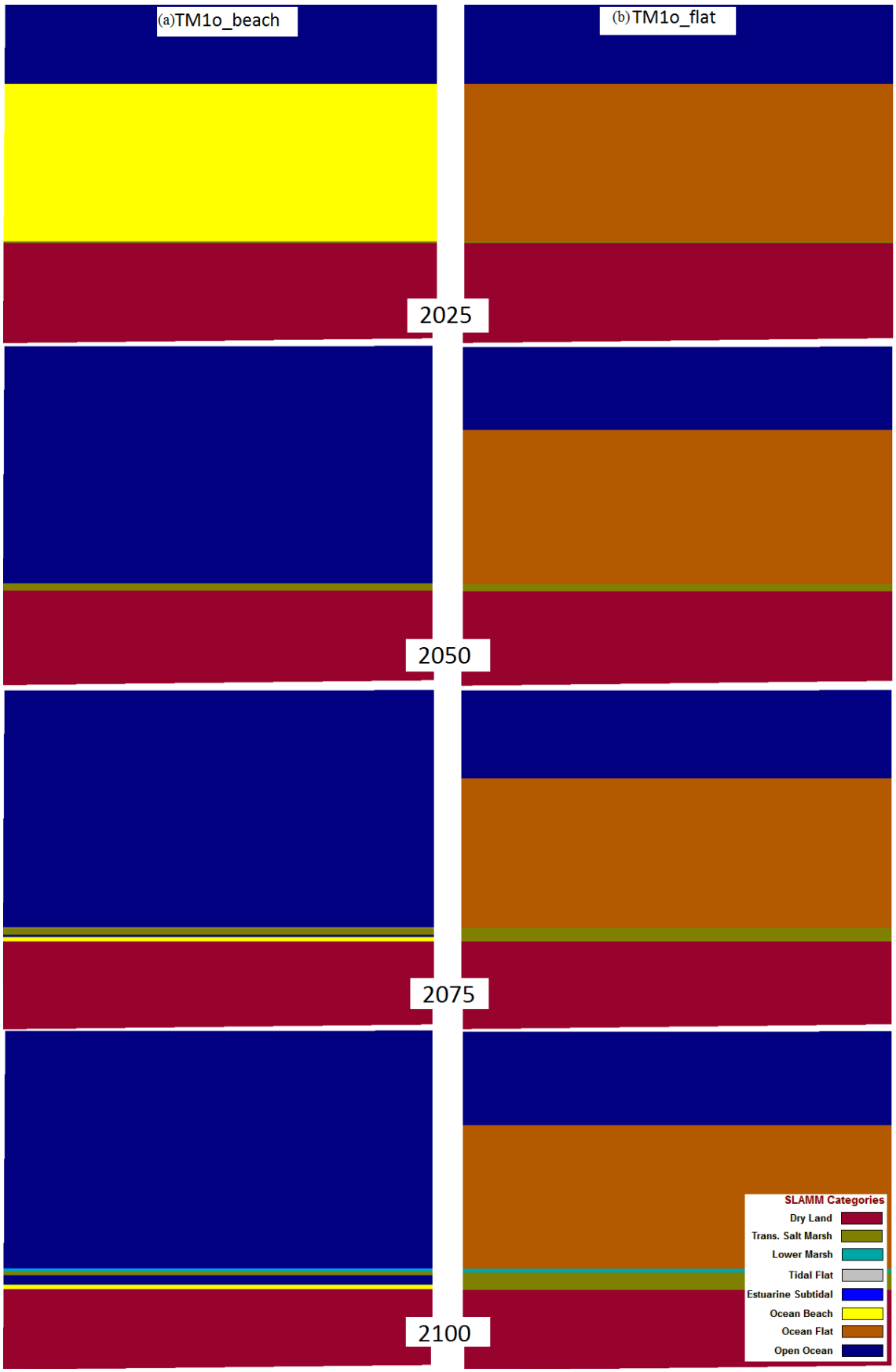

Figure 2.15: Different responses of the ocean environment (a: sandy shore, b: muddy shore) to sea-level rise.

Due to the appearance of marsh in both simulations, the second modification step needs to be benchmarked for each case ("TM2o_beach", "TM2o_flat" in Table 2.14). Different results are generated only at the last time-step of both simulations, where inundation of transitional marsh occurs. Similarly to the estuarine environment, transitional marsh is inundated to upper marsh instead of lower marsh, but the inundated area is the same, indicating that this conversion rule is applied correctly to the coastal model too. Consequently, the overall benchmarking of the code can be judged to have been successful, and therefore the modified code can be applied with confidence to other UK estuarine environments.

Table 2.14: Benchmark the 2nd modification step in the ocean model for a (a) sandy shore and a (b) muddy shore.

(a) Simulation "TM1o_beach" (1st modification step)

Date	SLR	DRYLAND	TRANS.	UPPER	LOWER	T. FLAT	ES. SUBT.	OC.BEACH	OC.FLAT	OP.OCEAN
0	0	356.3	0	0	0	0	0	567.8	0	280.7
2008	0	356.3	0	0	0	0	0	567.4	0	281.1
2025	0.0622	349.7	6.5	0	0	0	0	467.7	0	380.8
2050	0.2182	330.7	25.5	0	0	0	0	0.0	0	848.5
2075	0.4187	306.1	23.5	0	0	2	0	16.4	0	856.7
2100	0.6282	280.4	11.4	0	**12.1**	0	2	15.9	0	883.0

Simulation "TM2o_beach" (2nd modification step)

Date	SLR	DRYLAND	TRANS.	UPPER	LOWER	T. FLAT	ES. SUBT.	OC.BEACH	OC.FLAT	OP.OCEAN
0	0	356.3	0	0	0	0	0	567.8	0	280.7
2008	0	356.3	0	0	0	0	0	567.4	0	281.1
2025	0.0622	349.7	6.5	0	0	0	0	467.7	0	380.8
2050	0.2182	330.7	25.5	0	0	0	0	0.0	0	848.5
2075	0.4187	306.1	23.5	0	0	2	0	16.4	0	856.7
2100	0.6282	280.4	11.4	**12.1**	0	0	2	15.9	0	883.0

(b) Simulation "TM1o_flat" (1st modification step)

Date	SLR	DRYLAND	TRANS.	UPPER	LOWER	T. FLAT	ES. SUBT.	OC.BEACH	OC.FLAT	OP.OCEAN
0	0	356.3	0	0	0	0	0	0	567.8	280.7
2008	0	356.3	0	0	0	0	0	0	567.4	281.1
2025	0.0622	349.7	6.5	0	0	0	0	0	564.3	284.2
2050	0.2182	330.7	25.5	0	0	0	0	0	551.7	296.8
2075	0.4187	306.1	50.1	0	0	0	0	0	533.4	315.1
2100	0.6282	280.4	61.8	0	14.1	0	0	0	514.0	334.5

Simulation "TM2o_flat" (2nd modification step)

Date	SLR	DRYLAND	TRANS.	UPPER	LOWER	T. FLAT	ES. SUBT.	OC.BEACH	OC.FLAT	OP.OCEAN
0	0	356.3	0	0	0	0	0	0	567.8	280.7
2008	0	356.3	0	0	0	0	0	0	567.4	281.1
2025	0.0622	349.7	6.5	0	0	0	0	0	564.3	284.2
2050	0.2182	330.7	25.5	0	0	0	0	0	551.7	296.8
2075	0.4187	306.1	50.1	0	0	0	0	0	533.4	315.1
2100	0.6282	280.4	61.8	14.1	0	0	0	0	514.0	334.5

2.5 Model application and evaluation

2.5.1. Newtown Estuary, Isle of Wight, UK

Newtown estuary, on the Isle of Wight, southern England, was selected as a pilot study on account of its small size and computational tractability. Newtown is one of five estuaries on the Isle of Wight, UK (Figure 2.16). It is located on the north coast between the Western Yar and Medina estuaries. More generally, it is part of the estuarine system of Solent (Cope et al., 2008). The estuary has been under the protection of the National Trust since 1965 and includes the only National Nature Reserve of the Isle of Wight, the Newtown Harbour (which consists of the Newtown River and the surrounding land). This National Nature Reserve supports important and also threatened wildlife by providing feeding and over-wintering ground, especially for waders and other wildfowl, like Brent goose, widgeon, teal and black-tailed godwit (Gardiner et al., 2007; Isle of Wight SMP2, 2010). The Newtown River is also designated as an Area of Outstanding Natural Beauty (AONB) and has been designated as a Site of Special Scientific Interest (SSSI) since 1951.

The mouth of the estuary is dominated by intertidal sand backed by low maritime cliffs which are then backed by agricultural land. Habitats within the estuary include saltmarsh and mudflats, and an important saline lagoon, formed within the site of old salt workings, exists at the Newtown Quay. The Newtown estuary coastline, much like the rest of the north coastline of the island, is relatively undeveloped and has been subject to long-term retreat (Gardiner et al., 2007). Although the eroding cliffs produce a lot of sediment, most of it is transported offshore and therefore cannot protect local beaches from retreat (Isle of Wight SMP2, 2010).

The coastline is mesotidal, with a tidal range of 3.4 m calculated based on the closest tide gauge station at Cowes (around 8km to the northeast). Most of the marsh surfaces lay between 0.8m and 1.9m OD, with the highest astronomical tides reaching almost 2m OD (UK Hydrographic Office, 2000).

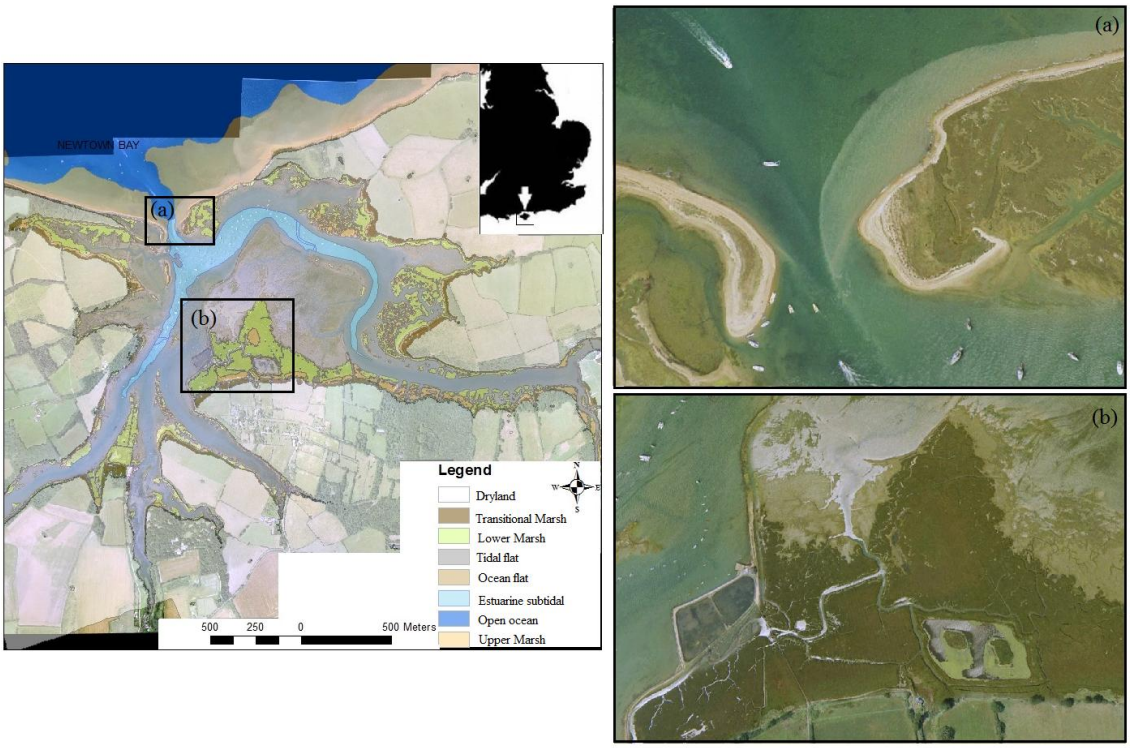

Figure 2.16: Aerial photo of the Newtown Estuary, Isle of Wight, with overlay of principal habitats, focusing on (a) the mouth of the estuary and (b) the saline lagoons existing at the Newtown Quay (Source: Google Earth).

In contrast to the southwest part of the island, which is exposed to storm waves within the English Channel, its north-west coast is protected from the open ocean. Thus, the waves generated in the West Solent are fetch-limited and do not exceed 1m in height (SCOPAC, 2003). As a consequence, the northern part of the island is undefended with only minor defences in limited locations.

The Newtown estuary is an undeveloped and naturally evolving inlet with only defence localised defence walls and embankments at Shalfleet Quay, Newtown Quay due to saltworks and on the upper part of Shalfleet Lake. These currently have a residual life 15 to 25 years (Isle of Wight SMP2, 2010; Figure 2.17). The general lack of coastal defences will allow the habitats to migrate inland, such that coastal squeeze is not a major concern here (Gardiner et al., 2007). The estuary entrance consists of two spits. Although the western spit is active and has rolled back, the eastern one does not show similar behaviour except for a landward shift between 1962 and 1995 of around 30 m (Gardiner et al., 2007). However, the eastern spit has breached, leaving some saltmarsh areas unprotected from the wave action (Bray and Cottle, 2003).

Figure 2.17: Coastal defences (Source: Isle of Wight SMP2, 2010).

The modified SLAMM code was applied in this pilot case study in order to undertake a sensitivity analysis of the various model parameters and external forcing involved. LIDAR data, available at no cost from the Channel Coastal Observatory (http://www.channelcoast.org/), were used to generate the required from SLAMM input layers, while site specific data are available from projects previously undertaken in this case study.

2.5.2. Blyth and Deben estuaries, Suffolk, UK

The Blyth and Deben estuaries, two small estuarine systems on Suffolk, eastern England, were selected in order to critically evaluate the ability of the model to produce meaningful projections of intertidal habitat change under a set of UKCP09 scenarios. As noted earlier, these sites were selected due to availability of background literature on habitats and sedimentary processes, as well as bathymetric datasets. The latter was supplemented the Environment Agency LiDAR data made available through the NERC iCOASST project (Nicholls et al., 2012; 2015).

The Blyth estuary is a barrier-enclosed system in a mainly rural catchment of 214 km^2 in Suffolk (Figure 2.18) with a dune-backed sand and gravel beach that extends southwards from an elevated headland where the town of Southwold is situated (French, 2008). It contains a mosaic of coastal, wetland and heathland habitats supporting a diverse fauna and flora, including nationally rare and scarce species. Thus, it is included within a Special Protection Area and Ramsar Site, the Minsmere-Walberswick SSSI. It

also lies within the Suffolk Coast and Heaths Area of Outstanding Natural Beauty (AONB) (Environment Agency, 1999a, 2009).

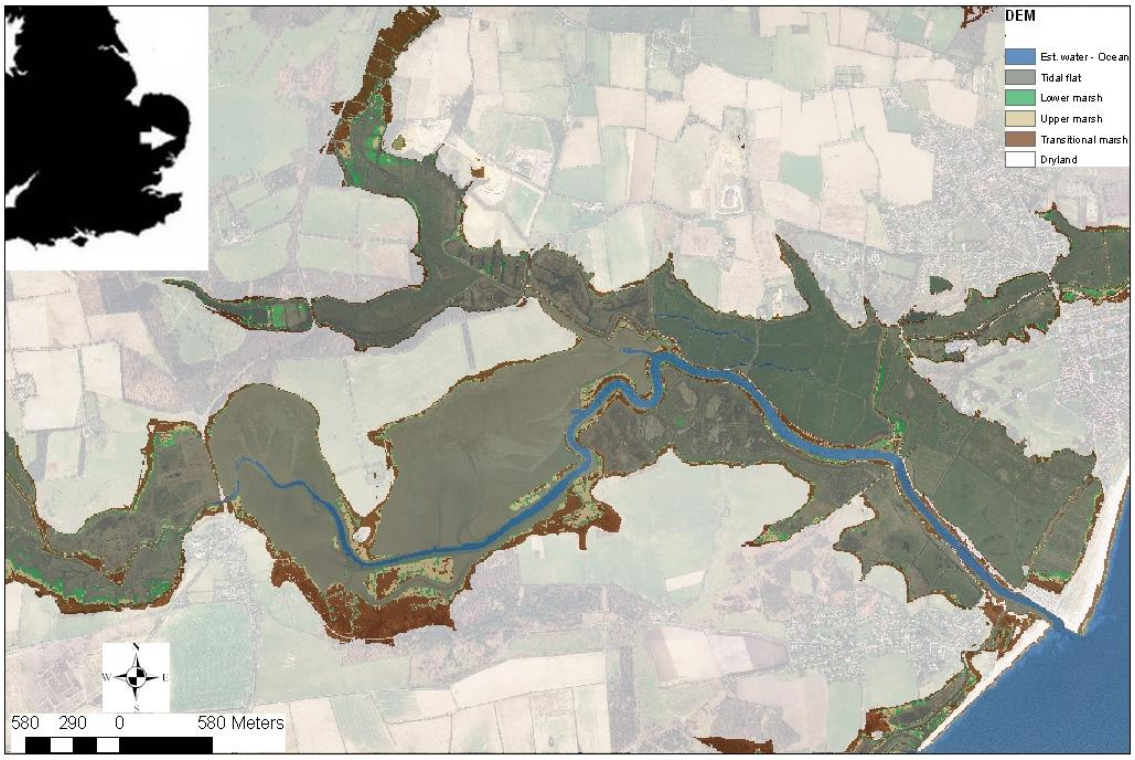

Figure 2.18: Aerial photo of the Blyth estuary, Suffolk, with overlay of principal habitats.

The Blyth estuary has a tidal length of 10.7 km (French, 2001), and it can be characterised as microtidal (Fairbridge, 1980; Davidson et al., 1991) with average ranges at Southwold of 2.0 m and 1.2 m at springs and neaps respectively. Highest Astronomical Tide (HAT), Mean High Water Springs (MHWS) and Mean sea-level (MSL) are approximately 1.6 m, 1.1 m and 0.2 m above Ordnance Datum (OD) respectively. The estuary is well-mixed, with a small freshwater inflow (0.4 m^3s^{-1} at Halesworth, (Institute of Hydrology, 1996)) in comparison with the tidal prism (3 x 10^6 m^3 on a mean spring tide) (French, 2008; French and Burningham, 2003; French et al., 2000, 2008).

Over 14 m of muddy sediment, with gravel and sand at the mouth, have been deposited in the estuary over the last 6,500 years (Brew et al., 1992). Taking into account the negligible sediment supply from the River Blyth itself, the sediment is derived from the North Sea and from the continuing process of erosion of the coastline further north, and

transported into the estuary driven by waves (French, 2008; French and Burningham, 2003; French et al., 2008).

Extensive reclamation of agricultural land took place in the second half of the 18th century (Lawrence, 1990), and by 1840 all tidal flat marshes were reclaimed (Beardall et al., 1991; Buncombe, 1994), confining the estuary to a narrow channel. The defences are primarily earth embankments, with protection at some places, and they are near the end of their life (Environment Agency, 2009). The Sandpit Marshes were abandoned in the 1920s, followed by the Bulcamp and Angel Marshes in the 1940s. Although the Angel Marshes are partially reverted to salt marsh, the other two are muddy tidal flats (Figure 2.19) (French, 2008; French and Burningham, 2003; French et al., 2000).

The narrow mouth of the estuary is maintained by two piled breakwaters, set 40m apart (French, 2008; French and Burningham, 2003; French et al., 2008). At the south of the mouth a narrow sand shingle beach exist, backed by dunes for the first 500 m south of the harbour, but then giving way to a narrow maintained shingle embankement. In contrast, the shore to the north comprises a wide sand shingle beach, backed by dunes. The dune strip, the Denes, has grown and stabilised since the north breakwater construction, forming the seaward flood barrier to the Havenbeach Marshes. The last one, together with the Woodsend and Town Marshes upstream, are below mean tide level and used as pastures (Environment Agency, 1999a).

Further upstream, the Buss Creek Marshes are located leading into Botany Marshes, where the main sewage works of the area exist. At its northwest side, the Reydon Marshes are located, opposite of which the Tinkers Marsh exist (Environment Agency, 1999a). At this point of the river, the defences are fronted by a 2 - 3 m plateau of intertidal saltmarsh. These widths have been eroded in many places, especially in response to the storm surges of 2007 (Environment Agency, 2009) and 2013 (Spencer et al., 2014). Combined with the deep channel bed in this area, this has led to serious problems of instability and the forward slumping failure of defences. It is worth mentioning here, that the Tinkers Marsh embankment, especially along its western end, is the lowest level of flood defence within the whole estuary. The Tinkers Marsh is divided by the Robinson's Marsh at the south by Squire's Hill and the sewage pipe embankment to the bridge (Environment Agency, 1999a, 2009).

Finally, upstream of the estuary and towards to Blyford Bridge, the narrow channel has a width of 300-500 m and is surrounded by low farmland. Here, the low embankments do not completely constrain the main river channel, leaving space for natural development of the channel. Also, they are failing due to storm surges in 2006 and 2007 (Environment Agency, 1999a, 2009).

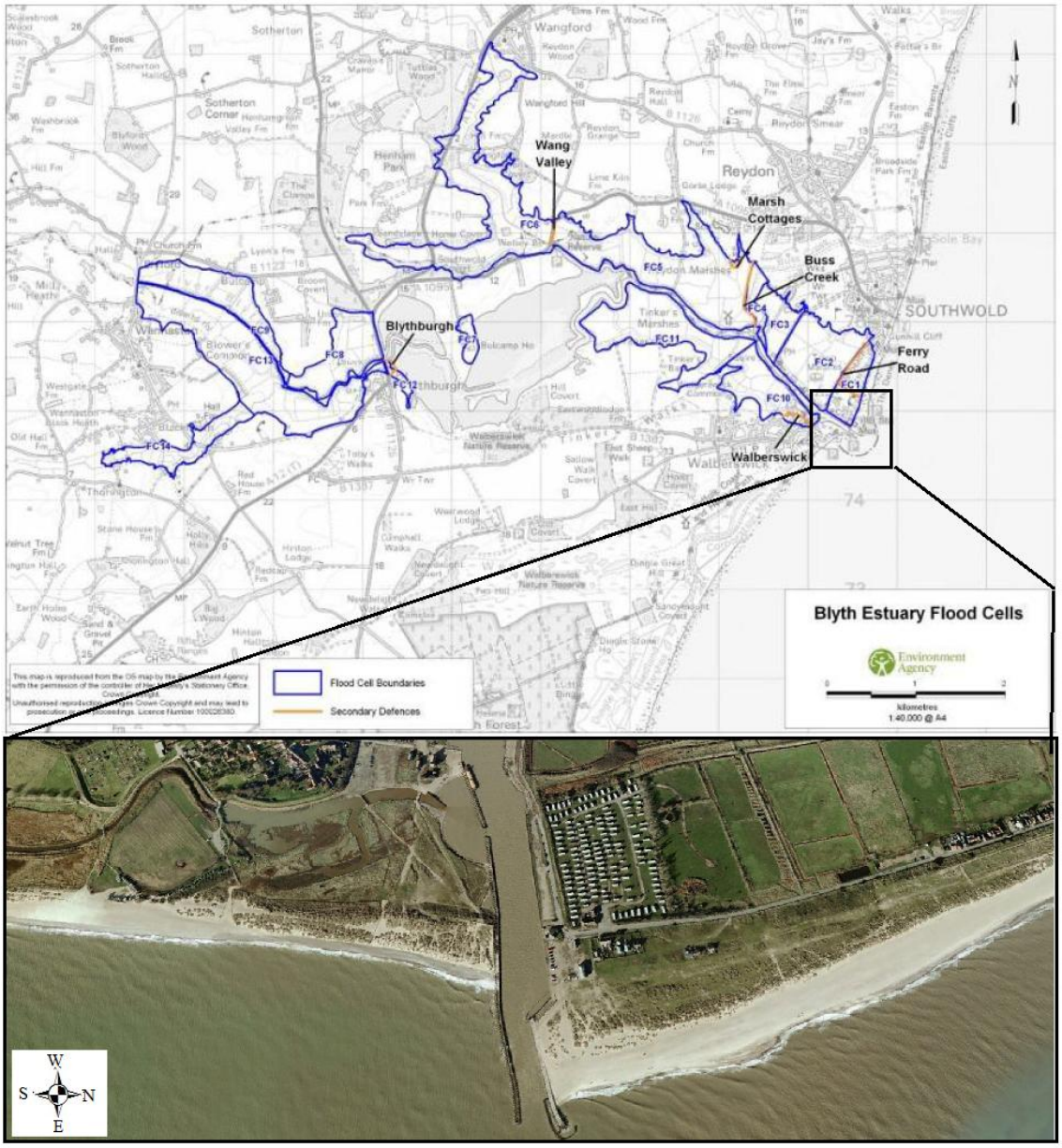

Figure 2.19: Flood compartments at the Blyth Estuary (Environment Agency, 2009), focusing on the piled breakwaters existing at the mouth of the estuary.

In contrast, the Deben is a long and narrow estuary extending for over 20 km south-eastwards from the town of Woodbridge to the sea north of Felixstowe (Figure 2.20). Most of its intertidal area is occupied by tidal flats, and it also occupies extensive and

diverse saltmarsh communities (approximately 28% of the total saltmarsh area of Suffolk; CHaMP, 2002), supporting overwintering waders and wildfowl. Thus, it is designated as a SSSI and a Special Protection Area and is also Ramsar Site. It is also included within the Suffolk AONB and its southern half is designated as Heritage Coast (Environment Agency, 1999b).

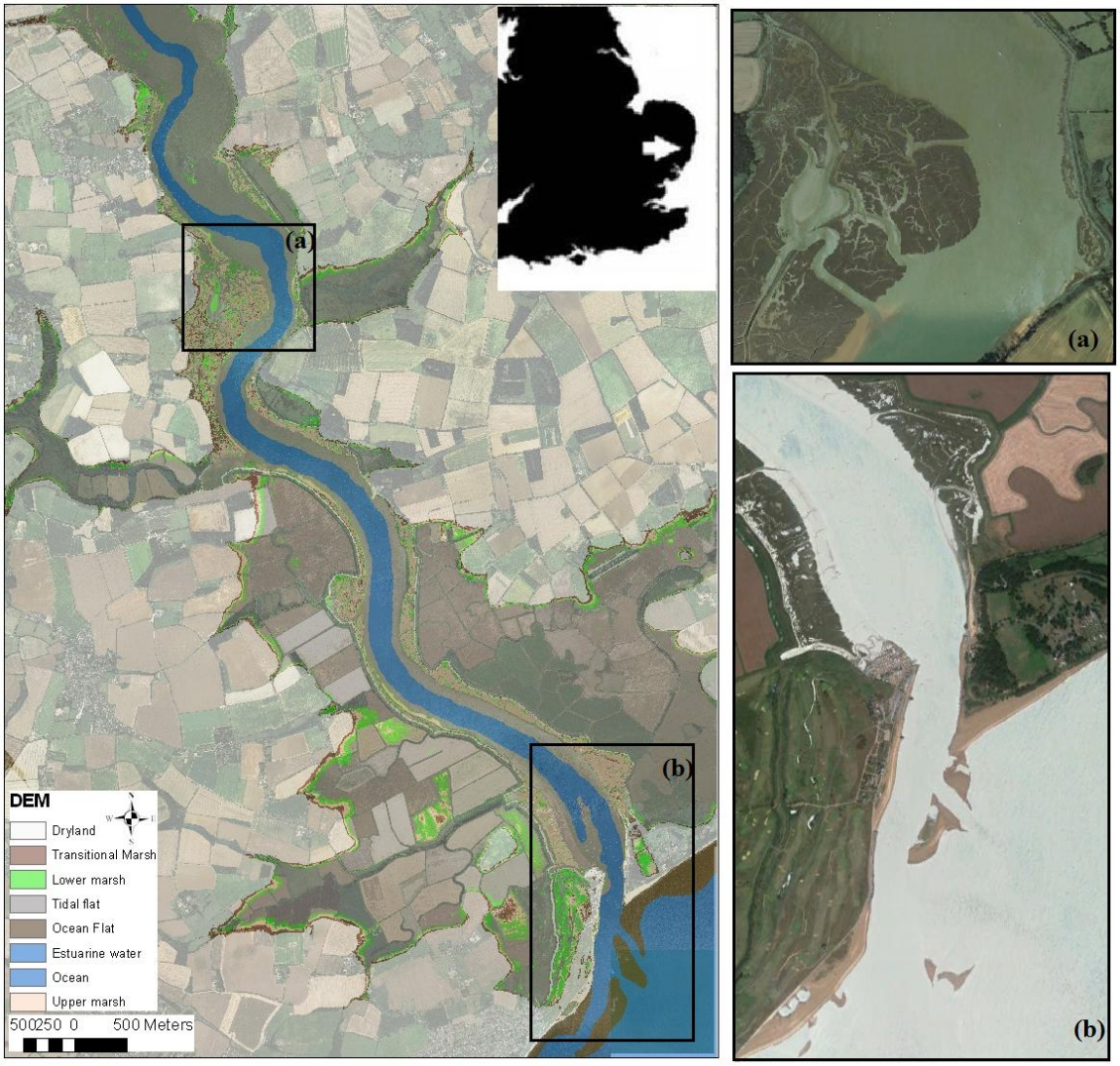

Figure 2.20: Aerial photo of the Deben estuary, Suffolk, with overlay of principal habitats, focusing on (a) the extensive saltmarsh area at the middle estuary and (b) the mouth of estuary (Source: Google Earth).

The Deben estuary can be characterised as mesotidal with 3.2 m tidal range on springs and 1.9 m on neaps at the mouth, and a higher (by about 0.3 - 0.4 m) range at Woodbridge. The estuary is dominated by tidal processes, and the influence of fresh

water is largely restricted to the upper part of the estuary (ChaMP, 2002; SMP7, 2010). The offshore sediment supply to the estuary has been estimated as 16 times greater than that supplied by the river (Beardall, 1991), being generally silt or silty sand in its upper and middle parts, but dominated by gravel and coarse sand close to the mouth (Burningham and French, 2006). The estuary is protected from offshore waves due to its narrow mouth, and ebb tidal delta (The Knolls; Figure 2.20b). The wider parts of the middle estuary are affected by fetch-limited waves that can still cause sediment suspension (SMP7, 2010).

Reclamation for agriculture took place in this estuary too, modifying it significantly, especially in its lower part. Approximately 25 km of defences protect 16 discrete compartments of former estuary floodplain from tidal inundation (Burningham and French 2006; Figure 2.21). The upper part is constricted to a narrow channel by rising ground to the east and the hard defences of Woodbridge town on the west bank. The channel almost dries at low water to the north of Woodbridge. Relatively small fringes of saltmarsh can be found here, the only exception being the east bank near Sutton, where the flood embankments were breached, recreating intertidal saltmarshes and tidal flats. Areas of brackish reed bed also exist here. The mid-estuary channel is flanked by large areas of intertidal flats and saltmarsh in front of the embankments and high ground. However, the channel becomes more restricted in the outer estuary due to more continuous runs of embankment and areas of higher ground on either side of the estuary. Fringing saltmarsh can be found along most of its length, especially on the northeast bank and in Falkenham Creek on the southwest bank. The mouth of the estuary narrows significantly just before connecting to the open sea due to a ridge of higher land on the north margin at Bawdsey and an extended area of beach ridges at Felixstowe Ferry on the opposite bank. The open coastline to the south is barrier beach backed by low-lying land (Environment Agency, 1999b; SMP7, 2010).

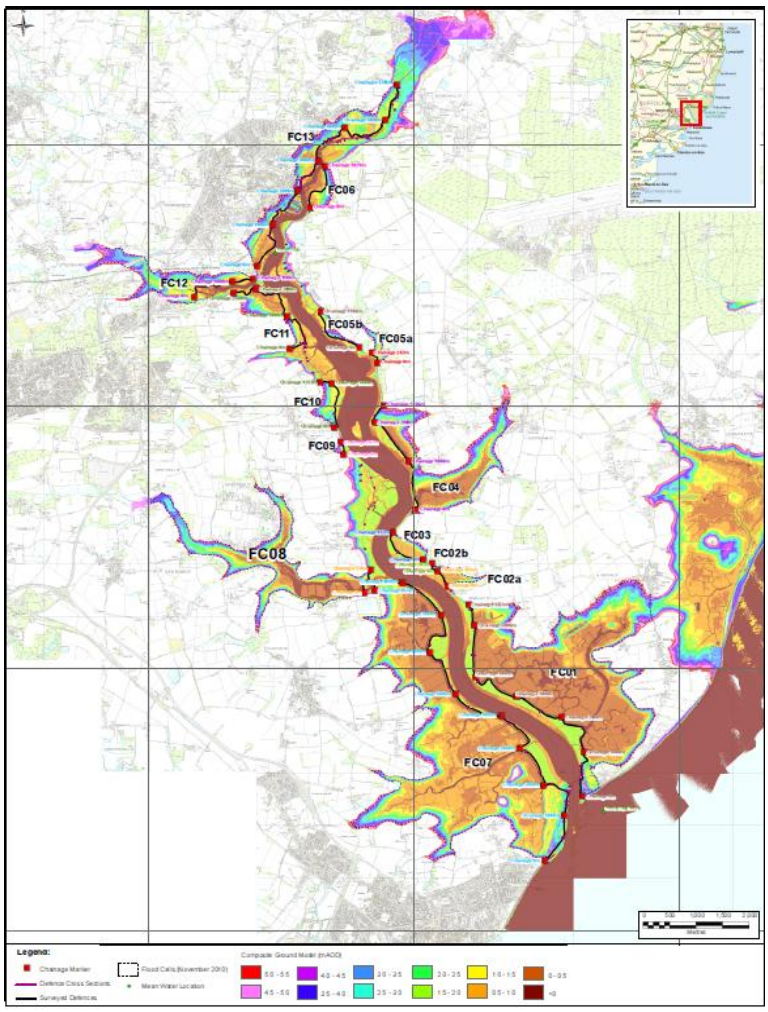

Figure 2.21: Flood compartments in the Deben Estuary (Deben Estuary Plan http://www.suffolkcoastandheaths.org/projects-and-partnerships/deben-estuary-partnership/deben-estuary-plan/)

2.5.3. Blakeney Point, Norfolk, UK

Blakeney Point, a gravel and dune barrier and backbarrier saltmarsh complex on North Norfolk, eastern England, was selected in order to evaluate the ability of SLAMM to produce meaningful projections of habitat change in a system influenced more directly by the evolution of the open coast. In the case of Blakeney Point, this involves historical retreat of an outer barrier under the influence of storm-driven overwash (Environment Agency, 2012).

Taken as a whole, the North Norfolk coast extends for a distance of around 40 km, consisting of extensive intertidal sand and mud flats with salt marsh units existing in the lee of recurved shingle barriers, many of which support vegetated dune systems (Figure 2.22; May, 2003). The saltmarshes of this area have been characterised by Steers (1946)

as the finest coastal marshes in Great Britain. The coastline is macrotidal, subjected to a strong tidal influence especially at the west with a mean range of 3.4 m at neaps and 6.4 m at springs, where most of the marsh surfaces lay between 2 m and 3.2 m OD; the larger dune-covered barriers reach a height of 15 - 20 m OD. The highest astronomical tides reach almost 4 m OD, although storm surges can increase water level to over 5m OD (French et al., 1990, 1995; French 1993; Reed et al, 1999).

Figure 2.22: The coast of North Norfolk (May, 2003).

Blakeney Point (Figure 2.23) is a large shingle spit extending from Sheringham westwards for over 17 km. The first 5.5 km enclose low cliffs of glacial till, while the central part forms a ridge of about 200 m width and almost 10m height, in front of the Salthouse Marsh and the Fresh Marsh. Finally, the western part continues for 3km as a single ridge and develops then a series of long recurves with a south/south-westward trend. These are the most recent members of a set of shingles, indicating the westwards growth of the spit (May, 2003). Consequently, the age of the marshes at either side of the Blakeney channel also increases eastwards, with the oldest one probably developed during the 15th century (Pethick, 1980), while lateral growth of new marsh has been occurring at the western end of Blakeney since the 1950s (Pye and French, 1993 in May 2003). Marshes also exist at the east side of Blakeney, but most of them have been land-claimed (May, 2003).

Figure 2.23: Aerial photo of Blakeney spit, Norfolk, including its associated backbarrier environments, and focusing on its western part (Source: Google Earth).

3 SLAMM SENSITIVITY ANALYSIS: APPLICATION TO NEWTOWN ESTUARY, ISLE OF WIGHT, UK

3.1 Previous work on the Newtown Estuary

3.1.1 Shoreline Management Plan SMP2

The current (phase 2) SMP for the Isle of Wight was developed by the Council of the Isle of Wight (Isle of Wight SMP2, 2010). It covers all the coastline of the island (110 km) which is divided it into seven zones, where the Newtown Estuary is part of the North-West Coastline (PDZ7). For each zone, future erosion and flood risk maps are produced for two different management scenarios:

- No Active Intervention (NAI) scenario: no further coastal defence work is necessary
- With Present Management (WPM) scenario: present practises are continued into the future.

Flood risk maps for the Newtown Estuary are presented in Figure 3.1. The erosion risk map is created by applying the future erosion rates, calculated by using the Walkden and Dickson (2008) formula (equation 3.1; Table 3.1), to GIS maps layers, thereby indicating the eroded zone for each year. When coastal defence structures exist, the erosion rates are applied from the point at which this structure is predicted to fail, otherwise it is applied from the first year (Isle of Wight SMP2, 2010).

$$\varepsilon_2=\varepsilon_1 * \sqrt{\frac{S_2}{S_1}}, \qquad (3.1)$$

where, ε_1= historic recession rate, ε_2= future recession rate, S_1=historic sea-level rise, S_2= future sea-level rise (produced in accordance to national government guidance issued by DEFRA in 2006, which aimed to define the sea-level allowances to be used in coastal management plans and schemes (DEFRA, 2006; Table 3.2)

Figure 3.1: Erosion and flood risk map for no active interaction scenario (a: Entrance to Newtown Estuary, b: Southern Newtown Estuary) (after Isle of Wight SMP2, 2010).

Table 3.1: Erosion Rates for the Newtown Estuary (Isle of Wight SMP2, 2010).

	Erosion Rates (m year^{-1})					
	Historic	**Current to 2025**	**2025 to 2055**	**2055 to 2085**	**2085 to 2105**	**Potential 100 year erosion (m) (unprotected)**
Western Spit	0.6	0.69	0.91	1.06	1.15	96
Eastern Spit	0.62	0.72	0.94	1.10	1.19	99
Inside Eastern Spit	0.2	0.23	0.30	0.35	0.35	32

Table 3.2: Sea-level rise for the Isle of Wight.

	Future Sea Level Rise (cm) (Isle of Wight SMP2, 2010)		Sea Level Rise Allowance (mm year^{-1}) (DEFRA, 2006)
	From 1990	From 2009	
By 2025	+14	+7	4
By 2055	+39.5	+32	8.5
By 2085			12
By 2105	+105.5	+98	15

The flood risk map created is based on the flood zones supplied by the Isle of Wight Strategic Flood Risk Assessment (Isle of Wight SFRA, 2009). The latter are based on ArcGIS shapefiles supplied by the Environment Agency, all taking into account sea-level rise data supplied by DEFRA (2006; Table 3.2) and PPS25 (2006). The outline for the SMP2 flood zones was created by using the worst case scenario supplied by Isle of Wight Council. This outline was then combined to the 'Tide Level map' supplied from the Environment Agency producing new water levels. These new water levels were overlaid on topography in order to provide the flood risk maps (Isle of Wight SMP2, 2010).

3.1.2 BRANCH Project

The BRANCH project is a trans-national project aiming to show how spatial planning can help biodiversity to adapt to climate change (BRANCH partnership, 2007). Its 'coastal package' aimed to develop and also test spatial planning tools for coastal and estuarine systems in order to inform their management with regard to climate change effects on biodiversity (BRANCH project partners, 2003). The Newtown Estuary is one of the local-scale case studies of this project. Historical data were used in order to establish the baseline information, and aerial photographs and LiDAR data to obtain the habitat distribution, all in GIS. Four sea-level rise scenarios are developed (Low, Medium-Low, Medium-High, High) for three time periods (2020s, 2050s, 2080s) based on the UKCIP (Hulme et al., 2002). However, rates of sea-level rise are necessary for modelling, thus the annual sea-level rise rates are calculated between these time-periods. Finally, two different modelling approaches are applied to the Newtown Estuary in order to assess the impacts of climate change; one for the intertidal habitats and one for the spits (Gardiner et al., 2007).

In the case of the spits, historic shoreline positions were compiled by digitising the mean high water (MHW) shorelines from past maps (Figure 3.2). Historic retreat rates were computed using the Leatherman's (1990) equation (eq. 3.2), in order to estimate the future retreat rates under the Medium-High emission scenarios, and further model the recession of the spits (Figure 3.3).

$$\varepsilon_2=\varepsilon_1 * \frac{S_2}{S_1} \qquad (3.2)$$

where, ε_1= Historic recession rate, ε_2= future recession rate, S_2= Future sea-level rise, S_1=Historic sea-level rise. This equation differs from the Walkden and Dickson (2008) equation; it is linear with sea-level rise and results follow the Bruun Rule's assumptions (Gardiner et al., 2007).

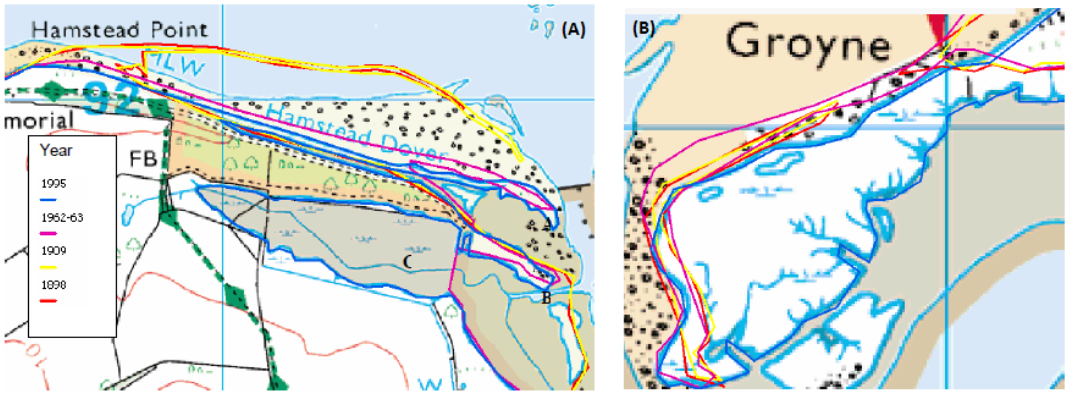

Figure 3.2: Historical analysis of the western (A) and eastern (B) spit at Newtown Estuary as part of the BRANCH project (after Gardiner et al., 2007).

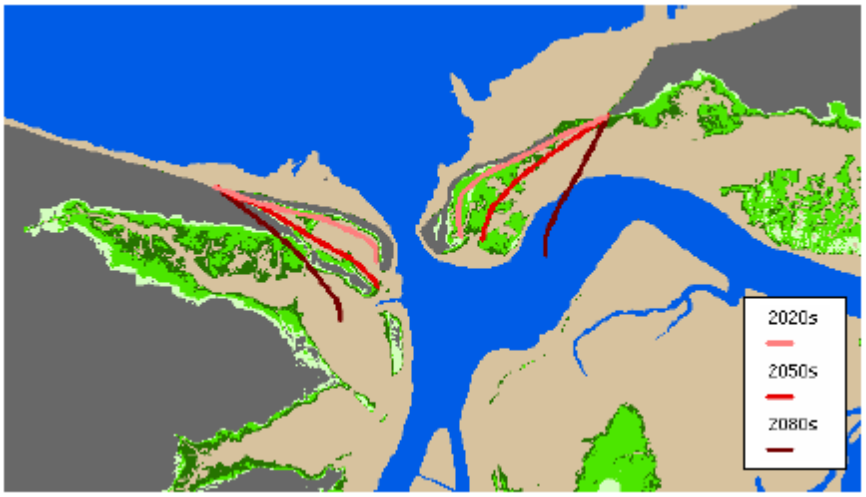

Figure 3.3: Recession analysis of the spits at Newtown Estuary (under the Medium-high emission scenario as part of the BRANCH project; Gardiner et al., 2007).

The distribution of intertidal habitats was generated using airborne LiDAR data, according to their elevation within the tidal frame (Figure 3.4). In order to assess the impacts of sea-level rise on these habitats, the new expected sea level was added onto the tidal parameters. For more realistic results, the analysis also included the effects of vertical accretion of 2mm/year and 4mm/year (Figures 3.4 b-d for the Medium-High emission scenario with 2mm accretion).

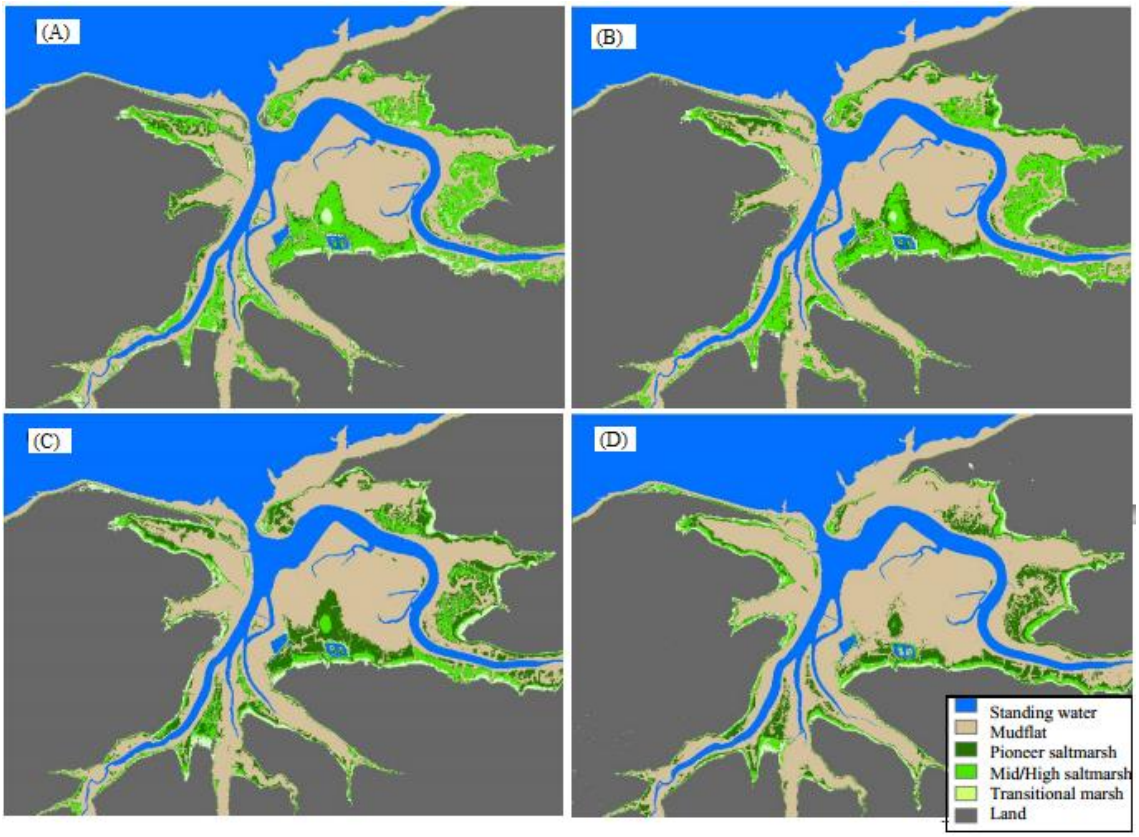

Figure 3.4: Newtown Estuary (A: current saltmarsh extent; B: saltmarsh in 2020s; C: saltmarsh in 2050s, D: saltmarsh in 2080s; the future positions are modelled for the Medium-High emission scenario and 2mm accretion rate as part of the BRANCH project; after Gardiner et al., 2007).

3.2 Preliminary application of the modified SLAMM code

In the present study, the modified SLAMM code was applied to Newtown, in order to undertake a sensitivity analysis of the various model parameters and external forcing involved. As noted previously, a key factor influencing the initial selection of the Newtown estuary was the availability of LiDAR data at no cost from the Channel Coastal Observatory (http://www.channelcoast.org/). At this stage in the project, LiDAR were not generally available for most of the estuaries in England and Wales. These data have a sampling interval of 1m and an indicative vertical accuracy of ±15 cm. LiDAR data combined with digitised bathymetry data in ARC-GIS 9.3 in order to create the input DEM for SLAMM (Figure 3.5). Given the quality of the LiDAR data, the elevation pre-processing option in SLAMM was not used. The DEM was used to derive the slope (Figure 3.6) and the land classification map based on wetland position in the tidal frame (Figure 3.7; Table 3.3), as described in Chapter 2. All input layers were resampled to a 5 m horizontal interval.

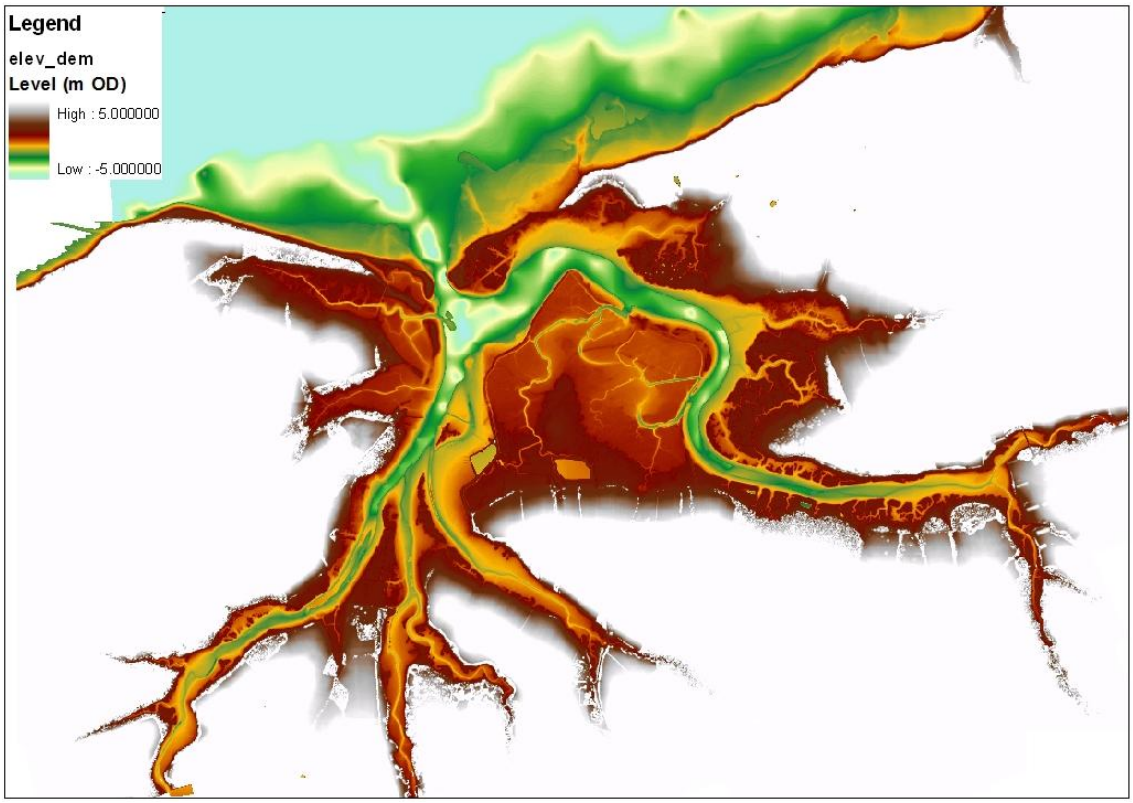

Figure 3.5: Elevation map of Newtown Estuary created using a GIS.

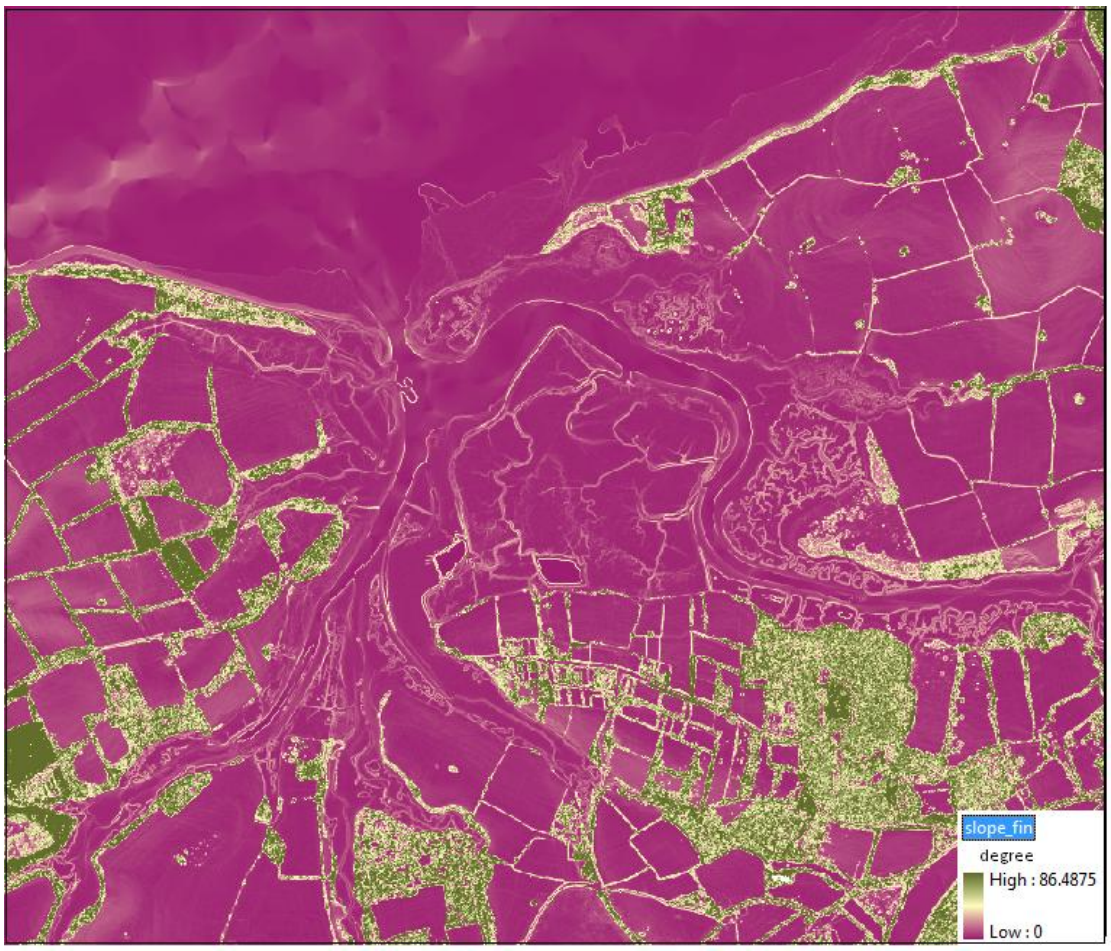

Figure 3.6: Slope map of Newtown Estuary created using a GIS.

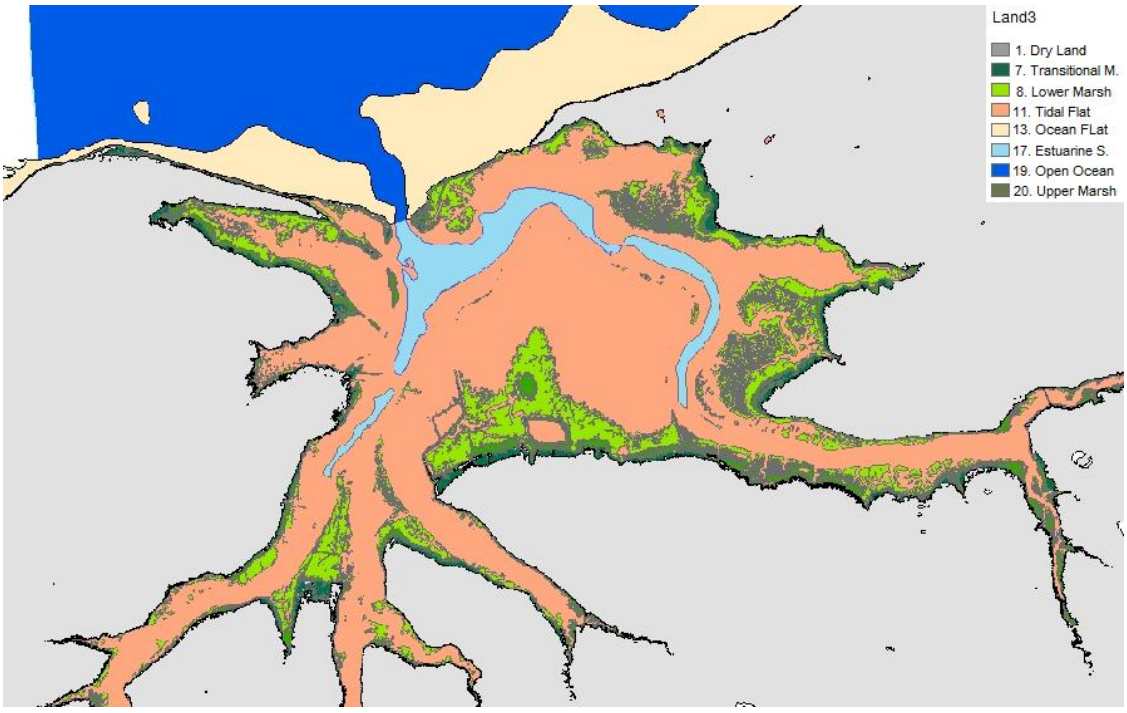

Figure 3.7: Land classification (habitat) map of Newtown Estuary created using a GIS.

Table 3.3: Tidal criteria for modelling vertical zonation of inter-tidal areas. Tidal levels are derived from the Admiralty tide tables (UK Hydrographic Office, 2000).

	Coastal habitats and land classification	Criteria for defining habitat position based on elevation and tidal level	
		Tidal level	Elevation (m)
Estuary model	1. Dry land	>HAT	> 1.9
	7. Transitional marsh	MHWS-HAT	1.5 - 1.9
	20. Upper marsh	MHW-MHWS	1.15 - 1.5
	8. Lower marsh	MHWN-MHW	0.8 - 1.15
	11. Tidal Flat	LAT-MHWN	(-2.6) - 0.8
	17. Estuarine Subtidal	<LAT	< (-2.6)
	13. Ocean Flat	LAT – HAT	(-2.6) - 1.9
	19. Open Ocean	<LAT	< (-2.6)

Table 3.4 summarises the additional site-specific parameters used in the sensitivity analysis model runs. The historic sea-level trend includes the effect of vertical land movements and is estimated at 1.49 mm yr^{-1} using the closest tide gauge station at Portsmouth (almost 25 km to the northwest). The greater diurnal tide range at this site is calculated by the difference between MHWS and MLWS (3.4 m), while erosion and accretion parameters are obtained from the SMP2 (Isle of Wight SMP2, 2010) and the BRANCH project (BRANCH partnership, 2007).

Table 3.4: Site parameter table for Newtown estuary.

Parameter	Newtown
DEM Date (YYYY)	2008
Direction Offshore[n,s,e,w]	N
Historic Sea Level Trend (mm y^{-1})	1.49
GT Great Diurnal Tide Range (m)	3.4
Salt Elevation (m above MTL)	1.9
HAT (m)	1.9
MHWS (m)	1.5
MHW (m)	1.15
MHWN (m)	0.8
LAT (m)	-2.6
Marsh Erosion (m y^{-1})	0.25
Tidal Flat Erosion (m y^{-1})	0.2
Lower Marsh Accr (mm y^{-1})	2 *
Upper Marsh Accr (mm y^{-1})	1.8 *
Beach Sedimentation Rate (mm y^{-1})	2

*Spatially varying accretion values for each wetland category. If the accretion model is to be used, these parameters are left blank.

For the purpose of the sensitivity analysis, simulations were executed under the UKCP09 SE mean sea-level rise scenario using a time-step of 25 years (Simulation 'N_UK'). Under this forcing scenario, the estuarine habitats are seemingly able to adapt to sea-level rise during the early time-steps, although changes in the lower marsh area are significant by the last time-step (Figure 3.8). In more detail, as presented in Table 3.5, sea-level drives enlargement of the estuarine subtidal by almost 30% by the year 2100. However, the area of the tidal flat increases from about 185 ha in year 2008 to about 208ha in year 2100, indicating that although part of it is inundated/eroded and therefore converted to estuarine subtidal, a larger part of it migrates upland to the marsh area. Consequently, the total area covered by marsh decreases by 2100. Most affected, though, is the lower marsh area with a decrease of 30%, because in most cases there is no space for upland migration. The transitional marsh remains quite stable by migrating upland to dryland, which is also inundated to ocean beach when it is adjacent to the ocean.

It is worth noting here that differences were not expected in the first time-step where SLAMM corrects the land classification based on the DEM, since the land classification is generated from the DEM based on the same conceptual model used in SLAMM. However, the resolution used for its creation can generate them. In this study, the land classification layer is generated by the original DEM file of 1m resolution, but they are both then resampled to 5 m, leading to small differences in the boundaries of some wetland categories between the two layers. SLAMM tries to correct these small differences at the first time-step by assuming inundation of the specific cells, ignoring the process of aggradation. Moreover, while inundation of a habitat within a specific cell is assumed, its transition to the correct one is based on empirical calculations which might result in bigger differences. Thus, it is wise to resample the DEM in the desired resolution first, and based on this generate the required land classification layer. In that case, the generated layers should have less differences and match he conceptual model used in SLAMM and therefore the current time-step could be skipped.

Table 3.5: Impacts of sea-level rise at the Newton Estuary by the year 2100 (changes in ha).

Simulation name: "N_UK"										
Date	**SLR**	**Dry Land**	**Trans. M.**	**Upper M.**	**Lower M.**	**Tidal Flat**	**Est. Subtidal**	**Ocean Beach**	**Ocean Flat**	**Open Ocean**
0	0	638.1	14.3	20.0	51.5	176.4	16.3	0.0	41.6	47.7
2008	0	628.7	19.5	15.8	49.2	185.0	17.3	0.8	41.2	48.4
2025	0.0563	627.7	14.5	15.9	51.7	187.6	17.8	0.4	40.8	49.5
2050	0.1583	625.7	14.4	14.1	49.6	192.5	18.6	0.0	39.7	51.2
2075	0.2778	623.0	14.6	13.4	46.5	197.1	20.2	0.0	37.7	53.4
2100	0.4123	619.5	14.8	13.5	36.8	208.2	21.6	0.0	35.4	56.2
0-2008		-9.4	5.3	-4.3	-2.3	8.6	1.0	0.8	-0.4	0.7
		-8.3	-3.1	-7.3	-9.6	-1.0	-1.1	-0.3	-0.4	-0.7
2008-2025		-0.9	-5.1	0.1	2.5	2.6	0.5	-0.5	-0.3	1.0
		-0.7	-5.8	-5.6	-3.2	-0.5	-0.2	-0.7	-0.3	-1.0
2025-2050		-2.0	0.0	-1.8	-2.07	4.93	0.80	-0.35	-1.17	1.73
		-1.8	-1.8	-3.7	-5.7	-0.80	-0.2	-0.6	-1.2	-1.73
2050-2075		-2.7	0.2	-0.7	-3.2	4.6	1.5	0.0	-2.0	2.2
		-2.4	-2.3	-3.0	-6.2	-1.5	-0.3	-0.3	-2.0	-2.2
2075-2100		-3.5	0.2	0.1	-9.7	11.0	1.4	0.0	-2.3	2.8
		-3.0	-2.8	-2.7	-12.4	-1.4	-0.5	-0.5	-2.3	-2.8

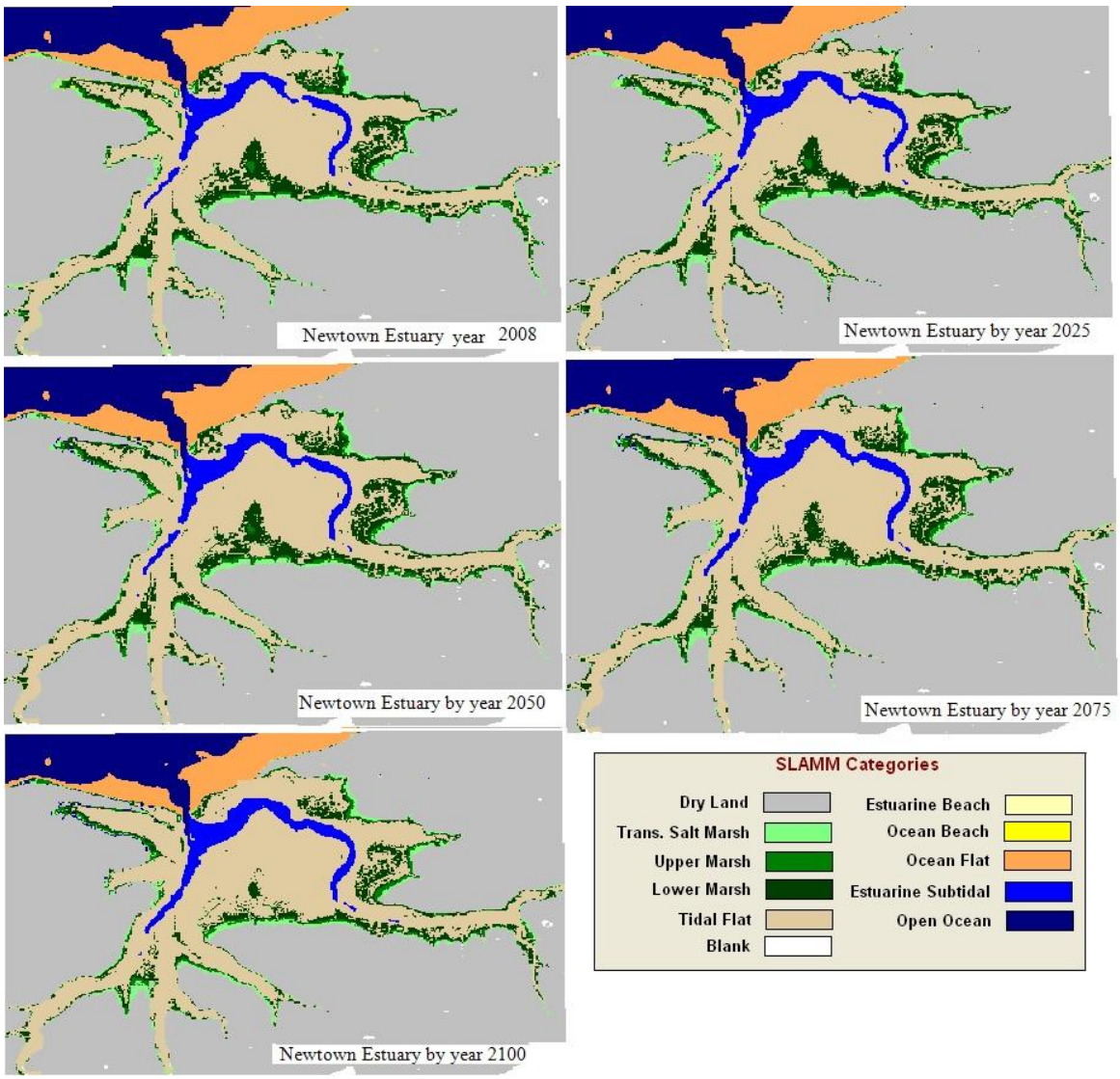

Figure 3.8: Habitat distribution in Newtown Estuary under the SE Mean UKCP09 sea-level rise scenario by the Year 2100 (Simulation 'N_UK').

The BRANCH project approach and SLAMM differ in that the former uses two different modelling approaches in order to assess the impacts of sea-level rise on an estuary; one for the open coast and one for the intertidal habitats. In contrast, SLAMM models the whole estuary at once. More specifically, in BRANCH the spits are modelled by using empirical relationships based on the assumption that the shoreline behaviour is included into the previous shoreline movements. However, the spits at the Newtown estuary have changed their shape and direction throughout the years, such that this approach tends to overestimate spit recession. On the other hand, SLAMM treats the open coastal flat in front of the spits exactly with the same way to the intertidal habitats within the estuary. Here, this tends to result in a more stable estuary mouth, and this approach therefore has its limitations.

Within the estuary proper, previous modelling efforts, including BRANCH, largely evolve the progressive drowning of the existing topography under sea-level rise. This approach does not incorporate any mechanistic modelling of habitat transitions, as SLAMM does by incorporating a flexible decision tree and qualitative relationships. In addition, the process of erosion is totally ignored in most previous models, and although the accretion parameter is taken into account by the BRANCH project, it only applies to areas colonised by saltmarsh. SLAMM introduces more sophistication in that different accretion and erosion values can be applied for each wetland category. Moreover, SLAMM can take into consideration the spatiality of the accretion parameter within each habitat type by calculating it as a time-varying function of elevation, distance to channel (and salinity, when this sub-model is activated). Given this additional complexity, a sensitivity analysis is necessary in order to evaluate how important these parameters are and how they affect the prediction of sea-level rise impacts on the various parts of the estuarine intertidal.

3.3 Sensitivity Analysis

The sensitivity analysis undertaken here investigates how each input factor within SLAMM affects the outputs of the model. This can potentially enhance our understanding of the model. More importantly, the sensitivity analysis will determine if the additional processes included in SLAMM generate predictions that are significantly different to those obtained using simpler approaches (such as the BRANCH method).

To this end, an array of SLAMM input parameters is initially defined (Table 3.6), each one of which is investigated separately. A Matlab-based shell was developed in order to execute multiple SLAMM simulations in a Monte Carlo framework (Figure 3.9). The results are presented as graphs showing the percentage change of each intertidal wetland category relative to the initial condition and the best estimated value of each parameter, i.e. the values used in Section 3.2 above.

Table 3.6: Statistical distribution of SLAMM input factors for sensitivity analysis.

		Parameters	Best estimate	Range of values for sensitivity analysis
Input	Elevation	- Error in DEM	0m	[-0.15:0.15:0.15]
		- Resolution	5m	[1, 5, 10, 20, 30]
	Land Cover	-Error in the classification		Misclassify 15%
SLR		Historic SLR	1.49 mm yr^{-1}	[1:0.1:3]
		Future SLR scenario	UKCP09 SE mean	[min, mean, max]
Site-	Erosion	-Marsh	0.25 m yr^{-1}	
		- Tidal Flat	0.2 mm yr^{-1}	[0:0.1:1]
	Accretion	- Upper Marsh	1.8 mm yr^{-1}	[1:0.1:8]
		- Lower Marsh	2 mm yr^{-1}	[1:0.1:10]
		- Tidal flat/ Beach Sed.	2 mm yr^{-1}	[1:0.1:10]

SLAMMshell.m*

```
matlabpool('open',4);       %Outline shell for running SLAMM within MC framework
nruns = 10;                 %Run control - number of Monte Carlo runs
%Setup parameter space
TFlatErosion_range=0:0.1:1;         %Tidal Flat Erosion range horizontal m/yr
MarshErosion_range=0:0.05:1;        %Marsh Erosion range horizontal m/yr
FixedLowerMarshAccr_range=0:0.1:10; %Fixed Lower Marsh Accretion mm/yr
FixedUpperMarshAccr_range=0:0.1:8;  %Fixed Upper Marsh Accretion mm/yr
Fixed_TF_Beach_Sed_range=0:0.1:10;  %Fixed Tidal Flat/Beach Sedimentation mm/yr
Historic_trend_range = 0:0.01:3;    % Historic sea-level rise trend mm/yr
parfor mc_run = 1:nruns             %Main run loop
  TFlatErosion=TFlatErosion_range(randi(length(TFlatErosion_range),1));
  MarshErosion=MarshErosion_range(randi(length(MarshErosion_range),1));
  FixedLowerMarshAccr=FixedLowerMarshAccr_range(randi(length(FixedLowerMarshAccr_range),1));
  FixedUpperMarshAccr=FixedUpperMarshAccr_range(randi(length(FixedUpperMarshAccr_range),1));
  Fixed_TF_Beach_Sed=Fixed_TF_Beach_Sed_range(randi(length(Fixed_TF_Beach_Sed_range),1));
  Historic_trend = Historic_trend_range(randi(length(Historic_trend_range),1));
  %Write input files
    inputFile=fopen('c:\Users\katerinapylarinou\Desktop\Sen_Analysis\N_UK_matlab.txt','rt+');
    outputFileName=['c:\Users\katerinapylarinou\Desktop\Sen_Analysis\InputFiles\SLR_historic\N_UK_input_slr_h',
        num2str(mc_run),'.txt'];
    outputFile=fopen(outputFileName,'wt+');
    counter=1;
    while (~feof(inputFile))
        tline = fgetl(inputFile);
        if counter==16
            tline=strcat('Historic_trend: ', num2str(Historic_trend));
            fprintf(outputFile,'%s\n',tline);
        elseif counter==238
            tline=strcat('OutputFileN:C:\Users\katerinapylarinou\Desktop\Sen_Analysis\OutputFiles\SLR_historic\N_UK_output_slr_h',
                  num2str(mc_run),'.txt');
            fprintf(outputFile,'%s\n',tline);
        else
            fprintf(outputFile,'%s\n',tline);
        end
        counter=counter+1;
    end
    fclose(inputFile);
    fclose(outputFile);
  %SLAMM Params = [TFlatErosion,MarshErosion,FixedLowerMarshAccr,FixedUpperMarshAccr,Fixed_TF_Beach_Sed,Historic_trend];
  Params = [Historic_trend];
  disp(['SLAMM run with params = ' num2str(mc_run),' ', num2str(Params)]);
  command=['c:\Users\katerinapylarinou\Desktop\5.SLAMM_UK\slamm6.exe ',
      'c:\Users\katerinapylarinou\Desktop\Sen_Analysis\InputFiles\SLR_historic\N_UK_input_slr_h',num2str(mc_run),'.txt'];
  system(command);
end   %End of main run loop
```

Figure 3.9: Matlab shell for execution of multiple SLAMM simulations.

Firstly the effect of the error in DEM is examined. This depends on the accuracy of the LiDAR data used to generate it. Usually, their vertical accuracies range from ±0.05 m to ±0.15 m, depending on the flight profile and the system configuration (Lillycrop et al., 1997; Gutelius et al., 1998; Gomes Pereira and Wicherson, 1999; French, 2003). Here, only the ±0.15 m error is examined since this is the typical UK elevation accuracy (CCO, 2013). Results show that the upper marsh is affected the most, with almost 100% and 50% change for an error of +0.15 m and -0.15 m respectively. Furthermore, differences in the initial condition also affect the projected areas, and more importantly their response to sea-level rise (Figures 3.10 – 3.11). These results indicate how important the quality of the basic terrain information when dealing with such low gradient environments in which small differences in elevation result in large differences in the habitat classification.

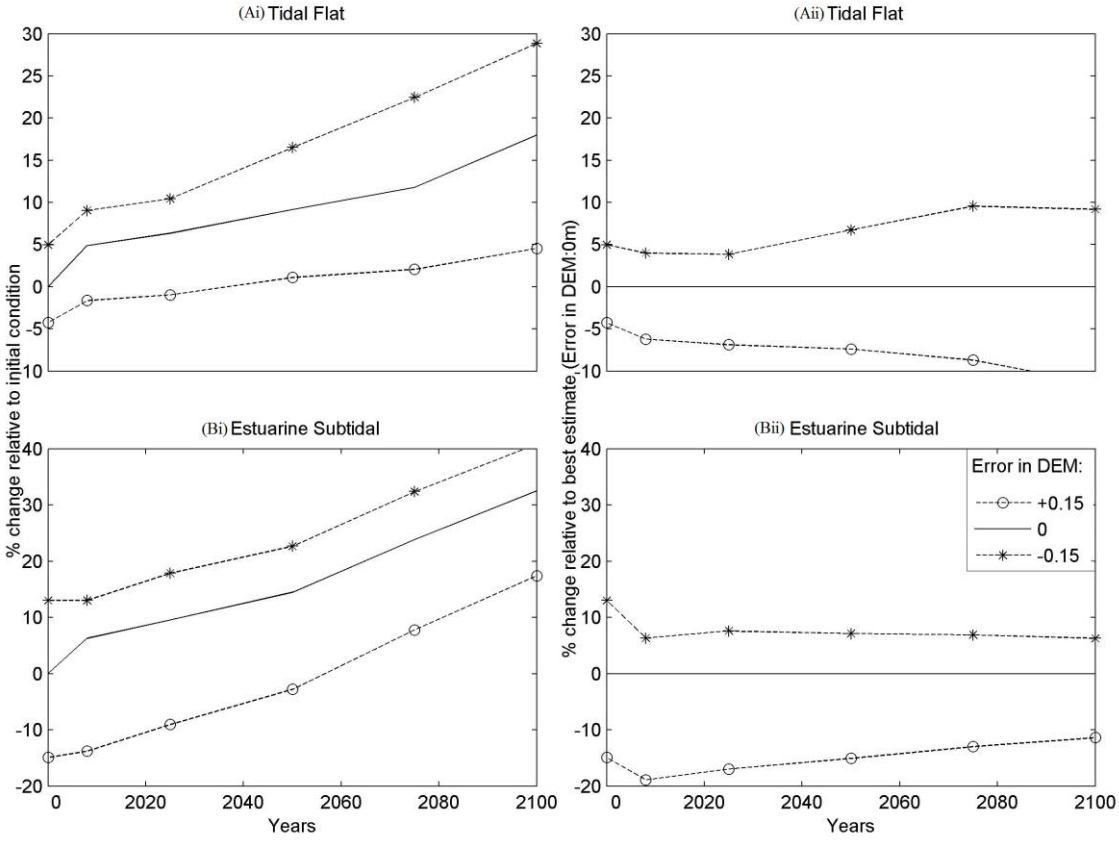

Figure 3.10: Percentage change in (A) tidal flat and (B) estuarine subtidal area relative to the (i) initial condition and (ii) the best estimation for different DEM errors.

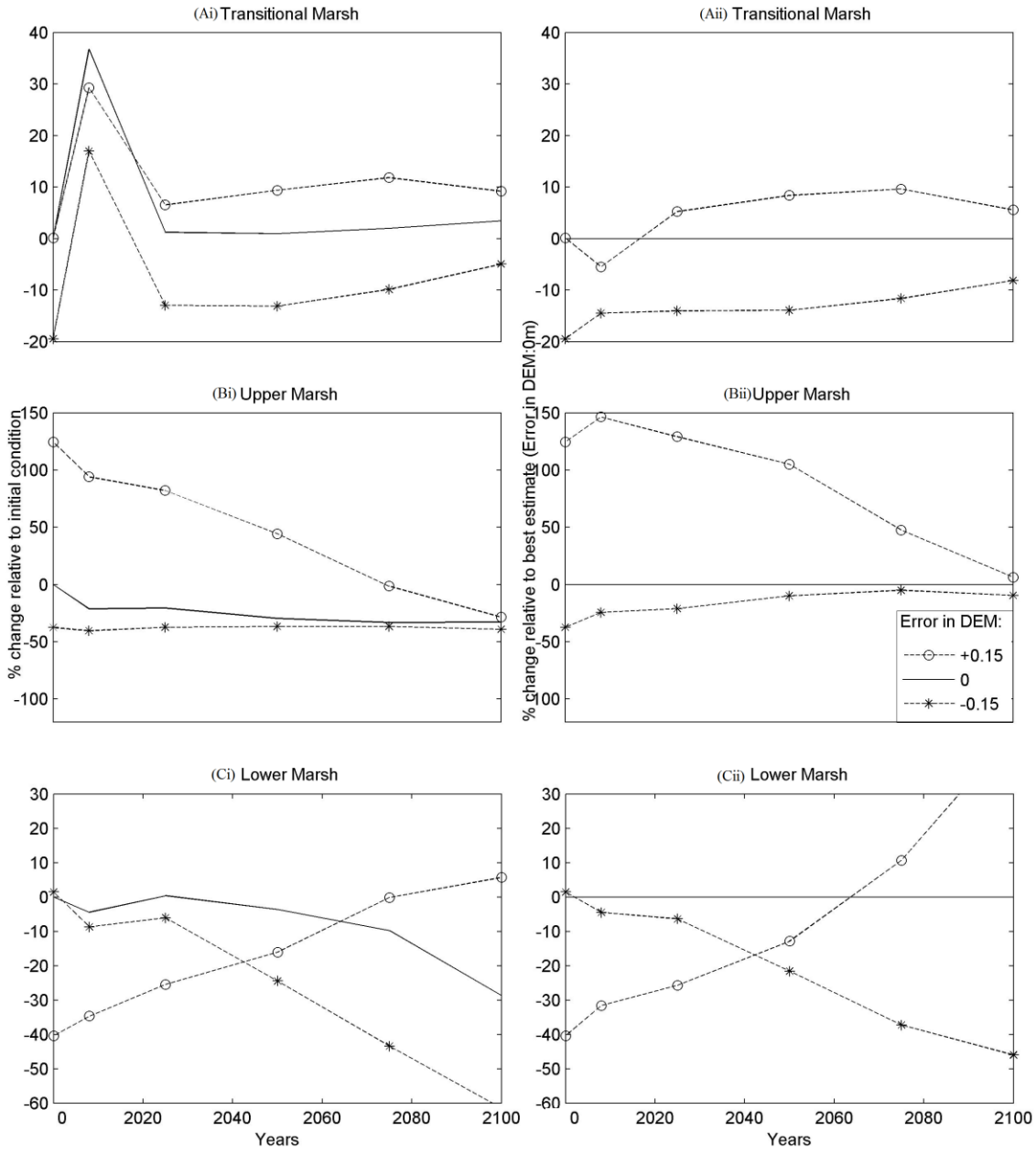

Figure 3.11: Percentage change in (A) transitional marsh, (B) upper marsh and (C) lower marsh area relative to the (i) initial condition and the (ii) best estimation for different DEM errors.

Secondly, the spatial resolution of the input data is examined. SLAMM is quite flexible with regards to cell-size, suggesting a range of 5 - 30 m sampling interval, depending on the size of the site and the availability of the data. The higher suggested resolution is considered here as the best estimation. Results differ from the initial simulation in a range of ±0-10% when high resolution data have been used, while big differences are observed for data with lower resolution, raising the question of whether SLAMM is really suitable for very large area simulations at resolutions of 30 m or lower (Figure 3.12 - 3.13). The most affected wetland category on this scale is the estuarine subtidal,

especially at the last time-steps, reaching a difference of 150% (Figure 3.13d). Significantly affected is also the lower marsh, presenting a difference of 50% for the year 2025 (Figure 3.12f), while the upper marsh (Figure 3.12d) and tidal flat (Figure 3.13b) present a maximum change of 20%. Consequently, the lower the resolution of the input data, less accurate the projected results are. Therefore, it is wise to use high resolution LiDAR data.

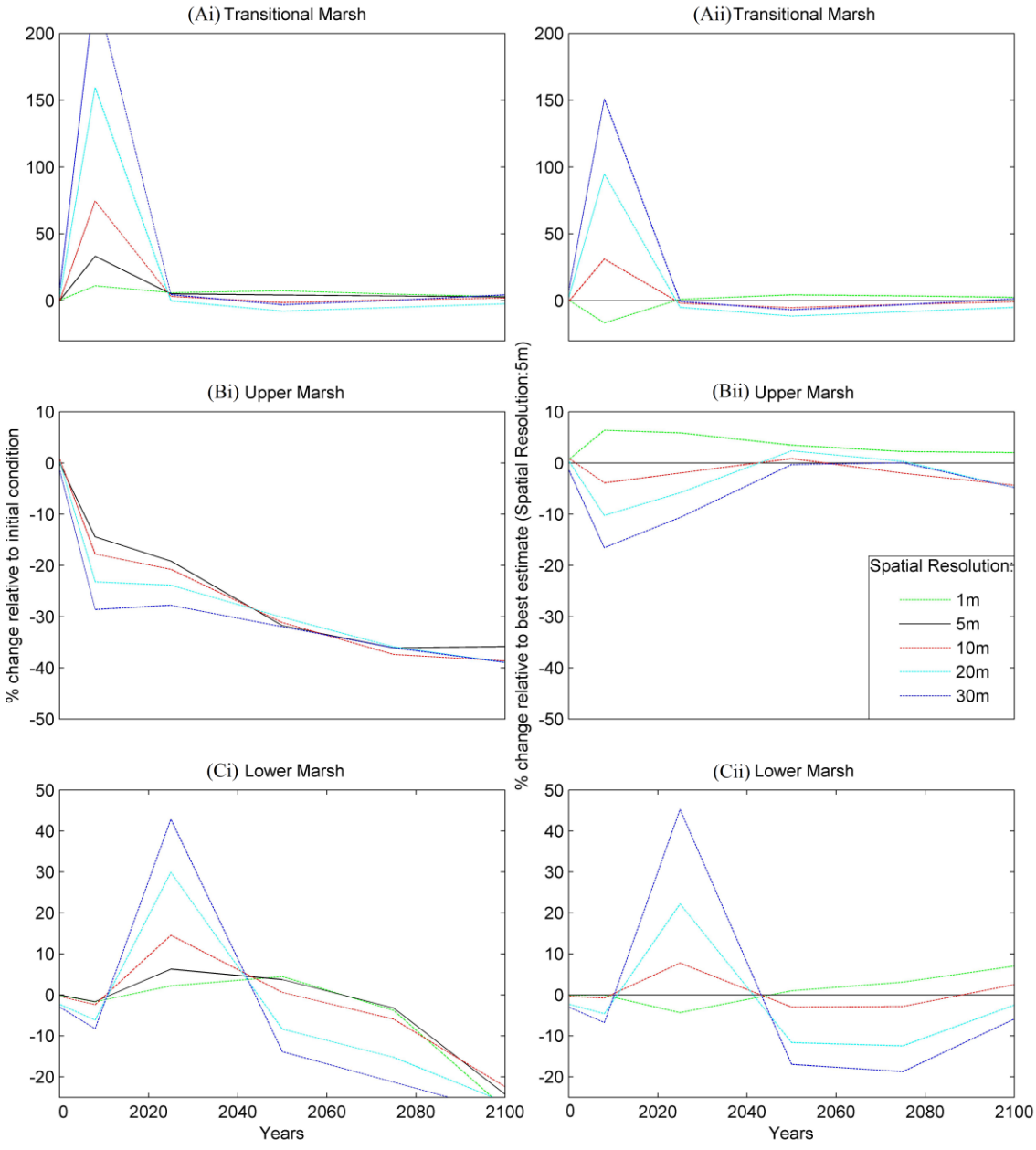

Figure 3.12: Percentage change in (A) transitional marsh, (B) upper marsh and (C) lower marsh area relative to the (i) initial condition and the (ii) 'best estimate' 5m resolution DEM for different resolutions.

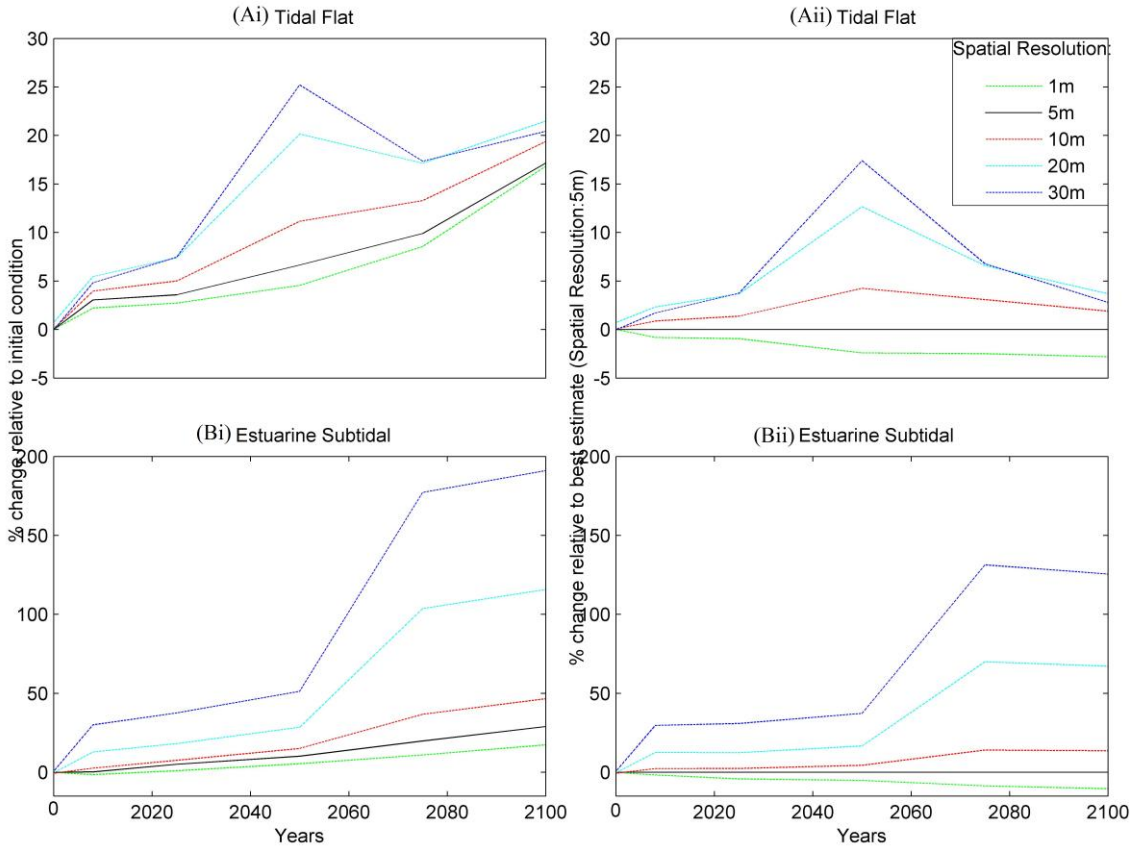

Figure 3.13: Percentage change in (A) tidal flat and (B) estuarine subtidal area relative to the (i) initial condition and the (ii) 'best estimate' 5m resolution DEM for different resolutions.

The last parameter that affects the input layers is an error in the land classification. Classification is usually dependent on the type of remotely-sensed data used, their interpretation and also their spatial analysis (Scott et al., 1987; Arbuckle et al., 1998). The minimum level of interpretation accuracy in the identification of land use and land cover categories from remote sensor data is 80-85% (Anderson, 1971; Anderson et al., 1971, 1976; Olson, 2008). Thus, in order to test the sensitivity of the model to misclassification, new land classification layers are generated in Matlab (Figure 3.14; Table 3.7) with 15% of each category randomly misclassified to the closest one.

Table 3.7: Basis of error analysis for the land classification.

	15% From	Misclassified To
1	Upper marsh	Lower marsh
2	Upper marsh	Transitional marsh
3	Transitional marsh	Dryland
4	Transitional marsh	Upper marsh
5	Tidal flat	Estuarine subtidal
6	Tidal flat	Lower marsh
7	Lower marsh	Upper marsh
8	Lower marsh	Tidal flat
9	Estuarine subtidal	Tidal flat

LandCover.m*

```
%Create the output file
outputFileName=['c:\Users\katerinapylarinou\Desktop\Sen_Analysis\OutputFiles\land_cover\land_s9.txt'];
outputFile=fopen(outputFileName,'wt+');

%read ASCII-delimited numeric data file (txt,delimiter=space,skip first 6 rows)
A=dlmread('c:\Users\katerinapylarinou\Desktop\Sen_Analysis\OutputFiles\land_cover\land3.txt','',6);

%parameters
lookingFor=17;
newvalue=11;

%find 'lookingFor' in the A matrix and also display it on the screen

Avalues=find(A==lookingFor);
disp('number of'); disp(lookingFor); disp(size(Avalues,1));

%change 15% to the 'newvalue'
a=datasample(Avalues,round(size(Avalues,1)*15/100),1,'Replace',false);
A(a)=newvalue;
disp('change 15%:');
disp(size(a,1));

%first write the 6 rows not included in the matrix tothe output file
fprintf(outputFile,'%s\n','ncols         759');
fprintf(outputFile,'%s\n','nrows         545');
fprintf(outputFile,'%s\n','xllcorner     440459.92056084');
fprintf(outputFile,'%s\n','yllcorner     89720.110536575');
fprintf(outputFile,'%s\n','cellsize      5');
fprintf(outputFile,'%s\n','NODATA_value  -9999');
%then write the new matrix
%(if append is not used dlmwrite overwrites the existing data)
dlmwrite('c:\Users\katerinapylarinou\Desktop\Sen_Analysis\OutputFiles\land_cover\land_s9.txt'...
    ,A,'-append','delimiter',' ');
```

Figure 3.14: Script to generate the misclassified land cover layers in Matlab.

In each simulation, only two categories are affected according to the error mapping summarised in Table 3.7. When a category is misclassified to one with a higher elevation, inundation is assumed leading to the transformation of this wetland category to the correct one. This is not the case when a category is misclassified to one characterised by a lower elevation (Figures 3.15 - 3.16). This behaviour is explained from the fact that the process of 'correction' is based on the process of inundation (see section 2.2), ignoring the process of aggradation. Thus, the need to include the

procedure of aggradation is a key finding of this part of the sensitivity analysis. However, even when inundation of the misclassified category is assumed, different habitat distribution is projected for the current time-step, since the conversions are based on empirical calculations. These differences range between around 5- 10% from the current time-step of the original simulation. Different habitat distribution on the current condition therefore projects different future habitat distribution.

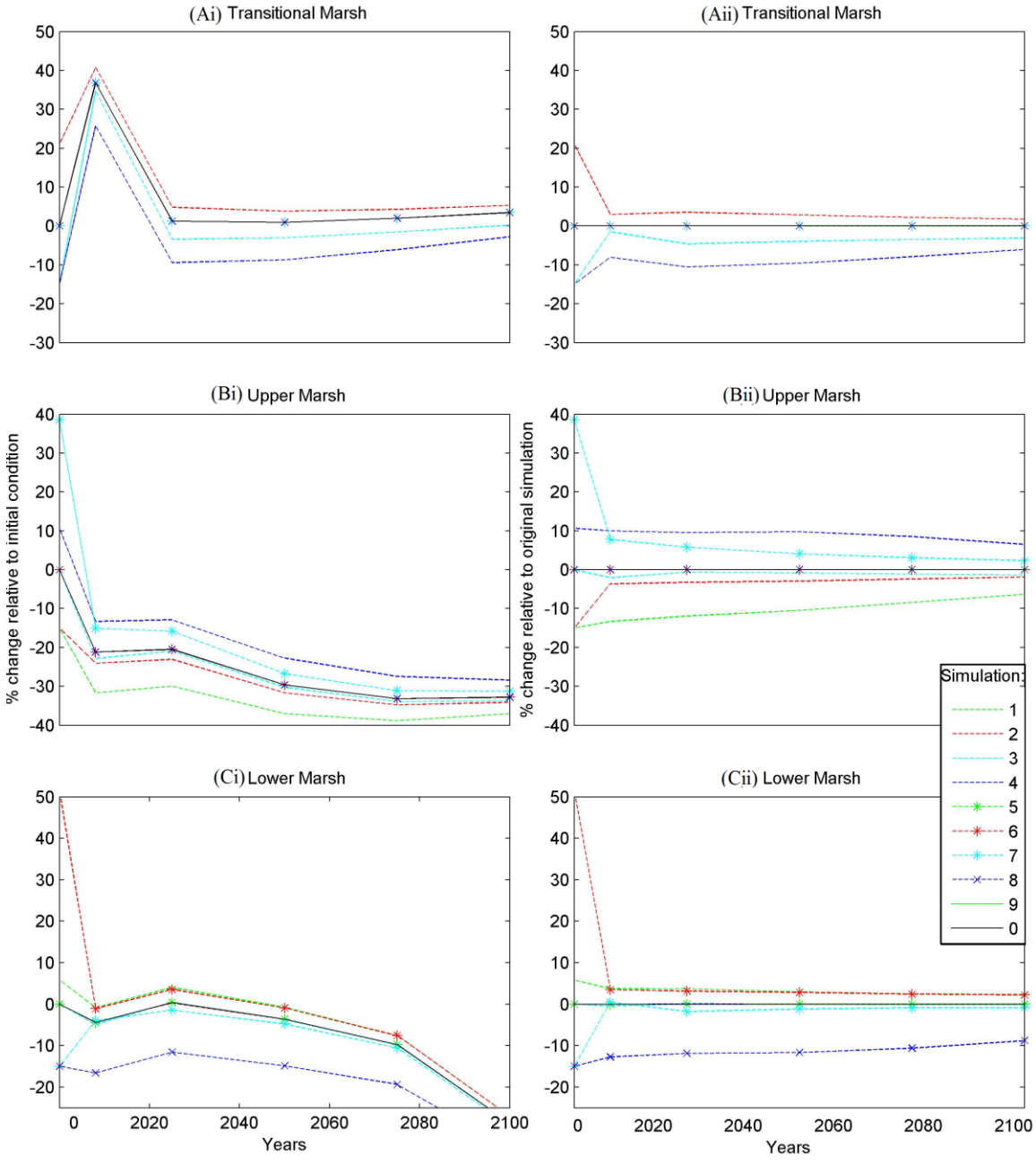

Figure 3.15: Percentage change in (A) transitional marsh, (B) upper marsh and (C) lower marsh area relative to the (i) initial condition and the (ii) original classification for different habitat misclassifications.

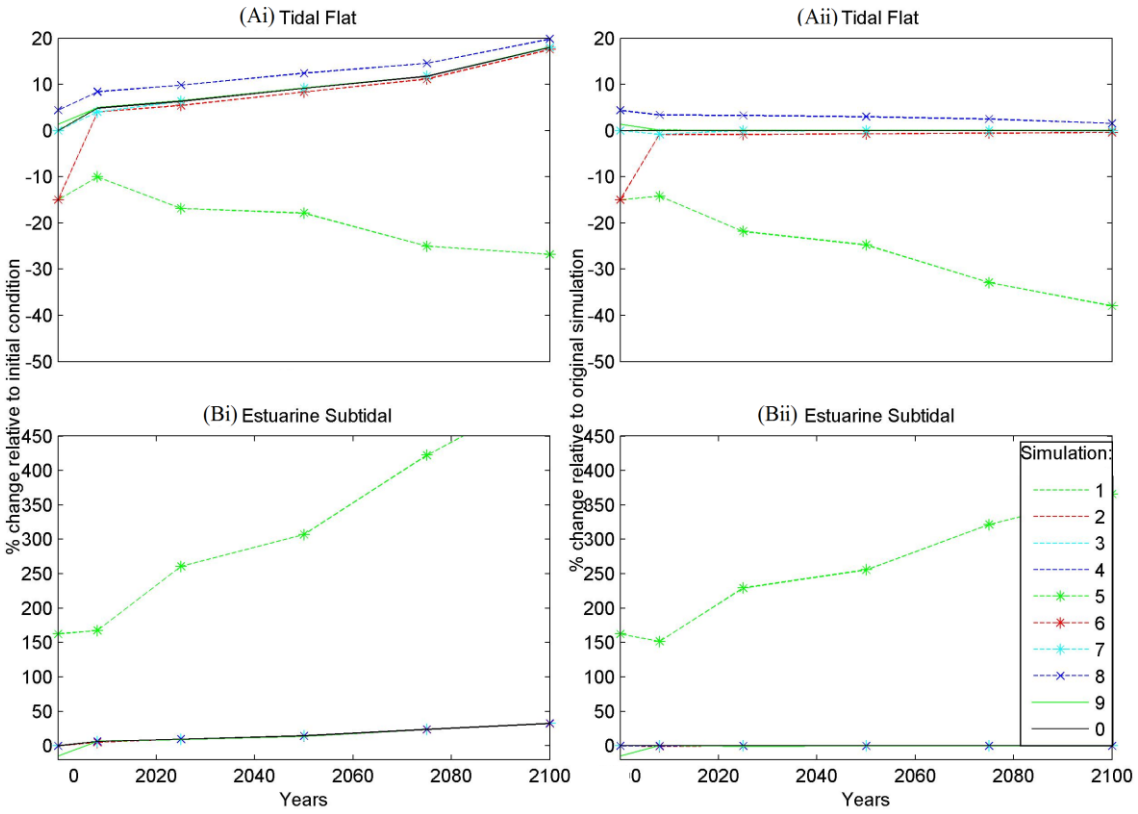

Figure 3.16: Percentage change in (A) tidal flat and (B) estuarine subtidal area relative to the (i) initial condition and the (ii) original classification for different habitat misclassifications.

The sensitivity of the modelled habitat changes to both historic and projected future sea-level rise rate was also examined. The results from this analysis are summarised in Figures 3.17 and 3.18. The response of the wetland categories to these two forcings are the same, because both are actually used to calculate the final sea-level rise applied at each time-step (see eq. 2.4). As expected, the more rapid the rate of sea-level rise, the larger the areas that are inundated. The estuarine subtidal and the tidal flat are enlarged, whilst the area of saltmarsh invariably decreases. Most affected is the lower marsh area reaching a difference of almost 50% from the original simulation at the last time-step (2100) for a historic sea-level rise rate of 3 mm yr^{-1}.

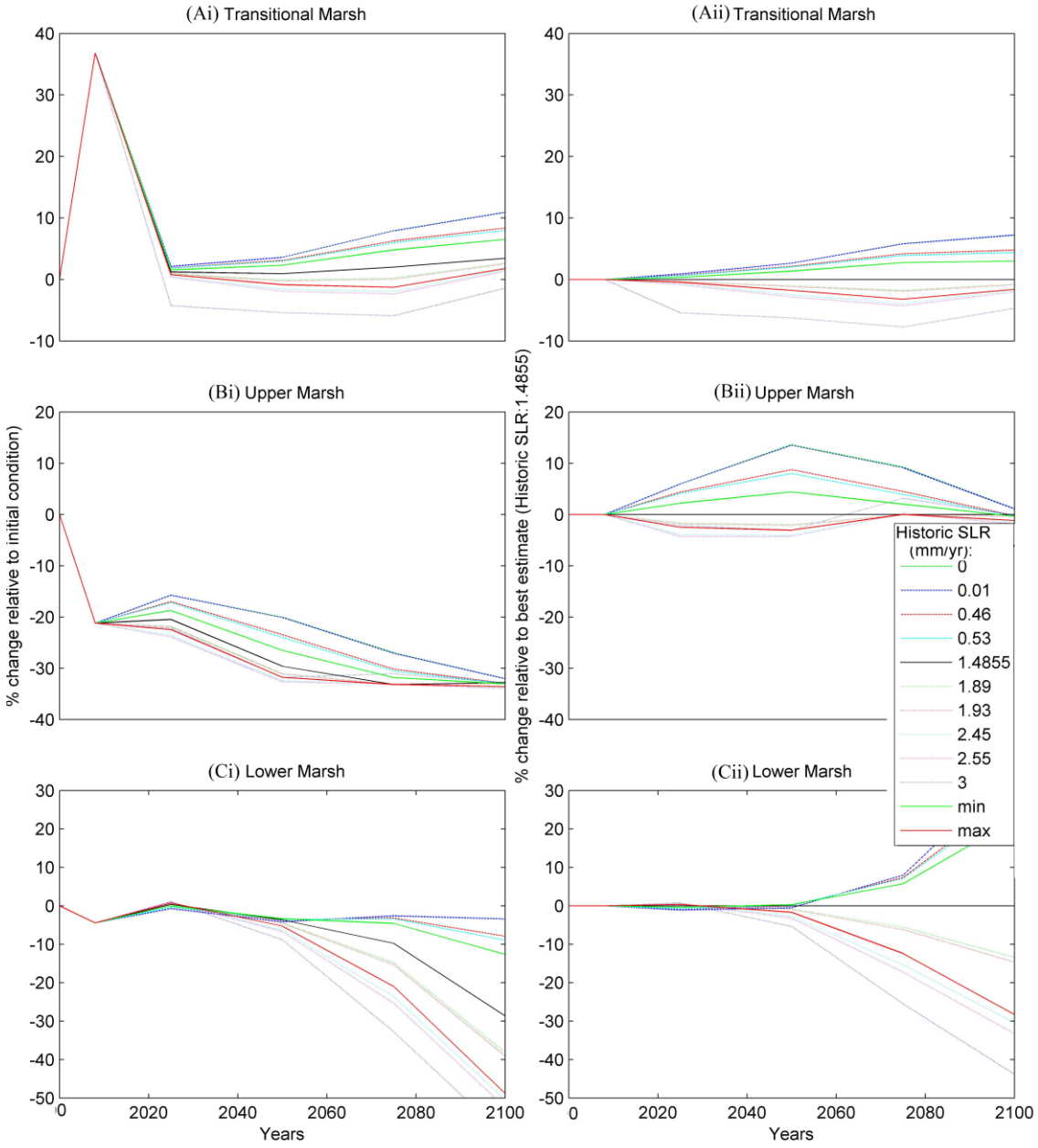

Figure 3.17: Percentage change in (A) transitional marsh, (B) upper marsh and (C) lower marsh area relative to the (i) initial condition and the (ii) best estimation for different historic and future sea-level rise scenarios.

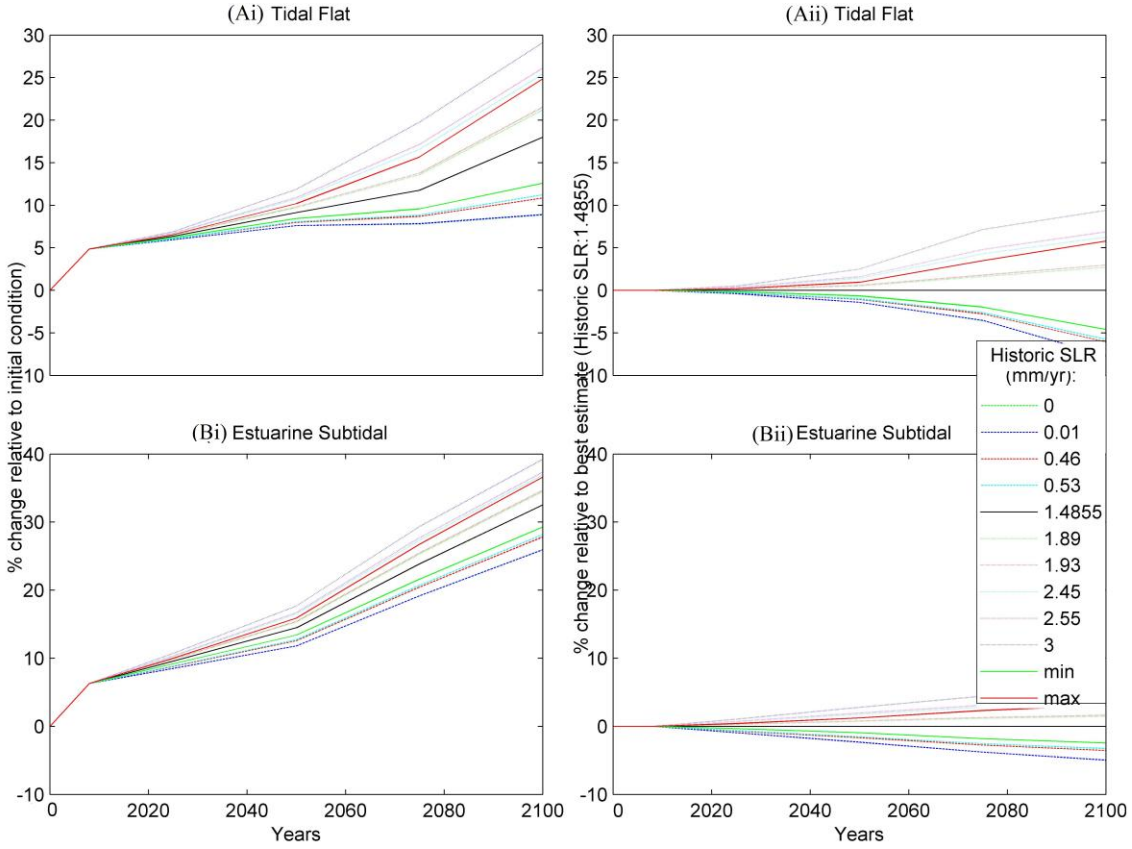

Figure 3.18: Percentage change in (A) tidal flat and (B) estuarine subtidal area relative to the (i) initial condition and the (ii) best estimation for different historic and future sea-level rise scenarios.

Finally, the basic processes included into the model are examined, with first one the process of accretion. This was accomplished by applying different accretion rates for the upper and lower saltmarsh and the tidal flat (Figures 3.19 – 3.21). Upper marsh accretion rates below the 'best estimate' value affect the upper marsh by 10%, but only at the middle time-steps (2025-2050). In contrast, lower and transitional marsh areas are affected during the whole simulation reaching a difference of 10% and 30% respectively at the last time-step. However, at higher accretion rates, all three zones are affected, with the transitional marsh being more vulnerable and reaching a difference of 40% from the best estimate by the year 2100 (Figures 3.19).

The most important outcome at this point is that the transitional marsh is affected by this parameter, although this was not expected according to the SLAMM structure. A further investigation into the model code indicates that this habitat is included into the upper marsh accretion model and thus treated with the same way. Although this is correct, it points out that the accretion module is under-documented.

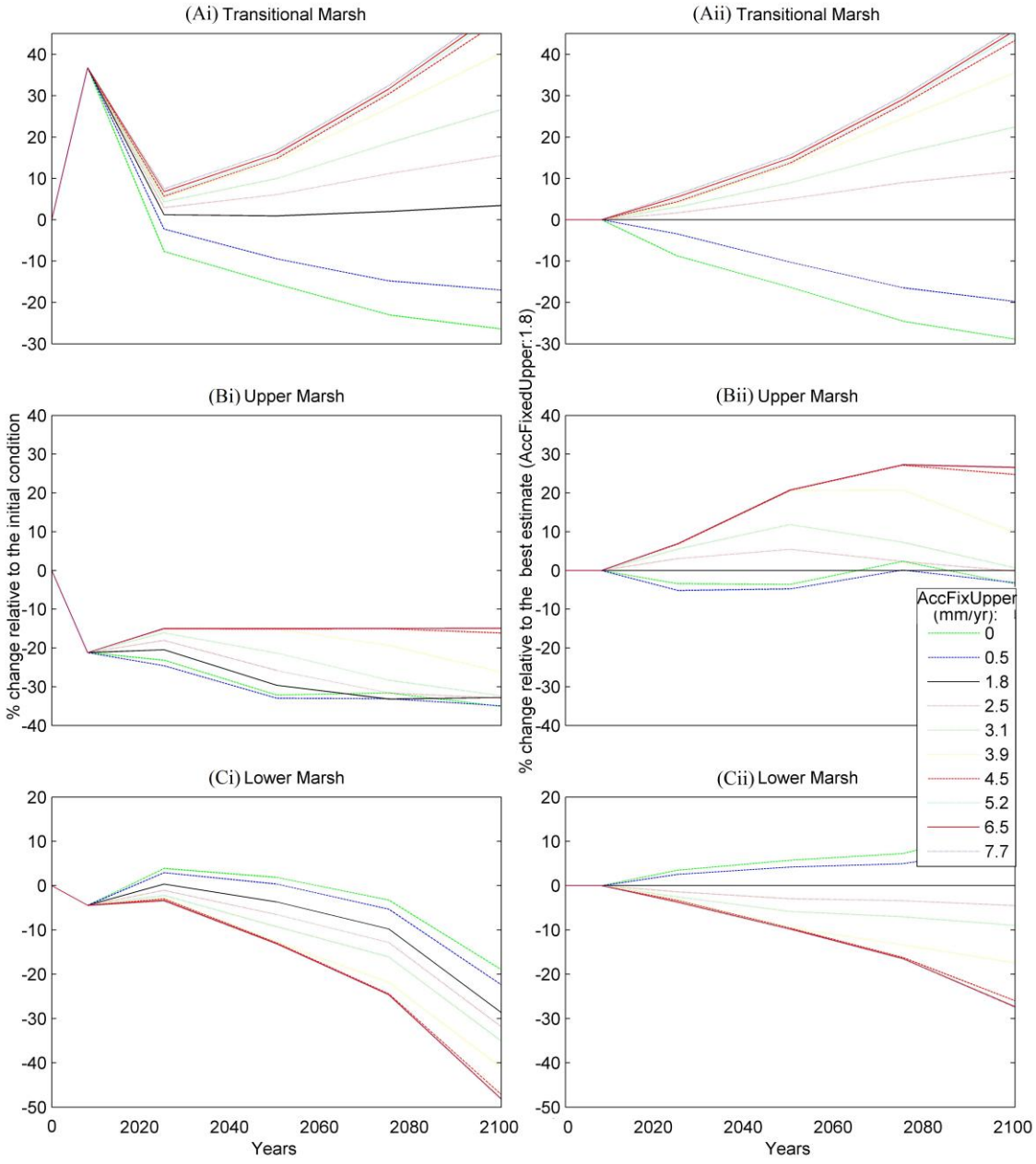

Figure 3.19: Percentage change in (A) transitional marsh, (B) upper marsh and (C) lower marsh area relative to the (i) initial condition and the (ii) best estimation for different upper marsh accretion rates.

The results also show that the lower marsh is very sensitive to changes in the lower marsh accretion parameter. In absence of accretion on the lower marsh, its area is very vulnerable to the sea-level rise and is gradually decreased during the simulation; up to half the low marsh area may be lost by 2100, with a corresponding increase in the area of tidal flat. The higher the accretion rate, more lower marsh area is capable to keep up with the sea-level rise, increasing its area and therefore decreasing the area of the tidal flat (Figure 3.20).

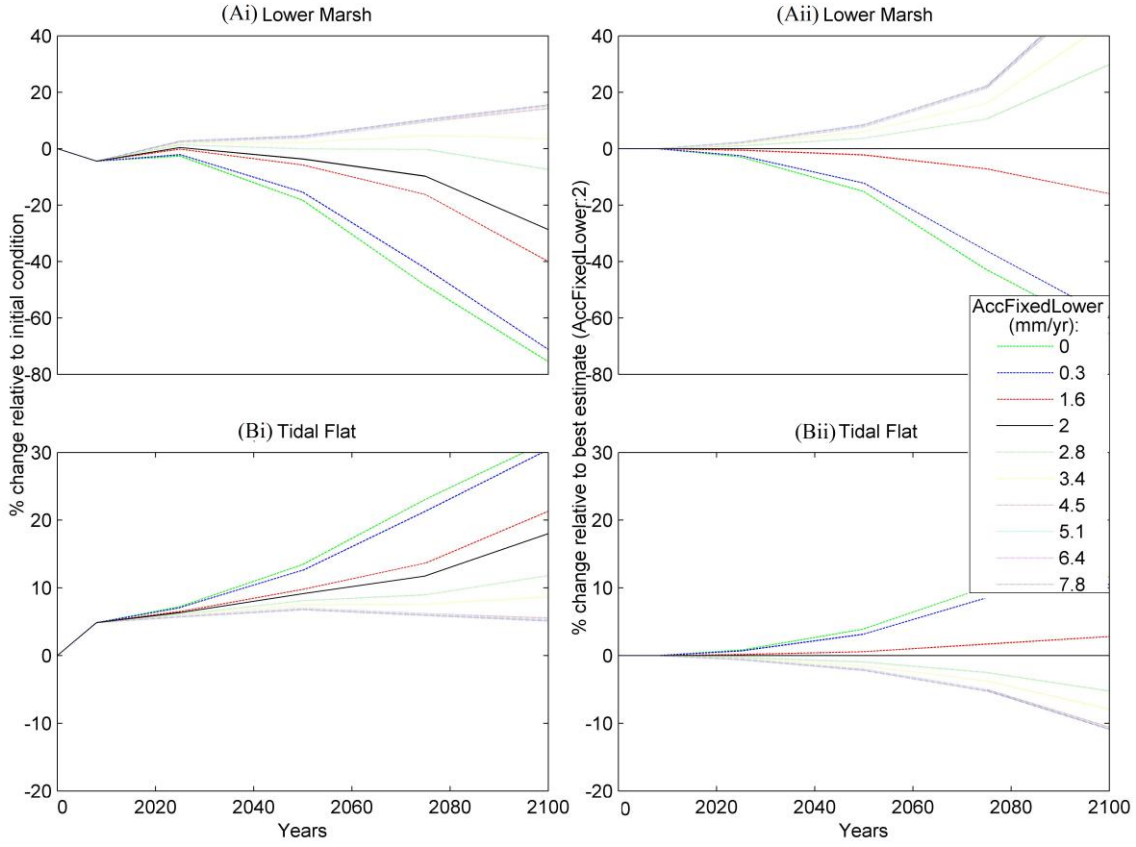

Figure 3.20: Percentage change in (A) lower marsh and (B) tidal flat area relative to the (i) initial condition and the (ii) best estimation for different lower marsh accretion rates.

The model is less sensitive to tidal flat accretion rate, with the tidal flat affected by only 2% at the last time-steps of the simulation (Figure 3.21). However, the most important outcome here is that accretion rates higher than 4.5 mm yr^{-1} for all three sub-models do not further affect the projected wetland categories, since these rates are higher than the sea-level rise rate, demonstrating again the need to include aggradational process in the model.

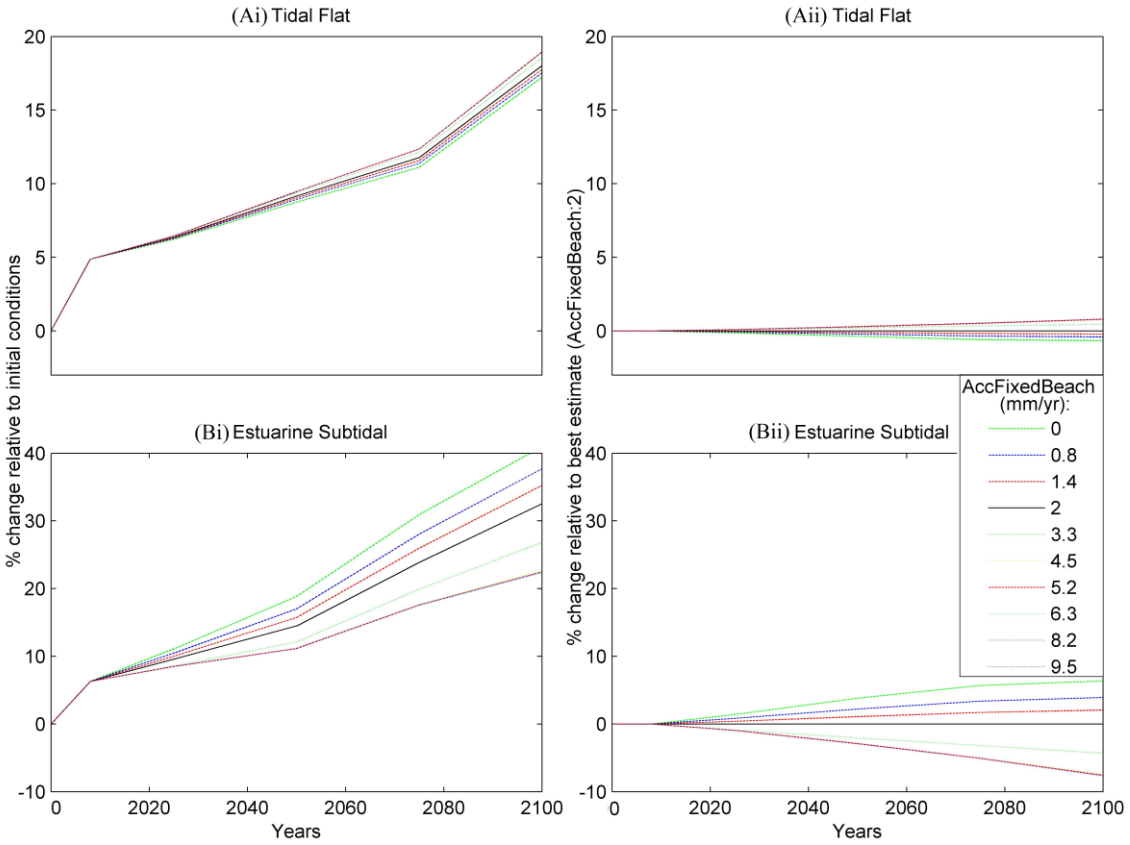

Figure 3.21: Percentage change in (A) tidal flat and (B) estuarine subtidal area relative to the (i) initial condition and the (ii) best estimation for different tidal flat accretion rates.

The last process examined is the process of erosion. As explained in Section 2.2, marsh erosion is assumed to occur within SLAMM when the fetch is more than 9 km. This criterion is not met for the small Newtown estuary, and therefore marsh erosion is not modelled. Thus, changes in the marsh erosion parameter do not affect its habitat distribution. However, evidence from studies at the southeast England (Burd, 1992; Cooper et al., 2001; van der Wal and Pye, 2004; Wolters et al., 2005) indicate that marsh erosion can be caused, even in estuaries with a smaller fetch, by a combination of high tides, strong winds, and increased wave height, pointing out the weakness of SLAMM to properly model the process of marsh erosion in the small UK estuaries. Thus, the need to incorporate a threshold of a smaller fetch within SLAMM has emerged through the sensitivity analysis.

On the other hand, the tidal flat is assumed to be eroded at each time-step with only the requirement of its adjustment to water. Therefore, changes at the tidal flat erosion parameter affect the vulnerability of the Newtown estuary to the sea-level rise; higher values of tidal flat erosion increase the eroded tidal flat area. Thus, the latter decreases

its total area by being converted to subtidal, which therefore is increased (Figure 3.22). It is worth noting here that values of tidal flat erosion >0.3 m yr^{-1} do not have a further influence on the projected results.

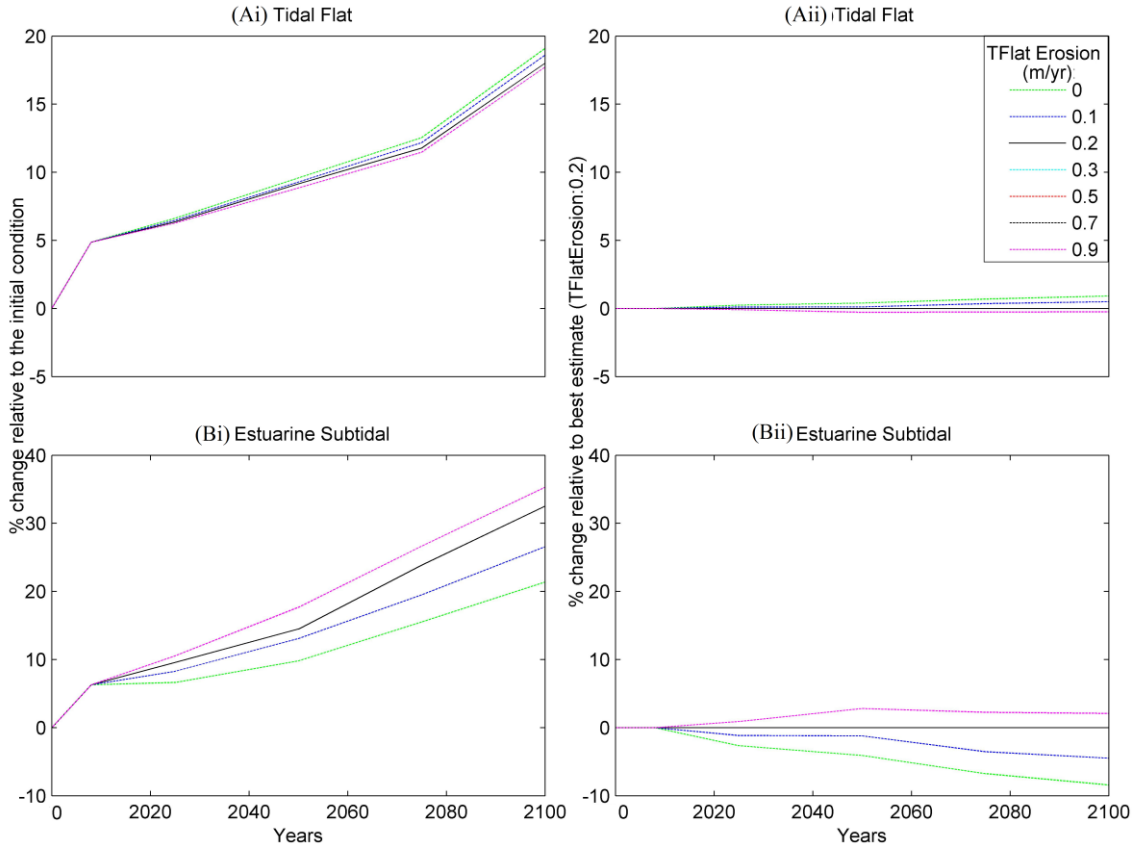

Figure 3.22: Percentage change in (A) tidal flat and (B) estuarine subtidal area relative to the (i) initial condition and the (ii) best estimation for different tidal flat erosion rates.

As shown in the previous chapter, more sophisticated spatial accretion routines are also available within SLAMM. These calculate the accretion rates for each habitat as a time-varying function of cell elevation, distance to channel and salinity. These are specified according to the following equations:

A_{elev} = accretion rate for a cell as a function of elevation

= MinAccr + ShapePctile * (MaxAccr-MinAccr) (3.3)

where MaxAccr = Max. accretion rate for the specific site given optimal distance to tidal channel, elevation and salinity (mm/year)

MinAccr = Min. accretion rate for the specific site (mm/year)

ShapePctile = (Shape(Elev)-MinShape) / (MaxShape-MinShape) (3.4)

Shape = $a\ (1\text{-}ElevPctile)^3 + b\ (1\text{-}ElevPctile)^2 + c\ (1\text{-}ElevPctile)$ (3.5)

ElevPctile = (Elev-ElevMin) / (ElevMax – ElevMin) (3.6)

Elev = elevation of the cell relative to MTL (m)

ElevMax = max. elevation for the specific wetland type (m above TL)

ElevMin = min. elevation for the specific wetland type (m above MTL)

a,b,c = cubic coefficients defining the shape of the curve (unitless)

D =factor representing distance to river or tidal channel

$$= \frac{1 - D2Channel}{DistEffectMax\ (1 - D_{min})} \quad (3.7)$$

where D2Channel =distance to channel (m)

DistEffectMax = not additional effect beyond this distance

D_{min} = min value of D factor (unitless)"

If there are no available data to parameterize this relationship, it should be ignored by setting the DistEffectMax to 0, and Dmin to 1 (Clough et al., 2010).

S = salinity factor representing salinity effects

$$\text{If } Salinity_{cell} \text{ in } [Salinity_{TMax} - (T\max Zone/2), Salinity_{TMax} + (T\max Zone/2)] \quad (3.8)$$

$$= S_{NonTMax} + (1 - S_{NonT\max})(1 - |Salinity_{TMax} - Salinity_{Cell}|/(TMaxZone/2)) \quad (3.9)$$

$$\text{otherwise } S = S_{NonTMax} \quad (3.10)$$

where $Salinity_{cell}$ = salinity at a given cell (ppt)

$Sailinity_{TMax}$ = salinity level at which max accretion rate occurs (ppt)

$S_{NonTMax}$ = accretion factor with no salinity effect (unitless)

TMaxZone = salinity range over which there is salinity effect (ppt)

The salinity factor is usually ignored because the rates of accretion can be described based on the elevation and distance to channel (Clough et al., 2010). At this stage, the distance to channel will also be ignored, due to lack of data availability. Therefore, the accretion rates are calculated based on the elevation only. The hypothetical accretion pattern is presented on Figure 3.23, based on which the accretion sub-model for each habitat is calibrated (Table 3.8; Simulation 'N_UK_a').

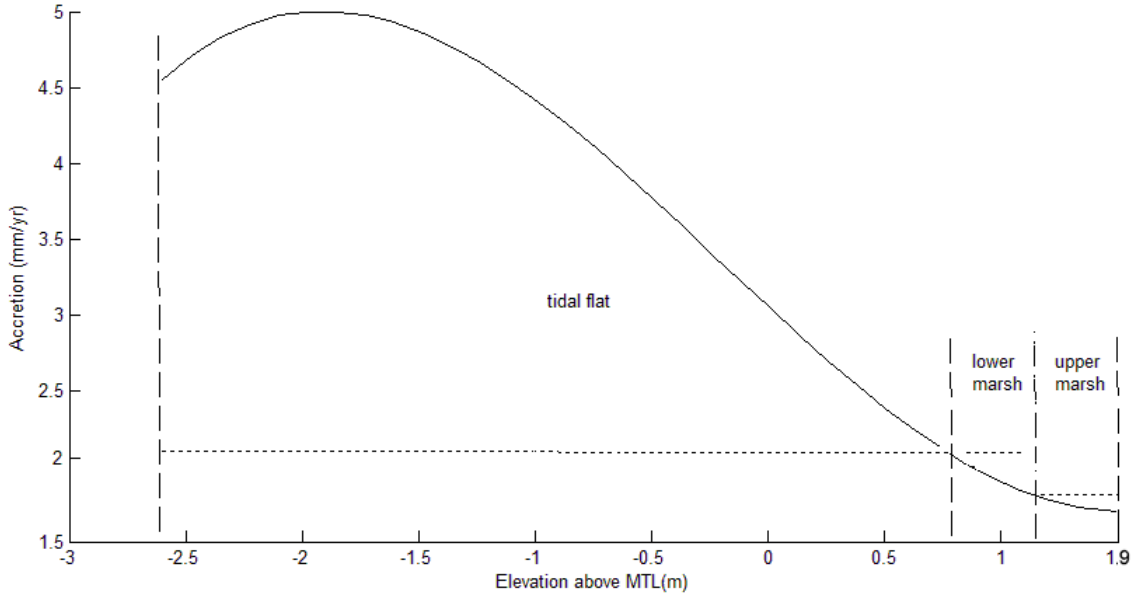

Figure 3.23: Elevation-dependent accretion rates calculated in SLAMM. Vertical dash lines illustrate the boundaries of each habitat, and horizontal dot lines demonstrate the constant accretion rate used for each habitat at the previous simulation.

Table 3.8: Accretion model parameters for the Newtown Estuary, Isle of Wight, UK.

Accretion model Parameters	**Upper and Transitional Marsh**	**Lower marsh**	**Tidal Flat**
Max Accretion rate (mm yr^{-1})	1.8	2	5
Min Accretion rate (mm yr^{-1})	1.7	1.8	2
a coefficient (cubic)	-0.8	-0.8	-1
b coefficient (square)	1	1	0.9
c coefficient (linear)	1	1	0.5

Compared with the previous simulation where constant accretion rates used (‘Simulation ‘N_UK’), the tidal flat experiences higher accretion rates making it more able to cope with sea-level rise. This tolerance of the tidal flat to sea-level rise combined with the lower accretion rates for the lower marsh area, forces the former to migrate landward, squeezing slightly the lower marsh (Table 3.9).

Table 3.9: Summary of the output from evaluation of the accretion sub-model for the Newtown estuary (areas in ha).

Simulation name: "N_UK"										
Date	**SLR**	**Dry Land**	**Trans. M.**	**Upper M.**	**Lower M.**	**Tidal Flat**	**Est. Subtidal**	**Ocean Beach**	**Ocean Flat**	**Ocean**
0	0	638.1	14.3	20.0	51.5	176.4	16.3	0.0	41.6	47.7
2008	0	628.7	19.5	15.8	49.2	185.0	17.3	0.8	41.2	48.4
2025	0.0563	627.7	14.5	15.9	51.7	187.6	17.8	0.4	40.8	49.5
2050	0.1583	625.7	14.4	14.1	49.6	192.5	18.6	0.0	39.7	51.2
2075	0.2778	623.0	14.6	13.4	46.5	197.1	20.2	0.0	37.7	53.4
2100	0.4123	619.5	14.8	13.5	36.8	208.2	21.6	0.05	35.4	56.2
Simulation name: "N_UK_A"										
Date	**SLR**	**Dry Land**	**Trans. M.**	**Upper M.**	**Lower M.**	**Tidal Flat**	**Est. Subtidal**	**Ocean Beach**	**Ocean Flat**	**Ocean**
0	0	638.1	14.3	20.0	51.5	176.4	16.3	0.0	41.6	47.7
2008	0	628.7	19.5	15.8	49.2	185.0	17.3	0.8	41.2	48.4
2025	0.0563	627.7	14.4	16.0	51.7	187.8	17.7	0.4	40.8	49.5
2050	0.1583	625.7	14.3	14.2	49.6	193.1	18.1	0.0	39.7	51.2
2075	0.2778	623.0	14.4	13.5	46.3	198.4	19.2	0.0	37.7	53.4
2100	0.4123	619.5	14.6	13.6	36.1	210.6	19.9	0.05	35.4	56.2
compare "N_UK" to "N_UK_A"										
TRUE	TRUE	TRUE	TRUE	TRUE	TRUE	TRUE	TRUE	TRUE	TRUE	TRUE
TRUE	TRUE	TRUE	TRUE	TRUE	TRUE	TRUE	TRUE	TRUE	TRUE	TRUE
TRUE	TRUE	TRUE	**FALSE**	**FALSE**	TRUE	**FALSE**	**FALSE**	TRUE	TRUE	TRUE
TRUE	TRUE	TRUE	**FALSE**	**FALSE**	TRUE	**FALSE**	**FALSE**	TRUE	TRUE	TRUE
TRUE	TRUE	TRUE	**FALSE**	**FALSE**	**FALSE**	**FALSE**	**FALSE**	TRUE	TRUE	TRUE
TRUE	TRUE	TRUE	**FALSE**	**FALSE**	**FALSE**	**FALSE**	**FALSE**	TRUE	TRUE	TRUE

3.4 Further modifications of the code

The pilot application of the modified SLAMM to the Newtown estuary reveals the need for a number of further modifications to the model code. First, it is evident that the process of aggradation (i.e. the seaward expansion of specific intertidal wetland units) must be included. This is accomplished by enabling the additional transitions depicted in Figure 3.24. The source code is detailed in A-0.27. The maximum elevation of each wetland category within a cell is computed at each time-step as a function of its minimum one, by assuming the same accretion rate. The changes made in the code assume that aggradation occurs when this maximum elevation is greater than the default maximum elevation for this wetland category. In contrast to the 'original' code, the modified one enables this procedure even for the current time-step, when it is necessary, and most importantly also includes the tidal flat wetland category. Under this procedure the wetland class then converts to one that is higher within the tidal frame. The fraction transformed is then computed for each time-step, as a function of the maximum elevation and the upper elevation boundary of that wetland and also the slope of that cell (equation 3.11).

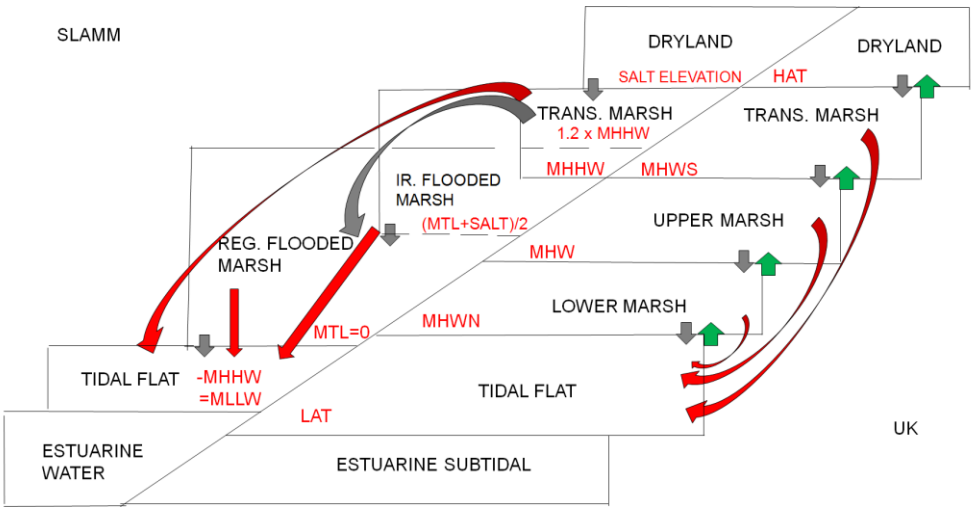

Figure 3.24: SLAMM decision tree modification including procedure of aggradation (grey arrows: inundation; red arrows: erosion, green arrows: aggradation).

$$FracLost_{Cat} = \frac{\left(\frac{UpperBound - MaxElev_{Cat,t}}{\tan Slope}\right)}{Width_{Cat}} \quad (3.11)$$

where FracLostCat = Fraction of wetland lost in time step (dimensionless)
MaxElev = Max elevation of the wetland class at time t (m)
UpperBound = Max elevation boundary of the wetland class (m)
Slope = Slope of the cell (degrees)
Width Cat = Width of the cell (m)

With the process of aggradation enabled, the response of the wetland categories to the UKCP09 SE mean sea-level rise scenario is changed (Figure 3.25). First, when the modified code is applied to the Newtown Estuary and compared to results obtained with previous code and the initial site-specific parameters clear differences are evident for accretion values larger than the sea-level rise; marsh areas can cope with sea-level rise and more importantly propagate seawards. Most sensitive is the model to the lower marsh accretion parameter where lower marsh loses more than half of its area by 2100 due to seaward propagation of the upper marsh by increasing its area by almost 200%. (Figure 3.25B). In addition, different results are projected even for the initial accretion values. The correction of the habitat distribution in the first time-step is not only determined by the minimum elevation of each wetland category, resulting to inundation, but the maximum elevation is also taken into consideration determining if the specific wetland category is subjected to aggradation too. Therefore, more differences can be corrected at this time-step. The fact that the projected habitat distribution for the current time-step is very similar to the initial one indicates the success of this modification step.

Second, it is clear that the marsh erosion procedure needs to be modified. As noted in Chapter 2, SLAMM assumes that marsh is eroded when it is adjacent to water where the fetch is more than 9 km. Although this could be the case for some of the larger estuaries of the US, such a long fetch is rare in UK estuarine systems where even a smaller fetch can cause wave-driven marsh-erosion (Wolters et al., 2005). In recognition of this, the fetch threshold within SLAMM is modified to 0.5 km as described in Figures A-0.28 and A-0.29. Marsh is thus projected to experience lateral erosion when it is adjacent to water where the fetch exceeds 0.5 km, increasing the tidal flat area (Simulation ‘N_2’). Finally it is notable that, although dryland should also be subjected to erosion, this

process is not actually implemented in the original SLAMM code. When this process is enabled (Figure A-0.30; Simulation 'N_3'), the results project a slight increase of the tidal flat area (Table 3.10).

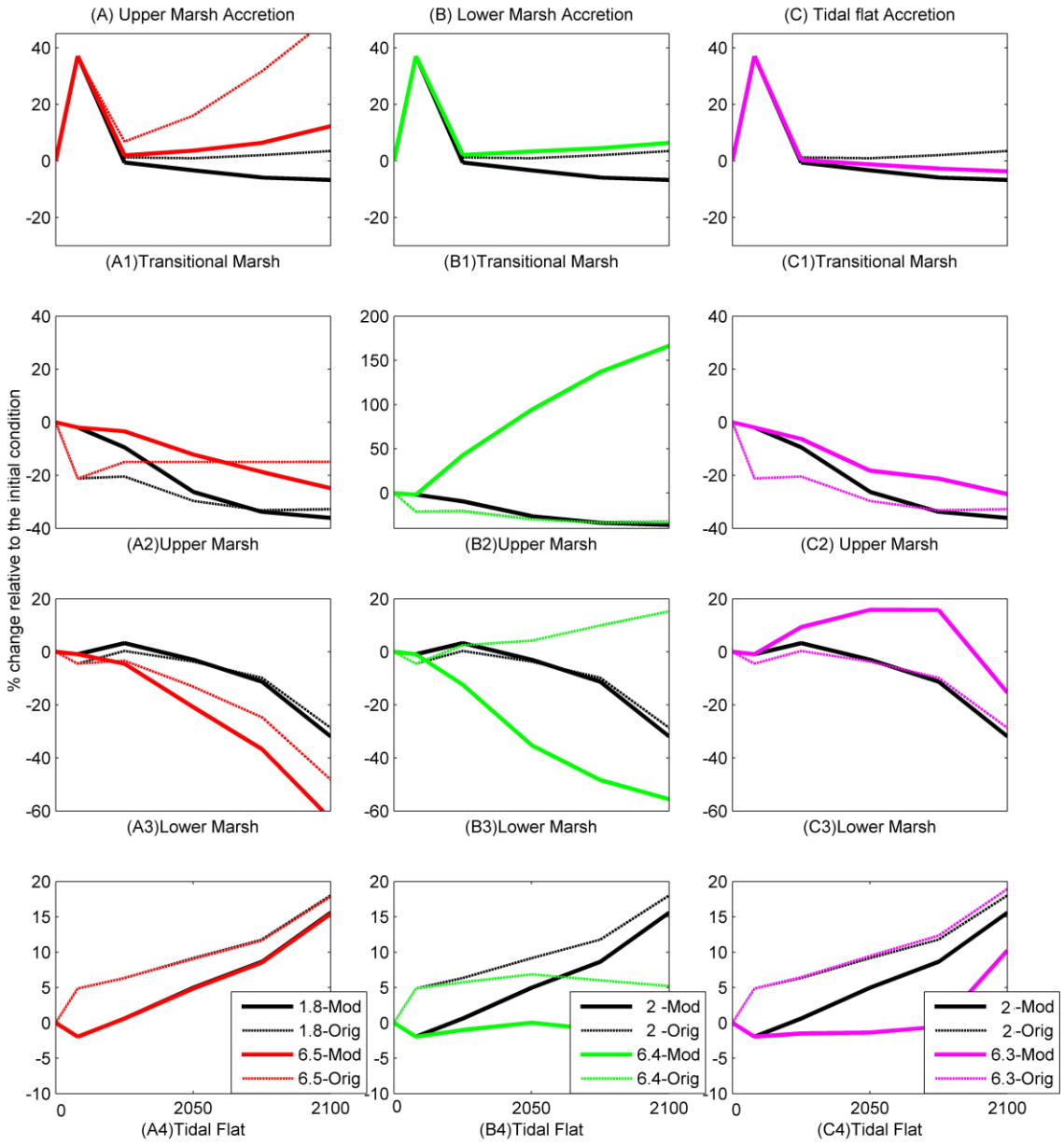

Figure 3.25: Response of the (1) transitional marsh, (2) upper marsh, (3) lower marsh and (4) tidal flat to different accretion values for the (A) upper marsh, (B) lower marsh and (C) tidal flat before (original) and after (modified) the inclusion of aggradation. In both cases, initial accretion rates of 1.8 and 2 mm yr^{-1} are used for the upper marsh and both the lower marsh and the tidal flat respectively, as well as accretion rates higher than the sea-level rise equal to 6.5, 6.4 and 6.3mm yr^{-1} for the upper, lower marsh and the tidal flat respectively.

Table 3.10: Impacts of sea-level rise during the modification of erosion process.

Simulation: "N_1": Fetch: 9 km							
Date	**SLR**	**Dry Land**	**Trans. M.**	**Upper M.**	**Lower M.**	**Tidal Flat**	**Est. Subt.**
0	0	638.1	14.3	20.0	51.5	176.4	16.3
2025	0.0563	633.7	19.9	17.2	53.0	173.8	17.9
2050	0.1583	631.3	14.5	14.7	53.9	181.8	18.5
2075	0.2778	629.5	13.4	13.3	46.0	192.3	19.9
2100	0.4123	626.7	13.2	12.9	35.1	204.4	21.5
Simulation:"N_2" Fetch: 0.5 km							
Date	**SLR**	**Dry Land**	**Trans. M.**	**Upper M.**	**Lower M.**	**Tidal Flat**	**Est. Subt.**
0	0	638.1	14.3	20.0	51.5	176.4	16.3
2025	0.0563	631.5	21.8	17.2	52.3	173.6	18.9
2050	0.1583	630.8	14.0	15.1	53.6	181.5	19.1
2075	0.2778	628.1	14.5	13.2	45.3	192.1	20.5
2100	0.4123	625.4	14.2	12.8	34.3	204.2	22.1
Simulation:"N_3": Dryland erosion included							
Date	**SLR**	**Dry Land**	**Trans. M.**	**Upper M.**	**Lower M.**	**Tidal Flat**	**Est. Subt.**
0	0	638.1	14.3	20.0	51.5	176.4	16.3
2025	0.0563	631.5	21.7	17.2	52.3	173.7	17.2
2050	0.1583	630.8	14.0	15.1	53.6	181.6	17.9
2075	0.2778	628.1	14.4	13.2	45.3	192.2	19.4
2100	0.4123	625.5	14.0	12.8	34.4	204.3	20.7

The final decision tree of the modified SLAMM is presented in Figure 3.26. This version of the source code provides the basis for the more substantive applications to the Suffolk estuaries and Norfolk barrier coastline summarised in the following Chapters.

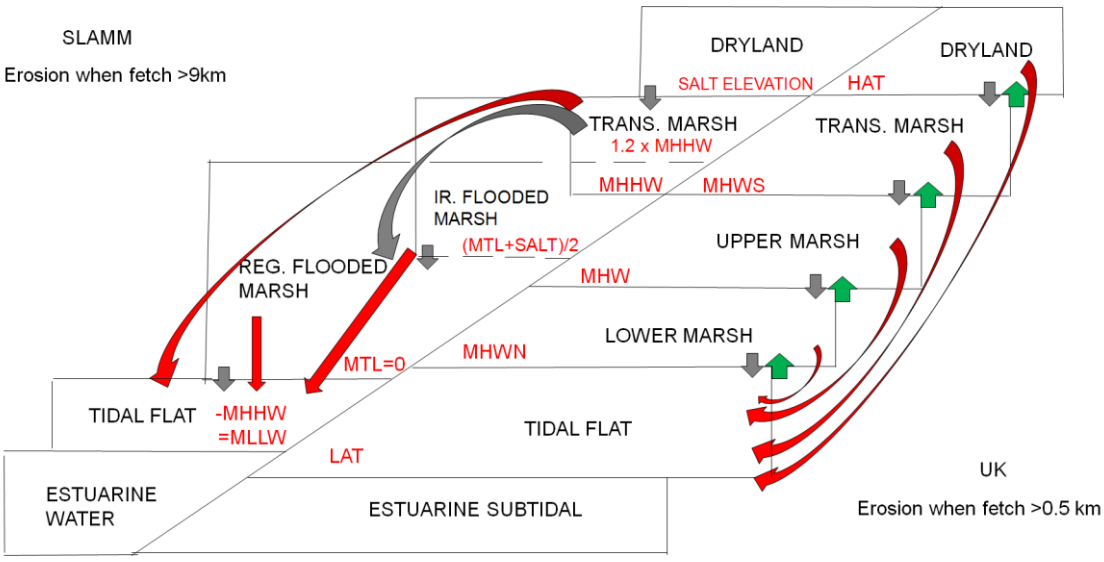

Figure 3.26: Updated SLAMM decision tree (grey arrows: inundation; red arrows: erosion, green arrows: aggradation).

4 APPLICATION OF THE MODIFIED SLAMM TO SUFFOLK ESTUARIES, UK

The modified SLAMM code is applied to selected estuaries in Suffolk, eastern England, in order to critically evaluate more fully its ability to produce robust projections of intertidal habitat change in more complex estuaries. A key factor influencing the initial selection of these estuaries was the availability of Environment Agency LiDAR data under the NERC iCOASST project (Nicholls et al., 2012; 2015). The Suffolk estuaries are of interest on account of their varied geomorphology and long history of reclamation. A starting point here is to use the modified SLAMM code to evaluate the likely changes of the existing intertidal environment due to the climate-driven sea-level rise. However, the flood defences that currently protect the extensive reclaimed areas will require upgrading in order to cope with the projected sea-level rise (French, 2008). In recognition of this, managed realignment has to be considered. In that case, the evolution of the protected areas needs to be investigated by assuming the defences inactive.

SLAMM is initially applied to the Blyth estuary in order to investigate the sensitivity of the projected habitat distribution to the different assumptions made in the underlying sub-models for the tidal flat and saltmarsh and the extent to which these can be tuned to allow simulation of the effects of removal or realignment of the flood defences that protect a large proportion of the natural estuary intertidal. A second application models intertidal change in the larger Deben estuary. This has a less complex morphology but fewer datasets exist with which to constrain the sedimentation sub-models in SLAMM.

4.1 Blyth Estuary

A composite LiDAR dataset (2 m resolution) produced by the Environment Agency from surveys undertaken in 2010 and 2012 was used as the base DEM for the Blyth. These data were integrated with subtidal bathymetry surveys undertaken by the UCL Coastal and Estuarine Research Unit between 1998 and 2001. The resulting elevation dataset, resampled to 5 m resolution, is presented in Figure 4.1. The derived slope and the land cover layers used to define the model domain are shown in Figures 4.2 and 4.3 respectively. However, one more layer is necessary now indicating the areas protected

by defences (Figure 4.4). These figures illustrate the varied geomorphology and reclamation patterns of the Blyth estuary. In the upper part it is enclosed by earth embankments that protect low farmland, but is enlarged in the middle part characterised by a large tidal prism of the abandoned Bulcamp, Sandpit and Angel marshes and by reedbeds. Finally, its entrance is restricted by defences that protect extended low-lands. Approximately 17 km of earth embankments protect around 67 ha of land from tidal flooding (CHaMP, 2002; French, 2003; French and Burningham, 2003).

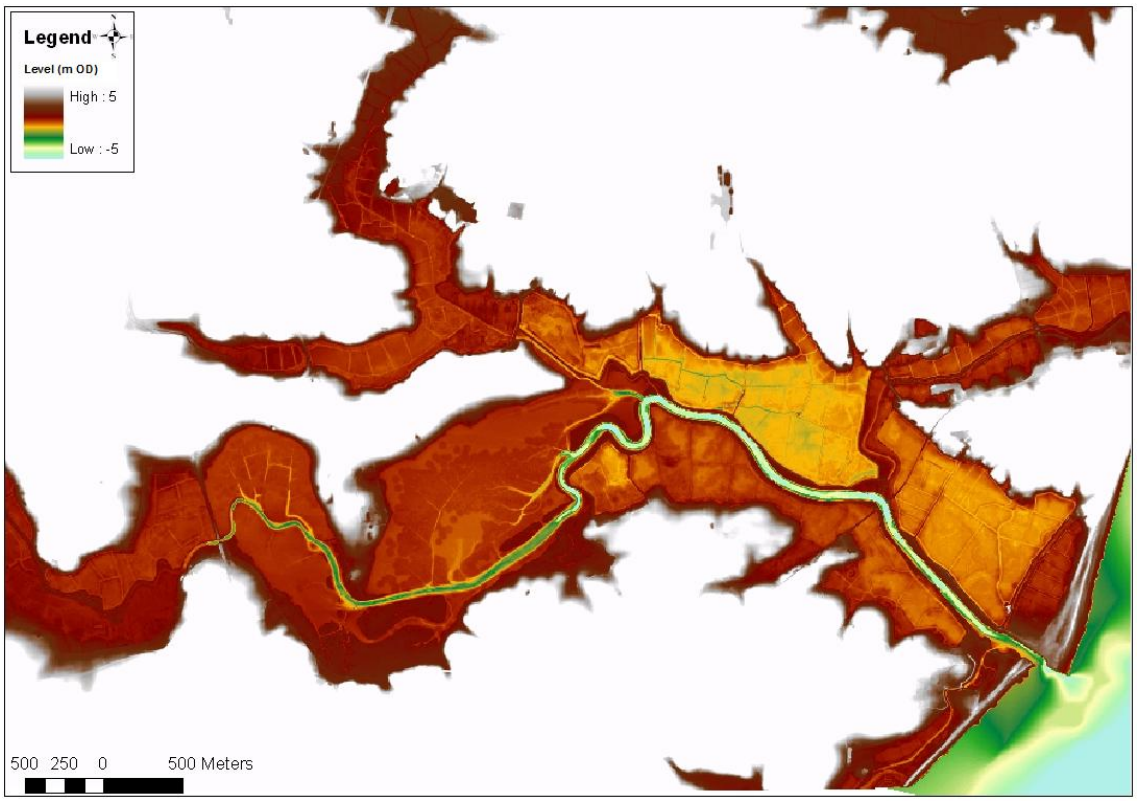

Figure 4.1: Topographic and bathymetric DEM of the Blyth Estuary.

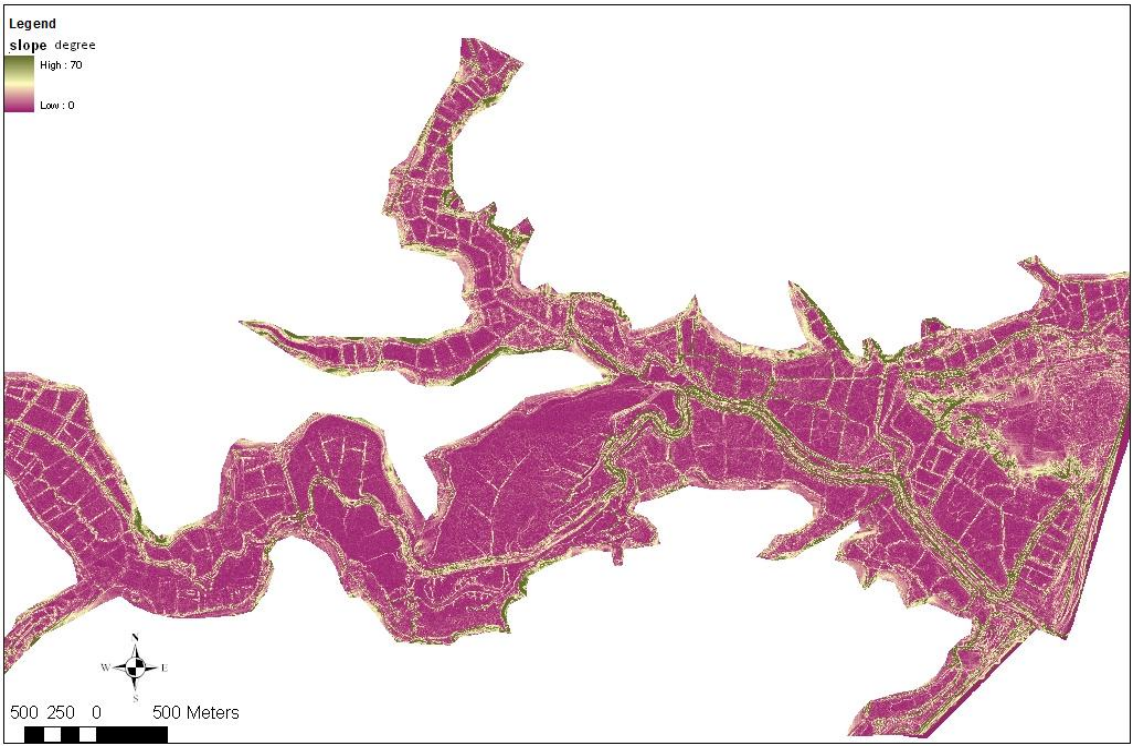

Figure 4.2: Slope map of the Blyth Estuary.

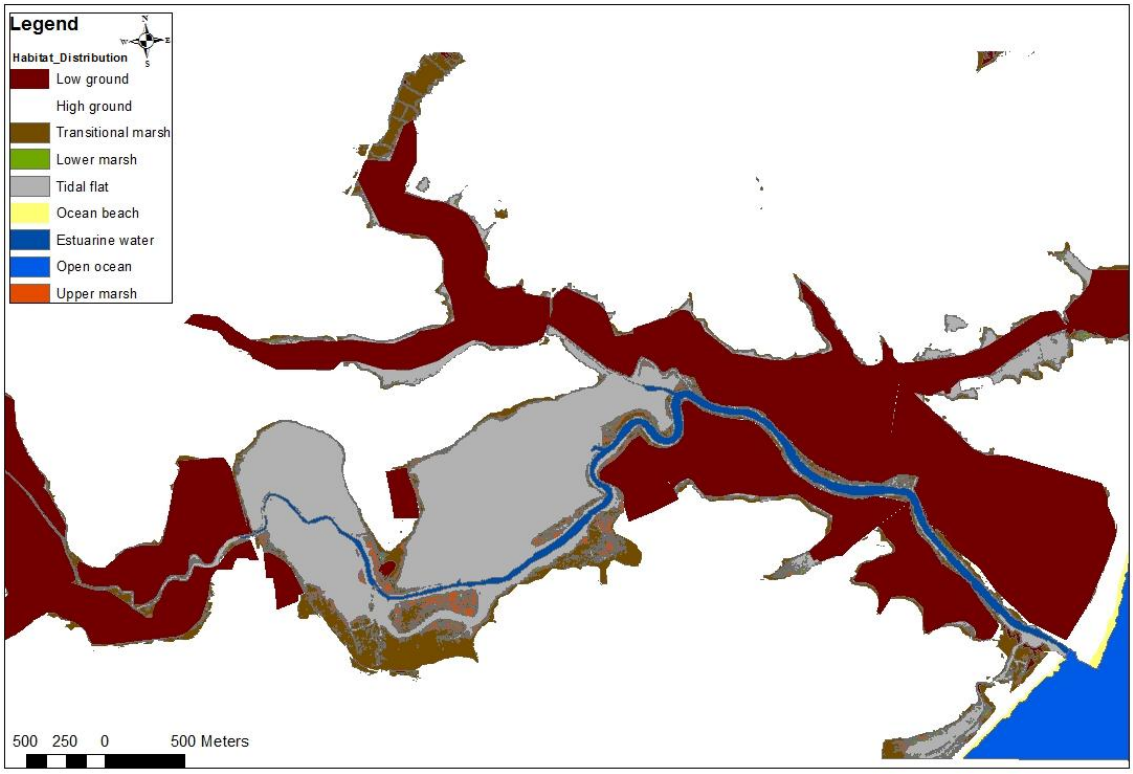

Figure 4.3: Land classification map of the Blyth Estuary.

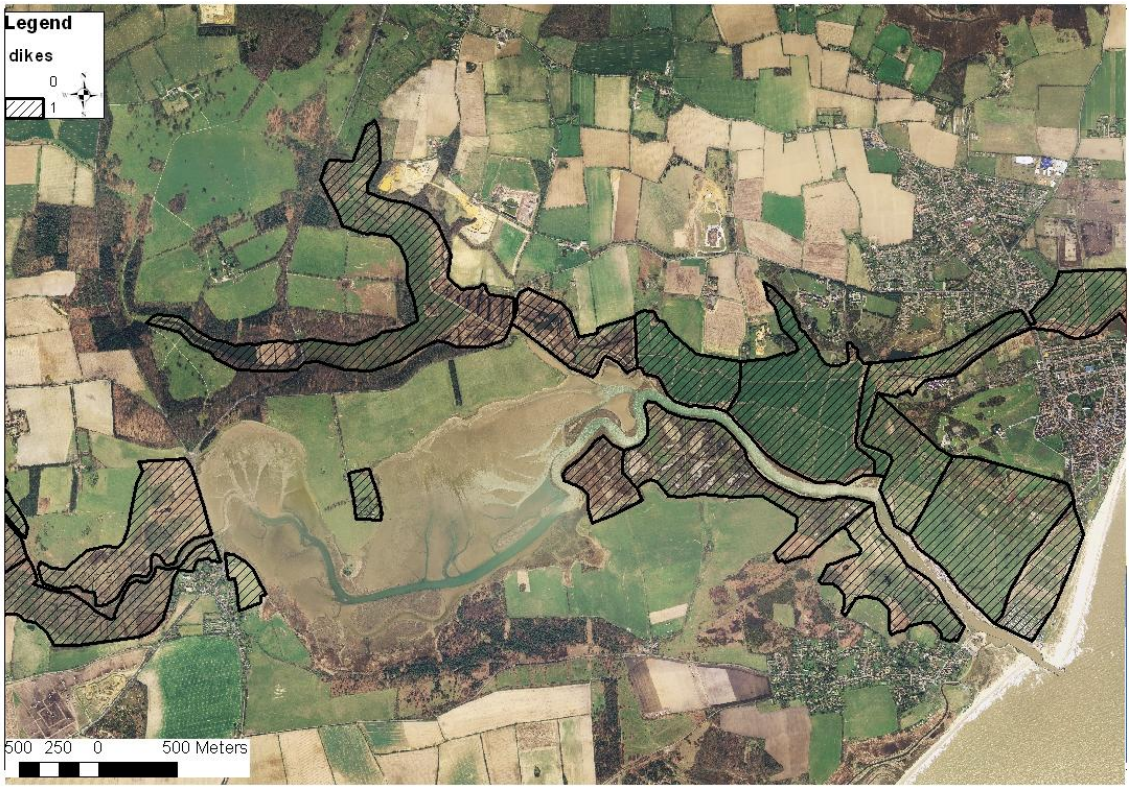

Figure 4.4: Flood compartments of the Blyth Estuary (after French 2008).

Table 4.1 summarises the required site parameters for the model runs. The historic sea-level trend includes the vertical land movements and is estimated at 2.7 mm yr^{-1} using the closest tide gauge station at Lowestoft (around 25 km to the northeast) (PSMSL, 2012). The tidal regime of the middle estuary is used to set up the model, as obtained from the Hydrographic Survey undertaken in the Blyth estuary by the Gardline Environmental Ltd in 2003 for the Environment Agency (Figure 4.5). A higher HAT is taken into account, though, taken into consideration the strong surge influence to the tides, and therefore to the habitat distribution; in 1953 the surge reached 3.6 m OD at Southwold (French, 2001; French and Burningham, 2003). Mean marsh accretion parameters are obtained from a survey undertaken by French and Burningham (2003) for the period 1997 and 2001, while observed tidal flat accretion rates are obtained from a sedimentation survey undertaken by Pye and Blott (2008b) in December 2008. Finally, the extensive literature on the Blyth estuary indicates that some of the abandoned defences in the Sandpit, Angel and Bulcamp marsh have been completely eroded over the last 50 years. Thus, an erosion of 0.1 m yr^{-1} can be assumed (Environment Agency, 1999a; French and Burningham, 2003; French, 2008; Pye and Blott, 2008b).

Figure 4.5: Tide levels (m OD) for 6 different sites in the Blyth Estuary (reproduced from Gardline Environmental Ltd, 2003). Data for site 4 are used at the present study.

Table 4.1: SLAMM site parameter table for the Blyth Estuary.

Parameter	**Blyth**
DEM Date (YYYY)	2010
NWI Date (YYYY)	2010
Direction Offshore[n,s,e,w]	E
Historic Sea Level Trend (mm yr^{-1})	2.7
Salt Elevation (m above MTL)	1.6
HAT (m)	1.6
MHWS (m)	0.9
MHW (m)	0.78
MHWN (m)	0.65
LAT (m)	-1.3
Marsh Erosion (m yr^{-1})	0.1
Tidal Flat Erosion (m yr^{-1}	0.1
Lower Marsh Accretion (mm yr^{-1})	6
Upper Marsh Accretion (mm yr^{-1})	5
Beach/Tidal flat Sedimentation Rate (mm yr^{-1})	6.4 (mean for all marshes) 20.7 (max in Bulcamp Old)

Nine simulations were performed, as summarised in Table 4.2, under the mid-range UKCP09 regional sea-level scenario, in order to investigate the effect of varied sedimentation models. First, the impacts of sea-level rise at the Blyth estuary are investigated assuming that all the present defences will continue to be maintained protecting the reclaimed areas behind them. The constant accretion module is simulated for the un-protected by defences estuary, based on either the mean ('RUN1') or max ('RUN2') tidal flat accretion rate of 6.4 and 20.7 mm yr^{-1} respectively, in order to investigate the response of the estuary to this parameter. In both simulations the mean constant accretion rate of 6 and 5 mm yr^{-1} is used for the lower and upper marsh respectively.

The defences are then considered inactive and the areas behind them are subjected to the processes related to the sea-level rise. Firstly, the constant accretion module is used by repeating the above scenarios of mean ('RUN3') and max ('RUN4') constant tidal flat accretion. The more dynamic spatial accretion module is then incorporated in its simplest form for the tidal flat ('RUN5') and the marsh area ('RUN6'). A final refinement is to also include the proximity to the channel influence into the marsh spatial accretion module by investigating three different scenarios ('RUN7', 'RUN8', 'RUN9') to further evaluate the sensitivity of the model to this parameter.

Table 4.2: Summary of modified SLAMM simulations for the Blyth estuary.

	Simulation	**Tidal Flat Accretion**	**Marsh Accretion**	
Active defences	RUN1	Mean Constant	Mean Constant	
	RUN2	Max Constant	Mean Constant	
No active defences	RUN3	Mean Constant	Mean Constant	
	RUN4	Max Constant	Mean Constant	
	RUN5	Spatial	Mean Constant	
	RUN6	Spatial	Spatial (elevation dependence)	
	RUN7	Spatial	Spatial (elevation and distance to channel)	Dmax=50m
	RUN8			Dmax=100m
	RUN9			Dmax=250m

A. Active defences

The results of the first two simulations, modelled using the mean ('RUN1') and max ('RUN2') constant tidal flat accretion rate are compared in Table 4.3 and Figure 4.6. In both simulations low-lying terrain remains protected by the defences. In the first simulation, the estuary seems to keep pace with the sea-level rise. More specifically, at the beginning of the first scenario, the tidal flat accretion rate is enough to outstrip the sea-level rise, forcing the lower marsh to migrate seaward over the tidal flat. However, the extended lower marsh cannot keep pace with the increased sea-level resulting to inundation at the next time-step. Thus, the tidal flat area is increased in 2050 but slightly inundated at the last time-steps as sea-level continues to rise. On the other hand, the maximum tidal flat accretion rate applied in the second simulation, always outstripping the sea-level rise, forcing the tidal flat to be almost totally converted to lower marsh by 2050. As the lower marsh area fills in over the tidal flat, its area is extremely increased, enhancing therefore the ability of the rest marsh area to keep up with the sea-level rise.

The coastal environment is not affected by changes in the tidal flat accretion parameter, since this parameter is not relevant to the specific coastal environment. In both simulations, the response of the beach at the sea-level rise is simulated within SLAMM by using the Bruun rule, projecting total beach erosion by year 2025. This projection, though, does not agree with the observed shoreline trend monitored by the EA (2011) for the period 1991-2010. As it is illustrated in Figure 4.7, the open coast shoreline presents a more complex pattern of up-drift accretion and downdrift erosion for the last two decades, than just a simple eroded beach along the coast, pointing out the limitation of SLAMM to include a complex shoreline response to the sea-level rise.

Table 4.3: Impacts of sea-level rise at the Blyth estuary as presently defended, modelled using different constant tidal flat accretion rates.

Simulation: 'RUN1'								
Date	SLR	Low Ground	High ground	Transitional Marsh	Upper Marsh	Lower Marsh	Tidal Flat	Subtidal
0	0	670.3	2779.6	113.4	25.6	13.9	249.4	30.4
2025	0.0497	687.1	2756.5	119.3	18.7	26.8	235.4	35.1
2050	0.1517	693.8	2746.0	120.5	21.0	16.1	244.4	35.9
2075	0.2712	701.7	2732.3	121.9	23.5	16.2	243.9	36.6
2100	0.4057	709.9	2717.3	120.3	26.9	17.9	244.6	37.1
Simulation: 'RUN2'								
Date	SLR	Low Ground	High ground	Transitional Marsh	Upper Marsh	Lower Marsh	Tidal Flat	Subtidal
0	0	670.3	2779.6	113.4	25.6	13.9	249.4	30.4
2025	0.0497	687.2	2756.5	126.7	21.5	41.2	211.2	34.6
2050	0.1517	699.1	2746.0	147.3	48.2	149.1	50.5	37.5
2075	0.2712	718.0	2732.3	155.2	56.1	156.3	20.0	38.2
2100	0.4057	732.0	2717.3	153.9	61.0	159.9	11.2	38.7

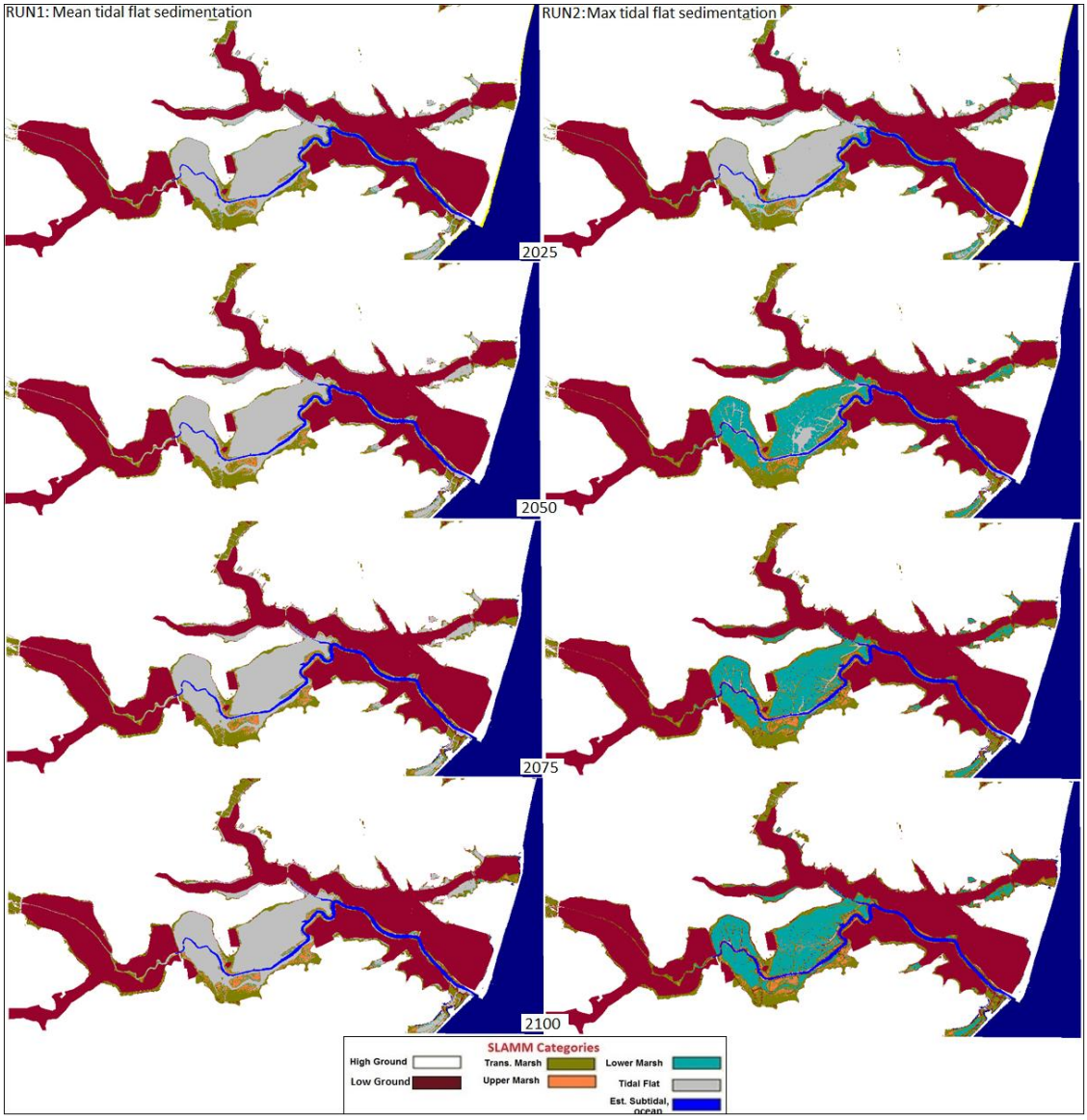

Figure 4.6: Changes in habitat distribution to 2100 for the Blyth estuary as presently defended, modelled using different constant tidal flat accretion rates.

Figure 4.7: Observed shoreline change at the entrance of the Blyth estuary for the period 1991-2010 (Environment Agency, 2011).

B. Inactive defences

In order the defences to be rendered as inactive, they have been assigned as long narrow hills of dryland, while the areas behind them as tidal flats, both subjected to the processes related to the sea-level rise. The two scenarios of mean and max constant tidal flat accretion simulated within the defended estuary are repeated for the undefended estuary too ('RUN3' and 'RUN4'). The results of these runs, as presented in Figure 4.8, indicate that the behaviour of the protected areas of the estuary is very similar to the unprotected ones, with marsh to be generated only in high elevations for a mean tidal flat accretion rate but almost filling in the tidal flat for a maximum rate. However, even this maximum rate is not enough to convert some very deep areas of tidal flat to lower marsh, even in 100 years.

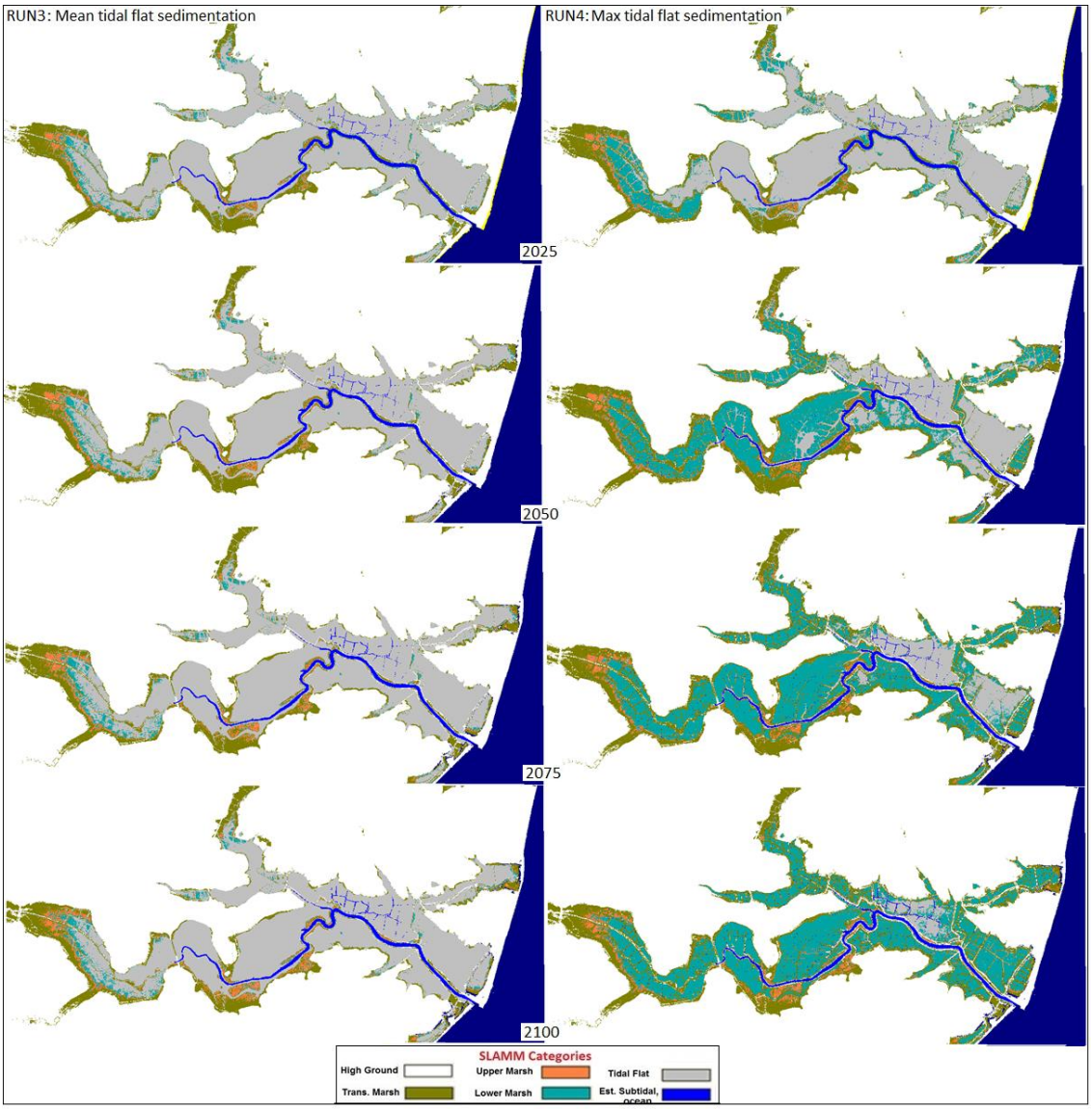

Figure 4.8: Changes in habitat distribution to 2100 for the Blyth estuary with the defences rendered inactive, modelled using different constant tidal flat accretion rates.

The annual tidal flat sediment demand required for each scenario is calculated at this point in order to evaluate the projected results in the context of sediment availability. The results are summarised in Table 4.4, and are critically compared with the potential annual deposition for the whole estuary as this is determined by French et al. (2008). More specifically, in this study the gross sediment flux for the whole estuary is estimated at 92.3 t x 10^3 yr^{-1}, which could sustain the required from the tidal flat sediment demands for all the scenarios. However, this could probably be constrained by the local supply estimated for the whole estuary at 1.4 t x 10^3 yr^{-1}. Although this implies all the scenarios as unrealistic, it is noted in the same study, that this residual sediment flux is not very reliable, because it is very difficult to be calculated, especially when bathymetric surveys and spatially representative measurements of contemporary deposition and erosion are missing.

Table 4.4: Annual sediment demand required for each scenario simulated within SLAMM for the Blyth Estuary.

		Defended Estuary	**Undefended Estuary**	**Intertidal annual deposition (French et al., 2008) (t x 10^3 yr^{-1})**	
Tidal Flat Area (m^2)		2,493,700	7,184,375		
		Tidal flat annual deposition demand (t x 10^3 yr^{-1})		**Gross**	**Residual**
Mean accr. rate (mm yr^{-1})	6.4	6	16	92.3	1.4
Max accr. rate (mm yr^{-1})	20.7	18	53		

However, constant accretion rates for the tidal flat cannot depict realistically its response to the sea-level rise, since they ignore any morphodynamic feedback as the elevation evolves within the tidal frame. Thus, the third simulation is repeated by incorporating this time the dynamic spatial accretion model for the tidal flat ('Run5'). This sub-model is parameterised based on observed tidal flat accretion data, as they obtained from the Pye and Blott (2008b) sedimentation survey. These elevation dependent accretion data are initially fitted with various empirical models (Figure 4.9a), which are used to constrain the relevant ones according to the SLAMM framework (Figure 4.9b). The best fit to the real data exponential curve is better characterised by the quadratic SLAMM curve. Thus, the last one is used to parameterise the tidal flat accretion sub-model. Table 4.5 summarises the parameters used to constrain the different elevation dependent tidal flat accretion models within SLAMM.

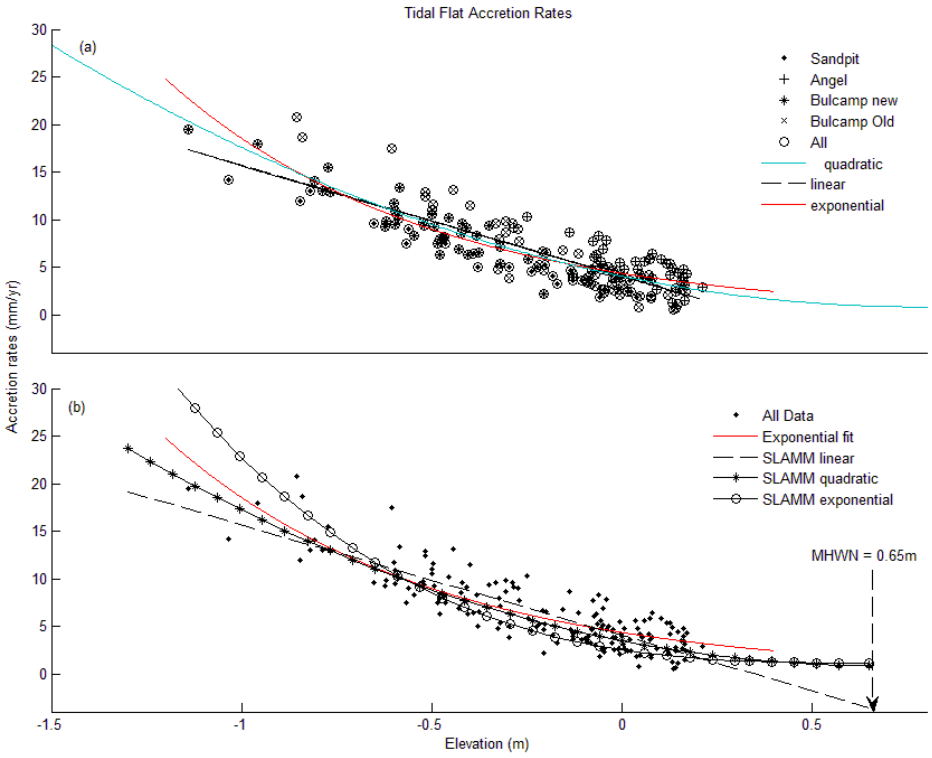

Figure 4.9: Observed tidal flat accretion rates (a) for the Blyth estuary used to constrain elevation-dependent accretion sub-model (b) (Source: Pye and Blott, 2008b).

Table 4.5: Parameter table for the elevation dependent tidal flat accretion model.

SLAMM Accretion model parameters	**Linear**	**Quadratic**	**Cubic**
Max Accretion rate (mm yr^{-1})	19.15	23.7	36.8
Min Accretion rate (mm yr^{-1})	-3.55	0.9	1.16
a coefficient (cubic)*	0	0	1
b coefficient (square)*	0	1	0
c coefficient (linear)*	1	0	0

*a,b,c: coefficients defining the shape of the accretion curve within SLAMM (see equations 3.3 to 3.6).

The response of the estuary to the specific sea-level rise scenario, modelled using the constant ('RUN3') and the spatial ('RUN5') tidal flat accretion models is presented in Table 4.6 and Figure 4.10. The much higher accretion rates generated by the spatial model for the low-lying tidal flat areas, consider it more capable to cope with the sea-level rise. Thus, less tidal flat is inundated in such low elevations in the last simulation, decreasing the projected subtidal. Parallel, the spatial tidal flat accretion rates generated in its higher elevations are much lower, getting very close to zero at some points. Thus, the estuary is less capable to form saltmarsh in the higher elevations of the upper estuary, decreasing the projected lower marsh area in the last simulation.

Table 4.6: Impacts of sea-level rise at the Blyth estuary with the defences rendered inactive, modelled using constant ('RUN3') and spatial ('RUN5') tidal flat accretion rates.

Simulation: 'RUN3'		High	Transitional	Upper	Lower	Tidal Flat	Subtidal
Date	SLR	Ground	Marsh	Marsh	Marsh		
0	0	2847.9	187.3	50.8	45.3	718.4	32.4
2025	0.05	2838.5	203.3	42.7	69.3	684.1	40.0
2050	0.15	2830.9	208.7	48.7	57.9	688.0	41.3
2075	0.27	2824.5	204.6	52.0	62.8	685.9	42.7
2100	0.41	2810.9	202.5	55.0	62.2	694.4	43.9
Simulation: 'RUN5'		**High**	**Transitional**	**Upper**	**Lower**	**Tidal Flat**	**Subtidal**
Date	**SLR**	**Ground**	**Marsh**	**Marsh**	**Marsh**		
0	0.00	2847.9	187.3	50.8	45.3	718.4	32.4
2025	0.05	2838.7	204.4	41.3	58.4	697.6	37.4
2050	0.15	2833.1	210.5	46.4	38.2	708.3	38.9
2075	0.27	2828.9	206.4	50.0	38.1	709.0	40.0
2100	0.41	2815.7	204.0	54.4	44.7	709.0	41.0

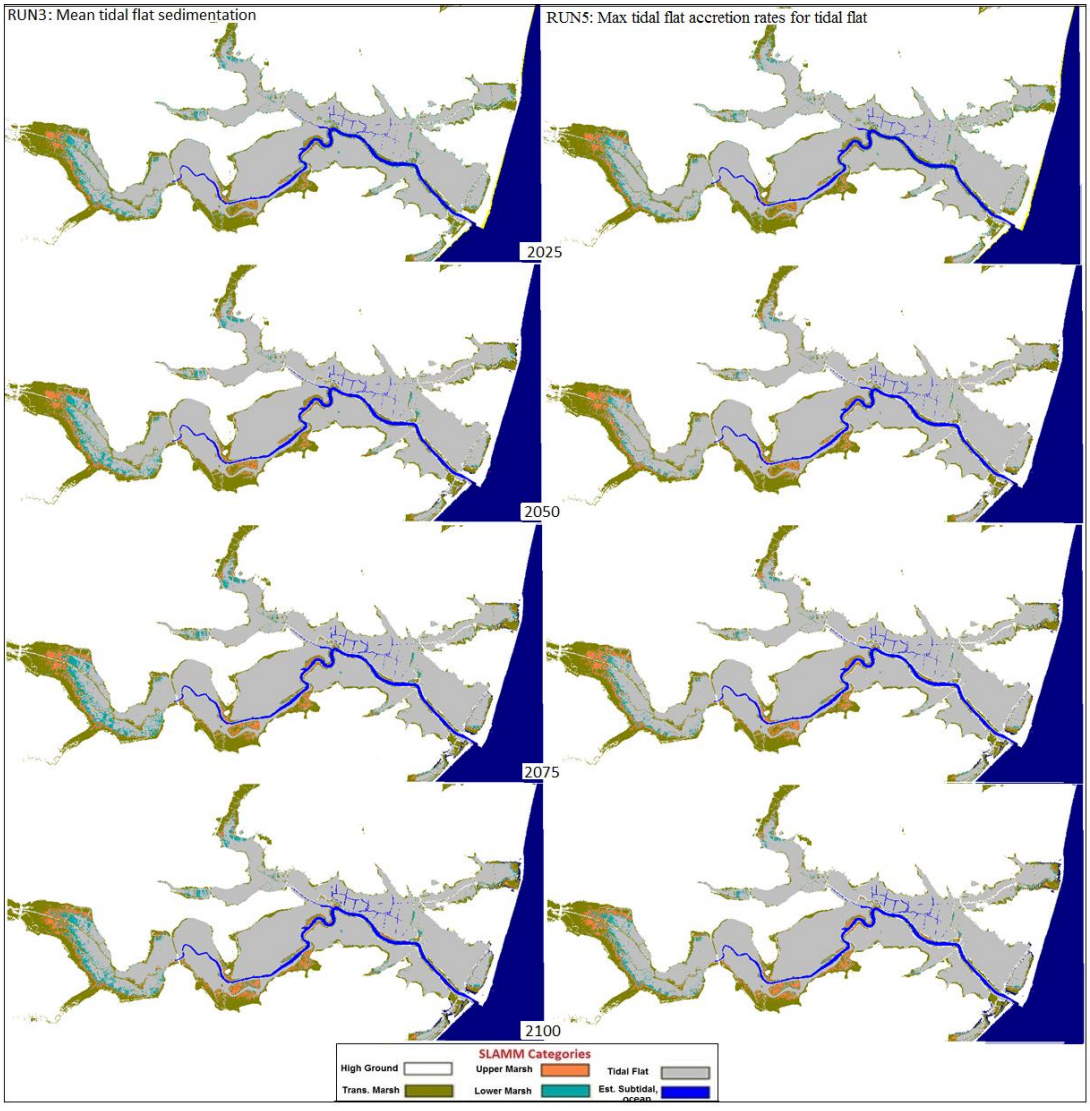

Figure 4.10: Changes in habitat distribution to 2100 for the Blyth estuary with the defences rendered inactive, modelled using constant ('RUN3') and spatial ('RUN5') tidal flat accretion rates.

Summarising it can be said that the Blyth estuary responds more dynamically to the specific sea-level rise scenario if a spatial accretion pattern is taken into account for the tidal flat. On the other hand, a mean constant tidal flat accretion rate overestimates the vulnerability of the estuary, forcing it to migrate landwards, while a maximum constant tidal flat accretion rate underestimates it, forcing it to migrate seawards.

A final refinement here is to also include a spatial accretion model for the saltmarsh ("RUN6"). Saltmarsh sedimentation in the Blyth has been investigated (see French and Burningham, 2003 for a study on the relationship between the marsh sedimentation and the sea-level rise; French et al., 2008 for a sediment flux study; French et al., 2000 for a study in the sedimentation movement within abandoned reclamations). However, the data are too sparse to permit generalisation into a spatial model. Accordingly, the aspatial MARSH-0D model (French, 2006) is used to compute the elevation dependence of marsh deposition rate given appropriate local vertical tidal limits and background sediment concentration. Modelled sedimentation as a function of time-evolving evolution was then fitted to the exponential empirical model, which used to constrain the SLAMM saltmarsh accretion model parameters (Figure 4.11; Table 4.7). However, the MARSH-0D simulations used only a simplified tidal regime (only four tidal constituents, M2, S2, O1, K1) and did not include the influence of the storm surge, a factor that is important to be taken into account into the accretion rate (Stumpf, 1983; Pugh, 1987; French, 2006; Schuerch et al., 2012). Therefore, it is necessary to fill in the missing data by assuming a zero- accretion rate at the highest elevation of the marsh.

Table 4.7: Parameter table for the elevation dependent marsh accretion model.

Accretion model Parameters	**Lower Marsh**	**Upper and Transitional Marsh**
Max Accretion rate (mm yr^{-1})	33	18
Min Accretion rate (mm yr^{-1})	18	0
a coefficient (cubic)*	0	1
b coefficient (square)*	1	0
c coefficient (linear)*	1	0

*a,b,c: coefficients defining the shape of the curve (see equations 3.3 to 3.6).

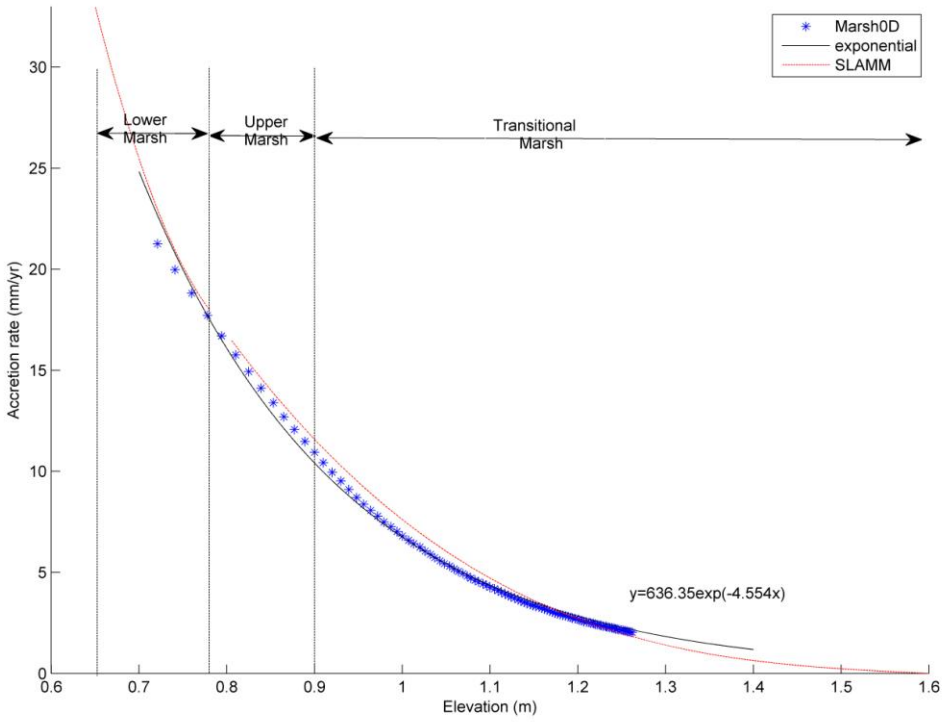

Figure 4.11: Modelled marsh accretion rates for the Blyth estuary generated by the MARSH-OD model and used to constrain the SLAMM sub-models.

The results of this simulation are compared to the one modelled using the constant marsh accretion model ('RUN5') in Table 4.8 and Figure 4.12. The spatial accretion rates applied to the lower and upper marsh area, even in their highest elevations, are much higher than the constant marsh accretion rate applied in the previous simulation. Thus, less lower marsh is inundated to tidal flat in low-lying areas, while in higher elevations more is capable to build up to upper marsh. The last one is therefore migrating now seawards over the lower marsh, while in higher elevations more is built up to transitional marsh. At these low elevations, the spatial accretion rates of the transitional marsh are still higher than the constant rate applied in the previous simulation, making the low-lying transitional marsh more capable to keep pace with the sea-level rise, and not be inundated to upper marsh. In higher elevations though, this rate is much smaller than the constant one, considering the transitional marsh less capable to build up, projecting less higher ground in the first time-steps. However, as the upper marsh continues to be converted to transitional marsh in the next time-steps, more of this is able to build up to higher ground.

Table 4.8: Impacts of sea-level rise at the Blyth estuary with the defences rendered inactive, modelled using constant ('RUN5') and spatial ('RUN6') marsh accretion rates.

Simulation: 'RUN5' Date	SLR	High Ground	Transitional Marsh	Upper Marsh	Lower Marsh	Tidal Flat	Subtidal
0	0.00	2847.9	187.3	50.8	45.3	718.4	32.4
2025	0.05	2838.7	204.4	41.3	58.4	697.6	37.4
2050	0.15	2833.1	210.5	46.4	38.2	708.3	38.9
2075	0.27	2828.9	206.4	50.0	38.1	709.0	40.0
2100	0.41	2815.7	204.0	54.4	44.7	709.0	41.0
Simulation: 'RUN6' Date	**SLR**	**High Ground**	**Transitional Marsh**	**Upper Marsh**	**Lower Marsh**	**Tidal Flat**	**Subtidal**
0	0.00	2847.9	187.3	50.8	45.3	718.4	32.4
2025	0.05	2834.6	223.5	54.9	38.8	688.6	37.4
2050	0.15	2838.0	217.1	79.5	18.2	684.1	38.9
2075	0.27	2840.5	208.1	88.1	12.6	683.8	40.0
2100	0.41	2828.2	196.9	105.1	14.2	683.2	40.9

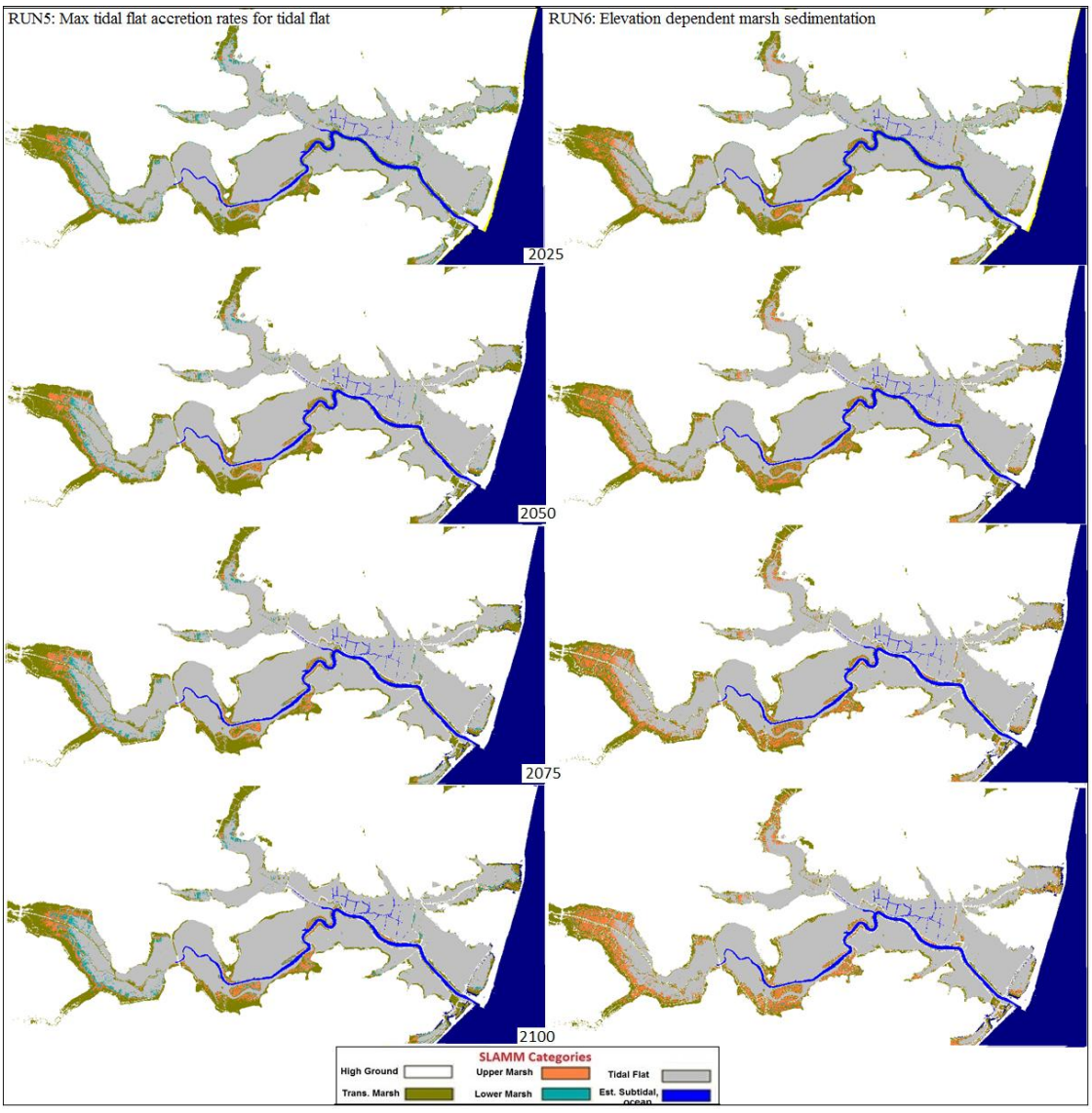

Figure 4.12: Changes in habitat distribution to 2100 for the Blyth estuary with the defences rendered inactive, modelled using constant ('RUN5') and spatial ('RUN6') marsh accretion rates. In both simulations spatial accretion rates have been used for the tidal flat.

In addition to the strong influence of elevation on the time-evolution of saltmarsh sedimentation, proximity to sediment sources (marshe edges, tidal creeks) is well documented as a driver of spatial variation in sedimentation (Reed, 1988; Stoddart et al., 1989; French and Spencer, 1993; French et al., 1995; Bartholdy, 1997; Reed et al., 1999; Bartholdy, 2010a, 2012). This factor is included in the SLAMM saltmarsh model via the D term in equation 3.7. Clough et al. (2010) suggest that this term is used to progressively reduce sedimentation over a range of 500 m (DistEffectMax), beyond which a minimum value (Dmin) of 0.1 is used for areas of marsh that are not affected by the proximity to channels or open water. Although this could be the case for the big estuaries in US, in the small UK estuaries, this threshold is approximately 100 m (French and Spencer, 1993). However, a sensitivity analysis of this threshold is investigated in order to evaluate the sensitivity of the model to this parameter. In that direction, three simulations are performed for ranges of 50 m (RUN7), 100 m (RUN8) and 250 m (RUN9). Figure 4.13 presents the values of the D term used into the equation 3.7 as a function of distance to channel for all the above simulations. It is worth mentioned here that the definition of the main channel must be manually done via the salinity sub-model, without activating it though.

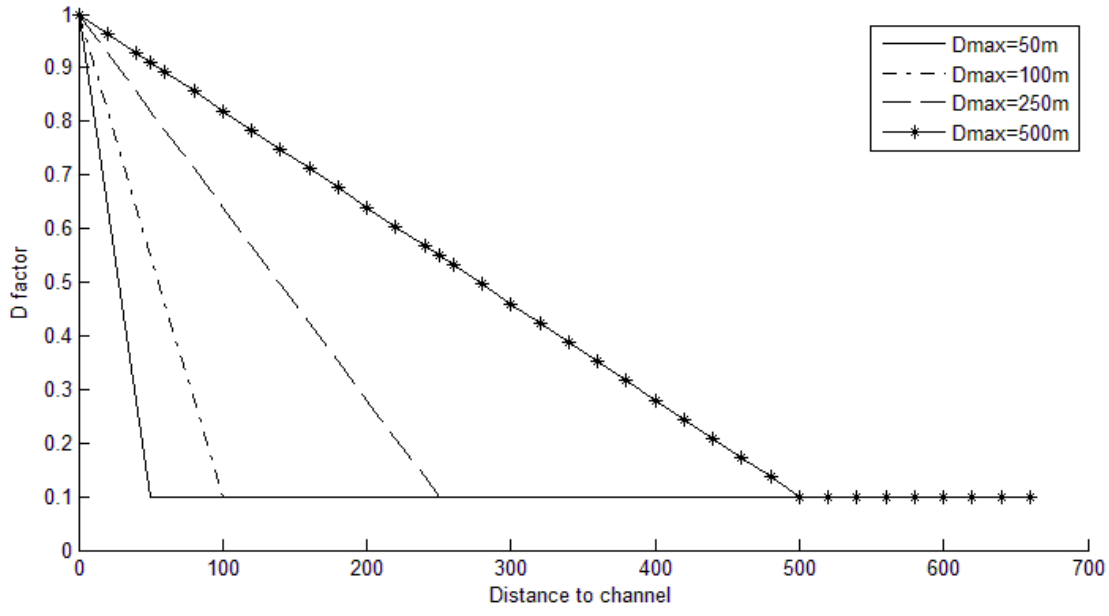

Figure 4.13: D term values as a function of distance to channel for different assumptions of proximity to channel influence.

Inclusion of the D term into the accretion sub-models tends to result in more extensive lower marsh at the expense of higher marsh. This reflects the preferential reduction in

sediment input to the higher marsh, which tends to be further away from the main estuary channel (Figure 4.14).

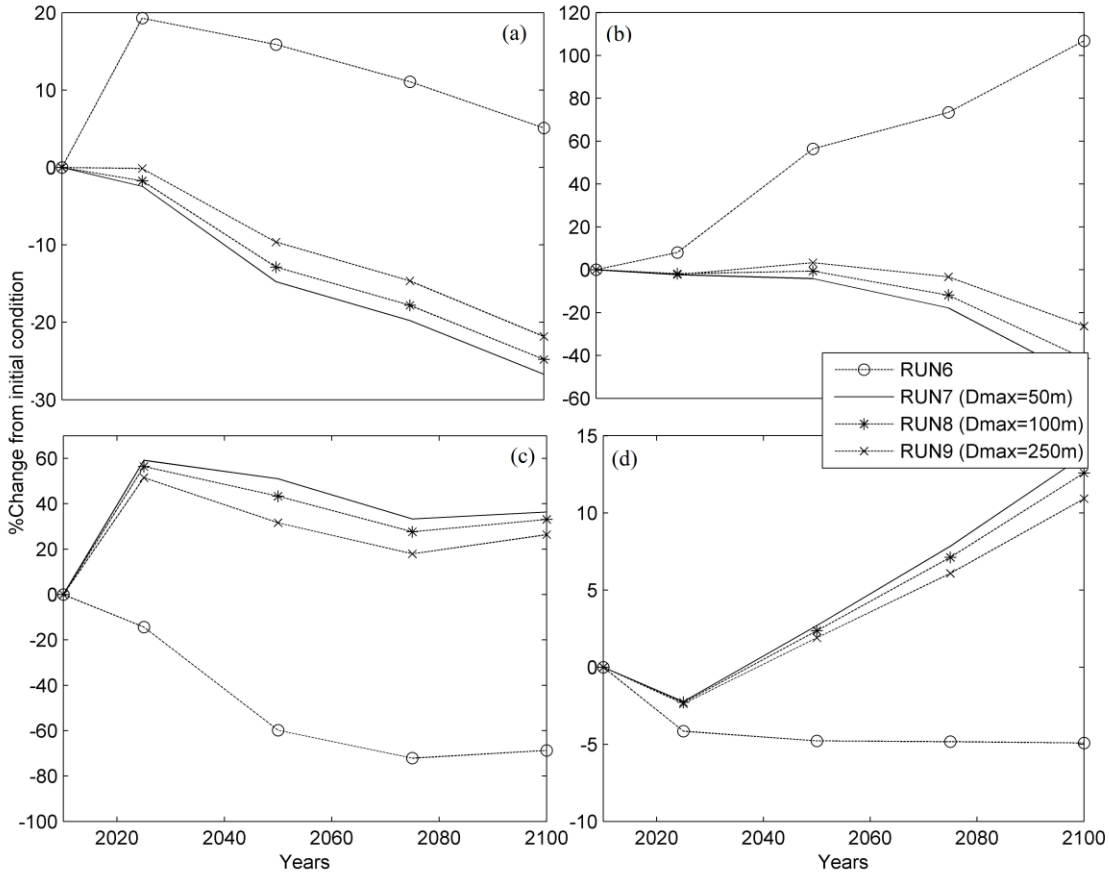

Figure 4.14: Sensitivity analysis for the distance to channel factor, D (a: transitional marsh, b: upper marsh, c: lower marsh, d: tidal flat).

Concluding, it can be said that although the Blyth estuary is more vulnerable to the specific sea-level rise scenario in the last simulation, as presented in Figure 4.15, it still responds quite dynamically to it. The lower part of the estuary keeps pace with the specific sea-level rise by 2100 due to the adequate tidal flat accretion, which is thought not enough to form marsh in such deep areas. On the other hand, the upper part of the estuary migrates landwards extending its tidal flat area over the lower marsh by the year 2100 and squeezing the higher marsh. More specifically, at the beginning of the simulation the higher marshes of the estuary cannot cope with the sea-level rise and are gradually inundated to lower marsh extending its area. However, the accretion capability of the lower marsh that further away from the main channel is not enough to outweigh the specific sea-level rise scenario. Consequently, the lower marsh is gradually inundated to tidal flat, while parallel higher marsh continues to be inundated to lower marsh at higher elevations as the sea-level continues to rise.

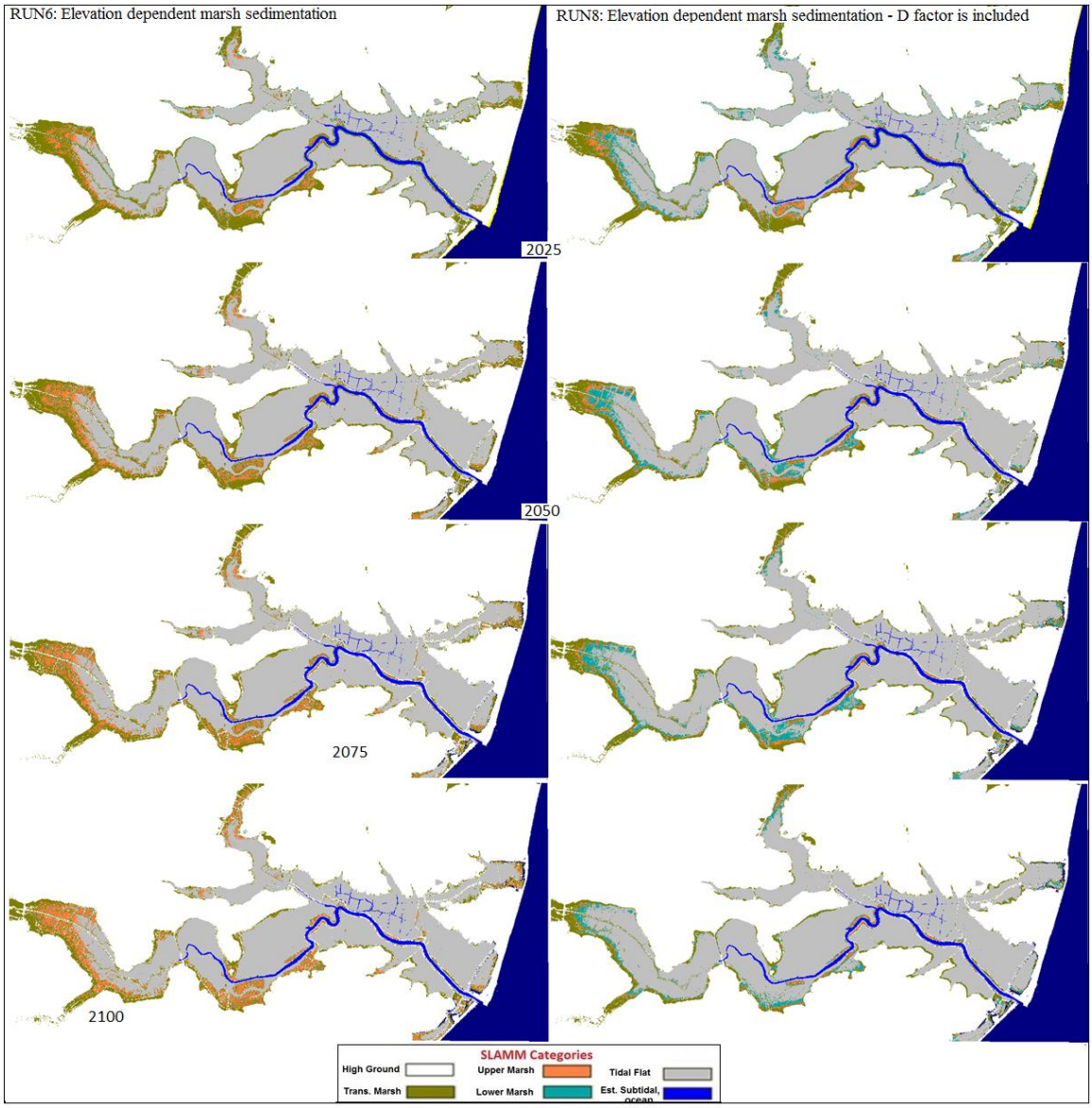

Figure 4.15: Changes in habitat distribution to 2100 for the Blyth estuary with the defences rendered inactive, modelled using spatial marsh accretion rates by including ('RUN8') or not ('RUN6') the proximity to channel factor.

Summarising it can be said that the predicted intertidal habitat changes are highly sensitive to assumptions made in the underlying sedimentation sub-models. This is especially so in the case of the different saltmarsh sub-environments (Figure 4.16). The higher marshes are not significantly affected from different assumptions on the tidal flat accretion sub-model. However, their areas are increased when the elevation dependent marsh accretion sub-model is activated, due to the more effective upland migration of the lower marsh. In contrast, lower accretion rates are assumed for the marshes when the distance to channel factor is also included into this model. Most affected of course are the higher marsh areas, since they are further away from the channel, considering them less able to cope with the sea-level rise, and therefore being inundated and

converted to lower marsh. Thus, the lower marsh area is increased, while some parts of it which are not very close to the channel are inundated and converted to tidal flat.

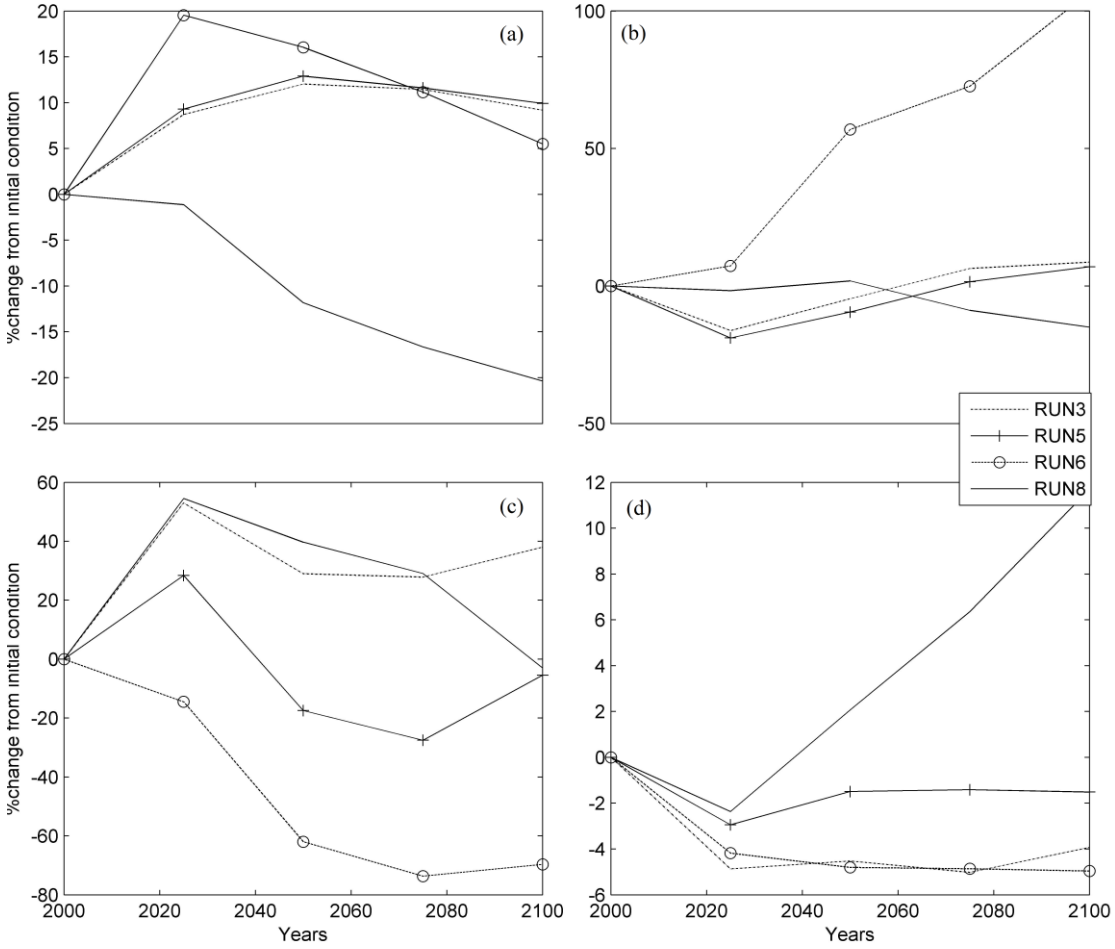

Figure 4.16: Sensitivity analysis for the sedimentation sub-models: constant deposition (RUN3); elevation dependant tidal flat deposition (RUN5); elevation dependant marsh deposition (RUN6); elevation dependant marsh deposition with D factor (RUN8) (a: transitional marsh, b: upper marsh, c: lower marsh, d: tidal flat).

As noted in Chapter 3, the elevation-dependence of the habitat decision tree means that SLAMM remains very sensitive to the quality of the underlying terrain data. Even a small error of ±0.15 m on the DEM may results to significant differences in habitat extents, which need to be identified when defining initial conditions. Most sensitive is the lower marsh. The error analysis presented in Figure 4.17 indicates that realistic LiDAR errors of ±0.15 m give rise to up to 50% variation in its initial extent. Interestingly, this sensitivity becomes much more apparent for the lower marsh when more sophisticated dynamic spatial accretion model is used. An error of +0.15 m on the DEM generates a more extended lower marsh. Thus, more lower marsh is now further away from the channel experiencing less accretion rates, considering it less capable to keep pace with the sea-level rise and parallel to build up to upper marsh.

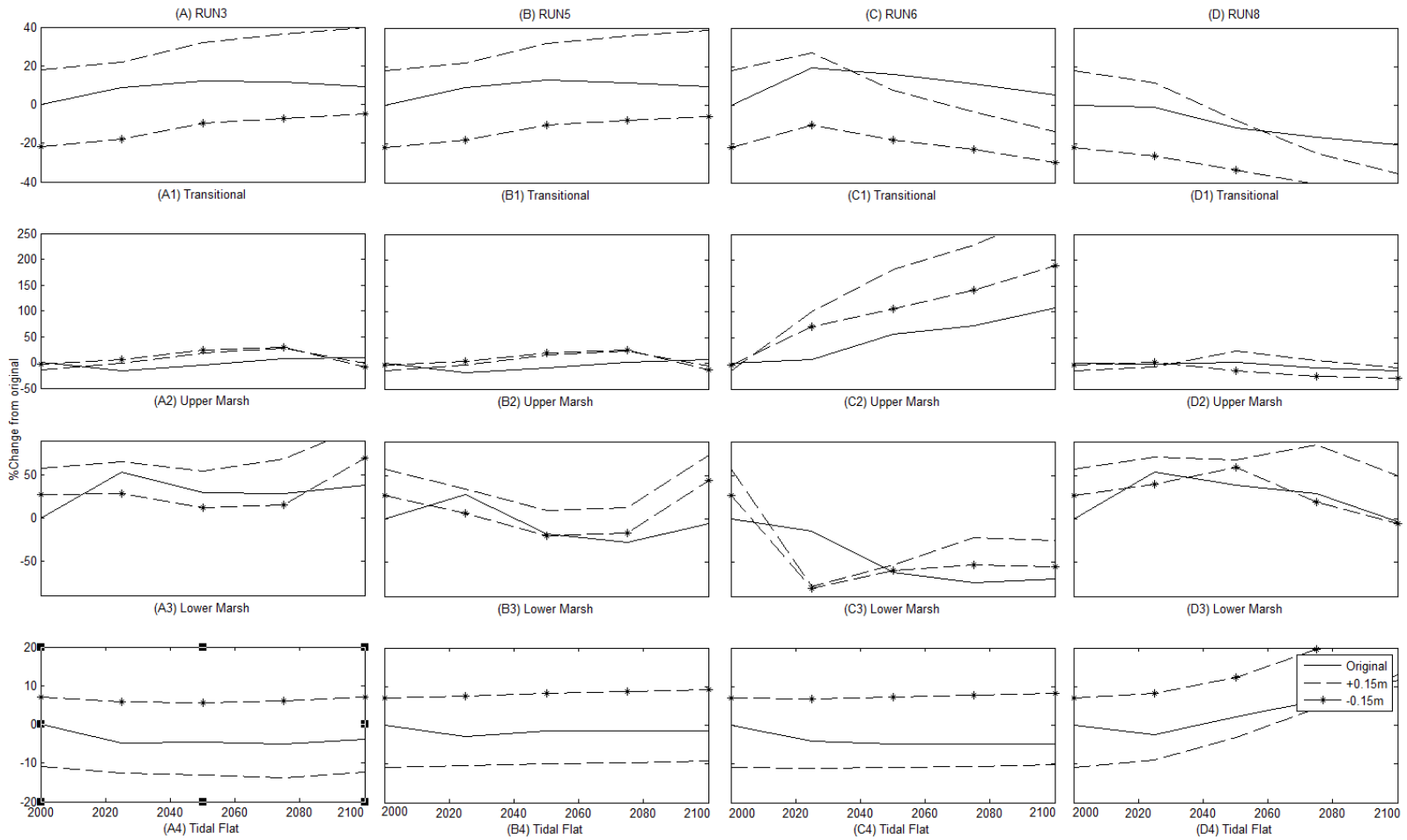

Figure 4.17: DEM Sensitivity analysis for the different sedimentation sub-models: (a) constant deposition (RUN3); (b) elevation dependant tidal flat deposition (RUN5); (c) elevation dependant marsh deposition (RUN6); (d) elevation dependant marsh deposition with D factor (RUN8).

Finally, the saltmarsh distribution generated by the original DEM can also be compared with observed extent, in order to investigate the accuracy of the habitat classification conceptual model used within SLAMM. Saltmarsh has been mapped in detail by the Environment Agency (EA), and a comparison of their saltmarsh polygons with the SLAMM classification for the Blyth estuary indicates a generally very close correspondence between model and data (Figure 4.18). However, local differences still exist either due to the different framework within each database is generated or due to an error. For example, Area 2 in Figure 4.18 is characterised as a saltmarsh by the EA when in reality is effectively a reedbed, a habitat that is determined based on the salinity. Similarly, the brackish marsh is outside of the SLAMM scope and therefore not included in its habitat classification, resulting to the misclassification of the area 5. Moreover, EA polygons miss some of the saltmarsh islands in the middle estuary (area 1), probably due to human error, while they also misclassify area 3 by assigning algae (*Enteromorpha spp*) as saltmarsh. On the other hand, area 4 is misclassified in the present study as saltmarsh when most its area is land/road that could be saltmarsh in terms of elevation ranges.

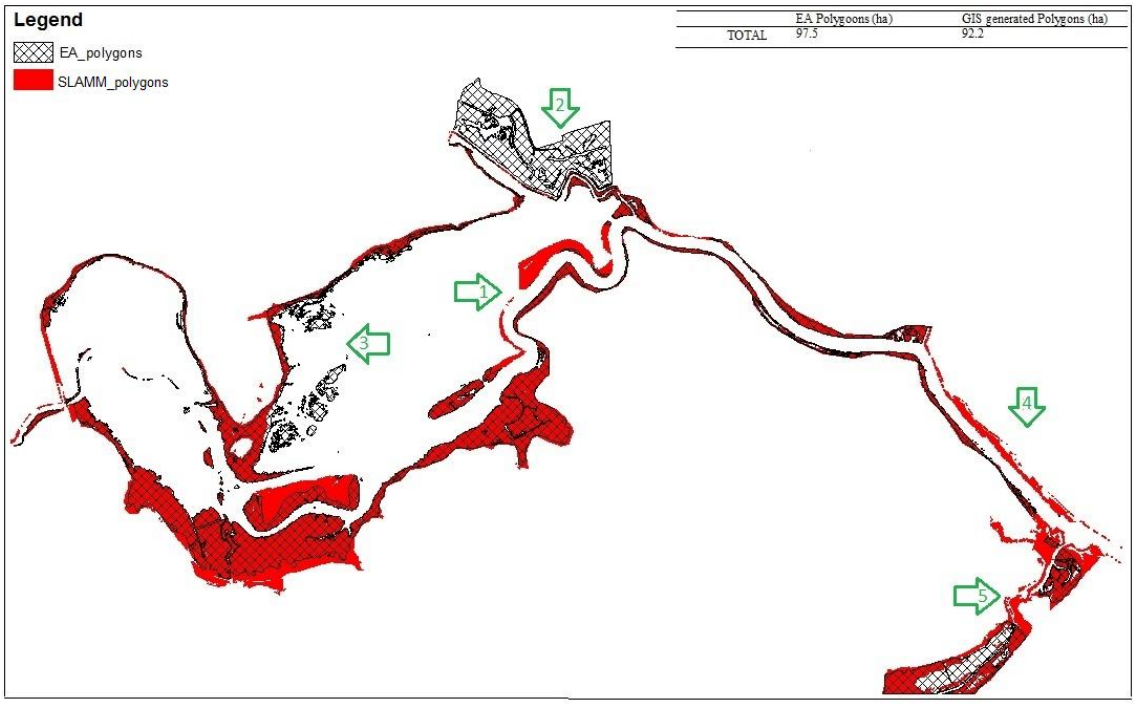

Figure 4.18: Comparison of saltmarsh distribution generated by the DEM classification SLAMM and saltmarsh extent determined by the Environment Agency.

4.2 Deben Estuary

A composite LiDAR dataset (2 m resolution) produced by the Environment Agency from surveys undertaken in 2010 and 2012 was used as the base DEM for the Deben estuary. These data were integrated with subtidal bathymetry surveys undertaken by the UCL Coastal and Estuarine Research Unit between 1998 and 2001. The resulting elevation dataset is resampled to 5 m resolution and is summarised in Figure 4.19a. The derived slope and the land cover layers used to define the model domain are shown in Figures 4.19b and 4.19c respectively. Finally, Figure 4.19d represents the protected by the defences area.

These figures illustrate the morphology and reclamation pattern found at the Deben estuary. Similarly to the Blyth estuary described in Section 4.1, the Deben is characterised by a relatively natural development of saltmarshes in its upper part, but it is enclosed by defences at its lower part, with the mouth being its narrowest section (CHaMP, 2002).

Table 4.9 summarises the required site parameters for the model runs. The historic sea-level trend includes the vertical land movements and is estimated at 2.1 mm yr^{-1} using the closest tide gauge station at Sherness (around 70 km to the south) (PSMSL, 2012). The tide regime in m OD for the Bawdsey is used to set up the model. An assumption of 0.1 m yr^{-1} for both tidal flat and the marsh area is also included.

Table 4.9: Site parameter table for the Deben estuary.

Parameter	**Deben estuary**
NWI and DEM Photo Date (YYYY)	2010
DEM Photo Date (YYYY)	2010
Direction Offshore[n,s,e,w]	S
Historic Trend (mm yr^{-1})	2.1
Salt Elevation (m above MTL)	2.25
HAT (m)	2.25
MHWS (m)	1.85
MHW (m)	1.5
MHWN (m)	1.15
LAT (m)	-2.15
Marsh Erosion (m yr^{-1})	0.1
Tidal flat erosion (m yr^{-1})	0.1

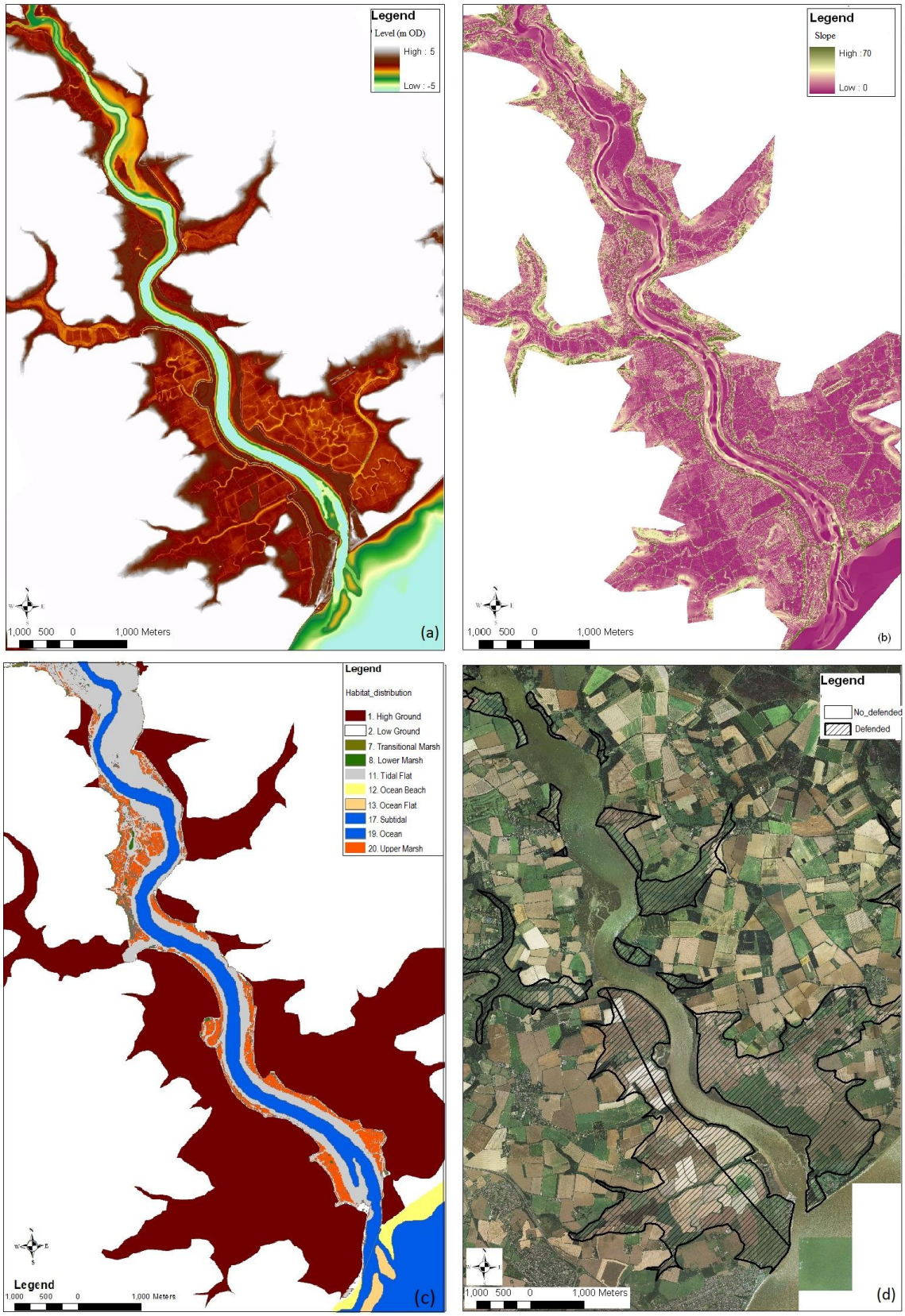

Figure 4.19: SLAMM Input layers for the Deben estuary: a) DEM; b) slope map; c) land classification; d) flood compartments.

Although there is a relatively large literature on management of the estuary's flood defences (Frostick and McCave, 1979; Environment agency, 1999b, SMP7, 2010), accretion rates have not been systematically measured to permit generalisation into a spatial model. To address this problem, the MARSH-0D model (French, 2006) is used to compute the elevation dependence of marsh deposition rate given appropriate local vertical tidal limits and background sediment concentration. Modelled sedimentation as a function of time-evolving elevation is best fitted to the quadratic empirical model, which is then used to constrain the SLAMM saltmarsh accretion model parameters (Figure 4.20; Table 4.10). As with the Blyth estuary simulations, it was necessary to constrain surge-drive sedimentation by assuming a zero deposition at the highest elevation. Finally, the distance to channel factor is also taken into account, as described in detail in Section 4.1.

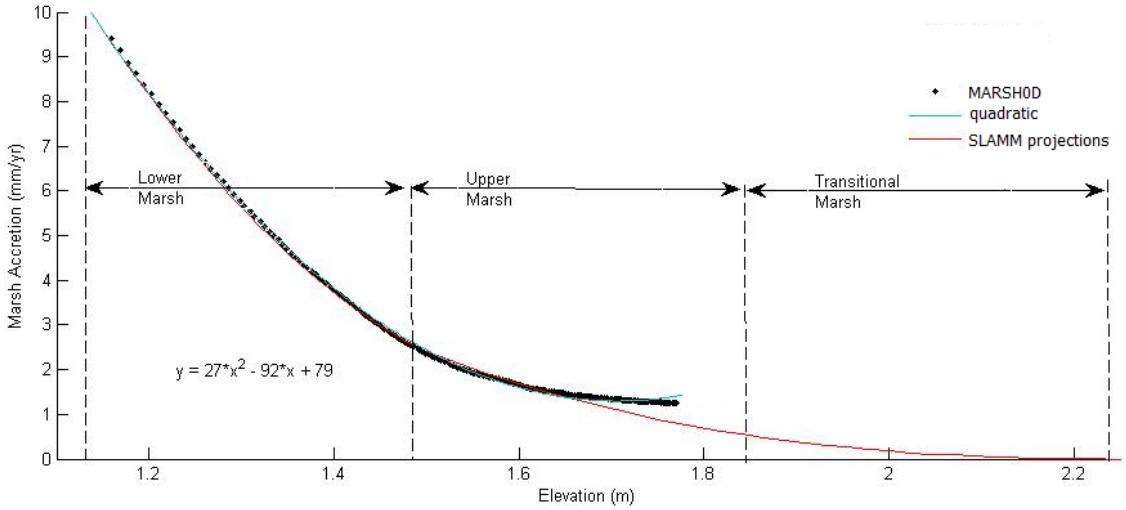

Figure 4.20: Modelled marsh accretion rates used to constrain the SLAMM sub-models for the Deben estuary.

Table 4.10:Parameters table for the SLAMM elevation and distance dependant marsh accretion model.

	Lower marsh	Upper and transitional marsh
Max Accretion (mm yr^{-1})	9.6	2.4
Min Accretion (mm yr^{-1})	2.4	0
Coefficient a (cubic)*	0	1
Coefficient b (square)*	1	1
Coefficient c (linear)*	1	0
DeffectMax (m)	100	100
Dmin (unitless)	0.1	0.1

*a,b,c: coefficients defining the shape of the curve (see equations 3.3 to 3.6).

Meanwhile, the composite LiDAR dataset is compared with past EA LiDAR data from 2003 in order to investigate the behaviour of the tidal flat for the period 2003 and 2010. At this point and based on French's (2003) study where the accuracy of the LiDAR data is investigated, the 2003 dataset is corrected for a systematic error of 10cm with respect to the 2010 data. The accuracy of the LiDAR dataset, though, could also be degraded from a random error which is much harder to constrain, and also by artifacts that arise in the LiDAR data processing. In addition, differences are also expected in vegetated areas due to the changing ground surface condition because of the different flight survey time during the year. The resulting elevation change map is presented in Figure 4.21. The tidal flat seems to be erosional along most of the eastern margin of the channel, but accretional on the western margin.

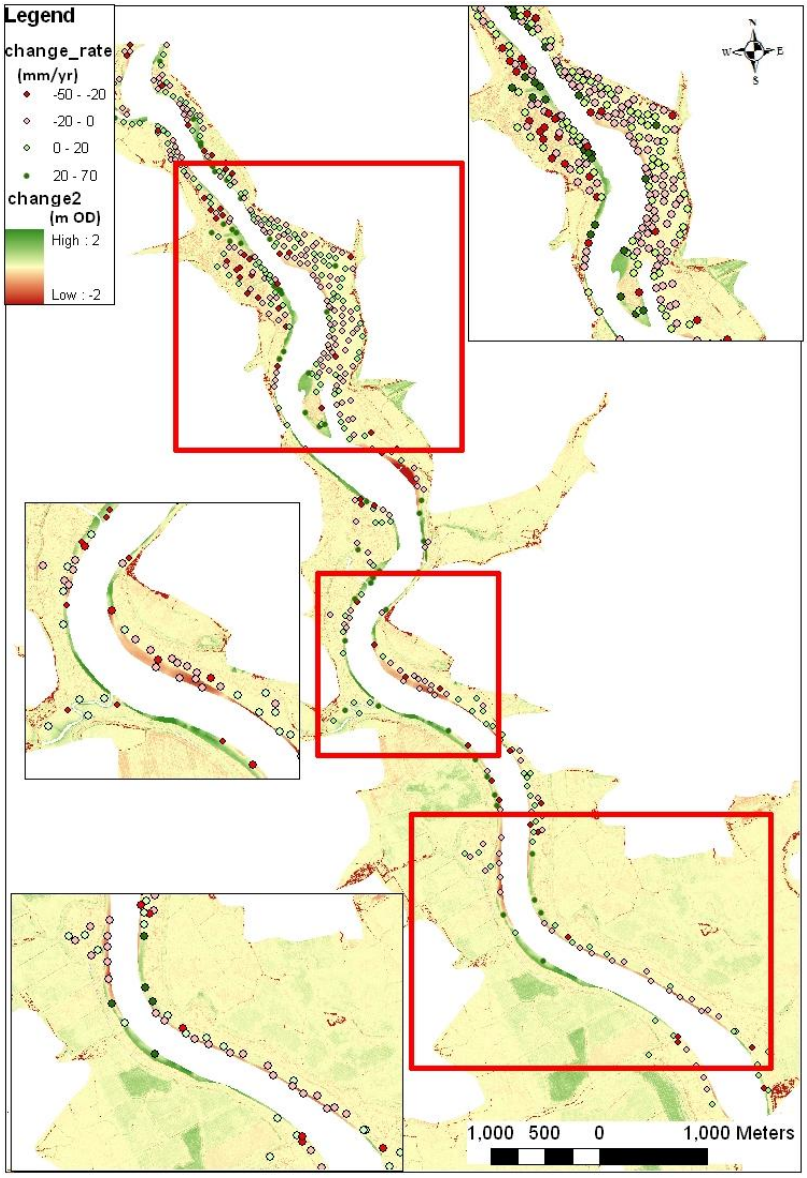

Figure 4.21: Topographic change for the Deben estuary intertidal flat for the period 2003-2010. Points visualise the rate of change in the tidal flat area.

The rate of the tidal flat change at locations where valid LiDAR data exist for both years is visualised in the same figure and analysed as a function of elevation and distance to the main channel in Figure 4.22. This analysis indicates that the tidal flat change on the Deben estuary does not depend in any simple way on these two factors. In addition, a survey undertaken by Frostick and McCave (1979) on the sediment change of the specific estuary over a calendar year reports a seasonal variation in accretion and erosion. The seasonal cycle of accretion is reported to be caused by the algal growth during summer, while the reduced wave action during the same period tends to allow the tidal flat to build-up. These data cannot be used to permit a generalisation into a spatial model, and therefore constant accretion rates must be applied for the tidal flat within SLAMM in order to investigate its fate under the specific sea-level rise scenario.

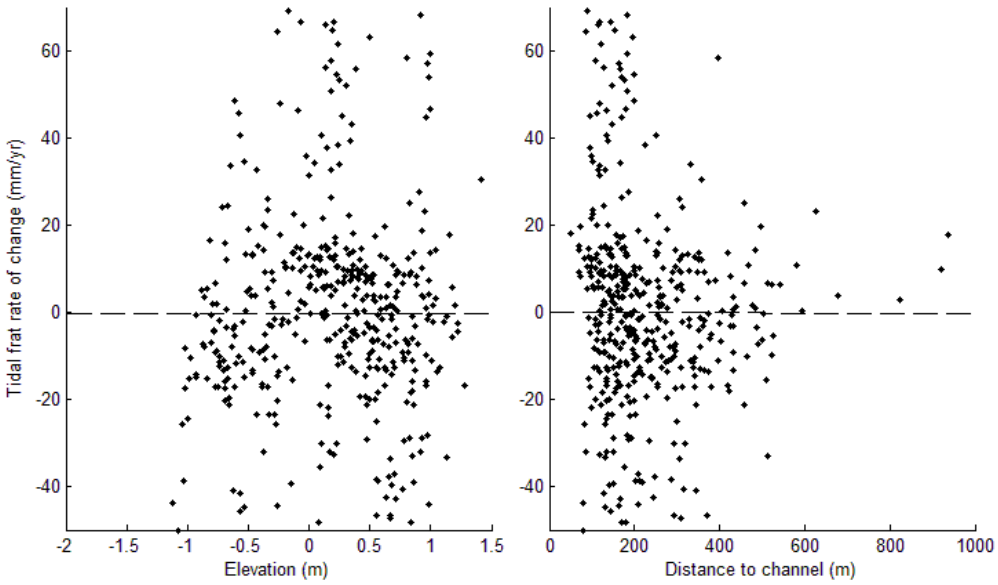

Figure 4.22: Tidal flat rate of change as a function of (a) elevation and (b) distance to channel.

Further investigation is necessary at this point in order to find a more specific pattern to describe the behaviour of the tidal flat, maybe by dividing the estuary in zones of different sedimentation behaviour. By applying a cross-sectional profile analysis in 6 locations along the Deben estuary, and based on Kirby's (2000) theory that a high and convex cross-sectional shape characterises accreting tidal flats, while a low and concave one characterises eroding ones (Figure 4.23), it is clear that the estuary can be zoned into a western accretional and eastern erosional side. This behaviour of the tidal flat can be partially related to the meandering platform of the estuary.

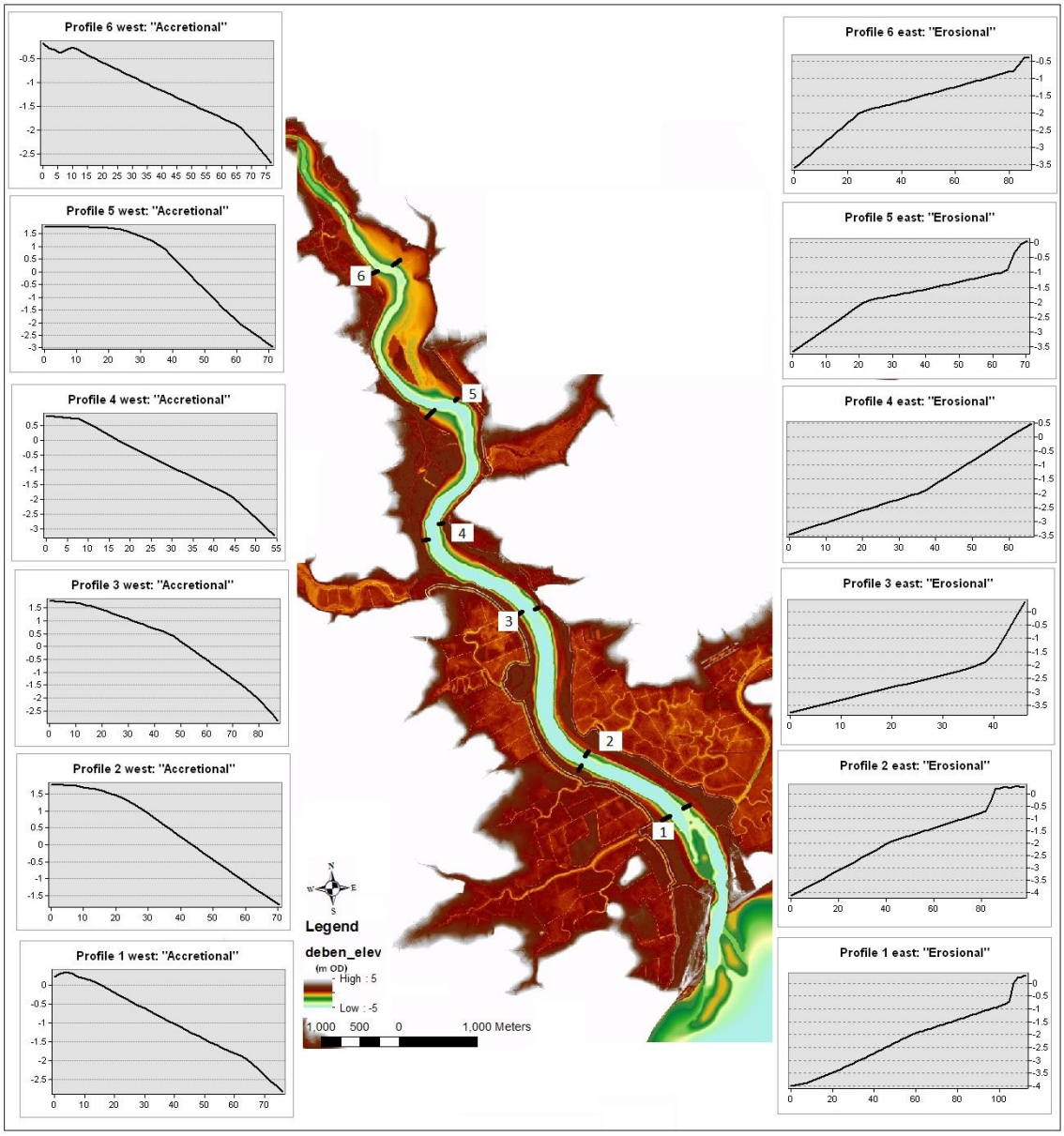

Figure 4.23: Tidal flat cross-sectional profiles at six locations along the Deben Estuary.

Four simulations were performed, as summarised in Table 4.11, under the mid-range UKCP09 regional sea-level scenario. Firstly, the impacts of sea-level rise at the Deben estuary are investigated assuming that all the present defences will continue to be maintained protecting the areas behind them. The area is simulated in zones of different tidal flat behaviour; the accretional western and the erosional eastern side ('RUN_A'). The defences are then considered inactive. In that case the above analysis for the tidal flat behaviour cannot describe the behaviour of the tidal flat behind the defences, and therefore three scenarios of different tidal flat behaviour are examined; a stable ('RUN_B'), an eroding ('RUN_C') and an accreting ('RUN_D') tidal flat.

Table 4.11: Different simulations of the modified SLAMM in the Deben estuary.

Simulation		Tidal flat accretion sub-model	Marsh accretion sub-model
Active defences	Run_A	Subsite 1 = 12.7 mm yr^{-1} Subsite 2 = -9 mm yr^{-1}	Spatial
No active defences	Run_B	accretion= 0 mm yr^{-1}	Spatial
	Run_C	Eroding tidal flat = -11.2mm yr^{-1}	Spatial
	Run_D	Accreting tidal flat = 10.8 mmyr^{-1}	Spatial

A. Active Defences

First, the impacts of sea-level rise at the Deben estuary are investigated assuming that all the present defences will continue to be maintained protecting the reclaimed areas behind them. The results are presented in Table 4.12 and Figure 4.24, where the zoning of the estuary into sub-sites of different input parameters for the tidal flat is also depicted.

At the beginning, the estuary seems to respond quite dynamically to the specific sea-level scenario. As the sea level continues to rise, higher marsh cannot keep pace and is inundated to lower marsh, increasing its area. The lower elevations of the estuary, though, respond differently within each sub-site. Along the western margin of the estuary, the accreting tidal flat outweighs the sea-level rise and forms marsh at its higher areas. On the other hand, the eroding tidal flat is inundated increasing the subtidal area. This is more obvious at the upper part of the estuary where this is not constrained by defences. In that direction, it can be said that the Deben estuary migrates eastwards by 2100 under the specific sea-level rise scenario, with the low lying terrain remaining protected by the defences.

Table 4.12: Impacts of sea-level rise at the Deben estuary as presently defended.

Simulation: 'RUN_A'		Low	High	Transitional	Upper	Lower		Estuarine	Ocean	Ocean	Open
Date	SLR	Ground	Ground	Marsh	Marsh	Marsh	Tidal Flat	Subtidal	Beach	Flat	Ocean
0	0.00	2017	7494	39	135	51	480	244	83	21	398
2025	0.05	2019	7489	35	129	66	472	238	52	19	444
2050	0.15	2019	7482	28	109	120	433	249	0.1	12	509
2075	0.27	2019	7475	25	61	201	393	264	0.1	7	516
2100	0.41	2020	7468	24	41	241	355	288	0.1	0	525

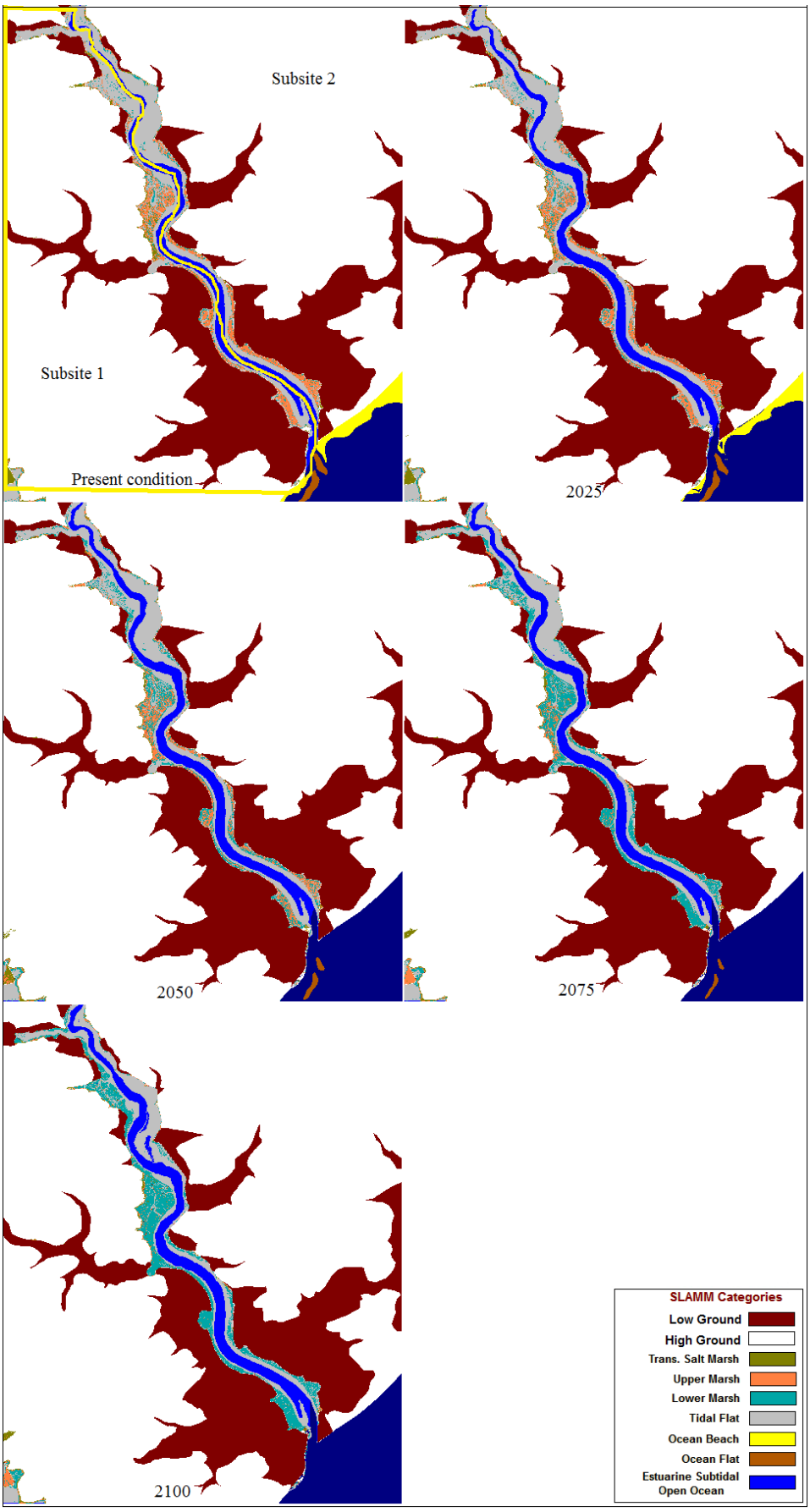

Figure 4.24: Modelled habitat distributions for the defended Deben estuary (‘RUN_A’).

B. Inactive Defences

As mentioned in Section 4.1, in order for the defences to rendered as inactive, they have been assigned as long narrow hills of dryland and the areas behind them as tidal flat, both subject to the processes related to sea-level rise. Three different scenarios of tidal flat behaviour are simulated here by assuming a more-or-less stable, an eroding and an accreting tidal flat. The results are presented in Figures 4.25 – 4.27 respectively and summarised in Table 4.13.

In the first scenario, the Deben estuary seems to migrate landwards under the specific sea-level rise scenario, with the previously protected by defences areas remaining quite stable (Figure 4.25). At the beginning, the higher marsh areas cope with the sea-level rise being slightly inundated to lower marsh in areas further away from the main channel where its accretion capability is very low. As the sea-level rises though at the next time-steps, its accretional capability even closer to the channel is not enough to keep pace with the sea-level rise, forcing it to lose half of its area by 2100. Consequently, the lower marsh area is increased. The expanded lower marsh in higher elevations of the estuary cannot cope with the increased sea level and therefore is inundated to tidal flat, which although is inundated to subtidal in the lower elevations of the estuary, its total area is increased by 10% in 2100.

Similar behaviour of saltmarsh landwards migration is observed in the next two simulations. However, the areas in lower elevations of the estuary respond totally different in each scenario. More specifically, in the second scenario, although the tidal flat is expanded landwards over the lower marsh, as described in the previous scenario, its eroding lower parts cannot cope with the sea-level rise and therefore are inundated increasing the subtidal area by 60% in 2100. As a result, this scenario considers the Deben estuary very vulnerable to the specific sea-level rise scenario, with the removal of the defences inundating parts of the areas behind them by creating small creeks within them (Figure 4.26).

On the other hand, the accretional response of the tidal flat under the third scenario is sufficient to outweigh sea-level rise, keeping the subtidal area steady by 2100. At the same time, it is also able to build up to lower marsh, quadrupling its area. The expanded lower marsh in such low elevations of the estuary is also capable of accreting to higher

marsh. Although its total area is decreased by 2100, this is still more than in the two previous simulations. Thus, this scenario shows the Deben estuary to be able to cope with sea-level rise, with the removal of the defences keeping stable the tidal flat at the deeper areas of the eastern estuary, but filling in its higher western side (Figure 4.27).

In the coastal environment, as mentioned in the previous case study, the impacts of the sea-level rise on the ocean beach are simulated within SLAMM using a Bruun formulation. This predicts total erosion of the beach by 2050. Particular interest presents the feature of the Knolls. In all three simulations the Knolls are assigned as ocean flat and therefore treated like the tidal flat in each simulation. Thus, in the first scenario the Knolls are not very capable to cope with the sea-level rise, losing almost half of its area by 2100. In the second scenario, the eroding Knolls are totally inundated by 2100. Finally, their accreting behaviour on the last scenario outweighs the sea-level rise, keeping their area steady. However, none of these simulations are able to include the complex morphodynamic behaviour of the ebb-tidal delta. According the survey undertaken by Burningham and French (2006), and presented in Figure 4.28, this system first experiences a small-scale intertidal breakdown by losing intertidal volume, followed by reconstruction and resumed growth.

Table 4.13: Impacts of sea-level rise at the undefended Deben estuary, modelled using different behaviour of the tidal flat area.

Simulation: 'RUN_B'		High	Transition	Upper	Lower	Tidal	Estuarine	Ocean	Ocean	Open
Date	SLR	Ground	al Marsh	Marsh	Marsh	Flat	Subtidal	Beach	Flat	Ocean
0	0.00	7897	138	235	189	1756	244	83	21	399
2025	0.05	7879	133	225	186	1787	237	59	20	436
2050	0.15	7843	124	194	202	1838	239	0.4	19	503
2075	0.27	7800	119	138	236	1888	253	0.9	15	511
2100	0.41	7755	117	113	228	1951	265	1.0	13	519
Simulation: 'RUN_C'		**High**	**Transition**	**Upper**	**Lower**	**Tidal**	**Estuarine**	**Ocean**	**Ocean**	**Open**
Date	**SLR**	**Ground**	**al Marsh**	**Marsh**	**Marsh**	**Flat**	**Subtidal**	**Beach**	**Flat**	**Ocean**
0	0.00	7897	138	235	189	1756	244	83	21	399
2025	0.05	7879	133	225	179	1779	251	48	17	450
2050	0.15	7843	124	193	197	1801	281	0.4	11	512
2075	0.27	7800	119	137	232	1819	327	0.9	6	521
2100	0.41	7754	116	112	225	1823	397	0.9	0	533
Simulation: 'RUN_D'		**High**	**Transition**	**Upper**	**Lower**	**Tidal**	**Estuarine**	**Ocean**	**Ocean**	**Open**
Date	**SLR**	**Ground**	**al Marsh**	**Marsh**	**Marsh**	**Flat**	**Subtidal**	**Beach**	**Flat**	**Ocean**
0	0.00	7897	138	235	189	1756	244	83	21	399
2025	0.05	7879	133	226	247	1728	233	63	21	431
2050	0.15	7844	126	207	418	1615	230	0.4	21	501
2075	0.27	7802	125	161	634	1483	230	1.0	21	505
2100	0.41	7759	125	144	832	1339	232	1.0	21	510

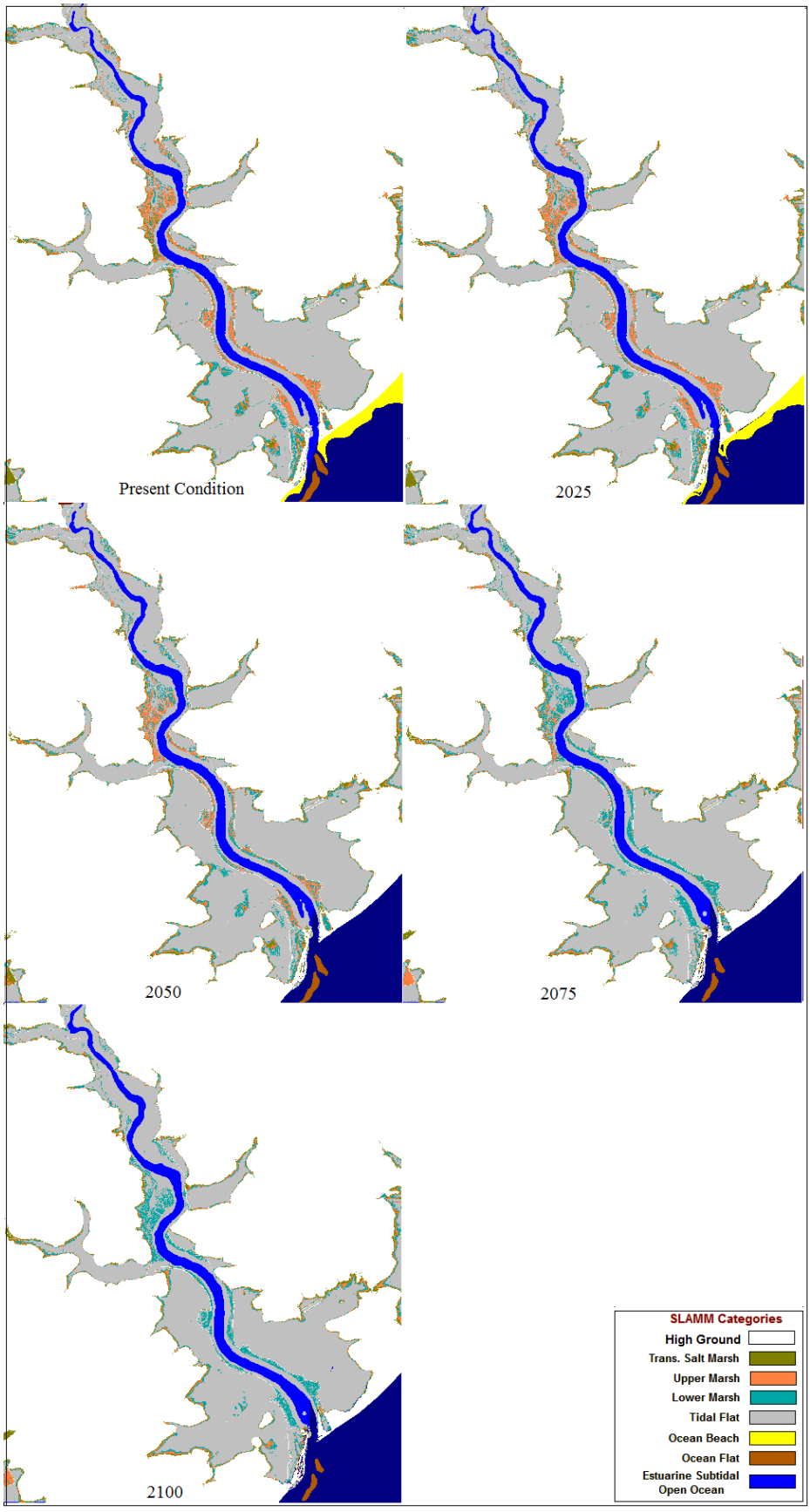

Figure 4.25: Modelled habitat distributions for the undefended Deben estuary, assuming a quite stable tidal flat ('RUN_B').

Figure 4.26: Modelled habitat distributions for the undefended Deben estuary, assuming an eroding tidal flat ('RUN_C').

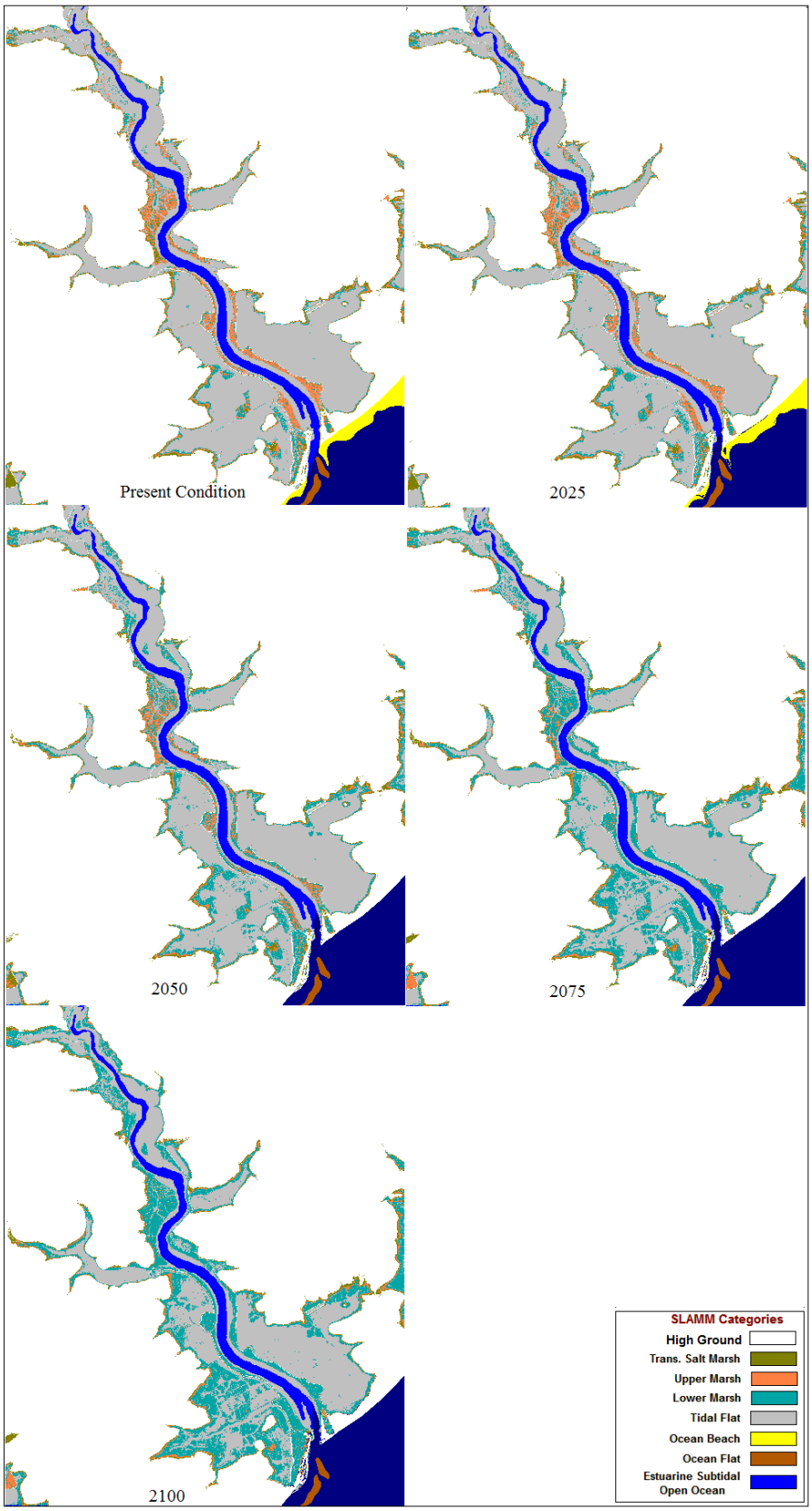

Figure 4.27: Modelled habitat distributions for the undefended Deben estuary, assuming an accreting tidal flat ('RUN_D').

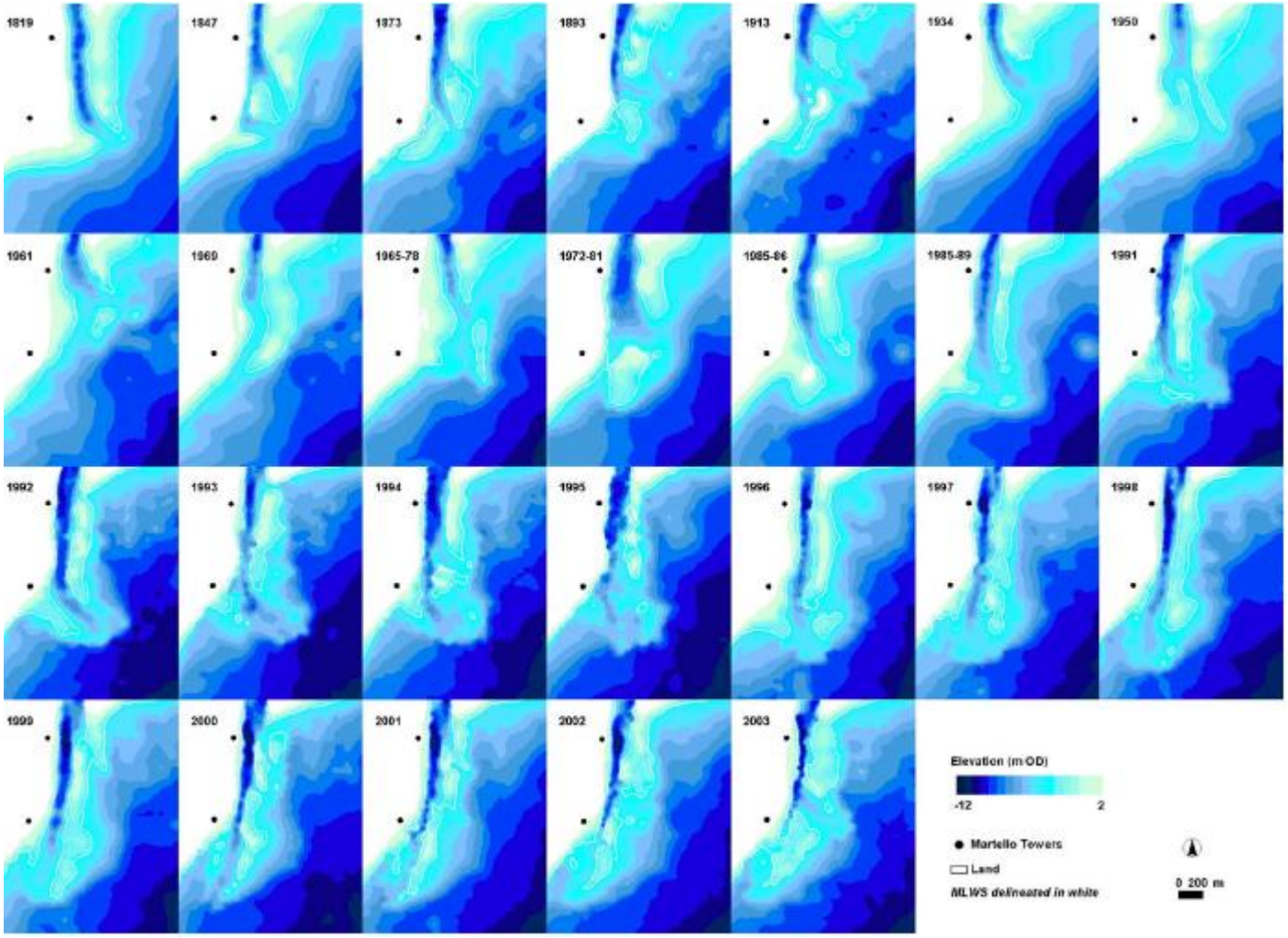

Figure 4.28: Historical bathymetries for the Deben inlet and ebb-tidal delta (data from Burningham and French, 2006).

Finally, the saltmarsh distribution generated by the original DEM can also be compared with observed extent, in order to investigate the accuracy of the habitat classification conceptual model used within SLAMM. Similarly to the Blyth estuary in Section 4.1, saltmarsh has been mapped in detail by the Environment Agency (EA), and a comparison of their saltmarsh polygons with the SLAMM classification for the Deben estuary is presented in Figure 4.29, indicating a generally very close correspondence between model and data. Localised differences though still exist, however. For example, Area 1 is characterised as a saltmarsh by the EA when in reality it is effectively a reedbed (*Phragmites spp*), a habitat that is determined partly by salinity rather than simple elevation. In addition, minor differences arise at the saltmarsh – tidal flat boundaries.

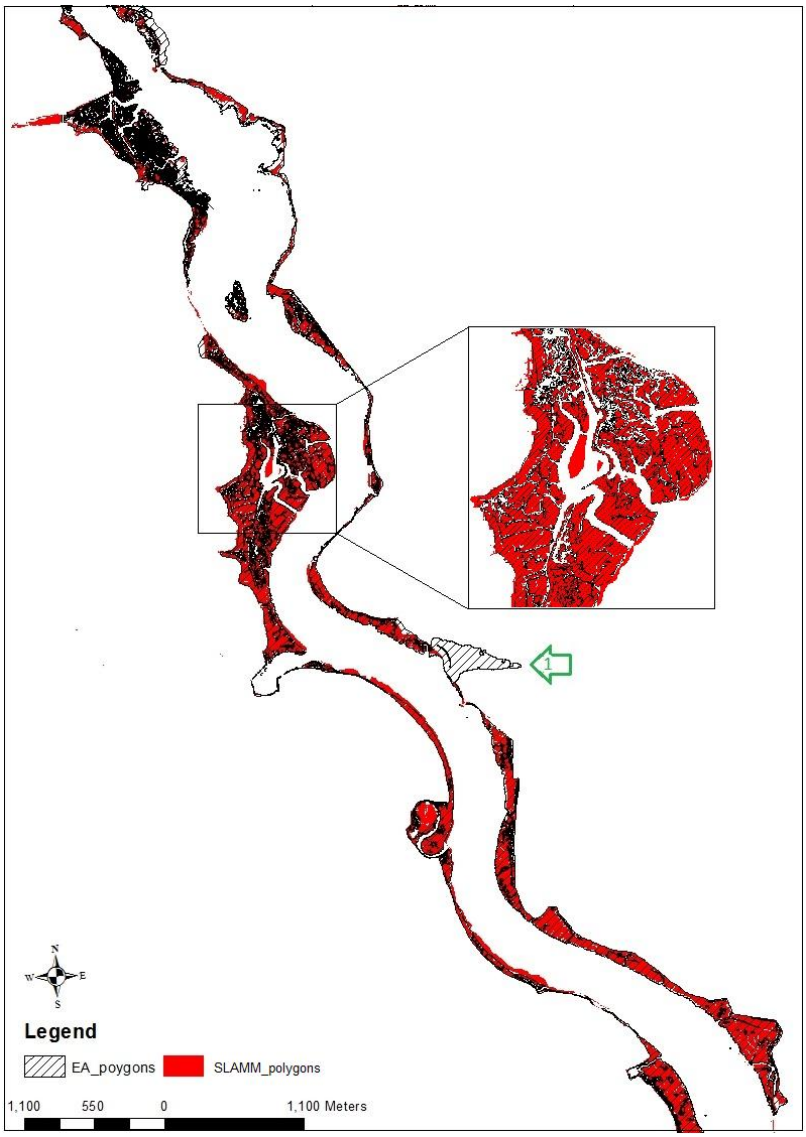

Figure 4.29: Comparison of saltmarsh distribution generated by the DEM classification in SLAMM and saltmarsh extent determined by the Environment Agency.

5 APPLICATION OF SLAMM TO COASTAL BARRIER COMPLEX OF BLAKENEY, NORFOLK, UK

5.1 Model parameterisation

As a follow-up to the simulations of estuarine habitat change, the modified SLAMM code was applied to the gravel and dune barrier and backbarrier saltmarsh complex of Blakeney, North Norfolk, eastern England. The aim here is to critically evaluate the ability of the modified model code to produce robust projections of habitat change in a system influenced more directly by the evolution of the open coast. In the case of Blakeney, this involves historic retreat of the outer barrier under the influence of storm-driven overwash (Clymo, 1964; Funnell et al., 2000)

As with the previous case studies, a key factor influencing the selection of this site was the availability of a composite LiDAR dataset; this was provided by the Environment Agency from surveys undertaken mostly between 2008 and 2010 at a 2 m resolution. These data were used as the base DEM and were integrated with subtidal bathymetry which was manually digitised based on UKHO bathymetry chart (chart no: 0108-0). The composite elevation dataset is resampled to 5 m resolution and visualised in Figure 5.1a. The derived land cover and slope layers used to define the model domain are presented in Figures 5.1b and 5.1c respectively.

Table 5.1 summarises the site-specific parameters used in the model runs. The historic sea-level trend is estimated at 2 mm yr^{-1} by interpolating the historic trend of the two closest tide gauge stations at Immingham and Lowestoft (PSMSL, 2012). The tidal reference levels for Blakeney, expressed in m OD, are obtained from the SMP2 project (SMP2-Appendix C, 2010). Due to missing data though, the highest and lowest astronomical levels are obtained by interpolating the relevant ones in Immingham and Cromer (Admiralty, 2000). Deposition rates have not been systematically measured at the backbarrier side of the island. Accordingly, the MARSH-0D model (French, 2006) is again used to compute the dependence of saltmarsh deposition rate on elevation; modelled sedimentation as a function of elevation was used to constrain the SLAMM saltmarsh accretion model parameters and a zero accretion rate assumed at the highest elevation of the marsh (Figure 5.2). In addition, the proximity to the creek network is

known to exert a strong control on sedimentation in the marshes of North Norfolk (French and Spencer, 1993; French et al., 1995), and the distance to channel factor is also used in the SLAMM marsh accretion sub-models. In the absence of both data and a more mechanistic model of tidal flat processes, sedimentation in this environment is simply assumed to track sea-level rise.

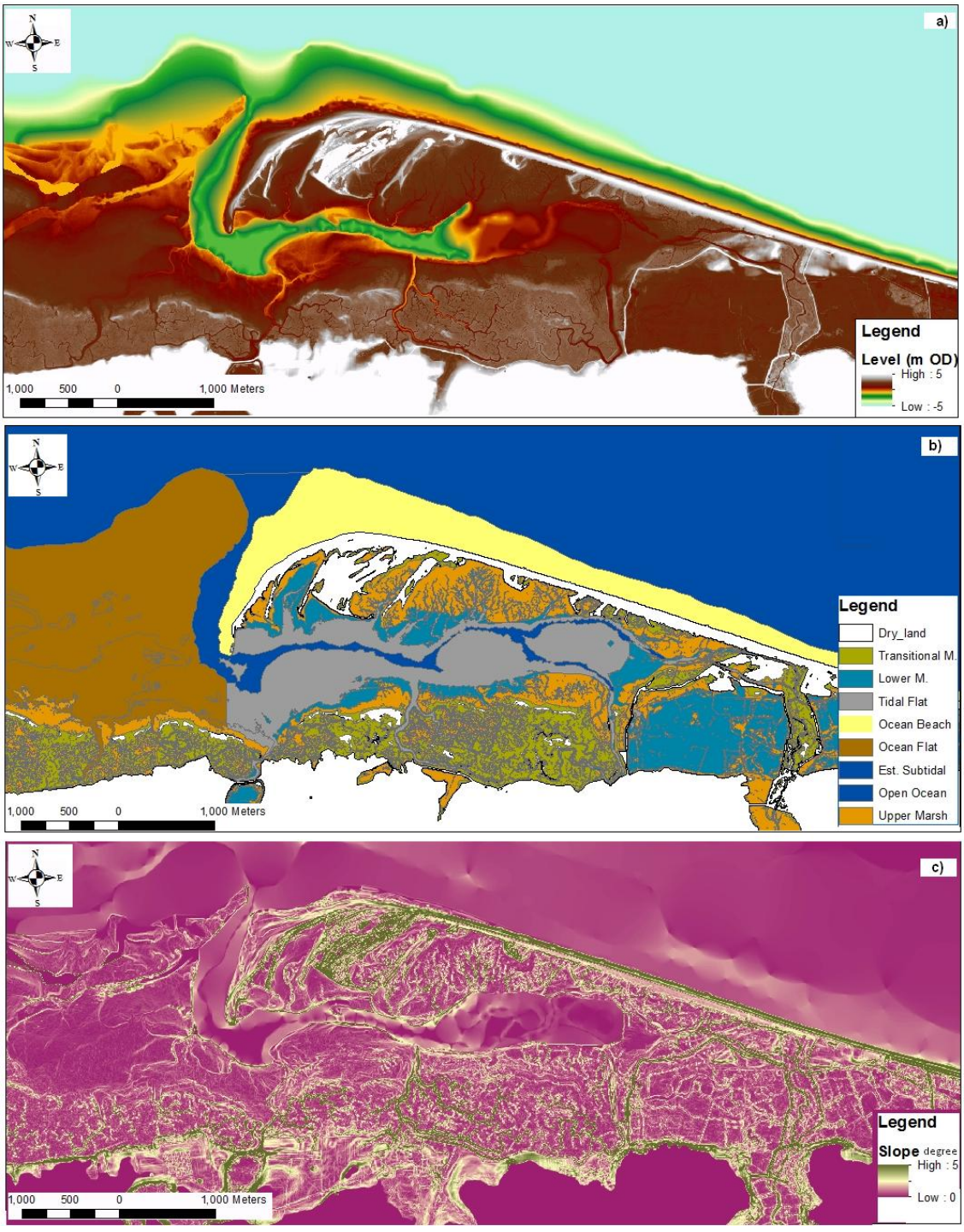

Figure 5.1: SLAMM input layers for the Blakeney barrier-backbarrier complex; a) DEM, b) Land classification, c) Slope map.

Table 5.1: SLAMM site parameter table for Blakeney.

Parameter		Value
Date (YYYY)		2010
Direction Offshore[n,s,e,w]		N
Historic Trend (mm yr^{-1})		2
Salt Elevation (m above MTL)		3
HAT (m)		3
MHWS (m)		2.6
MHW (m)		1.9
MHWN (m)		1.2
LAT (m)		-2.8
Marsh Erosion (m yr^{-1})		0.1
T.Flat Erosion (m y^{-1})		0.1
Beach Sedimentation Rate / Tidal Flat Accretion (mm yr^{-1})		2
LOWER MARSH ACCRETION MODEL	Max Accretion (mm yr^{-1})	24
	Min Accretion (mm yr^{-1})	9.9
	Coefficient a	0
	Coefficient b	1
	Coefficient c	3
	DeffectMax (m)	100
	Dmin (unitless)	0.1
UPPER MARSH ACCRETION MODEL	Max Accretion (mm yr^{-1})	9.9
	Min Accretion (mm yr^{-1})	0
	Coefficient a	0
	Coefficient b	1.4
	Coefficient c	1
	DeffectMax (m)	100
	Dmin (unitless)	0.1

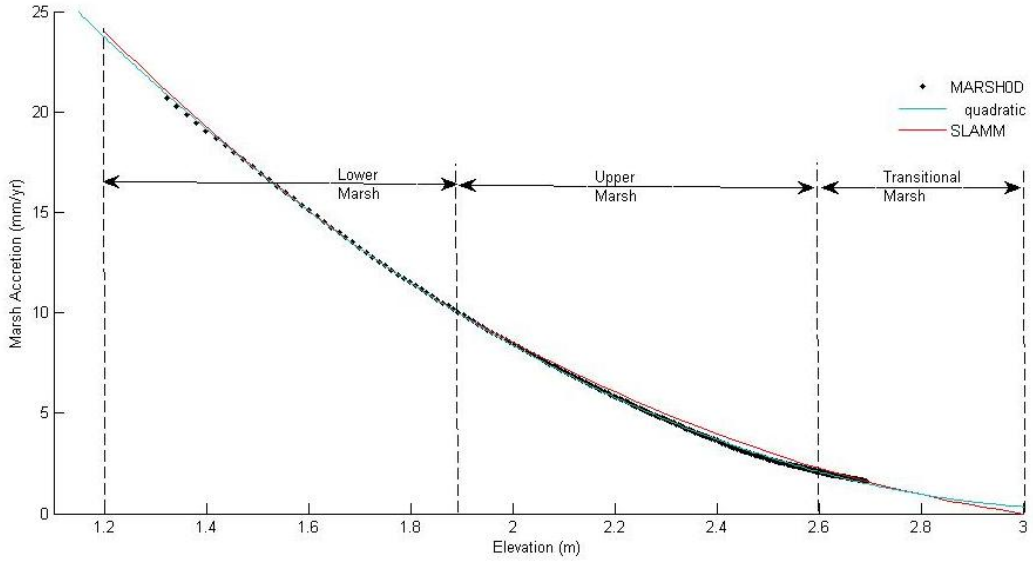

Figure 5.2: Modelled marsh accretion rates used to constrain the SLAMM marsh accretion sub-models for the Blakeney estuary.

The Blakeney barrier has retreated over recent historical timescale, in parallel with incremental westward extension of the spit through creation of sequential recurves

under storm conditions (Funnell et al., 2000; Environment Agency, 2012). This behaviour is visualised in Figure 5.3 according to the coastal trend analysis undertaken by the Environment Agency (2012) for the period 1991 to 2011; a 2 m advance in the dune line is evident in the transect N2C1, in parallel with a foredune retreat of 20 m in 20 years in transect N2C2. To the east and along the spit length, a roll back of the shingle ridge is occurring in response to natural processes, on average rate of 0.6 m yr^{-1}.

Figure 5.3: Coastal trend analysis for the Blakeney between 1991 and 2011, focusing on the a) westerly migration of the Blakeney Point system and b) the shoreline retreat along the barrier island (Environment Agency, 2012).

Overwash is an important process driving the landward rollover of a barrier over the landward saltmarsh and tidal channel environments. SLAMM includes an overwash module, as mentioned in Chapter 2, that applies to barrier islands less than 500 m in width due to storms with a frequency of 25 years. During overwash, the barrier beach rolls back by 30 m, and overwashed sediment is carried over the crest of the barrier and deposited onto the adjacent marsh, converting it to undeveloped dryland and estuarine beach (Table 5.2; Figure 5.4). This behaviour is based on observations from the large sandy barrier beaches in the USA (Leatherman and Zaremba, 1986; Clough et al., 2010).

Table 5.2: SLAMM overwash decision tree (Clough et al., 2010).

Converting from	to	Default values
Ocean Beach	Ocean	30 m
Dryland	Ocean Beach	30 m
Transitional and upper marsh	Undeveloped Dryland	50%
Lower marsh	Estuarine Beach	50%
Estuarine Subtidal	Estuarine Beach	60m

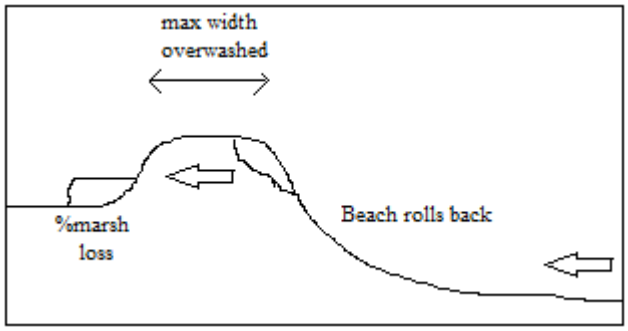

Figure 5.4: Overwash definition sketch within SLAMM

Accordingly, the overwash sub-model must be parameterised for the specific case study. An overwash frequency of 2 years is assumed, since the coast of North Norfolk experience extreme water levels almost every year (Figure 5.5). The maximum overwashed width is the width of the shingle ridge, estimated to be about 25 m, based on present aerial photos (Figure 5.6). The barrier roll over is estimated to be approximately 1.2 m in every overwash event, assuming that a retreat rate of 0.6 m yr^{-1} calculated on the coastal trend analysis undertaken by the Environment Agency (2012) is driven by the process of overwash (see Figure 5.3). Consequently, 1.2 m of sediment are overwashed in every event from the 25 m width shingle ridge and deposited on the marsh area at the back side of the ridge (‘marsh loss’: approximately 5%).

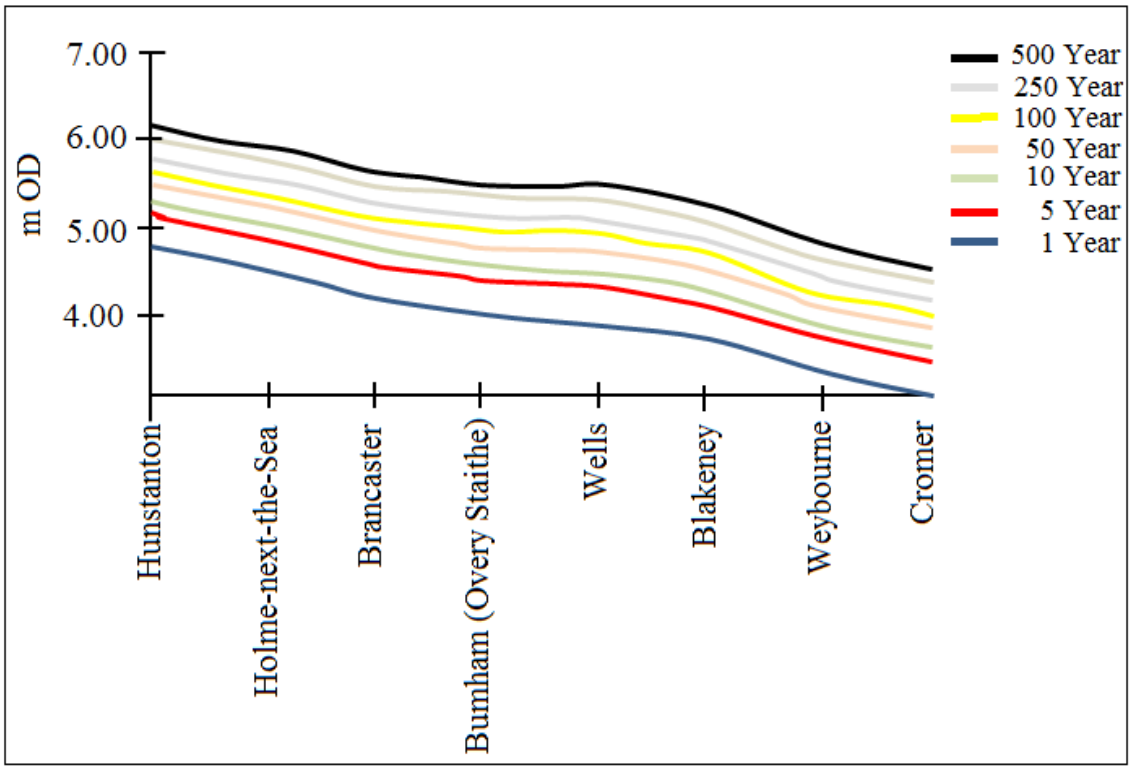

Figure 5.5: Distribution of extreme water levels in North Norfolk (after SMP2, 2010).

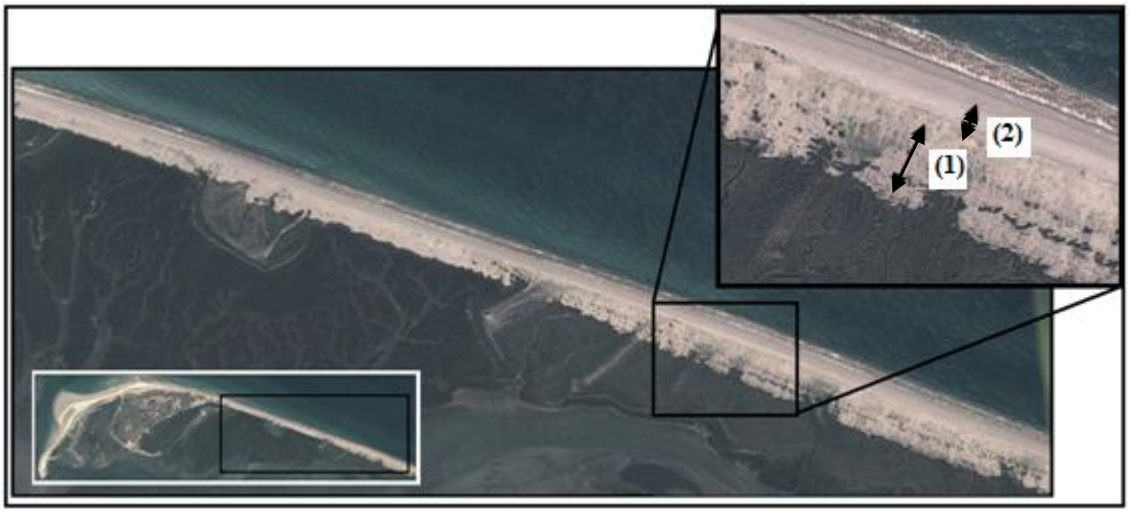

Figure 5.6: Overwash sub-model parameterisation based on analysis of aerial imagery in Google Earth: 1) marsh loss, 2) maximum overwash width.

Three different scenarios are simulated under the UKCP09 SE sea-level rise scenario, as presented in Table 5.3, in order to investigate how this process affects the habitat distribution of Blakeney. The overwash sub-model is not incorporated in the first simulation (RUN_1), but a comparative evaluation in two subsequent simulations applies an overwash of 5% (RUN_2) and 100% (RUN_3).

Table 5.3: SLAMM parameter table for the sensitivity analysis of the overwash model for Blakeney.

Overwash model parameters	RUN_1	RUN_2	RUN_3
Freq. overwash (years)	NO OVERWASH	2	2
Max width overwash (m)		25	25
Beach to Ocean (m)		1.2	1.2
Dryland to beach (m)		1.2	1.2
Marsh loss overwash (%)		5	100

5.2 Results

The results of these runs (summarised in Table 5.4) indicate a very small influence of the overwash process on habitat distribution. The differences are so small that they cannot be easily resolved in the SLAMM output maps. However, the map outputs of the first simulation (RUN_1) are presented in Figure 5.7 in order to understand how the whole system responds to the specific sea-level rise scenario. In all cases, the Blakeney complex responds quite dynamically to the specific sea-level rise scenario, by migrating inland. Tidal flat is slightly extended over the lower marsh in areas away from the main channel where the last one cannot keep pace with the sea-level rise, increasing its area by about 20% by 2100. In areas though closer to the main channel, the lower marsh accretion outweigh the sea-level rise and is significantly expanded over the upper marsh. However, the upper marsh area remains quite steady by 2100 by migrating inland squeezing the transitional marsh which cannot cope with the sea-level rise since its accreting capacity is close to zero that further away from the main channel.

The process of overwash slightly affects the habitat distribution of the Blakeney complex. The almost totally eroded beach seems to also slightly roll back, increasing the ocean area. The backbarrier environment is also affected with lower marsh being converted to estuarine beach, and higher marsh to gravel barrier, assigned to the 'undeveloped dryland' wetland category within SLAMM. The greater the assumed overwashed area, more estuarine beach and undeveloped dryland are produced.

However, the undeveloped dryland at the back side of the barrier island is unreasonably overwashed at the next time-steps, generating ocean beach at the backbarrier environment. Accordingly, this conversion rule was modified (Figure A-0.31 in Appendix) and the last two simulations repeated (RUN_4 and RUN_5; Table 5.5). The backbarrier environment is no longer able to be overwashed, and therefore more 'undeveloped dryland' is projected in the last simulations.

Table 5.4: Summary of the sensitivity analysis of the overwash sub-model for Blakeney.

Simulation: 'RUN_1' Date	Dry Land	Und. Dryland	Transitional Marsh	Upper Marsh	Lower Marsh	Estuarine Beach	Tidal Flat	Subtidal	Ocean Beach	Ocean Flat	Ocean
0	2377.8	0.0	333.2	507.8	405.6	0.0	284.2	103.4	296.0	473.0	3348.7
2025	2360.8	0.0	272.0	544.3	440.3	0.0	282.1	85.4	238.4	463.0	3443.5
2050	2332.4	0.0	156.2	603.2	500.3	0.0	296.0	82.7	2.1	457.9	3699.0
2075	2303.5	0.0	83.1	595.2	572.5	0.0	317.0	74.2	3.2	452.2	3729.0
2100	2276.8	0.0	48.5	544.6	624.1	0.0	360.4	70.4	3.3	446.0	3755.7
Simulation: 'RUN_2' Date	**Dry Land**	**Und. Dryland**	**Transitional Marsh**	**Upper Marsh**	**Lower Marsh**	**Estuarine Beach**	**Tidal Flat**	**Subtidal**	**Ocean Beach**	**Ocean Flat**	**Ocean**
0	2377.8	0.0	333.2	507.8	405.6	0.0	284.2	103.4	296.0	473.0	3348.7
2025	2357.6	0.0	271.1	544.4	440.3	0.1	282.1	85.4	239.5	463.0	3446.4
2050	2330.1	0.0	153.9	603.1	500.3	0.1	296.0	82.7	2.2	457.9	3703.6
2075	2301.6	0.0	81.1	594.8	572.5	0.0	316.8	74.2	3.2	452.2	3733.3
2100	2275.3	0.0	47.0	543.8	623.9	0.1	360.4	70.4	3.2	446.0	3759.7
Simulation: 'RUN_3' Date	**Dry Land**	**Und. Dryland**	**Transitional Marsh**	**Upper Marsh**	**Lower Marsh**	**Estuarine Beach**	**Tidal Flat**	**Subtidal**	**Ocean Beach**	**Ocean Flat**	**Ocean**
0	2377.8	0.0	333.2	507.8	405.6	0.0	284.2	103.4	296.0	473.0	3348.7
2025	2359.8	0.6	270.5	543.8	440.2	0.2	282.1	85.4	238.6	463.0	3445.8
2050	2332.0	0.2	153.2	602.0	500.0	0.3	296.0	82.7	2.3	457.9	3703.1
2075	2303.0	0.0	80.9	593.5	572.1	0.3	316.6	74.2	3.2	452.2	3733.8
2100	2276.5	0.0	47.0	542.2	623.5	0.3	360.0	70.4	3.2	446.0	3760.7

Table 5.5: Summary of the sensitivity analysis of the modified overwash sub-model for Blakeney for the second (RUN_4) and third (RUN_5) scenario respectively.

Simulation: 'RUN_4' Date	Dry Land	Und. Dryland	Transitional Marsh	Upper Marsh	Lower Marsh	Estuarine Beach	Tidal Flat	Subtidal	Ocean Beach	Ocean Flat	Ocean
0	2377.8	0.0	333.2	507.8	405.6	0.0	284.2	103.4	296.0	473.0	3348.7
2025	2357.5	0.8	271.2	544.3	440.3	0.1	282.1	85.4	239.3	463.0	3446.0
2050	2329.9	0.2	153.9	603.1	500.2	0.1	296.0	82.7	2.2	457.9	3703.6
2075	2301.3	0.1	81.2	594.9	572.5	0.1	316.9	74.2	3.2	452.2	3733.4
2100	2275.2	0.1	47.0	543.9	623.9	0.1	360.4	70.4	3.2	446.0	3759.8
Simulation: 'RUN_5' Date	**Dry Land**	**Und. Dryland**	**Transitional Marsh**	**Upper Marsh**	**Lower Marsh**	**Estuarine Beach**	**Tidal Flat**	**Subtidal**	**Ocean Beach**	**Ocean Flat**	**Ocean**
0.0	2377.8	0.0	333.2	507.8	405.6	0.0	284.2	103.4	296.0	473.0	3348.7
2025	2359.7	1.6	270.7	544.0	440.2	0.1	282.1	85.4	237.9	463.0	3445.1
2050	2331.9	0.9	153.3	602.2	500.1	0.2	296.0	82.7	2.4	457.9	3702.2
2075	2303.0	0.7	81.0	593.0	572.3	0.3	316.6	74.2	3.3	452.2	3733.2
2100	2276.5	0.5	47.0	541.7	623.4	0.5	360.0	70.4	3.2	446.0	3760.7

In order to investigate more deeply the effects of overwash on the habitat distribution, the projections to 2100 are examined in more detail in Figure 5.8. Under the extreme scenario of a completely overwashed shingle ridge (RUN_5), it is clear that the overwash sub-module produces unreasonable results with the overwashed sediment being deposited far away from the shingle ridge.

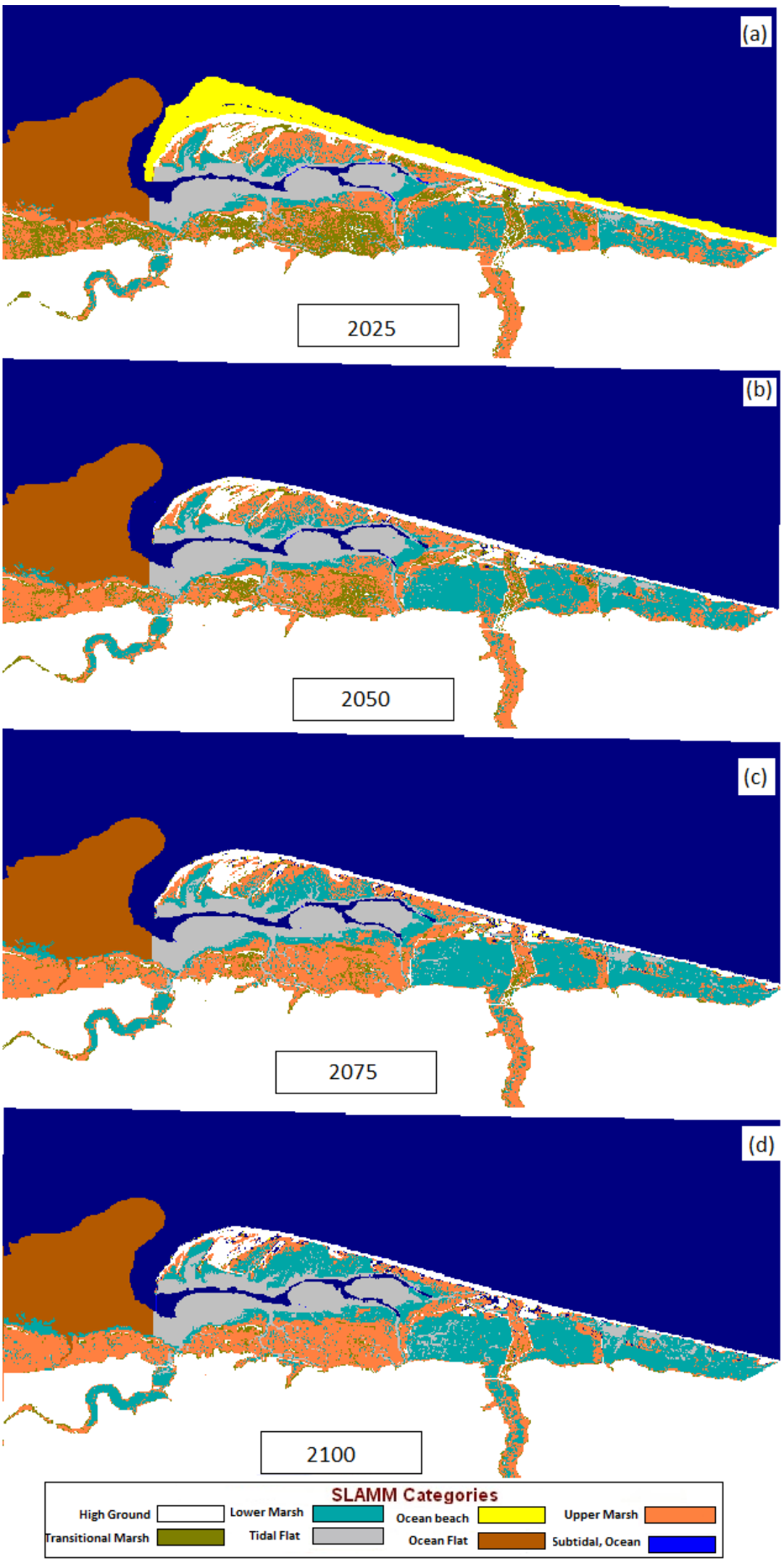

Figure 5.7: Habitat distribution for the Blakeney complex up to 2100 (RUN_1).

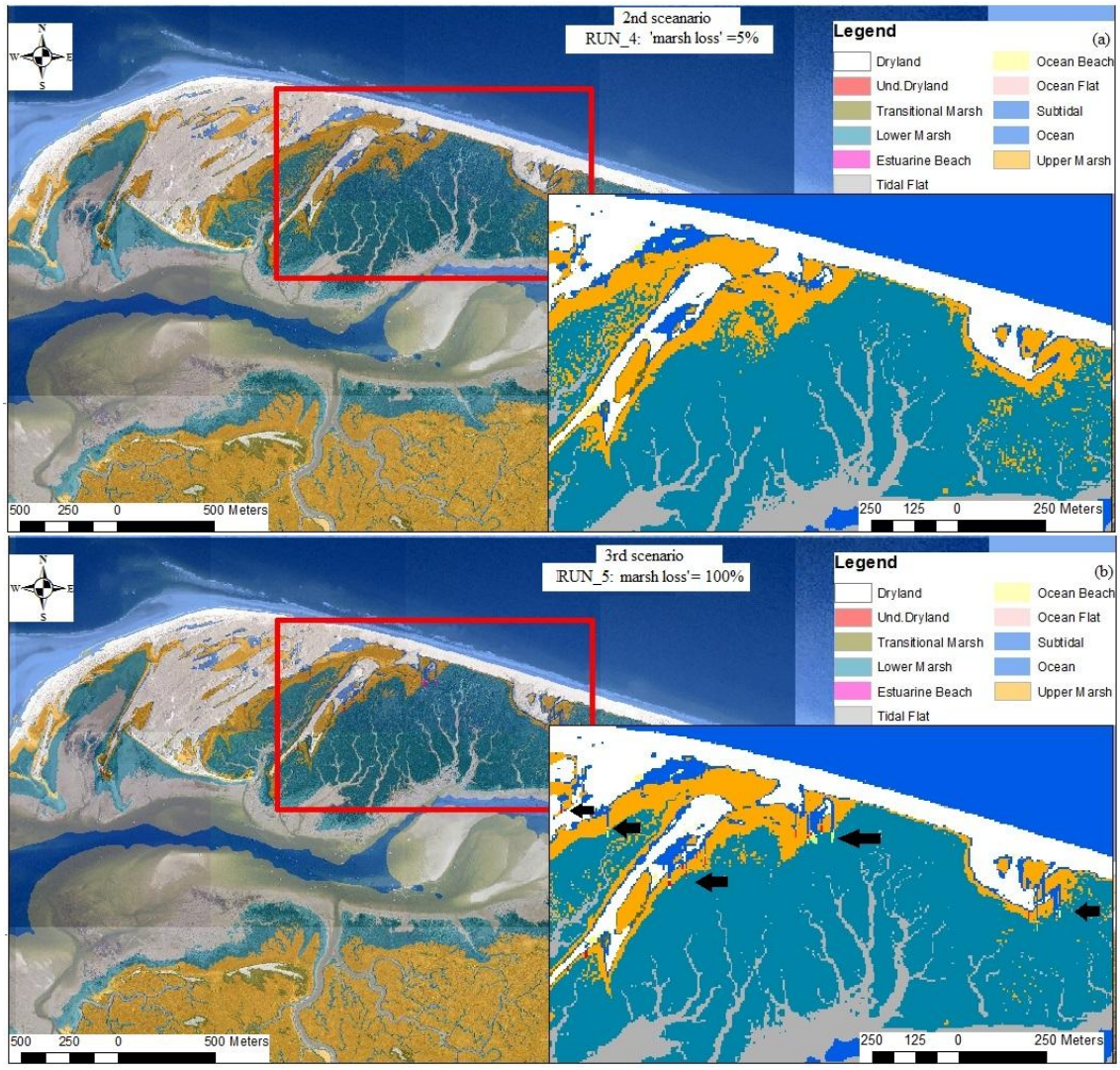

Figure 5.8: Changes in habitat distribution to 2100 for Blakeney, modelled using the modified source code under the second (RUN_4) and third (RUN_5) scenario.

The weakness of SLAMM to properly simulate the process of overwash has been acknowledged by the developers for simulations undertaken at a fine (<30m) resolution. Following this, the second scenario (RUN_4) is repeated using 30m resolution (RUN_6). The ocean beach responds more dynamically, by slightly rolling back instead of being totally eroded under the Bruun Rule. In parallel, the overwashed sediment has been deposited at the backbarrier environment affecting only the 5% of the adjacent to the barrier island marsh, evenly distributed across the island (Table 5.6; Figure 5.9).

Table 5.6: Impacts of sea-level rise at the Blakeney complex under the second scenario, modelled at 30m resolution (RUN_6).

Simulation: 'RUN_6'											
Date	Dry Land	Und. Dryland	Transitional Marsh	Upper Marsh	Lower Marsh	Estuarine Beach	Tidal Flat	Subtidal	Ocean Beach	Ocean Flat	Ocean
0	2373.6	0.0	334.6	511.5	404.1	0.0	284.8	102.7	296.2	474.0	3346.9
2025	2366.7	0.2	274.3	519.2	436.9	0.0	289.7	88.9	296.8	462.6	3393.1
2050	2354.5	1.0	160.3	571.1	477.2	1.0	314.0	91.0	292.0	457.9	3408.4
2075	2329.3	0.8	109.1	566.6	525.3	1.4	335.9	90.3	285.9	452.4	3431.3
2100	2305.3	0.8	83.8	523.8	568.2	1.6	372.6	89.9	278.4	446.4	3457.5

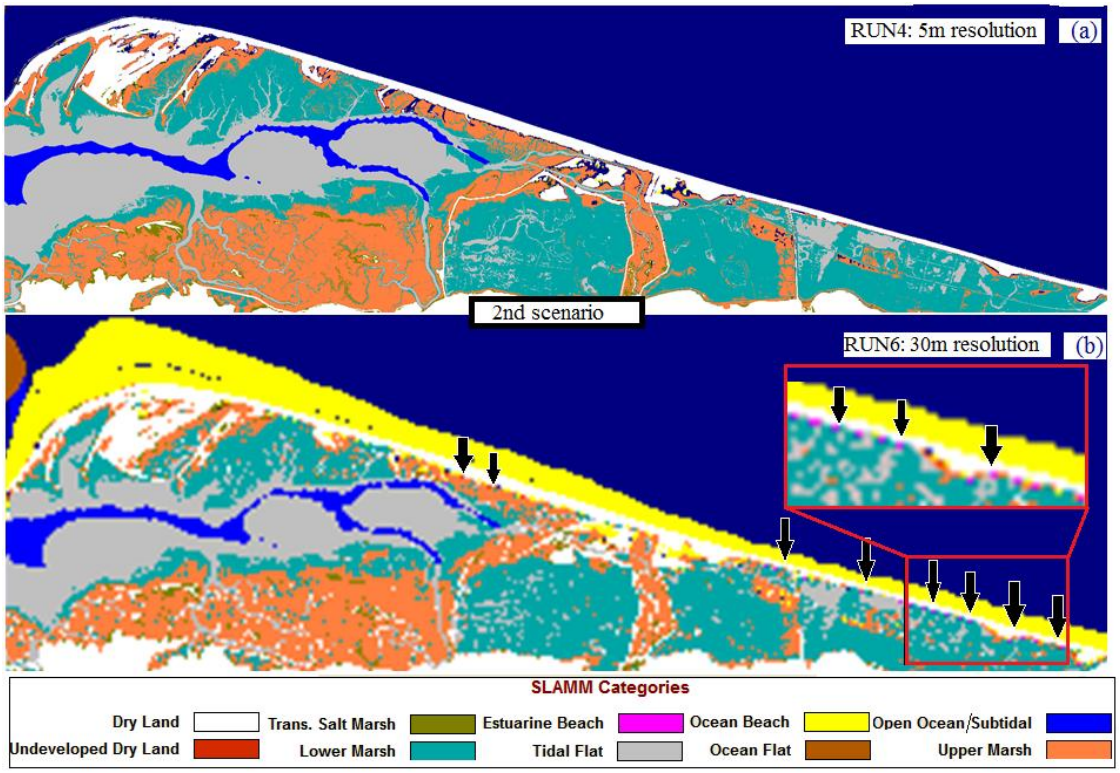

Figure 5.9: Habitat distribution for the Blakeney complex for the year 2100 under the second scenario, modelled at a) 5m (RUN_4) and b) 30m (RUN_6) resolution.

5.3 Indicative evaluation of the model

In both resolutions, SLAMM cannot include the tendency of the spit to develop westwards. This westward growth of Blakeney is evident in Figure 5.10 with the growth stages over the last century being marked by the formation of the different recurves. The recurves are shaped by westerly and northwesterly wave action, with the most recent extension having been added after a storm surge in 1978 (Bird, 2008). This analysis indicates that the western end of the Blakeney system is mainly affected by storm driven processes, considering it far more complex than SLAMM could ever handle. Therefore, this complex part is not included within the further analysis of the model.

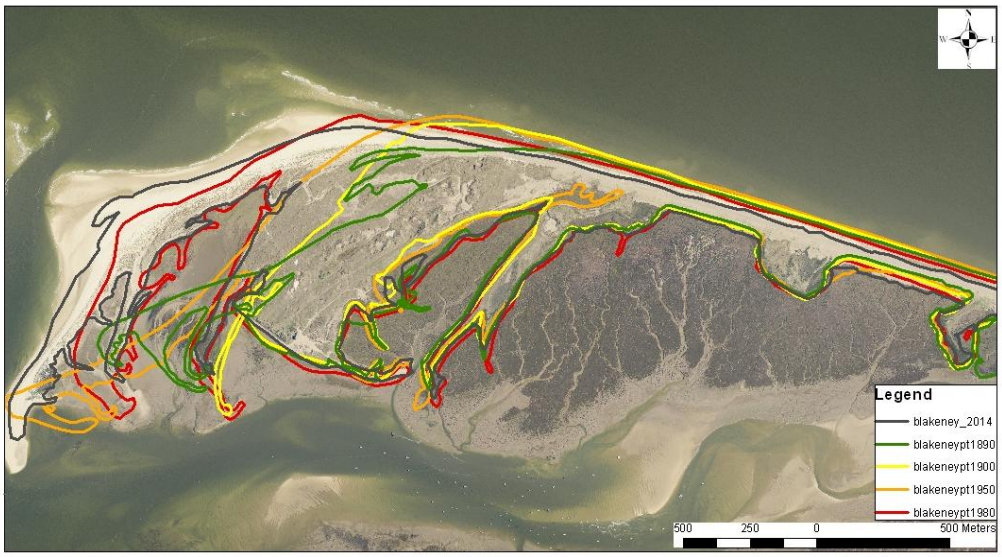

Figure 5.10: Historic shoreline positions of the Blakeney coast (generated in GIS based on historic maps available on digimap).

A hindcast analysis could be useful at this point to validate the model performance within the barrier and backbarrier environment. Unfortunately, this is not possible due to lack of historic terrain information, and this is clearly a limitation of the SLAMM approach given the short archive of LiDAR data (dating back no earlier than 1995 in the UK). However, Historic Trend Analysis (HTA) (National Research Council, 1987; Leatherman, 1990), widely used in coastal management and planning, is used here to validate the projected by SLAMM shoreline behaviour. As mentioned in Chapter 1, this approach assumes that the observed coastal behaviour encompasses the kind of behaviour that is expected in the future (National Research Council, 1990; Fenster et al., 1993; Hooke and Bray, 1996), with the sea-level rise being the dominant influence (Bray and Hooke, 1997; Whitehouse et al., 2009).

The analysis is summarised in Figure 5.11. The historic behaviour of the shoreline is analysed based on available historic OS Ordnance Survey maps, by digitising the mean high water (MHW) line. As presented in graphs a, b and c the shoreline is quite steady, with its western end advancing seawards, until 1950, when it starts to retreat linearly. This behaviour, coupled with the observed in the region linear sea-level rise since 1950 (graph d), leads to the assumption that the post-1950 shoreline retreat is driven by historic sea-level rise.

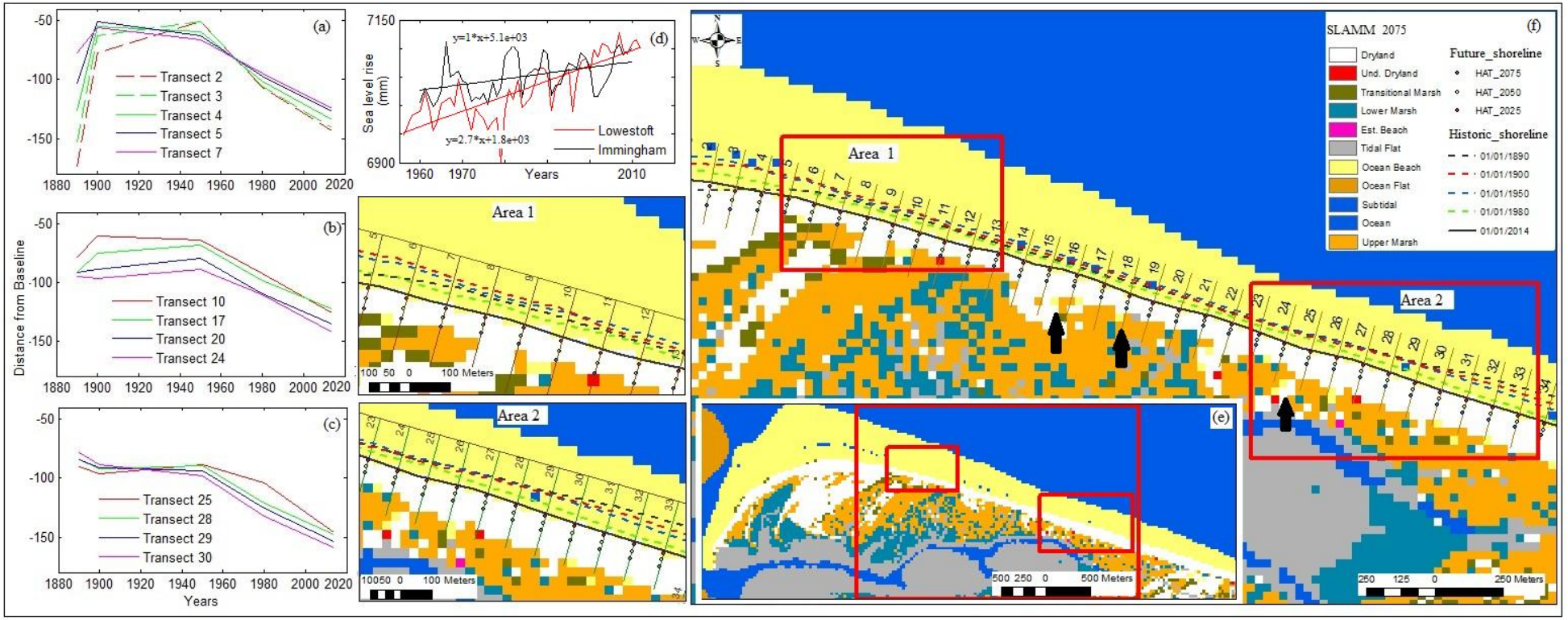

Figure 5.11: a, b, c: Analysis of the historic shoreline position; d: Historic sea-level rise at the two closest tide gauges, e: Habitat distribution for the year 2075, projected within SLAMM, by assuming that the sea-level will continue to rise at a rate equal to the historic one (2.6 mm yr^{-1}); f: Projected shoreline position within HTA for the years 2025, 2050, 2075.

In that direction, the historic rates of change calculated, based on the post-1950 behaviour by using the DSAS extension (Thieler et al., 2009) in GIS. These historic retreat rates are then used in the equation 5.1 (Leatherman's 1990) to extrapolate them into the future, and therefore compute the shoreline position for the years 2025, 2050 and 2075 (Table 5.8).

$$R_2 = R_1 \frac{S_2}{S_1} \quad , \qquad (5.1)$$

where R_2= future retreat rate (m yr^{-1}), R_1= historic retreat rate (m yr^{-1}),

S_2 = future sea-level rise (mm yr^{-1}), S_1 = historic sea-level rise (mm yr^{-1}).

In order to compare the two modelling approaches, the last simulation performed within SLAMM (RUN_6) is repeated by assuming that the sea-level will continue to rise under the same rate in the future (RUN_7). In that direction a custom simulation is performed by assuming a global sea-level rise equal to 0.2 m by 2100, in order an eustatic sea-level rise of 0.13 m by 2075 to be calculated. The results are presented at the Table 5.7 up to year 2100 and in the Figure 5.11e for the year 2075. The ocean beach converts to ocean by about 0.1% by year 2075, while at the backbarrier environment a slight inland marsh migration occurs squeezing the transitional marsh, which lose almost half of its area.

Table 5.7: Impacts of sea-level rise at the Blakeney complex for the second scenario, assuming that sea level rises at a rate equal to the historic one (RUN_7).

Simulation: 'RUN_7'												
Date	SLR (eustatic)	Dry Land	Und. Dryland	Transitional Marsh	Upper Marsh	Lower Marsh	Estuarine Beach	Tidal Flat	Subtidal	Ocean Beach	Ocean Flat	Ocean
0.0	0	2373.6	0.0	334.6	511.5	404.1	0.0	284.8	102.7	296.2	474.0	3346.9
2025.0	0.02	2378.5	0.3	301.3	509.8	416.4	0.0	285.0	85.5	298.7	471.1	3381.8
2050.0	0.07	2382.4	0.4	226.0	558.0	426.4	0.3	293.9	86.3	300.1	470.5	3384.2
2075.0	0.13	2365.1	0.7	181.0	588.2	451.6	0.6	292.8	90.3	301.4	463.2	3393.6
2100.0	0.20	2353.0	0.6	142.5	603.5	481.0	0.9	292.7	92.2	302.9	461.5	3397.7

Focusing on the shoreline position, the projected habitat distribution generated within SLAMM for the year 2075 is overlaid by the historic and future shoreline positions, as the last ones are calculated within the HTA modelling approach for the years 2025, 2050 and 2075, as presented in Figure 5.11f. The fact that the 2014 shoreline position is depicted at the seaward lower boundary of the dryland is due to the low quality input data. Thus, the importance for high quality data is once again highlighted (see sensitivity analysis at Section 3.3). Most importantly, though, the future shoreline positions computed within the HTA approach, driven by the process of overwash, are projected within the dryland wetland category of SLAMM. Consequently, this process

is not captured within the overwash sub-model incorporated within SLAMM, indicating the limitation of the model to properly simulate this process without a hydrodynamic model.

On the other hand, ocean beach is generated at the backbarrier environment, even after the last modification of the source code (Figure 5.11f). This, coupled with the inundated areas projected at high elevations of the backbarrier environment at high resolution simulations (see simulations RUN_4 and Run_5 in Figure 5.7), is explained by the fact that the adjacent to the ocean dryland, i.e. within 500 m, is inundated to ocean beach and therefore to ocean (see Table 2.5).

Accordingly, the source code was further modified, and the adjacent to the ocean threshold is determined as a variable parameter that must be specified by the user for each case study (Figures A-0.32; update Figures A-0.2 to A-0.4 and A-0.6 to A-0.10 in Appendix). For Blakeney, this threshold is estimated at approximately 50 m, based on present aerial photos (Figure 5.12), by taking into account that the beach will be totally eroded, and the first scenario is repeated with the modified code (RUN_ 8) in order to simulate the impacts of sea-level rise at the Blakeney complex, ignoring the process of overwash. The results, presented in Table 5.9 and Figure 5.13, project a different respond of the backbarrier environment, with the dryland considered part of the estuarine system, and being inundated to transitional marsh.

Figure 5.12: Parameterisation of the adjacent to the ocean threshold based on analysis of aerial imagery in Google Earth.

Table 5.8: Projection of future shoreline position within the HTA approach.

	DSAS				HTA			Distance from Baseline				Transect coordinates			Projected Shoreline Coordinates					
															2025		2050		2075	
ID	LRR	LR2	Linear ??	Historic retreat (m/yr)	Historic SLR (mm/year)	Future SLR by 2075	Future Retreat Rate by 2075	in 2014	in 2025	in 2050	in 2075	StartX	StartY	Azimuth	X	Y	X	Y	X	Y
1	n/a	n/a	n/a	n/a	n/a	n/a	n/a	n/a	n/a	n/a	n/a	n/a	n/a	n/a	n/a	n/a	n/a	n/a	n/a	n/a
2	-1.4	0.98	YES	1.44	2	2	1.44	143	159.3	195.3	231.3	600457	346759	191	600427	346603	600421	346567	600414	346532
3	-1.4	0.98	YES	1.4	2	2	1.4	141	156.4	191.4	226.4	600554	346739	194	600517	346587	600508	346553	600500	346519
4	-1.2	0.99	YES	1.17	2	2	1.17	134	147.1	176.3	205.6	600651	346715	194	600616	346572	600609	346544	600602	346515
5	-1.0	0.99	YES	1	2	2	1	127	138.2	163.2	188.2	600748	346690	194	600714	346557	600708	346532	600702	346508
6	-1.1	1.00	YES	1.05	2	2	1.05	126	137.3	163.5	189.8	600845	346664	195	600809	346532	600802	346507	600795	346481
7	-0.9	1.00	YES	0.92	2	2	0.92	125	135.0	158.0	181.0	600941	346638	195	600906	346508	600900	346485	600894	346463
8	-0.8	0.99	YES	0.79	2	2	0.79	122	130.5	150.2	170.0	601038	346611	195	601003	346485	600998	346466	600993	346447
9	-0.8	1.00	YES	0.84	2	2	0.84	122	130.9	151.9	172.9	601134	346585	196	601098	346459	601093	346438	601087	346418
10	-1.0	1.00	YES	0.97	2	2	0.97	126	136.3	160.6	184.8	601230	346557	196	601193	346426	601186	346403	601180	346379
11	-1.0	0.99	YES	1.03	2	2	1.03	128	139.2	164.9	190.7	601327	346530	196	601288	346396	601281	346371	601274	346346
12	-1.0	1.00	YES	1.02	2	2	1.02	126	137.0	162.5	188.0	601423	346502	196	601385	346370	601378	346346	601371	346321
13	-0.9	0.97	YES	0.89	2	2	0.89	117	126.8	149.0	171.3	601519	346474	196	601483	346353	601476	346331	601470	346310
14	-1.0	0.99	YES	0.96	2	2	0.96	121	131.2	155.2	179.2	601615	346446	196	601577	346320	601571	346297	601564	346274
15	-0.9	0.99	YES	0.86	2	2	0.86	116	125.5	147.0	168.5	601710	346418	196	601675	346297	601669	346277	601663	346256
16	-0.8	0.98	YES	0.78	2	2	0.78	113	121.2	140.7	160.2	601806	346389	196	601773	346273	601768	346254	601763	346235
17	-0.8	0.99	YES	0.84	2	2	0.84	122	131.6	152.6	173.6	601903	346365	194	601872	346237	601867	346217	601862	346196
18	-1.0	0.99	YES	0.96	2	2	0.96	135	145.5	169.5	193.5	602001	346341	194	601966	346200	601961	346177	601955	346153
19	-1.0	1.00	YES	0.95	2	2	0.95	140	150.8	174.5	198.3	602097	346316	197	602052	346172	602045	346150	602038	346127
20	-0.9	0.99	YES	0.87	2	2	0.87	136	145.1	166.9	188.6	602193	346286	197	602149	346148	602143	346127	602136	346106
21	-0.7	0.99	YES	0.72	2	2	0.72	128	136.4	154.4	172.4	602288	346256	197	602247	346126	602242	346109	602236	346092
22	-0.7	0.99	YES	0.73	2	2	0.73	129	137.1	155.4	173.6	602384	346226	197	602342	346095	602337	346078	602331	346061
23	-0.8	1.00	YES	0.78	2	2	0.78	135	143.1	162.6	182.1	602479	346198	195	602441	346060	602436	346041	602431	346022
24	-0.8	0.99	YES	0.84	2	2	0.84	143	152.0	173.0	194.0	602576	346171	195	602535	346025	602530	346004	602524	345984
25	-0.9	0.95	YES	0.91	2	2	0.91	146	156.5	179.3	202.0	602672	346145	195	602631	345994	602624	345972	602618	345950
26	-0.9	1.00	YES	0.85	2	2	0.85	142	151.2	172.4	193.7	602769	346118	195	602728	345972	602723	345952	602717	345931
27	-0.9	0.98	YES	0.86	2	2	0.86	142	151.6	173.1	194.6	602865	346091	195	602825	345945	602819	345924	602813	345904
28	-0.9	0.99	YES	0.92	2	2	0.92	148	158.1	181.1	204.1	602961	346065	195	602919	345912	602913	345890	602907	345868
29	-0.9	1.00	YES	0.94	2	2	0.94	154	164.1	187.6	211.1	603058	346038	196	603014	345880	603007	345857	603001	345835
30	-1.0	0.99	YES	0.95	2	2	0.95	159	169.6	193.4	217.1	603154	346011	196	603108	345848	603102	345825	603095	345802
31	-1.0	0.97	YES	0.95	2	2	0.95	162	172.7	196.5	220.2	603250	345984	196	603204	345818	603197	345795	603191	345772
32	-0.9	0.94	YES	0.91	2	2	0.91	165	174.8	197.5	220.3	603347	345957	196	603299	345789	603293	345767	603287	345745
33	-0.9	0.96	YES	0.86	2	2	0.86	167	176.7	198.2	219.7	603443	345930	196	603395	345760	603389	345739	603384	345718
34	-0.8	0.94	YES	0.84	2	2	0.84	171	180.0	201.0	222.0	603539	345903	196	603491	345730	603485	345710	603479	345689
35	n/a	n/a	n/a	n/a	n/a	n/a	n/a	n/a	n/a	n/a	n/a	n/a	n/a	n/a	n/a	n/a	n/a	n/a	n/a	n/a
36	n/a	n/a	n/a	n/a	n/a	n/a	n/a	n/a	n/a	n/a	n/a	n/a	n/a	n/a	n/a	n/a	n/a	n/a	n/a	n/a
37	n/a	n/a	n/a	n/a	n/a	n/a	n/a	n/a	n/a	n/a	n/a	n/a	n/a	n/a	n/a	n/a	n/a	n/a	n/a	n/a

Table 5.9: : Impacts of sea-level rise at the Blakeney complex for the first scenario, modelled with the adjacent to the ocean threshold equal to 500m (RUN_1) and 50m (RUN_8).

Simulation: 'RUN_1' Date	Dry Land	Transitional Marsh	Upper Marsh	Lower Marsh	Tidal Flat	Subtidal	Ocean Beach	Ocean Flat	Ocean
0	2377.8	333.2	507.8	405.6	284.2	103.4	296.0	473.0	3348.7
2025	2360.8	272.0	544.3	440.3	282.1	85.4	238.4	463.0	3443.5
2050	2332.4	156.2	603.2	500.3	296.0	82.7	2.1	457.9	3699.0
2075	2303.5	83.1	595.2	572.5	317.0	74.2	3.2	452.2	3729.0
2100	2276.8	48.5	544.6	624.1	360.4	70.4	3.3	446.0	3755.7
Simulation: 'RUN_8' Date	**Dry Land**	**Transitional Marsh**	**Upper Marsh**	**Lower Marsh**	**Tidal Flat**	**Subtidal**	**Ocean Beach**	**Ocean Flat**	**Ocean**
0	2377.8	333.2	507.8	405.6	284.2	103.4	296.0	473.0	3348.7
2025	2360.8	275.4	544.3	440.3	282.2	105.2	236.7	463.0	3422.1
2050	2332.4	167.6	603.4	500.1	296.2	104.1	0.0	457.9	3668.1
2075	2303.7	101.5	595.9	572.2	319.0	102.0	0.1	452.2	3683.3
2100	2277.5	74.5	547.2	624.1	362.1	100.4	0.1	446.0	3697.9

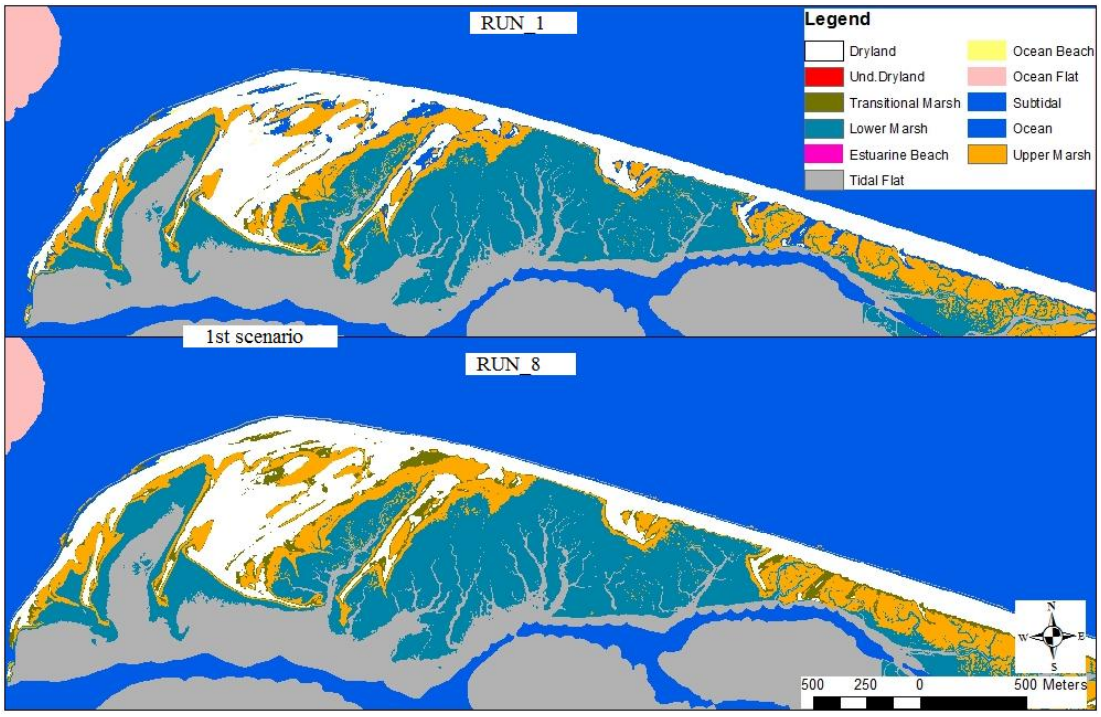

Figure 5.13: Habitat distribution for the Blakeney complex for the year 2100 under the first scenario, modelled with the adjacent to the ocean threshold equal to 500m (RUN_1) and 50m (RUN_8).

Summarising, it can be said that the open to the ocean part of the Blakeney complex responds differently than its inner one under the UK-CP sea-level rise scenario. The former one is projected to be unable to cope with the sea-level rise and being totally eroded, while the estuarine part responds very dynamically by migrating inland. However, the more complex process of the westward development of the spit and the process of overwash that mostly control the response of the specific case study to the sea-level rise cannot be captured within SLAMM. Thus, the need for further development of the model is emerged by including more robust sub-models.

6 DISCUSSION

6.1 Spatial models for simulation of estuarine and coastal habitat changes

The research presented here has explored the potential of reduced complexity, spatial landscape models to represent mesoscale impacts of sea-level rise on estuarine environments in the UK. The Sea Level Affecting Marshes Model (SLAMM) (Clough et al., 2010) was used as a starting point, because, after 20 years of development, it has been characterised as an important forecast and simulation model in coastal research (Liao et al., 2011). Notably, it has been widely used in US for the North American estuaries and wetland environments (SLAMM2: Park et al., 1989; Park, 1991; Titus et al., 1991, SLAMM3: Lee et al., 1991,1992; Park et al., 1991, 1993, SLAMM4: Galbraith et al., 2002, 2003, SLAMM4.1: NWF, 2006, SLAMM5: Craft et al., 2009, SLAMM6: used by many consultancy projects by Warren Pinnacle Consulting on behalf of the U.S. Fish and Wildlife Service, the National Wildlife Federation, the Gulf of Mexico Alliance, the Nature Conservancy and the Indiana University; Chu et al., 2014; Geselbracht et al., 2011; Glick et al., 2013; Linhoss et al., 2013, 2015; Wang et al., 2014).

SLAMM is a rule-based spatial model, which simulates the dominant processes involved in shoreline modifications and wetland conversions during sea-level rise. Like other spatial models used in the past in the US (e.g. Sklar et al., 1985, 1989, 1994; Costanza et al., 1988, 1990), the area of interest is simulated on a cell-by-cell basis, and habitat change is determined by using a decision tree. Whilst previous spatial models have often been based on cellular automata principles (see also Dearing et al., 2006), SLAMM places greater reliance on global rules to determine the evolution of habitat type according to elevation and relative position within a rasterised landscape. As a consequence, cells are not connected to their neighbours by exchanges of water and suspended materials, and this limits the ability of the model to represent the constraining influence of sediment supply, which is known to be important in estuarine and intertidal wetland systems (French, 2006; Kirwan et al., 2010). On the other hand, SLAMM can handle a range of spatial resolutions (cell sizes), depending on the size of the site and the availability of the data input. For example, a resolution of 10 m was used for the Grand Bay Estuarine Research Reserve and the Southern Jefferson County

at the Gulf of Mexico (Warren Pinnacle Consulting Inc, 2011a,b), 15 m for the southeastern Louisiana (Glick et al., 2013) and the Cape May National Wildlife Reserve in New Jersey (Warren Pinnacle Consulting Inc, 2011c) and 30m resolution for the more extended Kenai Peninsula and Anchorage in Alaska (Clough and Larson, 2009) and the Chesapeake Bay Region in the US (Glick et al., 2008). SLAMM can also recognise the existence of more than one land cover category within a cell and simulate them separately. Consequently, SLAMM is suitable to simulate quite complex environments and is capable of spatially detailed projections.

Although spatial models have been widely applied to coastal and estuarine problems in the US, little previous work of this kind has yet been carried out in the UK. Preliminary work on an estuary model based on cellular automata principles was carried out by Dearing et al. (2006), including a pilot application to the Blackwater Estuary, UK. Probably the only operational use of spatial modelling is the BRANCH project (BRANCH partnership, 2007), which simulated the impacts of sea-level rise at six local case studies on the south coast of the UK. This approach is GIS-based, and in contrast to SLAMM, which simulates the whole estuary at once, divides the area of interest into the open coast and the intertidal habitats and assesses the impacts of sea-level rise on each one of them individually.

Modelling of the open coast in the UK has focused on the shoreline movement under different sea-level rise scenarios, by using empirical relationships (e.g. Futurecoast study (Defra, 2002); Pye and Blott, 2008; Isle of Wight SMP2, 2010), or more sophisticated process-based models with representative example the SCAPE model (Walkden and Hall, 2005, 2011; Dickson et al., 2007; Addo et al., 2008; Walkden and Dickson, 2008). The former technique is based on the assumption that shoreline behaviour is only driven by the sea-level rise (Bray and Hooke, 1997; Whitehouse et al., 2009). Therefore, it is not suitable for coasts that are also affected by other factors. An example of this type of more complex shoreline behaviour is the barrier island and spit complex of the North Norfolk coast. These exhibit progressive landward retreat of gravel and dune-capped barriers, in parallel with incremental westwards extension driven by episodic storm conditions (Steers et al., 1979; Funnell et al., 2000). On the other hand, the SCAPE model is a reduced complexity model that includes several modules in order to describe more complex responses. However, its application is restricted to a specific range of coastal types (cliffs, beaches and shore platforms), and

therefore must be used in conjunction with other predictive models (Walkden and Hall, 2005, 2011; Dickson et al., 2007; Addo et al., 2008; Walkden and Dickson, 2008).

Current estuarine modelling approaches (see also Brooks et al., 2006; Snoussi et al., 2009; Tian et al., 2010) are largely based on the progressive drowning of the existing topography under different sea-level rise scenarios, lacking any physically–based modelling of habitat transition. SLAMM represents a step forward here in that it incorporates a flexible decision tree and qualitative relationships in order to determine the fate of each habitat. More importantly, more processes than just inundation are included, with most important vertical accretion within intertidal marsh and flat environments. Importantly, accretion can either be specified as a constant value for each habitat, when insufficient data are available, or as a time-varying function of cell elevation, wetland type, distance to channel and salinity.

SLAMM has already been used in US as a tool to help environmental managers understand the effects of sea-level rise and consequently identify strategies to minimise them (Glick et al., 2013). Building on this experience, this thesis has investigated the potential for UK estuary management policy to be informed more effectively by using models such as SLAMM. To this end, the SLAMM source code has been examined in detail and, where appropriate, modifications made to allow its application outside the US. Its component sub-models have also been examined and their limitations explored in the context of case studies on the south and east coast of England. Of particular importance is the dependence of SLAMM not only on high resolution topographic data but also on the availability of background information on the tidal regime and on indicative rates of intertidal sedimentation with which to constrain the operation of its various rules. Whilst the former are now increasingly available in the form of airborne LiDAR data (e.g. French, 2003, Brock and Purkis, 2009), observations of intertidal sedimentation processes and rates are still lacking for many sites. Moreover, the historic archive of airborne LiDAR data is still quite short (the earliest Environment Agency coastal datasets are for 1995). This makes longer – term hindcast validation difficult.

6.2 Modification of SLAMM for application to UK estuaries

The architecture of SLAMM is slightly unconventional in terms of the land cover classification. This is hard coded according to the US National Wetland Inventory

(NWI) scheme (U.S. Fish and Wildlife Service, 1974), which is not widely used elsewhere. In addition, the forcing scenarios and various aspects of the sub-models are also embedded in the source code rather being read from external files. Consequently, changes in its source code are required in order to apply the model to sites outside North America, and to explore changes resulting from a wider set of regional sea-level forcing scenarios.

To this end, the SLAMM code was modified in order to suit the tidal sedimentary environments and habitats more typical of the UK. A simpler land classification is included as it is defined by the INTERREG funded BRANCH project (BRANCH partnership, 2007). In parallel, the land classification conceptual model within SLAMM was modified to automatically update the elevation range of each habitat according to their position to the tidal frame, as used in the BRANCH project (after Chapman, 1960; Pye and French, 1993; Leggett and Dixon, 1994; Blott and Pye, 2004). Consequently, in contrast to the original model, the modified scheme more readily accommodates specific case studies. In addition, the habitat transition rules were modified to include a smoother habitat conversion due to inundation; the transitional marsh is inundated to upper marsh instead of lower marsh, and the dryland to transitional marsh instead of estuarine beach when it is adjacent to the subtidal. Finally, UK-specific sea-level rise scenarios were incorporated into the modified code. Consequently, the modified code can be used to simulate the impacts of sea-level rise in the UK estuarine systems.

The estuarine systems in the UK are generally much smaller in extent than many of the North American systems previously investigated using SLAMM. Their intertidal habitats are also often fragmented, with many saltmarsh units been only a few meters in width. This necessitates application of the modified SLAMM at a higher spatial resolution. Thus, although the highest resolution used to date in the US is 10m (see case studies of Brand Bay NERR and Southern Jefferson County in Mexico (Warren and Pinnacle Inc, 2011a,b)), a 5 m resolution is used in the present UK applications. This corresponds to the upper resolution limit suggested by the original model authors (Clough et al., 2010).

The modified code was firstly applied to a small case study estuary, on the south coast of England, the Newtown estuary, Isle of Wight. Initial simulations indicated significant changes in the distribution of intertidal flat and saltmarsh under the UKCP09 SE mean

sea-level rise scenario (UKCP, 2009).These changes were compared with results from a previous modelling effort for the Newtown estuary carried out as part of the BRANCH project (BRANCH partnership, 2007). As already noted above, the approach used within the BRANCH project is based on the progressive drowning of the existing topography lacking any mechanistic modelling of habitat transition. In particular, lateral erosion at the tidal flat – saltmarsh transition is totally ignored, while accretion is only taken into account for areas already colonised by saltmarsh vegetation. In contrast, SLAMM presents a step forward by incorporating a flexible decision tree and qualitative relationships to determine the habitat transition. It also takes into account of more processes related to sea-level rise than just inundation, with most important being vertical accretion within the intertidal marsh and flat environments. Importantly, this accretion is also allowed to vary spatially.

The small size of the Newtown estuary allows a comprehensive sensitivity analysis of the basic processes and parameters included in the model. Firstly, the effect of an error at the DEM was investigated, by examining the typical elevation accuracy of the UK LiDAR data, which is generally quoted as being equal to ±0.15 m (French, 2003; CCO, 2013). The results highlighted out the importance of the quality of the terrain information, especially for such low gradient environments, by affecting the initial condition of the habitat distribution, and therefore their further response to the sea-level rise.

The importance of fine resolution simulations was also highlighted. The recommended cell size range of 5 to 30m (Clough et al., 2010) was extended to include a higher resolution of 1m. The results indicate the significant influence of this parameter to the projected habitat distribution. The lower the resolution used, greater the differences are to the projected habitat distribution relevant to the present condition. However, this parameter affects the run time of the simulation, which is significantly increased for fine resolution simulations. For the small Newtown estuary, the run time of a simulation varied from 1 minute for a low resolution simulation (30 m) to ten minutes and six hours for a fine resolution simulation of 5 and 1 m respectively (using a single 2.4GHz cpu). This limits the application of fine resolution simulations in very large areas, where resolution need to be sacrificed for a shorter simulation time.

A further factor that could affect the quality of the input data is the interpretation accuracy in the identification of the habitat distribution from remote sensor data. The smallest recommended level of accuracy equal to 85% (Anderson, 1971; Anderson et al., 1971, 1976; Olson 2008) is examined here by randomly misclassifying 15% of each category to the closest in terms of elevation one. This analysis highlights the capability of SLAMM to correct errors in the habitat distribution (Clough et al., 2010) based on their position into the tidal frame. However, this process is simulated solely in terms of inundation, ignoring the equally important process of aggradation (i.e. the seaward expansion of specific intertidal wetland units). Therefore the source code was further modified to incorporate this process, enabling SLAMM to capture a more accurate present habitat distribution. The latter considers SLAMM a valuable tool in decision making strategies for case studies with poorly represented habitat distribution data.

Most fundamentally, the process of aggradation further affects the representation of accretional processes into the future habitat projections. The sensitivity of the projected habitat distribution on this extremely important factor was examined here by applying different accretion values for the upper and lower marsh and the tidal flat. The higher the accretion rate applied in a given habitat, the better it is able to cope with the sea-level rise (Reed, 1990; Doody, 2001; Day et al., 2008). However, with the procedure of aggradation disabled, the model cannot capture the process of upland migration in areas with sufficient sediment supply. This particular modification of the source code is therefore vital to the performance of the model.

Finally, the process of lateral erosion was investigated for the tidal flat and the marsh area by applying different erosion rates for each one of them. Based on evidence from studies in southeast England (Burd, 1992; Cooper et al., 2001; van der Wal and Pye, 2004; Wolters et al., 2005) that marsh edge erosion can occur even in estuaries with a small fetch, the model code was modified to reduce the fetch threshold to 0.5 km. The code was also edited to allow erosion of the ‘dryland’; this allows the model to represent the erosion of inactive flood defences. This modification is mostly relevant for estuaries where embankments have failed but continue to limit the fetch until they eroded away (French et al., 2000).

This sensitivity analysis focuses mainly on the output uncertainty at each time-step, due to individual input parameters. An analysis of the cumulative representation would also

be interesting, but this is outside the scope of this thesis. A deeper investigation of the uncertainty factor could also explore the inter-dependencies between the different input uncertainties and how this might propagate into model projection errors. That would most logically involve a Monte Carlo simulation possibly involving several hundred simulations to cover all the parameters. One of the challenges that might arise here is the selection of appropriate estuarine state indicators (cf Van Koningsveld et al., 2005) to match model output to management needs.

The various source code modifications reported here allow meaningful use of SLAMM beyond the North American context for which it was designed. The modified code accommodates a simplified classification of intertidal habitats that is better suited to application in the UK, and potentially elsewhere in northwest Europe. It might also be argued that a simpler classification is more commensurate with the ability of this kind of rule-based model to resolve changes in habitat based largely on elevation as a determining factor. The detailed floristic composition of wetland subtypes clearly reflects not only the elevation (and its direct effect on hydroperiod) but also factors such as soil structure and chemistry, drainage and competition that may exhibit a much weaker dependence on elevation (Paul, 1993; Boorman et al., 1998; Callaway, 2001; Silvestri et al., 2005).

6.3 Application of modified SLAMM to contrasting estuarine and barrier systems in Eastern England

The variously modified SLAMM code was subsequently applied to the more complex environments of the Suffolk estuaries and Norfolk barrier coast in eastern England in order to critically evaluate its ability to produce meaningful projections of habitat change under the UKCP09 sea–level rise scenarios. The choice of the sites was mainly based on the availability of the LiDAR data from the Environment Agency, since topographic data at high resolution and accuracy is vital for meaningful application of the model (Clough et al., 2010). The LiDAR data were supplemented by the available background literature on habitats and sedimentary processes within these environments and by application of a simpler 0-dimensional model of saltmarsh sedimentation (French, 2006) to derive the required functional dependencies between sedimentation and elevation.

Initially, SLAMM was applied into two estuarine systems on the Suffolk of eastern England; the Blyth and the Deben estuary. Both of them are of particular interest due to extensive reclamation of their intertidal margins since the 17th century (French and Burningham, 2003; French et al., 2008), and large potential intertidal area that is presently protected from inundation by earth embankments. Simulations were performed with the assumption that these defences were maintained in situ and also for the entirely hypothetical case that all defences are removed. Since the effect of restoring tidal exchange to individual flood compartments is purely additive (i.e. they do not feedback into estuary tidal prism, hydrodynamics and sedimentation; French, 2008), this extreme scenario is also sufficient to evaluate any more incremental reduction in the defended area.

A key focus of this work was to explore the appropriateness of the various assumptions in the under-lying accretion sub-models. The model was empirically parameterised based on observed historic sedimentation data (French and Burningham, 2003; Pye and Blott, 2008b), while the MARSH-0D (French, 2006) model (essentially an aspatial box model; Hearn, 2008) was used to further constrain saltmarsh sedimentation by generating a functional relationship between elevation and sedimentation rate under the local tidal regime. A limitation of the MARSH-0D (French, 2006) model as used here is that its uses a simplification of the tidal regime (only four tidal constituents, M2, S2, O1, K1), and in the mode used here, does not include aperiodic surge effects. The latter can be an important contributor to marsh sedimentation, especially in micro- and meso-tidal settings (Stumpf, 1983; Pugh, 1987; French, 2006; Schuerch et al., 2012). This was addressed by extrapolating the computed accretion rates by assuming a zero-deposition in the highest elevation of the marsh. A further refinement through the distance to channel effect was also included.

This approach is reasonably effective in representing one of the major morphodynamic feedbacks that is known to condition the adjustment of marsh elevation (which is here the chief control of habitat type) within the tidal frame at centennial timescales (Allen, 2000; French and Reed, 2001; Friedrichs and Perry, 2001; French and Burningham, 2003; Temmerman et al., 2003; French, 2006). The analysis highlights that the projected changes in the habitat distribution are clearly very sensitive to the various assumptions in the accretion sub-models, and that it is often difficult to justify particular values with reference to observations. Experimentation with constant accretion rates

indicated that the rule based approach is the only way forward given that SLAMM does not keep track of sediment mass balance and cannot adjust sedimentation rate according to local sediment supply.

Importantly, tidal flats are rather more dynamic than saltmarshes and frequently exhibit temporal variation between accretion and erosion at seasonal, low interannual and decadal timescales (Anderson et al., 1981; O'Brien et al., 2000; French and Burningham, 2003). However, inferences based on historic sedimentation are occasionally possible. The Blyth is as good example here, where measured sediment accumulation over a dated horizon following abandonment of flood defences can be used to generate functional relationship between sedimentation and elevation. This approach assumes a tendency towards accretion, with any intermediate erosional episodes clearly not resolved.

Also, in the case of the Blyth, historic sedimentation within newly created intertidal areas seemingly leads to an equilibrium elevation that lies below that at which saltmarsh would ordinarily establish. This can be interpreted as evolution towards a wave-dominated equilibrium (Fagherazzi and Wiberg, 2009), which cannot be captured in SLAMM since the influence of the waves is not incorporated into the model. This is clearly a limitation of the model, since the upper intertidal flats are significantly affected by the waves (Nicholls et al., 1999, 2004; Simas et al., 2001; Syvitski et al., 2005; Gardiner et al., 1992, Gardiner and Porter 2001; Pethick, 2001; Davidson–Arnott et al., 2002; Cahoon et al., 2006; Moller, 2006; Reed et al., 2009). Handling this kind of situation, and the resolution of alternative divergent states (Phillips, 2014), would clearly require a more mechanistic treatment of the interaction between intertidal sedimentation, locally generated wind waves, and the tidal regime.

In the Deben case study, an attempt was made to resolve recent changes in tidal flat elevation from the EA LIDAR data and also to relate these to characteristically erosional or accretional tidal profiles, following the approach of Kirby (2000). Based on this, the tidal profiles are classified according to the contributions of tidal currents and wind waves to the sediment transport, and the intertidal flat within SLAMM is then zoned accordingly. However, this approach is still very crude and highlights once again the need for a more mechanistic treatment of the tidal flat. This is a major weakness of SLAMM, but it is not clear that the necessary models actually exist, although progress

is being made with explanatory numerical models for simplified geometries (e.g. Mariotti and Fagherazzi, 2013; Thornhill et al., 2015). Moreover, the poorly modelled tidal flat within SLAMM also controls the evolution of the subtidal, which depends on the surrounding environment rather than being modelled itself. In other words, SLAMM is a model that focuses into the intertidal environment.

Particular interest presents in the case of the Deben estuary the feature of the Knolls, which are assigned here as ocean flat and therefore treated within SLAMM similarly to the tidal flat environment. A comparison of the projections with a survey undertaken by Burningham and French (2006) indicates that SLAMM is not able to capture the complex historic behaviour of the ebb-tidal delta in the absence of an effective wave model. Morphodynamic of ebb deltas shores is complex, involving waves, tides and, in the case of the Deben, mixed sediments. Resolving this behavirour requires a dedicated sub-model that is presently lacking in SLAMM. Moreover, in both case studies, the response of the beach at the sea-level rise is simulated within SLAMM by using the Bruun rule, projecting total beach erosion. This projection though does not agree with the observed historic shoreline trend which indicates a more complex pattern of shoreline response. This is clearly a limitation of the model which also enhances the idea that the Bruun rule is an inadequate model of shoreline retreat (Kaplin and Selivanov, 1995; List et al., 1997; Pilkey et al., 2000; Sallenger et al., 2000; Thieler et al., 2000), highlighting the need to incorporate a wave hydrodynamic model.

The fairly simple open coastal beach and barrier sub-model within SLAMM is evaluated with reference to the complex barrier coast of Norfolk. In particular, simulations of the Blakeney spit complex are used to test the ability of SLAMM to reproduce coastal retreat driven by storm overwash (Clymo, 1964; Funnell et al., 2000). The MARSH-0D (French, 2006) model was again used to parameterise the marsh accretion sub-model, while in the absence of both data and a more mechanistic model of tidal flat processes, this environment was assumed to simply track the sea-level rise.

The overwash sub-model is currently rather experimental in SLAMM and has been used rather infrequently and only at low resolution. Modifications were found to be necessary to resolve the unreasonable projection of ocean beach at the backbarrier environment. The overwash transition rule of the backside of the ridge was de-activated, and the threshold that considers the ‘dryland’ part of the coastal environment, and therefore

considers it subjected to be inundated to ocean beach, was determined as variable in order to be specific for each case study. The latter makes the model capable of application in a broader range of environmental contexts.

With the overwash model inactive, the beach is rapidly eroded according to the Bruun Rule. However, the procedure of erosion is de-activated during the simulation when overwash is assumed to be the main cause of coastal retreat. In that case, the outer barrier seems to slightly retreat, while in parallel the overwashed sediment is deposited in the backbarrier environment. A big limitation of the model though, in both cases, is that it cannot include the westwards development of the spit (Clymo, 1964; Funnell et al., 2000). It is thus unable to simulate planform evolution in systems that are influenced by storm-driven processes.

A hindcast analysis was not possible to evaluate the performance of the model due to the restricted terrain information with which a historic simulation could be initialised. Although a digital elevation model could be generated by adjusting the present elevations to account of the effects of relative sea-level rise and deposition rates for the intervening period, this could inevitably lead to project the initial elevations. Differences might exist, though, to the projected habitat distribution since the affected areas are calculated based on empirical equations by taking into account only the minimum and maximum elevation of each wetland category in each cell. At this end, an indicative evaluation was achieved for the Blakeney spit and barrier case study by comparing historic migration of the shoreline and outer barrier with projected future change. The Historic Trend Analysis (National research Council, 1987; Leatherman, 1990) approach was used for the comparison, by using the same (linear) sea-level forcing in both modelling approaches. The results showed that although SLAMM seems to capture a slight roll back of the barrier island, this is weakly represented with such a simple empirical model. Further development therefore is required by including a hydrodynamic model, which can also take into account the magnitude and the extent of the overwash deposits (Donnelly et al., 2006; Roelvink et al., 2009).

The modifications to the habitat type classification and certain elements of the decision tree have been successfully tested in a selection of UK estuarine and backbarrier settings. High spatial resolution of 5m is computationally tractable for the modelled domains, allowing multiple model runs to investigate the model sensitivity and the

projected outcomes under a wide range of scenarios. SLAMM performs best in the upper intertidal, where the elevational adjustment of saltmarsh surfaces is mainly governed by patterns of sedimentation that can be expressed as relatively robust functions of elevation and position with respect to channels or open water. Projections under the UKCP09 sea-level rise scenario show a dynamic response of the estuaries by migrating landwards squeezing the upper marsh zones where landward migration is prevented by low accretion rates in higher elevations away from the main channel. However, the tidal flat is modelled less convincingly. Tidal flat morphodynamics are more complex and more difficult to parameterise as simple functions of elevation and location relative to the main channel. As such, crude assumptions must necessarily be made. The major consequence of this is that rather arbitrary changes are projected in the tidal flat extent leading to possible mis-representation of the crucial transition between tidal flat and lower marsh.

Finally, a key habitat in the Suffolk estuaries that is not treated directly within the modified SLAMM is the brackish reedbed. Reedbeds dominated by *Phragmites spp* occur within the upper reaches of both Deben and Blyth estuaries and function as important habitats, especially for rare bird species (French and Burnignham 2003; JNCC, 2008). Whilst SLAMM does incorporate a salinity sub-model, this is founded on the assumption of a salt-wedge estuary (Clough et al., 2010). In Suffolk, the strong tidal exchange, even in the micro-tidal Blyth (French et al., 2008) means that the estuaries stratify only partially and intermittently in their upper reaches. Significant modification to the salinity model would thus be required to parameterise this salinity regime and thereby resolve the changing distribution of brackish habitats.

6.4 Comparison of SLAMM and GIS-based modelling

It is instructive to compare results generated by the modified SLAMM code with those obtained using the methodology of the BRANCH project (BRANCH partnership, 2007). The BRANCH approach is based on the progressive drowning of the topography, by adding the new expected sea level onto the tidal parameters, based on which the future habitat distribution is generated for each scenario (Figure 6.1a). For more realistic results, the effects of vertical accretion are represented by applying a constant accretion rate to areas colonised by saltmarsh (Figure 6.1b). Spatial variation in accretion is not represented. Thus, the present study applies different constant accretion

rates for each habitat, as SLAMM does in its simplest form. This was easily accomplished within the last version of GIS (ArcGIS 10), which can integrate complex algebraic statements within Python in order to generate the desired DEM.

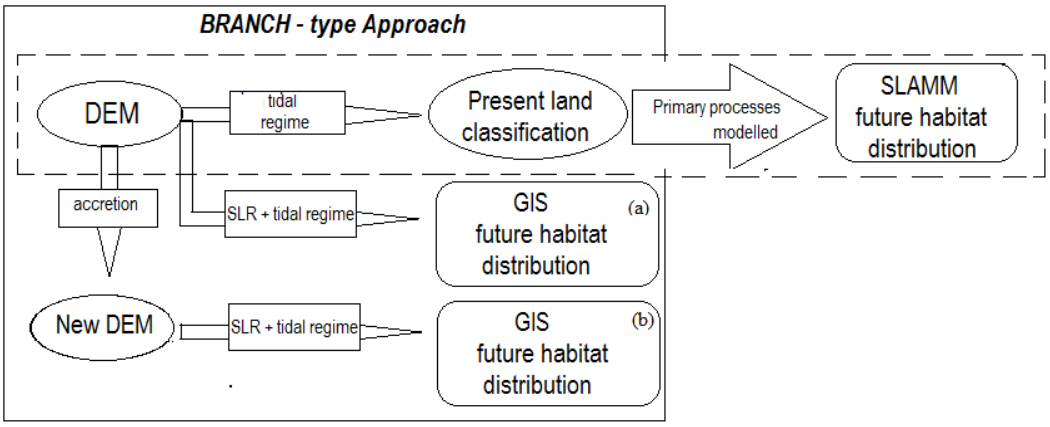

Figure 6.1: BRANCH (2007) modelling approach compared to SLAMM.

Five different scenarios of accretion pattern are investigated for the Newtown estuary, under the UKCP09 SE mean sea-level rise scenario, as described in Table 6.1. In the first simulation, accretion is not taken into account (RUN0), while the accretion patterns simulated using the final version of the modified SLAMM are represented by RUN1 to RUN4.

Table 6.1: Summary of additional simulation runs with both the SLAMM and BRANCH approaches for the Newtown estuary.

	Accretion rate (mm yr^{-1})		
	Tidal flat	Lower marsh	Upper and Transitional marsh
RUN0	-	-	-
RUN1	2.0	2.0	1.8
RUN2	6.3	2.0	1.8
RUN3	2.0	6.4	1.8
RUN4	2.0	2.0	6.5

The habitat distribution projected by 2100 under the first simulation (RUN0) is compared to the initial condition of the estuary in Figure 6.2. A simple drowning of the topography renders the estuary very vulnerable to the rise in sea level. Most of the existing saltmarsh reverts to tidal flat, a rather dramatic outcome that clearly fails to account for the sedimentary response to an increase in the frequency and depth of tidal inundation (Redfield, 1972; McCaffery and Thomson, 1980; Pethick, 1981; Shaw and Ceman, 1999; French, 2006).

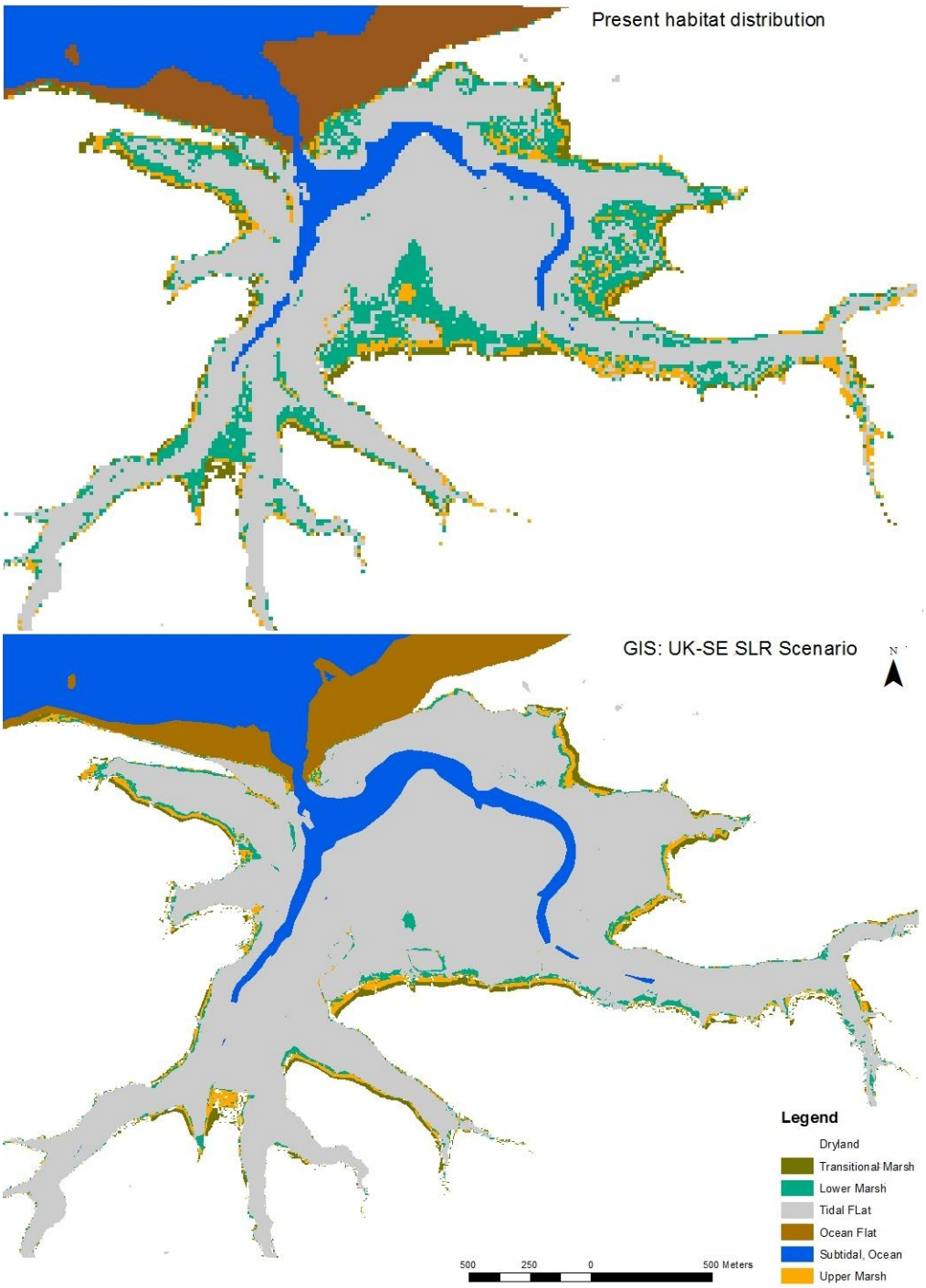

Figure 6.2: Change in habitat distribution to 2100 for the Newtown estuary under the UKCP09 SE sea-level rise scenario, modelled within the BRANCH approach without taking into account the process of accretion (RUN0).

The habitat distributions projected by 2100 under the next four scenarios are compared to the ones projected with the modified SLAMM in Figure 6.3. Although the maps produced by the two modelling approaches seem to project similar behaviour of the estuary within each scenario, significant differences are observed in the percentage loss of each habitat, with SLAMM overestimating the affected areas. These differences are

clearly explained by the different framework incorporated within each approach. BRANCH simulates each scenario based on the DEM, while SLAMM is mainly focused on the land cover, where in a cell-by-cell basis decides the fate of each habitat by using empirical equations based only on the minimum and maximum elevation of the specific cell.

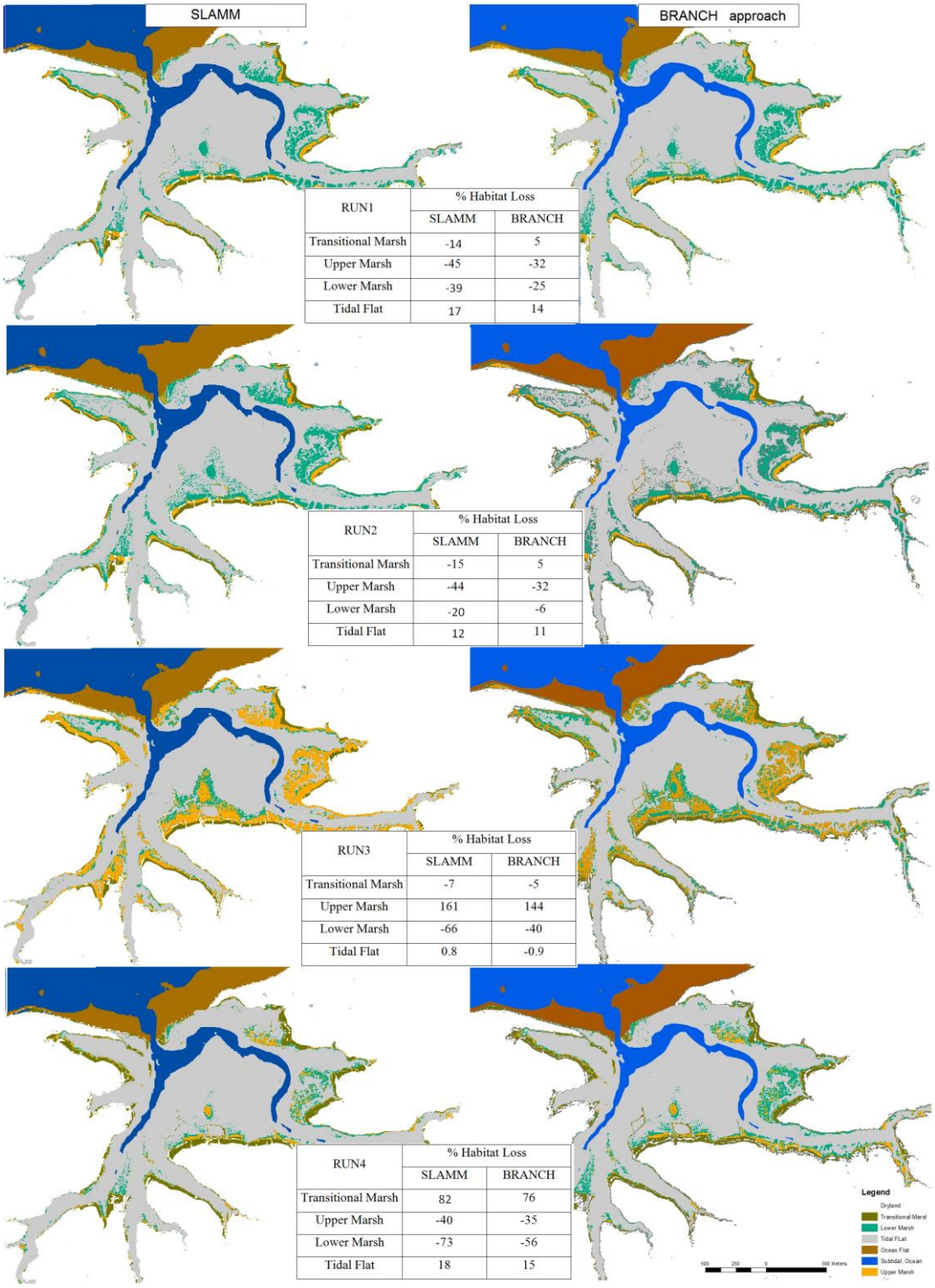

RUN1	% Habitat Loss	
	SLAMM	BRANCH
Transitional Marsh	-14	5
Upper Marsh	-45	-32
Lower Marsh	-39	-25
Tidal Flat	17	14

RUN2	% Habitat Loss	
	SLAMM	BRANCH
Transitional Marsh	-15	5
Upper Marsh	-44	-32
Lower Marsh	-20	-6
Tidal Flat	12	11

RUN3	% Habitat Loss	
	SLAMM	BRANCH
Transitional Marsh	-7	-5
Upper Marsh	161	144
Lower Marsh	-66	-40
Tidal Flat	0.8	-0.9

RUN4	% Habitat Loss	
	SLAMM	BRANCH
Transitional Marsh	82	76
Upper Marsh	-40	-35
Lower Marsh	-73	-56
Tidal Flat	18	15

Figure 6.3: Change in habitat distribution to 2100 for the Newtown estuary under the UKCP09 SE sea-level rise scenario, modelled for different accretion scenarios using the SLAMM and BRANCH approaches.

This difference between the two approaches is investigated more fully with reference to the Blyth estuary. Three different scenarios of tidal flat accretion pattern are implemented for this case study (Table 6.2). In the first one (RUN0) accretion is not taken into account, while the two scenarios of mean (RUN1) and max (RUN2) tidal flat accretion, as described in Chapter 4, are repeated for the two modelling approaches.

Table 6.2: Summary of simulations runs with SLAMM and a BRANCH approach for the Blyth estuary.

	Accretion rate (mm yr^{-1})		
	Tidal flat	Lower marsh	Upper and Transitional marsh
RUN0	-	-	-
RUN1	6.4 (Mean)	6.0	5.0
RUN2	20.7 (max)	6.0	5.0

The results are compared in Figure 6.4. As with the Newtown estuary, the Blyth intertidal cannot cope with the sea-level rise when the accretion is ignored (RUN0). The low-lying tidal flat area at the lower part of the estuary is mostly flooded, while the rest of the estuary intertidal migrates landwards, squeezing the marsh area. Under the second scenario (RUN1), the estuary is more able to cope with sea-level rise. The BRANCH produces a significant increase in the marsh area, reaching approximately 90% for the lower marsh. This difference is attributed to its neglect of lateral edge erosion. Finally, an unrealistic scenario of tidal flat accretion (RUN2) produces almost total loss of the tidal flat in both cases. However, its conversion to a different habitat is treated differently in each modelling approach. Under the BRANCH simulation the estuary almost dries out, instead of gradually being converted to saltmarsh as is projected by SLAMM. In the latter case, the rate of saltmarsh accretion then constrains further progression towards a higher in terms of elevation habitat. The more sophisticated decision tree implemented in SLAMM thus generates far more meaningful final outcomes in situations where accretion is known to be significant.

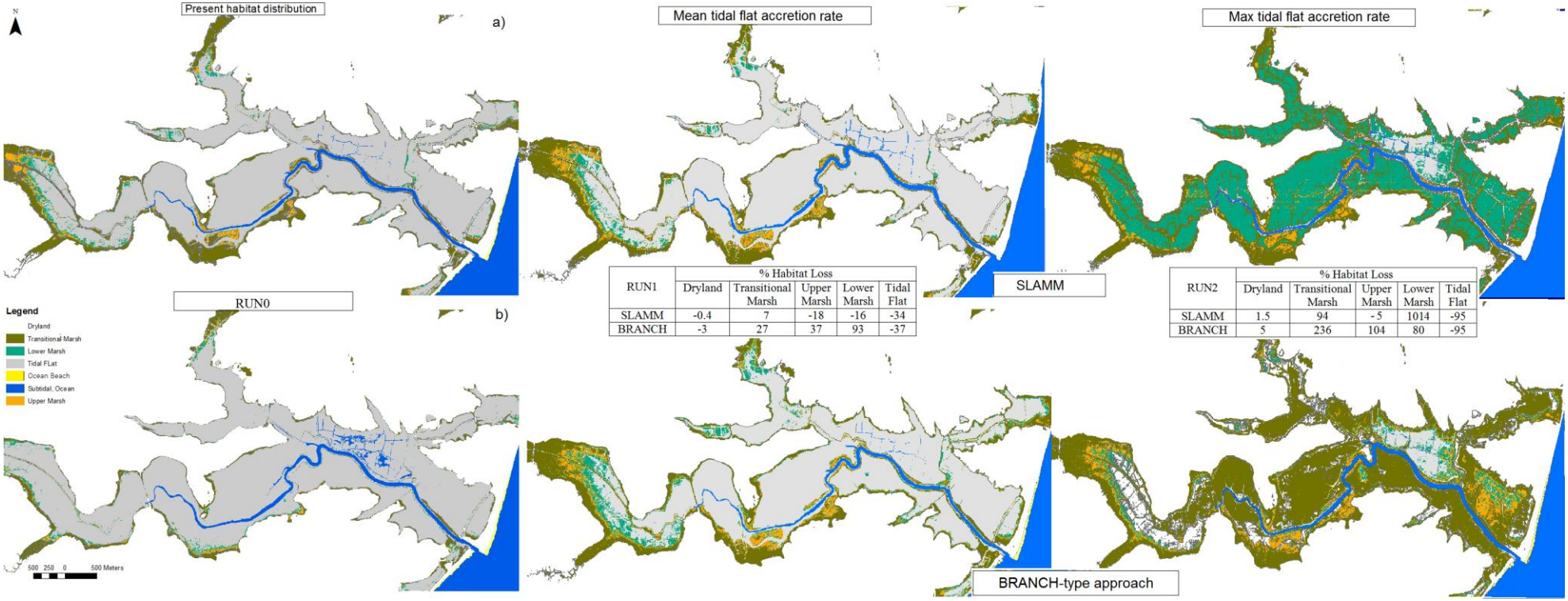

RUN1	% Habitat Loss				
	Dryland	Transitional Marsh	Upper Marsh	Lower Marsh	Tidal Flat
SLAMM	-0.4	7	-18	-16	-34
BRANCH	-3	27	37	93	-37

RUN2	% Habitat Loss				
	Dryland	Transitional Marsh	Upper Marsh	Lower Marsh	Tidal Flat
SLAMM	1.5	94	-5	1014	-95
BRANCH	5	236	104	80	-95

Figure 6.4: Change in habitat distribution to 2100 for the Blyth estuary under the UKCP09 SE sea-level rise scenario, modelled for different tidal flat accretion scenarios using the SLAMM and BRANCH approaches.

6.5 Ability of spatial landscape modelling to produce meaningful projections of future habitat distribution

Overall, the evaluation of SLAMM presented here has demonstrated the ability of reduced complexity models in general to simulate mesoscale impacts of sea-level rise on estuarine and coastal environments. However, such models are often very dependent on rather restrictive underlying assumptions. In the case of SLAMM, its performance is dependent on the provision of accurate elevation data, since this is the crucial variable that determines the transition between habitat types. Until very recently the availability of high quality LiDAR and bathymetry datasets has been limited, even in the UK, where access to datasets has often been a limited factor. Given a move towards open data access, this should be less of an issue in the future. Even a small error in the elevation could affect significantly the representation of the initial habitat distribution, as well as the projected changes. The former implication further includes the uncertainty from the interpretation accuracy in the classification of the habitat distribution from the underlying terrain information. However, this can be partially corrected into SLAMM, given an accurate DEM.

For a given DEM, accuracy resolution also plays an important role in the performance of the model. The finer the resolution used, the more realistic the projected changes are likely to be, since SLAMM simulates the area of interest in a cell-by-cell basis based on the minimum and maximum elevation of each cell. However, the choice of the resolution depends on the size of the area on account for the required run time of the simulation, which is significantly increased in finer resolution simulations. For the small Newtown estuary, for example, the run time of a simulation varied from 1 minute for a low resolution simulation (30m) to ten minutes and six hours for a fine resolution simulation of 5 and 1m respectively. This is a limitation of the model in comparison with the GIS-based modelling approach used in the BRANCH project (BRANCH partnership, 2007), whilst a 5m resolution was found to work well in the three application domains in Suffolk and Norfolk, which were all much larger than the Newtown estuary and a large number of model runs were required for each one.

Furthermore, accurate observation data are necessary to parameterise the embedded sub-models for more efficient projections. Although the absence of fieldwork data can be addressed for the saltmarsh by using the MARSH-0D (French, 2006) model to

constrain saltmarsh sedimentation as a function of elevation, the complex tidal flat morphodynamics are difficult to be parameterised based on elevation and location from the main channel, constraining its modelling to crude assumptions. However, in all cases, the amount of area affected is computed by empirical equations, leading to potential misrepresentation of the projected changes.

The uncertainty of the model to the factors described above is illustrated in Figure 6.5 by using the Newtown estuary as a case study due to its small size. Table 6.3 describes the range of the model's input factors. The parameter uncertainty effect seems to be quite large for most environments, with the large range in the outputs occurring due to the choice of key parameter values. Accretion is clearly a key here; only sufficient data available to fully constrain dependence on elevation and the use of a simple supplementary model (e.g. French, 2006) is the only way forward here. In addition, the sensitivity of the model outputs to the quality of the DEM is quite large, since, as already noted above, the elevation is the crucial parameter that determines the transition between the habitat types. Finally, sea-level rise scenario uncertainty is surprisingly small, reflecting the resilience of the saltmarsh environments to sea-level rise (Redfield, 1972; McCaffery and Thomson, 1980; Pethick, 1981; Shaw and Ceman, 1999; French, 2006).

Table 6.3: Range of SLAMM input factors for uncertainty sensitivity analysis.

SLAMM Input Factors		min	mean	max
Vertical Accretion	Tidal flat (mm yr^{-1})	0.0	2.0	6.3
	Lower marsh (mm yr^{-1})	0.0	2.0	6.4
	Upper marsh (mm yr^{-1})	0.0	1.8	6.5
Lateral Erosion	Tidal flat (m yr^{-1})	0.0	0.2	1.0
	Marsh (m yr^{-1})	0.0	0.25	1.0
DEM	DEM error (m)	-0.15		+0.15
	Spatial resolution (cell size) (m)	1	5	30
SLR	Sea-level rise scenario: SE UKCP09	min	mean	max

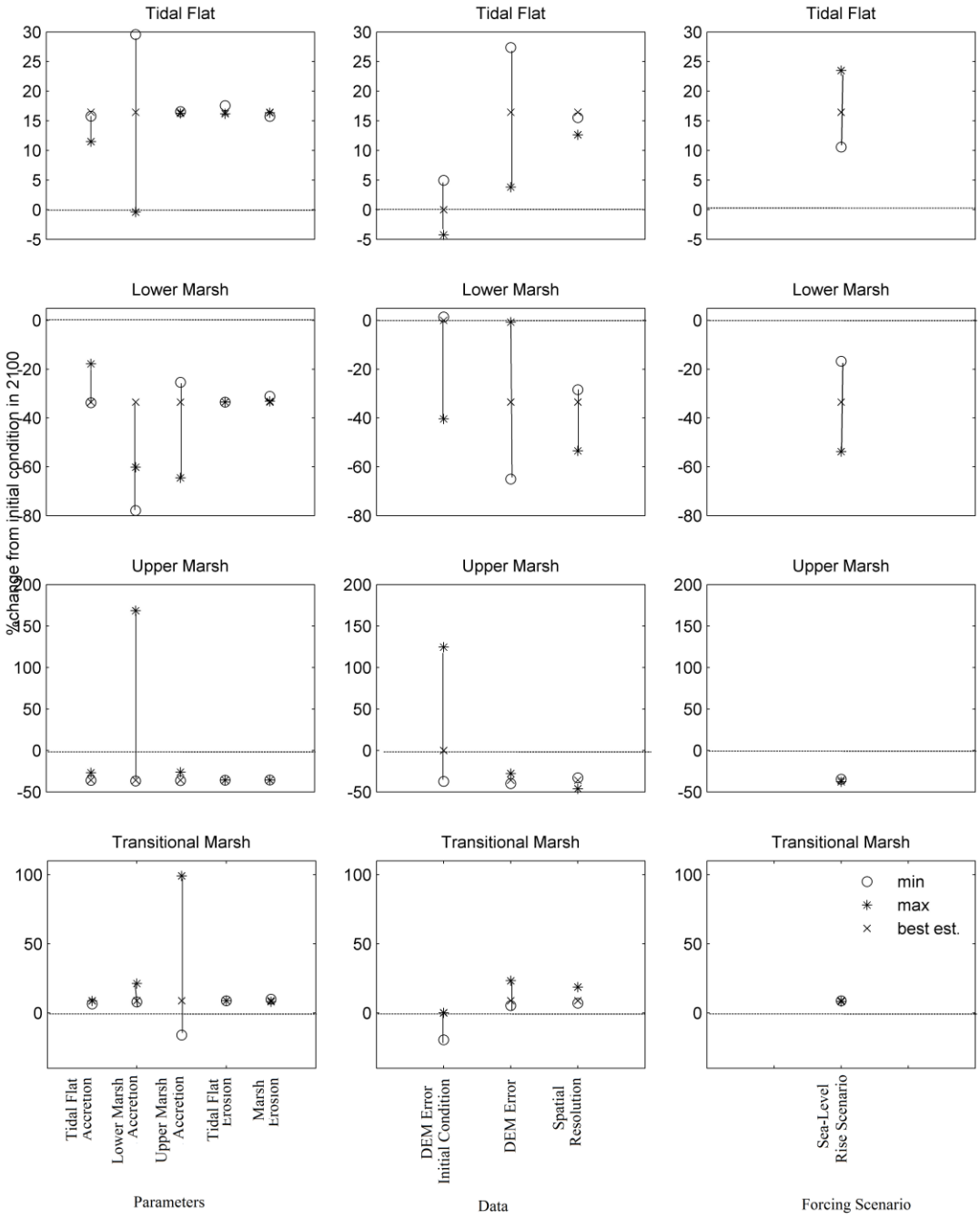

Figure 6.5: Uncertainty sensitivity analysis of the modified code for the Newtown Estuary.

More importantly, though, reduced complexity models are based on simplified parameterisations that focus on the key linkages and feedbacks between the major morphological components (Walkden and Hall, 2005, 2011; Dickson et al., 2007; Walkden and Dickson, 2008). In this repsect, the embedded sub-models within SLAMM are empirically parameterised based on a simplified kinematic response to sea-level rise, and linear erosion terms that neglect the complex processes of wave-driven

erosion. Although progress has been made to address this issue (e.g. Bassoulet et al., 2000; Le Hir, 2000; Di Silvio et al., 2010; Mariotti and Fagherazzi, 2013), it is important to further develop models in order to capture more complex processes (French et al., 2015; Thornhill et al., 2015).

7 CONCLUSIONS

This thesis sets out to investigate the potential of reduced complexity models as a tool to more effectively inform estuary management, with particular reference to the effects of sea-level rise on intertidal habitat distribution. The Sea Level Affecting Marshes Model (SLAMM), widely used in the USA, has here been adapted and evaluated for application to UK estuarine environments.

SLAMM includes a complex habitat classification based on the US National Wetlands Inventory, which is hard-coded, making application outside North America problematic. Numerous other potentially user-adjustable parameter values are embedded with the source code. Accordingly, the original code has been modified to incorporate a simpler habitat classification that is appropriate for a UK (and broader northwest European) context and which is, arguably, commensurate with the ability of a relatively simple model to resolve specific habitats largely on the basis of their elevation within the tidal frame. At the same time, numerous other changes were made to the embedded sub-models, especially those for the tidal flat, saltmarsh and the treatment of barrier overwash.

The modified source code was applied to different estuarine and coastal environments in UK. The small size of the UK case studies allows the model to run at higher resolution than has hitherto been attempted in US applications. However, accurate data are necessary to calibrate the model for more efficient projections. In absence of field data, this is addressed for the saltmarsh by using the MARSH-0D model (French, 2006) to constrain saltmarsh sedimentation by generating a functional relationship between elevation and sedimentation rate under the local tidal regime. However, the more complex tidal flat morphodynamics are difficult to parameterise based purely on elevation and location from the main channel, constraining its modelling to crude assumptions that may lead to misrepresentation of its fate under specific sea-level rise scenarios.

The analysis presented here demonstrates that reduced complexity models are more sophisticated than the GIS-based approaches used to date in the UK (BRANCH

partnership, 2007), and are able to resolve a wider range of suited responses and behaviours. In the case of SLAMM, however, the use of empirical sub-models to handle key systems linkages means that important processes are neglected. This, in turn, makes it very easy to generate projections that, whilst visually appealing to stakeholders and policy makers, are actually quite misleading. A key area of weakness concerns the representation of tidal flat processes. There is clearly a need for further work to translate scientific understanding of hydrodynamics and morphodynamics into better mesoscale model formulations (Di Silvio et al., 2010; Mariotti and Fagherazzi, 2013; Thornhill et al., 2015). In addition, a sediment transport model that could take into account the exchange of sediment between the neighbouring sections and conserve the sediment budget would also be a major improvement in SLAMM.

REFERENCES

Adam, P. (2002) 'Saltmarshes in a Time of Change' *Environmental Conservation*, 29, 39-61.

Addo, K.A., Walkden, M., Mills, J.P. (2008) 'Detection, Meausurement and Prediction of Shoreline Recession in Accra, Ghana' *ISPRS Journal of Photogrammetry & Remote Sensing*, 63, 543-558.

Admiralty (2000) *Admiralty Tide Tables, Volume 1: United Kingdom and Ireland (Including European Channel Ports).* The United Kingdom Hydrographic Office.

Akumu, C., Pathinara, S., Baban, S., and Butcher, D. (2010) 'Examining the Potential Impacts of Sea Level Rise on Coatsal Wetlands in North-Eastern NSW', *Journal of Coastal Conservation, 15,* 15-22.

Allan, J.C. and Komar, P.D. (2006) 'Climate Controls on US West Coast Erosion Processes' *Journal of Coastal Research*, 22, 511-529.

Allen, J.R.L. (1981) 'Beach Erosion as a Function of Variations in the Sediment Budget, Sandy Hook, New Jersey, USA' *Earth Surface Processes and Landforms*, 6, 139- 150.

Allen, J.R.L. (1989) 'Evolution of Saltmarsh Cliffs in Muddy and Sandy Systems: A Qualitative Comparison of British West-Coast Estuaries' *Earth Surface Processes and Landforms,* 14, 85-92.

Allen, J.R.L. (1990) 'Salt-marsh Growth and Stratification: A Numerical Model with Special Reference to the Severn Estuary, Southwest Britain' *Marine Geology*, 95, 77-96.

Allen, J.R.L. (1990a) 'The Seven Estuary in Southwest Britain: Its retreat under Marine Transgression and the Fine Sediment Regime', *Sedimentary Geology* 66, 13.28.

Allen, J.R.L. (1991) 'Saltmarsh Accretion and Sea-level Movement in the inner Severn Estuary: The Archeological and Historical Contribution' *Journal of Geological Society*, 148, 485-494.

Allen, J.R.L. (2000) 'Morphodynamics of Holocene Salt Marshes: A Review Sketch from the Atlantic and Southern North Sea coasts of Europe' *Quaternary Science Reviews*, 19, 1155-1231.

Allen, J.R.L. and Duffy, M.J. (1998) 'Medium-term Sedimentation on High Intertidal Mudflats and Salt Marshes in the Severn Estuary, SW Britain: The Role of Wind and Tide' *Marine Geology*, 150, 1-27.

Allen, J.R.L. and Pye, K. (1992) 'Coastal Saltmarshes: Their Nature and Importance', In Allen, J. and Pye, K. (eds.) *Saltmasshes: Morphodynamics, Conservation and Engineering Significance*, Cambridge University Press, 1-18.

Allison, R.J. (1989) 'Rates and Mechanisms of Change on Hard Rock Coastal Cliffs' *Zeitschriftfur Geomorphologie Supplement Band*, 73, 125-138.

Alexander, L., Tett, S., & Johnsson, T. (2005) 'Recent Observed Changes in Severe Storms over the United Kingdom and Iceland' *Geophysical Research Letters, 32*, L13704.

Anderson, J.R. (1971) 'Land Use Classification Schemes used in Selected recent Geographic Applications of remote Sensing', *Photogrammetric Engineering*, 37, 379-387.

Anderson, J.R., Hardy, E.E., Roach, J.T. (1971) 'A Land-use Classification System for Use with Remote-sensor data', *U.S. Geological Survey Circular,* 671, 16pp.

Anderson, J.R., Ernest, E.H., Roach, J.T., Witmer, R.E. (1976) *A Land Use and Land Cover Classification System for Use with Remote Sensor Data*. Geological Survey Professional Paper 964, United States Government Pronting Office, Washington, 1976.

Anderson, F.E., Black, L., Watling, L.E., Mook, W., Mayer, L.M.A. (1981) 'A Temporal and Spatial Study of Mud Flat Erosion and Deposition' *Journal of Sedimentary Research*, 51, 726-736.

Anderson, K.E., Cahoon, D.R., Gill, S.K., Gutierrez, B.T., Thieler, E.R., Titus, J.G., and Williams,S.J. (2009) '*Executive Summary' In:* J.G. Titus, K.E., Anderson, D.R., Cahoon, D.B., Gesch, S.K., Gill, B.T., Gutierrez, E.R., Thieler, and S.J., Williams (ed.) *Coastal Sensitivity to Sea-Level Rise:A Focus on the Mid-Atlantic Region.* A report by the U.S.Climate Change Science Programme and the Subcommittee on Global Change Research, U.S. Environmentan Protection Agency, Washington DC, 1-8.

Arbuckle, C.J., Huryn, A.D., Israel, S.A. (1998) 'Applications of Remote Sensing and GIS to Wetland Inventory: Upland Bogs' *10th Colloquium if the Spatial Information Research Centre, University of Otago, New Zealand, Novemebr 16-19 1998.*

Austin, G.E., Rehfisch, M.M., Vilew, H.A., Berry, P.M. (2001) 'Impacts on Coastal Environments' In: Harrison, P.A., Berry, P.M., Dawson, T.P. (eds) *Climate Change and Nature Conservation in Britain and Ireland: Modelling Natural Resource Responses to Climate Change (the MONARCH project)* UKCIP Technical Report, Oxford, 177 – 228.

Baldwin, A., Egnmotovich, M., Ford, M., Platt, W. (2001) 'Regeneration in Fringe Mangrove Forests damaged by Hurricane Andrew' *Plant Ecology*, 157, 151-164.

Barnett, T.P. (1983) 'Recent Changes in Sea Level and their Possible Causes' *Climate Change*, 5, 15-38.

Barnett, T.P. (1984) 'The Estimates of Global Sea level Change: A Problem of Uniqueness' *Journal of Geophysical Research*, 89, 7980-7988.

Barnett, T.P. (1988) 'Global Sea Level' in NCPO, *Climate Variations Over the Past century and the Greenhouse Effect*, A Report based on the First Climate Trends Workshop, 7-9 September 1988, Washington, DC, National Climate Prorgam Office/NOAA, Rockville, MD.

Barth, M.C. and Titus, J.G. (1984) *Greenhouse Effect and Sea Level Rise*, New York: Van Nostrand Reinhold.

Bartholdy, A.T., Bartholdy, J., Kroon, A. (2010a) 'Salt Marsh Stability and Patterns of Sedimentation Across a Backbarrier Platform' *Marine Geology*, 278, 31-42.

Bartholdy, J. (1997) 'The Backbarrier Sediments of the Skallingen Peninsula, Denmark' *Geografisk Tidskrift-Danish Journal of Geography*, 97, 11-32.

Bartholdy, J. (2012) 'Salt Marsh Sedimentation' In: Davis Jr., R.A. and Dalrymple, R.W. (eds) *Principles of Tidal Sedimentology*, Springer Science and Business Media, 151 – 185.

Bartholdy, J., Christiansen, C., Kunzen, H. (2004) 'Long Term Variations in Backbarrier Slat Marsh Deposition on the Skallingen Peninsula – The Danish Wadden Sea, *Marine Geology*, 278, 31-42.

Bartholdy, J., Pedersen, J.B.T., Bartholdy, A.T. (2010b) 'Autocompaction in Shallow Silty Salt Marsh Clay' *Sediment Geology*, 223, 310-319.

Bassoulet, P., Le Hir, P., Gouleau, D., Robert, S. (2000) 'Sediment Transport over an Intertidal Mudflat: Field Investigations and Estimations of Fluxes within the Bay of Marennes-Oleron (France), *Continental Shelf Research*, 20, 1635 – 1653.

Baumman, R.H., Day, J.W., Miller, C.A. (1984) 'Mississipi Deltaic Wetlands Survival: Sedimentation versus Coastal Submergence', *Science*, 224, 1093-1095.

Beardall, C.H., Dryden, R.C., Holzer, T.J. (1991) *The Suffolk Estuaries: A Report by the Suffolk Wildlife Trust on the Wildlife and Conservation of the Suffolk Estauries* Segment Publications, Ipswich, UK.

Beckley, B.D., Lemoine, F.G., Luthcke, S.B., Ray, R.D., Zelensky, N.P. (2007) 'A Reassessment of Global and Regional Mean Sea Level Trends from TOPEX and Jason-1 Altimetry based on Revised Reference Frame and Orbits' *Geophysical Research Letter*, 34.

Bijlsma, L., Ehler, C.N., Klein, R.J.T., Kulshrestha, S.M., McLean, R.F., Mimura, N., Nicholls, R.J., Nurse, L.A., Perez Nieto, H., Turner, R.K., Warrick, R.A. (1996) 'Coastal Zones and Small Islands' In: Watson, R.T., Zinyowera, M.C., Moss, R.H. (eds) *Impacts, Adaptations and Mitigation of Climate Change: Scientific-Technical Analyses(The Second Assessement Report of the Intergovermental Panel on Climate Change, Working Group II),* Cambridge University Press, 289-324.

Bird, E.C.F. (1985) *Coastline Changes – A Global Review*, New York: John Wiley and Sons. 219pp.

Bird, E.C.F. (1993) *Submerging Coasts: The Effects of a Rising Sea Level on Coastal Environments* John Wiley, Chichester, UK.

Bird, E. (2008) 'Spits, Barriers and Bars' in Bird, E. (ed) *Coastal Geomorphology An Introduction*, John Wiley & Sons Ltd.

Blot, S.J. and Pye, K. (2004) 'Application of LiDAR Digital Terrain Modelling to Predict Intertidal habitat Development at a Managed Retreat Site: Abbotts Hall, Essex, UK' *Earth Surface Processes and Landforms*, 29, 893-905.

Bobba, A.G. (2002) 'Numerical Modellling of Salt-Water Intrusion due to Human Activities and Sea-Level Change in the Godavari Delta, India' *Hydrological Sciences*, 47 (S), S67-S80.

Bondesan, M.G., Castiglioni, G., Elmi, C., Gabbianelli, G, Marocco, R., Pirazzoli, P., Tomasin, A. (1995) 'Coastal Areas at Risk from Storm Surges and Sea-Level Rise in Northeastern Italy' *Journal of Coastal Research*, 11, 1354-1379

Boomans, R.M.J., Day, J.W. Jr. (1993) 'High Precision Measurements of Sediment Elevation in Shallow Coastal Areas using a Sedimentation – Erosion Table' *Estuaries*, 16, 375 – 380.

Boorman, L.A. (1998) 'Salt-Marshes – Present Functioning and Future Change' *Mangroves and Salt Marshes*, 3, 227-241.

Boorman, L.A., Goss-Custard J.D., McGrorty S. (1989) 'Climatic Change, Rising Sea Level and the British Coast', LONDON, HMSO, 24pp (ITE research publication, no. 1).

Boorman, L.A., Garbutt, A., Barratt, D. (1998) 'The Role of Vegetation in Determining Patterns of the Accretion of Salt Marsh Sediment' In: Black, K.S., Paterson, D.M., Cramp, A. (eds) *Sedimentary Processes in the Intertidal Zone*, Geological Society, London, Special Publications, 139, 389-399.

Bouttier, F. and Courtier, P. (1999) 'Data Assimilation Concepts and Methods' *Meteorological Training Course Lecture Series*, ECMWF.

Brampton, A.H. (1992) 'Engineering Significance of British Saltmarshes' In: Allen, J.R.L. and Pye, K. (eds) *Saltmarshes, Morphodynamics, Conservation and Engineering Significance*, University Cambridge Press, Cambridge, UK, 115-122.

BRANCH project (2003) INTERREG IIIB North-West Europe Application Form Part A – Project Content and Management.

BRANCH partnership (2007) *Planning for Biodiversity in a Changing Climate – BRANCH Project Final Report*, Natural England, UK.

Bray, M.J. and Cottle, R. (2003) *Solent Coastal Habitat Management Plan*. Report by Posford Haskoning and University of Portsmouth to English Nature and Environment Agency. Volume 1 Summary of Habitat Change, Volume 2 Technical Report.

Bray, M.J. and Hooke, J.M. (1997) 'Prediction of Soft-cliff Retreat with Accelerating Sea-Level Rise' *Journal of Coastal Research*, 13, 453-467.

Brew, D.S., Funnell, B.M., Kreiser, A. (1992) 'Sedimentary Environments and Holocene Evolution of the Lower Blyth Estuary' *Proceedings of the Geologists' Association, 103, 57-74.*

Britsch, L.D. and Dunbar, J.B. (1993) 'land Loss Rates: Louisiana Coastal Plain' *Journal of Coastal Research*, 9, 324-338.

Brochier, F., and Ramieri, E. (2001) 'Climate Change Impacts on the Mediterranean Coastal Zones' *Nota di Lavoro, April 2001, Fondazione Eni Enrico Mattei*, No 27.

Brock, J.C. and Purkis, S.J. (2009) 'The Emerging Role of Lidar Remote Sensing in Coastal Research and Resource Management', *Journal of Coastal Research,* SI (53), 1-5.

Brooks, N., Nicholls, R., Hall, J. (2006) 'Sea Level Rise: Coastal Impacts and Responses' *Expertise for WBGU on Oceans and Global Change, Final Draft*, Berlin, 2006.

Bruun, P. (1954) 'Coastal Erosion and Development of Beach Profile', *U.S. Army Beach Eros. Board Tech.Memo. No 44*, U.S. Army Corps Eng., Waterw. Exr. Stn., Vicksburg, MS.

Bruun, P. (1962) 'Sea-level Rise as a Cause of Shore Erosion' *Proceedings of the American Society of Civil Engineers. Journal of the Waterways and Harbors Division*, 88,117-130.

Bruun, P. (1983) 'Review of Conditions for uses of the Bruun Rule of Erosion' *Coastal Engineering*, 7, 77-89.

Bruun, P. (1988) 'The Bruun Rule of Erosion by Sea-Level Rise: A Discussion on Large-Scale Two- and Three-dimensional Usages' *Journal of Coastal Research*, 4, 627-648.

Bryan, B., Harvey, N., Belperio, T., Bourman, B. (2001) 'Distributed process modeling for regional assessment of coastal vulnerabilty to sea-level rise' *Environmental Modeling and Assessment*, 6, 57-65.

Buncombe, W. (1994) *Osprey Pocket Guide to the River Blyth*, Waveney Valley Products, Beccles, Suffolk.

Burd, F. (1992) *Erosion and Vegetation Change on the Saltmarshes of Essex and North Kent Between 1973 and 1988*, Research and Survey in Nature Conservation, No42, Nature Conservancy Council, Peterborough, UK.

Burningham, H. and French, J. (2006) 'Morphodynamic behaviour of a mixed sand-gravel ebb-tidal delta: Deben Estuary, Suffolk, UK', *Marine Geology*, 225, 23-44.

Cahoon, D.R. (2006) 'A Review of Major Storm Impacts on Coastal Wetland Elevations' *Estuaries and Coasts*, 29, 889-898.

Cahoon, D.R. and Reed, D.J. (1995) 'Relationships among Marsh Surface Topography, Hydroperiod, and Soil Accretion in a Deteriorating Louisiana Salt Marsh; Sediment Dynamics, Deposition and Erosion in Temperate Salt Marshes' *Journal of Coastal Research*, 11, 357-369.

Cahoon, D.R., Reed, D.J., Day, J.W.Jr. (1995a) 'Estimating Shallow Subsidence in Macrotidal Salt Marshes of the Southeastern United States: Kaye and Barghoorn Revisited' *Marine geology*, 128, 1-9.

Cahoon, D.R., Reed, D.J., Day Jr, J.W., Steyer, G.D., Boumans, R.M., Lynch, J.C., McNally, D., Latif, N. (1995b) 'The Influence of Hurricane Andrew on Sediment Distribution in Louisiana Coastal Marshes' *Journal of Coastal Research*, SI 21, 280-294.

Callaway, J.C. (2001) 'Hydrology and Substrate' In: Zedler, J.B. (ed) *handbook for Restoring Tidal Wetlands*, CRC Press LLC, Chapter 3, 89-118.

Callaway, J.C., Nyman, J.A., DeLaune, R.D. (1996) 'Sediment Accretion in Coastal Wetlands: A Review and a Simulation Model of Processes' *Current Topics in Wetland Biogeochemistry*, 2, 2-23.

Callaway, J.C., Delaune, R.D., Patrick, W.H. (1997) 'Sediment Accretion Rates from four Coastal Wetlands along the Gulf of Mexico' *Journal of Copastal Research*, 13, 181-191.

Carling, P.A. (1982) 'Temporal and Spatial Variation in Intertidal Sedimentation Rates' *Sedimentology*, 29, 17-23.

Carter, R.W.G. (1988) *Coastal Environments: An Introduction to the Physical, Ecological and Culutural Systems of Coastline,* Academic Press, London, 199-244.

Carter, R.W.G. and Woodroffe, C.D. (1994) 'Coastal Evolution: An Introduction' In: Carter, R.W.G. and Woodroffe C.D. (eds) *Coastal Evolution: Late Quaternary Shoreline Morphodynamics*. Cambridge, Cambridge University Press, 1-31.

Cassar, M. (2005) *Climate Change and the Historic Environment* Centre for Sustainable Heritage, University College London.

Cailleux, A. (1952) 'Recentes Variations du Niveau des Mers et des Terres' *Rev. gen. Hydraul.*, 48, 310-315.

Cayocca, F. (2001) 'Long Term Morphological Modelling of Tidal Inlet: The Arcachon Basin, France, *Coastal Engineering*, 42, 115-142.

Cazenave, A., Nerem, R.S. (2004) 'Present-day Sea Level Change: Observations and Causes' *Reviews of Geophysics*, 42, RG3001, doi:10.1029/2003RG000139.

CCO (2013) http://www.channelcoast.org/southwest/survey_techniques/ /airborne_remote_sensing_topo_surveys/?link=LIDAR_surveys_of_cliffs_and_saltmarsh_systems.html

ChaMP (2002) *Suffolk Coast and Estuaries Coastal Habitat Management Plan*, Final Report, 3G547201, English Nature/ Environment Agency, 3G547201/R00002/JGLG/PBor.

CHaMP (2003) *North Norfolk Coastal Habitat Management Plan* Final Report G5472, English Nature, G5472/R/RS/PBor.

Channel Coastal Observatory (http://www.channelcoast.org/).

Christian, R.R., Stasavich, L., Thomas, C., Brinson, M.M. (2000) 'Reference is a Moving Target in Sea-Level Controlled Wetlands' In: Weinstein, M.P., Kreeger, D.A. (eds) *Concepts and Controveries in Tidal Marsh Ecology*, The Netherlands: Kluwer Press, 805-825.

Chu, M.L., Guzman, J.A., Munoz-Carpena, R., Kiker, G.A., Linkov, I. (2014) 'A Simplified Approach for Simulating Changes in Beach Habitat due to the Combined Effects of Long-Term Sea Level Rise, Storm Erosion, and Nourishment' *Environmental Modelling and Software*, 52, 111-120.

Church, J.A., and White, N.J. (2011) 'Sea-Level Rise from the Late 19th to the early 21st century', *Surveys in Geophysics*, 32, 585-602.

Church, J.A., White, N.J., Coleman, R., Lambeck, K., Mitrovica, J.X. (2004) 'Estimates of the Regional Distribution of Sea-Level Rise over the 1950-2000 Period' *Journal of Climate*, 17, 2609-2625.

Chust, G., Caballero, A., Marcos, M., Liria, P., Hemandez, C., Borja, A. (2010) 'Regional Scenarios of Sea Level Rise and Impacts on Basque (Bay of Biscay) coastal habiats, throughout the 21st century' *Estuarine, Coastal and Science*, 87, 113-124.

Chust, G., Borja, A., Liria, P., Galparsoro, I., Marcos, M., Caballero, A., Castro., R. (2009) 'Human Impatcs Overwhelm the Effects of Sea-Level Rise on Basque Coastal Habitats (N Spain) between 1954 and 2004' *Estuarine, Coastal and Shelf Science*, 84, 453- 462.

Clark, J.A., Farrell, W.E., Peltier, W.R. (1978) 'Global Changes in Postglacial Sea Level: A Numerical Calculation' *Quaternary Research*, 9, 265-287.

Clayton, K. and Shamoon, N. (1998) 'New Approach to the Relief of Great Britain II. A Classification of Rocks based on Relative Resistance to Denudation' *Geomorphology*, 25, 155-171.

Clough, J.S. and Larson, E.C. (2009) *SLAMM Analysis of Kenai Peninsula and Anchorage, AK, Final Report,* Warren Pinnacle Consulting Inc.

Clough, J.S., Larson, E.C. (2010) 'SLAMM 6.0.1 beta, Users Manual' Warren Pinnacle Consultingm Inc.

Clough, J.S., Park, R.A., Fuller, R. (2010) 'SLAMM 6 beta Technical Documentation' Warren Pinnacle Consulting, inc.

Clymo, R.S. (1964) 'Movement of the Main Shingle Bank at Blakeney Point, Norfolk', *Norolk and Norwich Naturalists Society Transaction*, 21, 3-6.

CoastBase http://www.coastbase.org.

Conner, W.H. and Day Jr., J.W. (1991) 'Variations in Vertical Accretion in a Louisiana Swamp' *Journal of Coastal Research*, 7, 617-622.

Cooper, J., and Pilkey, O. (2004) 'Sea-level Rise and Shoreline Retreat: Time to Abandon the Bruun Rule' *Global and Planetary Change*, 43(3-4), 157-171.

Cooper, N., Cooper, T., Burd, F. (2001) '25 Years of Salt Marsh Erosion in Essex: Implications for Coastal Defence and Nature Conservation' *Journal of Coastal Conservation*, 9, 31-40.

Cope, S.N., Bradbury, A.P., Gorcznska, M. (2008) *Solent Dynamic Coast Project: Main Report*, New Forest District Council/ Channel Coastal Observatory.

Costanza, R., Farber, S.C., Maxwell, J. (1989) 'The Valuation and Management of Wetland Ecosystems' *Ecological Economics*, 1, 335-361.

Costanza, R., Sklar, F.H., White, M.L. (1990) 'Modeling Coastal Landscape Dynamics' *Bioscience*, 40, 91-107.

Costanza, R, Sklar, F.H., White, M.L., Day, Jr., J.W. (1988) 'A Dynamic Spatial Simulation Model of Land Loss and Marsh Succession on Coastal Louisiana' In: Mitsch, W.J., Straskraba, M., Jorgensen, S.E. (eds) *Wetland Modelling*, Elsevier Science Publisher, 99-114.

Coulthard, T.J., Macklin, M.G., Kirkby, M.J. (2002) 'A Cellular Model of Holocene Upland River Basin and Alluvial Fan Evolution' *Earth Surface Processes and Landform*, 27, 269-88.

Covey, R. and Laffoley, D. d'A. (2002) *Maritime State of Nature Report for England; Getting onto an Even Keel*, English Nature, Petrborough, UK.

Coward, L., Corbett, D.R., Walsh, J.P. (2011) 'Shoreline Change along Sheltered Coastlines: Insights from te Neuse River Estuary, NC, USA' *Remote Sensing*, 3, 1516-1534.

Cowell, P.J. and Thom, B.G. (1994) 'Morphodynamics of Coastal Evolution' In: Carter, R.W.G. and Woodroffe (eds), *Coastal Evolution, Late Quaternary Shoreline Morphodynamics*, Cambridge University Press, 33-86.

Cowell, P.J., Stive, M.J.F., Niederoda, A.W., de Vriend, H.J., Swift, D.J.P., Kaminsky, G.M. and Capobianco, M. (2003) 'The Coastal Tract (part 1): A Conceptual Approach to Aggregated Modelling of Low Order Coastal Change' *Journal of coastal research*, 19, 812-827.

Craft, C., Clough, J., Ehman, J., Joye, S., Park, R., Pennings, S., Guo, H., Machmuller, M. (2009) 'Forecasting the Effects of Accelerated Sea-level Rise on Tidal Marsh Ecosystem Services' *Frontiers in Ecology and the Environment*, 7, 73-78.

Crooks, S. (2004) 'The Effect of Sea-Level Rise on Coastal Geomorphology' *IBIS*, 146, 18-20.

D'Alpaos, A., Lanzoni, S., Mudd, S.M., Fagherazzi, S. (2006) 'Modeling the Influence of Hydroperiod and Vegetation on the Cross-Sectional Formation of Tidal Channels' *Estuarine, Coastal and Shelf Science*, 69 (3-4), 311-324.

Dalrymple, R.A., Biggs, R.B., Dean, R.G, Wang, H. (1986) 'Bluff recession Rates in Chesapeake Bay' *Journal of Waterway, Port, Coastal and Ocean Engineering*, 112, 164-169.

Dasgupta, S., Laplante, B., Meinser, C., Wheeler, D., Yan, J. (2009) 'The Impact of Sea Level Rise on Developing Countries: A Comparative Analysis' *Climatic Change*, 93, 379-388.

Davidson, N.C., Laffoley, D.d'A, Doody, J.P., Way, L.S., Gordon, J., Key, R., Drake, C.M., Pienkowski, M.W., Mitchell, R., Duff, K.L. (1991) *Nature Conservation and Estuaries in Great Britain*, Nature conservancy Council.

Davidson-Arnott, R.G.D., van Proosdij, D., Ollerhead, J., Schostak, L. (2002) 'Hydrodynamics and Sedimentation in Salt Marshes: Examples from a Macrotidal Marsh, Bay of Fundy' *Geomorphology*, 48, 209-231.

Davidson-Arnott, R.G.D. (2005) 'Conceptual Model of the Effects of Sea Level Rise on sandy Coasts' *Journal of Coastal Research*, 21(6), 1166-1172

Day, J., Ibanez, C., Scarton, F., Pont, D., Hensel, P., Day, J., Lane, R. (2011) 'Sustainability of Mediterranean Deltaic and Lagoon Wetlands with Sea-Level Rise: The Importance of River Input' *Estuaries and Coasts*, 34, 483-493.

Day, J.W., Christian, R.R., Boesch, D.M., Yanez-Arancibia, A., Morris, J., Twilley, R.R., Naylor, L., Schaffner, L., Stevenson, C. (2008) 'Consequences of Climate Change on the Ecogeomorphology of Coastal Wetlands' *Estuaries and Coasts*, 31, 477-491.

Day, Jr., J.W., Pont, D., Hensel, P.F., Ibanez, C. (1995) ' Impacts Of Sea Level Rise on Deltas in the Gulf of Mexico and the Mediterranean: The Importance of Pulsing Events to Sustainability' *Estuaries*, 18, 636-647.

Dean, R.G. (1977) *Equilibrium Beach Profiles: U.S. Atlantic and Gulf Coasts*, Technical Report No.12, Department of Civil Engineering, University of Delaware, 45p.

Dean, R.G. (1987) ‘Additional Sediment Input to the Nearshore Region’ *Shore Beach*, 55, 76-81.

Dean, R.G. (1991) ‘Equilibrium Beach Profiles: Characteristics and Applications’ *Journal of Coastal Research*, 7, 53-84.

Dean, R.G. and Maurmeyer, E.M. (1983) ‘Models for Beach Profile Response’ In: Komar, P.D. (ed.) *Handbook of Coastal Processes and Erosion*, Boca Raton, Florida: C.R.C. Press, 151-166.

Dearing, J., Richmond, N., Plater, A., Wolf, J., Prandle, D., and Coulthard, T. (2006) ‘Modelling Approaches for Coastal Simulation based on Cellullar Automata: The Need and Potential’ *Philosophical Transactions of the Royal Society A, 364*, 1051-1071.

Defeo, O., McLachlan, A., Schoeman, D.S., Schlacher, T.A., Dugan, J., Jones, A., Lastra, M., Scapini, F. (2009) ‘Threats to Sandy Beach Ecosystems: A Review’ *Estuarine, Coastal and Shelf Science*, 81, 1-12.

DEFRA (2002) *Managed Realignment Review*, Policy research Project FD 2008, Department for Environment, Food and Rural Affairs, London. Department of Environment Food and Rural Affairs, London.

DEFRA (2006b) *Flood and Coastal Defence Appraisal Guidance FCDPAG3 Economic Appraisal – Supplementary note to Operating Authorities – Climate Change Impacts* Department for Environment, Food, and Rural Affairs, London.

DeLaune, R.D., Smith, C.J., Patrick Jr., W.H. (1983) ‘Relationship of Marsh Elevation, Redox Potential, and Sulfide to Spartina Alterniflora Productivity’ *Soil Science Society of America Journal*, 47, 930-935.

DeVriend, H.J., Zyserman, J., Nickolson, J., Roelvink, J.A., Pechon, P., Southgate, H.N. (1993a) ‘Medium Term 2DH Coastal Area Modelling’ *Coastal Engineering, 21, 193-224.*

DeVriend, H.J., Capobianco, M., Chasher, T., De Sward, H.E., Latteux, B., Stive, M.J.F. (1993b) ‘Approaches to Long-Term Modelling of Coastal Morphology: A Review’ *Coastal Engineering*, 21, 225-269.

Dickson, M.E., Walkden, M.J.A., Hall, J.W. (2005) ‘Systematic Impacts of Climate Change on an Eroding Coastal Region over the Twenty-First Century’ *Climatic Change*, 84, 141-166.

Dickson, M., Walkden, M., Hall, J., Pearson, S., Rees, J. (2005) ‘Numerical Modelling of Potential Climate-Change Impacts on Rates of Soft-cliff Recession, Northeast

Norfolk, UK' *Coastal Dynamics 2005 Proceedings of the 5th International Conference*, 4-8 April, 2005, Barcelona, Spain.

Dijkema, K.S. (1987) 'Geography of Saltmarshes in Europe' *Zeitschrift fur Geomorphologie*, 31, 489-499.

DINAS-COAST Consortium (2006) *DIVA 1.0* Postdam Institute for Climate Impact Research, Postdam, Germany, CR-ROM.

Di Silvio, G. (1989) 'Modelling the Morphological Evolution of Tidal Lagoons and their Equilibrium Configurations' *XXII Congress of the IAHR. Ottawa, Canada*

Di Silvio, G., Dall'Angelo, C., Bonaldo, D, Fasolato, G. (2010) 'Long-term Model of Planimetric and Bathymetric Evolution of a Tidal Lagoon', *Continental Shelf Research*, 30, 894-903.

Dissanayake, D.M.P.K., Ranasinghe, R., Roelvink, J.A., Wang, Z.B. (2011) 'Process-based ans Semi-Empirical Modelling Approaches on Tidal Inlet Evolution' *Journal of Coastal Research*, SI 64 (Processings of the 11th International Coastal Symposium), 1013-1017, Szezecin, Poland, ISSN 0749-0208

Dolan, R., Fenster, M., Holme, S. (1991) 'Temporal Analysis of Shoreline Recession and Accretion' *Journal of Coastal Research*, 7, 723-744.

Doody, J.P. (1992) 'The Conservation of British Saltmarshes' In: Allen, J.R.L. and Pye, K. S*altmarshes, Morphodynamics, Conservation abd Engineering Significance*, University of Cambridge Press, Cambridge, UK, 80-114.

Doody, J.P. (2001) *Coastal Conservation and Management: An Ecological Perspective*, Kluwer Academic Publishers, Dordrecht, the Netherlands.

Doody, J.P. (2012) 'Coastal Squeeze and Managed Realignment in Southeast England, does it tell us anything about the future?' *Ocean and Coastal Management* (article in press).

Douglas, B.C. (1991) 'Global Sea Level Rise' *Journal of Geophysical Research*, 95, 6981-6992.

Douglas, B.C. (1992) 'Global Sea Level Acceleration' *Journal of Geophysical Research*, 97 (C8), 12699-12706.

Douglas, B.C. (1997) 'Global Sea Level Rise: A Redetmination' *Surveys in Geophysics*, 18, 279-292.

Dougla, B.C. (2001) 'An Introduction to Sea Level' In: Douglas, B.C., Kearney, M.S., Leatherman, S.P. (eds) *Sea Level Rise, History and Consequences*, London Academic Press.

Douglas, B.C. and Peltier, W.R. (2002) 'The Puzzle of Global Sea Level Rise' *Physics Today*, 55, 35-40.

Douglas, B.C., Crowell, M., Leatherman, S.(1998) 'Considerations for Shoreline Position Prediction' *Journal of Coastal Research*, 14, 1025-1033.

Dubois, R.N. (1977) 'Predicting Beach Erosion as a Function of Rising Water Level' *The Journal of Geology*, 85, 470-476.

Dubois, R.N. (1992) 'A Re-evaluation of Bruun's Rule and Supporting Evidence' *Journal of Coastal Research*, 83, 618-628.

Eisma, D. and Kalf, J. (1987) 'Dispersal, Concentration and Deposition of Suspended Matter in the North Sea' *Journal of the Geological Society*, 144, 161-178.

El-Raey, M. (1997) 'Vulnerability Assessment of the Coastal Zone of the Nile Delta of Egypt, to the Impacts of Sea Level Rise' *Ocean and Coastal Management*, 37, 29-40.

Emery, K.O. (1980) 'Relative Sea Levels from Tide-Gauge Record' *Proceedings of the national Academy of Science*, USA, 77,6968-72.

Emery, K.O. and Aubrey, D.G. (1991) *Sea Levels, land levels, and tide gauges*, New York, Springler-Verlag.

English Nature (1992) *Coastal Zone ConservationEnglish Nature's Rationale, Objectives and Practical Recommendations*, English Nature, Peterborough, UK.

Environment Agency (1999a) *Suffolk Estuarine Strategies, Phase II – Report A, Blyth Estuary.*

Environment Agency (1999b) *Suffolk Estuarine Strategies, Phase II – Report C, Deben Estuary.*

Environment Agency (2007) *Saltmarsh Management Manual*. R&D Technical Report PFA-076/TR, Environment Agency, Bristol, 123pp.

Environment Agency (2009) *Suffolk Estuarine Strategies, Blyth, Strategy Approval Report*.

Environment Agency (2011) *Coastal Trends Report – Suffolk (Lowestoft to Languard Point, Felixstowe)*, RP022/S/2011, February 2011.

Environment Agency (2012) *Coastal Trends Report – North Norfolk (Old Hunstanton to Kelling)*, RP028/L/2011, October 2012.

Evans, E., Ashley, R., Hall, J., Penning-Rowsell, E., Saul, A., Sayers, P., Thorne, C., Watkinson, A. (2004) *Foresight Future Flooding Scientific Summary: Volume I Future Risks and their Drivers* Office of Science and Technology, London.

EUROSION (2004) *Living with Coastal Erosion in Europe: Sediment and Space for Sustainability*, Report to Directorate General Environment, European Comission, http://www.eurosion.org.

Fagherazzi, S. and Wiberg, P.L. (2009) 'Importance of Wind Conditions, Fetch, and Water Levels on Wave-generated Shear Stress om Shallow Intertidal Basins', *Journal of Geophysical Research*, 114, F03022.

Fagherazzi, S. and Priestas, A.M. (2010) 'Sediments and Water Fluxes in a Muddy Coastline: Interplay Between Waves and Tidal Channel hydrodynamics' *Earth Surface Processes and Landforms,* 35, 284-293.

Fairbridge, R.W. (1980) 'The Estuary: Its Definition and Geodynamic Cycle' In: Olausson, E., Cato, I. (eds) *Chemistry and Biochemistry of Estuaries*, Wiley, New York, 1-35.

Fairbridge, R.W. and Krebs, O.A. (1962) 'Sea Level and the Southern Oscillation' *Geophysical Journal,* 6, 532-545.

Fenster, M.S., Dolan, R. (1993) 'Historical Shoreline Trends Along the Outer Banks, North Carolina: Processes and Responses' *Journal of Coastal Research*, 9, 172-188.

Fenster, M.S., Dolan, R., Elder, J.F. (1993) 'A New Method for Predicting Shoreline Positions from Historical Data' *Journal of Coastal Research*, 91, 147-171.

Ferguson, G. and Gleeson, T. (2012) 'Vulnerability of Coastal Aquifers to Groundwater Use and Climate Change' *Nature Climate Change*, DOI:10.1038/NCLIMATE1413.

FitzGerald, D.M., Fenster, M.S., Argow, B.A, and Buynevich, I.V. (2008) 'Coastal Impacts Due to Sea-Level Rise*' Annual Review of Earth and Planetary Sciences*, *36*(1), 601-647.

Forbes, D.L., Taylor, R.B., Shaw, J. (1989) 'Shorelines and Rising Sea Levels in Eastern Canada' *Episodes*, 12, 23-28.

French, C.E., French, J.R., Clifford, N.J., Watson, C.J. (2000) 'Sedimentation-erosion Dynamics of Abandoned Reclamation: The Role of Waves and Tides' Continental Shelf Research, 20, 1711-1733.

French, G.T., Awosika, L.F., Ibe, C.E. (1995) 'Sea-Level Rise and Nigeria: Potential Impacts and Consequences' *Journal of Coastal Research*, 14, 224-242.

French, J.R. (1993) 'Numerical Simulation of Vertical Marsh Growth and Adjustment to Accelerated Sea-Level Rise, North Norfolk, U.K' *Earth Surface Processes and Landforms, 18* (1), 63-81.

French, J.R. (1994) ‘Wetland Response to Accelerated Sea-Level Rise: A European Perspective’ In: Finkl, C.W. (ed.) ‘Coastal Hazards: Perception, Mitigation and Susceptibility’ *Journal of Coastal Research Special Issue,* 12, 94-105.

French, J.R. (2001) *Hydrodynamic Modelling of the Blyth Estuary: Impast of Sea-Level Rise,* Coastal and estuarine research Unit, University College London, Report for Environment Agency, Anglian Region.

French, J.R. (2003) ‘Airborne LiDAR in Support of Geomorphological and Hudraulic Modelling’ *Earth Surface Processes and Landfroms*, 28, 321-335.

French, J.R. (2004) *Critical Concepts in Coastal Geomorphology,* London, Routledge.

French, J.R. (2006) ‘Tidal Marsh Sedimentation and Resilience to Environmental Change:Exploratory modelling of Tidal, Sea-Level and Sediment Supply Forcing in Predominantly Allocthonous Systems’ *Marine Geology*, 235, 119-136.

French, J.R. (2008) ‘Hydrodynamic Modelling of Estuarine Flood Defence Realignment as an Adaptive management Response to Sea-level Rise’ *Journal of Coastal Research,* 24, 1-12.

French, J.R and Burningham, H. (2003) ‘Tidal Marsh Sedimentation Versus Sea-level Rise: A Southeast England Estuarine Perspective’ *Proceedings Coastal Sediments ’03, Sheraton Sand Key, Vlearwater, Florida.*

French, J.R. and Burningham, H. (2009) ‘Coastal Geomorphology: Trends and Challenges’ *Progress in Physical Geography*, 33, 117-129.

French, J.R. and Burningham, H. (2011) ‘Qualitative Mathematical Modelling of Coupled Coast and Estuary Morphodynamics: A Modified Boolean Network Approach’ *American Geophysical Union*, Fall Meeting 2011.

French, J.R. and Burningham, H. (2013) ‘Coasts and Climate: Insights from Geomorphology’ *Progress in Physical Geography,* 37, 550-561.

French, J.R. and Reed, D.J. (2001) ‘Physical Contexts for Saltmarsh Conservation’ In: Warren, A. and French, J.R. (eds) *Habitat Conservation: Managing the Physical Environment*, John Wiley & Sons, LTD, 179-228.

French, J.R. and Spencer, T. (1993) ‘Dynamics of Sedimentation in a Tide-Diminated Backbarrier Salt Marsh, Northfolk, UK’ *Marine Geology*, 110, 315-331.

French, J.R. and Spencer, T. (2001) ‘Sea-level Rise’ In: Warren, A. and French, J.R. (eds) *Habitat Conservation: Managing the Physical Environment*, John Wiley & Sons, LTD, 305-349.

French, J.R. and Stoddart, D.R. (1992) 'Hydrodynamis of Salt-Marsh Creek Systems – Implications for Marsh Morphological Development and Material Exchange' *Earth Surface Processes and Landforms*, 17, 235-252.

French, J.R., Spencer, T., Stoddart, D. (1990) 'Backbarrier Salt marshes of the North Norfolk Coast: Geomorphic Development and Response to Rising Sea-Levels' *Discussion papers in Conservation, Ecology and Conservation Unit, UCL*, 54.

French, J.R., Burningham, H., Benson, T. (2008) 'Tidal and Meteorological Forcing of Suspended Sediment Flux in a Muddy Mesotidal Estuary' *Estuaries and Coasts*, 31: 843-859.

French, J.R., Spencer, T., Murray, A.L., Arnold, N.S. (1995) 'Geostatistical Analysis of Sediment Deposition in Two Small Tidal Wetlands, Norfolk, UK' *Journal of Coastal Research*, 11, 308-321.

French, J., Payo, A., Murray, B., Orford, J., Elliot, M., Cowell, P. (2015) 'Appropriate Complexity for the Prediction of Coastal and Estuarine Geomorphic Behaviour at Decadal to centennial Scales' *Geomorphology*, In Press.

French, P.W. (1997) *Coastal and Estuarine Management* Routledge Environmental Management Series, pp 251.

French, P.W. (2001) *Coastal Defences. Processes, Problems and Solutions*, Routledge, London, UK.

Friedrichs, C.T. and Perry, J.E. (2001) 'Tidal Saltmarsh Morphodynamics: A Synthesis', *Journal of Coastal Research Special Issue*, 27, 7-37.

Frostick, L.E. and McCave, I.N. (1979) 'Seasonal Shifts of Sediment within an Estuary Mediated by Algal Growth' *Estuarine and Coastal Marine Science*, 9, 569-576.

Funnell, B.M., Boomer, I., Jones, R. (2000) 'Holocene Evolution of the Blakeney Spit Area of the North Norfolk coastline', *Proceedings of the Geologists' Association*, 111, 205-217.

Galbraith, H., Jones, R., Park, R., Clough, J.S. , Herrod-Julius, S., Harrington, B., Page, G. (2002) 'Global Climate Change and Sea Level Rise: Potential Losses of intertidal Habitat for shorebirds' *Waterbird*, 25, 173-183.

Galbraith, H., Jones, R., Park, R., Clough, J., Herrod-Julius, S., Harrington, B., Page, G. (2003) 'Global Climate Change and Sea Level Rise: Potential Losses of intertidal habitat for shorebirds' In: Valette-Silver, N.J. and Scavia, D. (eds) *Ecological Forecasting: New Tools for Coastal and marine Ecosystem Management*, NOAA, Silver Spring, Maryland, 19-22.

Galbraith, H., Jones, R., Park, R., Clough, J., Herrod-Julius, S., Harrington, B., Page, G. (2005) *Global Climate Change and Sea Level Rise: Potential Losses of intertidal habitat for shorebirds.* USDA Forest Service Gen. Tech. Rep. PSW-GTR-191.2005.

Garbutt, R.A., Reading, C.J., Wolters, M., Gray, A.J., Rothery, P. (2006) 'Monitoring the Development of Intertidal Habitats on Former Agricultural Land after the Managed Realignment of Coastal Defences at Tollesbury, Essex, UK' *Marine Pollution Bulletin*, 53, 155-164.

Garcin, M., Yates, M., Le Cozannet, G., Walker, P., Donato, V. (2011) 'Sea Level Rise and Coastal Morphological Changes on Tropical Islands: Examples from New Caledonia and French Polynesia (SW Pacific)' *Geophysical Research Abstracts*, 13EGU2011-3504.

Gardiner, L.R., Porter, D.E. (2001) 'Stratigraphy and Geologic History of a Southeastern Salt Marsh Basin, North Inlet, South Carolina, USA' *Wetlands Ecology and Management*, 9, 371-382.

Gardiner, L.R., Smith, B.R, Michener, W.K. (1992) 'Soil Evolution along a Forest-Marsh Transect under a Regime of slowly Rising Sea Level, North Inlet, South Carolina, USA' *Geoderma*, 55, 141-157.

Gardiner, S., Ingleby, A., Jude, S., Nicholls, R.J., Rauss, I., Williams, A (2007) 'Developing Spatial Planning Tools and Guidance to Enable Coastal Biodiversity to Adapt to Climate Change, Annex 3' of *Planning for Biodiversity in a Changing Climate – BRANCH project Final Report,*, Natural England, UK.

Gardline Environmental Ltd (2003) *River Blyth Hydrographic Survey: Hydrodynamics and Sediment Study, Data Period: April 24th to May 27th*.

Gesch, D.B., Gutierrez, B.T., Gill, S.K. (2009) 'Coastal Elevations*' In:* J.G., Titus, K.E., Anderson, D.R., Cahoon, D.B., Gesch, S.K., Gill, B.T., Gutierrez, E.R., Thieler, S.J., Williams (ed.) *Coastal Sensitivity to Sea-Level Rise:A Focus on the Mid-Atlantic Region.* A report by the U.S.Climate Change Science Programme and the Subcommittee on Global Change Research, U.S. Environmentan Protection Agency, Washington DC, 25-42.

Geselbracht, L., Freeman, K., Kelly, E., Gordon, D.R., Putz, F.E. (2011) 'Retrospective and Prospective Model Simulations of Sea Level Rise Impacts on Gulf of Mexico Coastal Marshes and Forests in Waccasassa Bay, Florida' *Climatic Change*, 107, 35-57.

Ghyben, B.W. (1888) 'Nota in Verband Met de Voorgenomen putboring Nabij Amsterdam (Notes on the Probable Results of the Proposed Well Drilling Near Amsterdam)' *Tijdschrift van het Koninklijk Institunt van Ingeniers, The Hague*, 8-22.

Glick, P., Clough, J., Nunley, B. (2008) *Sea-Level Rise nas Coastal Habitats in the Chesapeake Bay Region, Technical Report*, National Wildlife Federation.

Glick, P., Clough, J., Polaczyk, A., Couvillion, B., Nunley., B. (2013) 'Potential Effects of Sea-Level Rise on Coastal Wetlands in Southeastern Louisiana' *Journal of Coastal Research*, 63, 211-233.

Gomes Pereira, L.M. and Wicherson, R.J. (1999) 'Suitability of Laser Data for Deriving geographical Information. A Case Study in the Context of Manageemnt of Fluvial Zones' *ISPRS Journal of Photogrammetry and Remote Sensing*, 54, 105-114.

Gornitz, V. (1991) 'Global Coastal Hazards from Future Sea Level Rise' *Global Planet Change*, 89, 379-98.

Gornitz, V. (1995) 'Sea-level Rise:A Review of Recent past and Near – Future trends' *Earth and Surface Processes and Landfroms*, 20, 7-20.

Gornitz, V., Lebedeff, S., Hansen, J. (1982) 'Global Sea Level Trend in the Past Century' *Science*, 215, 1611-1614.

Gornitz, V. and Lebedeff, S. (1987) 'Global Sea Level Changes during the Past Century' In: Nummedal, D., Pilkey, O.H., Howard, J.D. (eds), *Sea Level Fluctuation and Coastal Evolution* , SEPM Spec.Publ. 41, 3-16.

Gornitz, V., Cough, S., Hartig, E. (2001) 'Impacts of Sea Level Rise in the New York Metropolitan Area' *Global and Planetary Change*, 32, 61-88.

Gray, A.J. (1977) 'Reclaimed Land' In: Barnes, R.S.K. (ed) *The Coastline*, Wiley, London, 253-270.

Grinsted, A., Moore, J.C., Jevrejeva, S. (2009) 'Reconstructing Sea Level from Paleo and Projected Temperatures 2000 to 2100 AD' *Climate Dynamics*, 34, 461-472.

Green, D. and King, S. (2003) 'Progress in Geographical Information Systems and Coastal Modeling: An Overview' In: Lakhan, V. (ed) *Advances in Coastal Modeling*, Elsevier Science, 553-580.

Groger, M. and Plag, H.P. (1993) 'Estimations of a Global Sea-Level Trend: Limitations from the Structure of the PSMSL Global Sea Level Data Set' *Global and Planetary Change*, 8, 161-9.

Gulve, S.K., and Hasse, L. (1999) ‘Changes of Wind Waves in the North Atlantic Over the Last 30 Years’ *International Journal of Climatology*, 19, 1091-1117.

Gulve, S.K., and Grigorieva, V. (2004) ‘Last Century Changes in Ocean Wind Wave Height from Global Visual Wave Data’ *Geophysical Research Letters*, 31, L24302.

Guntenspergen, G.R., Cahoon, D.R., Grace, J.B., Steyer, G.D., Fournet, S., Townson, M.A., Foote, A.L. (1995) ‘Disturbance and Recovery of the Louisiana Coastal Marsh Landscape from the Impacts of Hurrican Andrew’ *Journal of Coastal Research*, SI 21, 324-339.

Gutelius, W., Carter, W., Shrestha, R., Medvedev, E., Gutierez, R., Gibeaut, J. (1998) ‘Engineering Applications of Airborne Scanning Lasers: Reports from the Field’ *Photogrammetric Engineering & Remote Sensing*, 64, 246-253.

Gutenberg, B. (1941) ‘Changes in Sea Level, Post-glacial Uplift and Mobility of the Earth’s Interior’*Bulletin of the Geological Society of America*, 52, 721-72.

Hackney, C.T., Cleary, W.J. (1987) ‘Saltmarsh Loss in Southeastern North Carolina Lagoons: Importance of Sea Level Rise and Inlet Dredging’ *Journal of Coastal Research*, 3, 93-97.

Hadley, D. (2009) ‘Land Use and the Coastal Zone’ *Land Use Policy*, 26S, S198-S203.

Hall, J.W., Meadowcroft, I.C., Lee, E.M., Van Gelder, P.H.A.J.M (2002) ‘Stochastic Simulation of Episodic Soft Coastal Cliff Recession’ *Coastal Engineering*, 46, 159-174.

Han, M., Hou, J., Wu, L. (1995) ‘Potential Impacts of Sea-Level Rise on China’s Coastal Environment and Cities: A National Assessment’ *Journal of Coastal Research*, 14, 79-95.

Hands, E.B. (1983) ‘The Greta Lakes as a Test Model for Profile Responses to Sea-Level Change’ In: Komar, P.D. (ed.) *Handbook of Coastal Processes and erosion*, Boca Raton, CRC Press, 167-189.

Hanson, H. and Kraus, N. (1989) *GENESIS: Generalized Model For Simulating Shoreline Change* Technical Report CERC -89-19, 85 p, Vicksburg, Mississippi, US Army Corps of Engineers.

Hanson, H., Connell, K.J., Larson, M., Kraus, N.C., Beck, T.M., Frey, A.E. (2011) ‘Coastal Evolution Modeling at Multiple Scales in Regional Sediment Management Applications’ *Proceedings of Coastal Sediments 2011*, Miami, Fl., 3, 1920-1932.

Hanson, H., Aarninkhof, S., Capobianco, M., Jimenez, J.A., Larson, M., Nicholls, R.J., Plant, N.G., Southgate, H.N., Steetzel, H.J., Stive, M.J.F., de Vriend, H.J. (2003) 'Modelling of Coastal Evolution on Yearly to decadal Time Scales' *Journal of Cooastal research*, 19, 790-811.

Hatton, R.S., DeLaune, R.D., Patrick Jr., W.H. (1983) 'Sedimentation, Accretion, and Subsidence in Marshes of Bataria Basin, Louisiana' *Limnology and Oceanography*, 28, 494-502.

Hayden, B.P., Santos, C.F.V., Shao, G., Kochel, R.C. (1995) 'Geomorphological Controls on Coastal Vegetation at the Virginia Coast Reserve' *Geomorphology*, 13, 283-300.

Hearn, C.J. (2008) *The Dynamics of Coastal Models, Cambridge University Press.*

Henderson-Sellers, A., Zhang, H., Berz, G., Emanuel, K., Gray, W., Landsea, C., Holland, G., Lighthill, J., Shieh, S.L., Webster, P., McGuffie, K. (1998) 'Tropical Cyclones and Global Climate Change: A Post-IPCC Assessment' *Bulletin Americal Meteorological Society*, 79, 19-38.

Herzberg, A. (1901) 'Die Wasserversorgung einiger Nordseeb~ider (The Water Supply on Parts of the North Sea Coast in Germany)' *Journal Gabeleucht ung und Wasserversorg ung*, 44, 815-819, 824-844.

Hibma, A., Stive, M.J.F., Wang, Z.B. (2004) 'Estuarine Morphodynamics' *Coastal Engineering*, 51, 765-775.

Higinbotham, C.B., Alber, M.M., Chalmers, A.G. (2004) 'Analysis of Tidal Marsh Vegetation Patterns in Two Georgia Estuaries using Aerial Photography and GIS' *Estuaries*, 27, 670-683.

Hinkel, J. (2005) 'DIVA: An Iterative Method for Building Modular Integrated Models' *Advances in Geosciences*, 4, 45-50.

Hinkel, J. and Klein, R.J.T. (2007) 'Integrating Knowledge for Assessing Coastal Vulnerability to Climate Change' In: McFadden, L., Nicholls, R.J., Penning-Rowsell, E.C. (eds) *Managing Coastal Vulnerability: An Integrated Approach*, Amsterdam: Elsevier Science, 61-78.

Hinkel, J., and Klein, R.J.T. (2009) 'Integrating Knowledge to Assess Coastal Vulnerability to Sea-Level Rise: The Development of the DIVA Tool' *Global Environmental Change*, 19, 384-395.

Hoffman, J.S., Keyes, D., Titus, J.G. (1983) 'Projecting Future Sea Level Rise; Methodology, Estimates to the Year 2100 and Research Needs' Washington DC:US Environmental Protection Agency, 121pp.

Hoffman J.S., Wells, J.B., Titus, J.G. (1986) 'Future Global Warming and Sea Level Rise. In: Sigbjarnarson, G. (ed) *Proceedings Iceland Coastal and River Symposium '85.* Reykjavik, National Energy Authority, 246-66.

Holgate, S.J., Woodworth, P.L. (2004) 'Evience for Enhanced Coastal Sea Level Rise during the 1990s' *Geophysic Research Letters*, 31, 4.

Hooke, J.M., Bray, M.J. (1996) 'Approaches to Analysis and Prediction of Coastal Processes and Morphology' In: Taussik, J., Mitchell, J. (eds) *Partnership in Coastal Zone Management*, Samara Publishing, Cardigan, 167-174.

Hoozemans, F.M.J., Marchand, M., Pennekamp, H.A. (1993) 'Sea Level Rise: A Global Vulnerability Analysis: Vulnerability Assessments for Population, Coastal Wetlands and Rice Production on Global Scale' *Second Revised Edition,* Delft Hydraulics and Rijkswaterstaat, Delft and The Hague, The Netherlands, 184.

Horton, R., Herweijer, C., Rosenzweig, C., Liu, J., Gornitz, V., Ruane, A.C. (2008) 'Sea level rise projections for current generation CGCMs based on the semi‐empirical method' *Geophysical Research Letters*, 35, L02715.

Howe, M.A. (2002) *A Review of the Coastal Soft Cliff Resource in Wales, with particular reference to its Importance for Invertebrates,* CCW Natural Science Report No. 02/5/1.

Hughes, R.G. and Paramor, O.A.L. (2004) 'On the Loss of Saltmarshes in South-East England and methods for their restoration' *Journal of Applied Ecology*, 41, 440-448.

Hull, C.H.J. and Titus, J.G. (1986) *Greenhouse Effect, Sea Level Rise and Salinity in the Delaware Estuary*, EPA 230-50-86-010, 86pp.

Hulme, M., and Jenkins, G. (1998) *Climate Change Scenarios for the United Kingdom UKCIP Technical Report No.1.* Climatic Research Unit, University of East Anglia and Hadley Centre, Met. Office.

Hulme, M., Turnpenny, J., Jenkins, G. (2002) *Climate Change Scenarios for the United Kingdom - The UKCIP02 Briefing Report.* Tyndall Centre for Climate Change Research, School of Environmental Sciences, University of East Anglia, Norwitch, UK.

HydroQual, Inc. (2002) *A Primer for ECOMSED* Users Manual, Version 1.3, HydroQual, Inc., Mahwah, New Jersey, pp 188.

Ibanez, C.A., Canicio, A., Day, J.W., Curco, A. (1997) 'Morphologic Evolution, Relative Sea Level Rise and Sustainable Management of Water and Sediment in the Ebre Delta' *Journal of Coastal Conservation*, 3, 191-202.

Ibanez, C., Sharpe, P.J., Day, J.W., Day, J.N., Prat, N. (2010) 'Vertical Accretion and Relative Sea Level Rise in the Ebro Delta Wetlands (Catalonia, Spain) *Wetlands*, 30, 979-988.

Institute of Hydrology (1996) *UK National River Flow Archive,* Station no. 035014, Wallingford, UK.

Isle of Wight Shoreline Management Plan 2, (Isle of Wight, SMP2) (2010) *Main Report Chapter 4: Policy Development Zone 7- North West Coastline (PDZ7); & Appendix C: Baseline Process Understanding: C1: Assessment of Shoreline Dynamis, C2: Defence Appraisal, C3: Baseline Scenarios of Future Shoreline Change, Appendix D: Natural and Built Environment Baseline,* Coastal Management, Isle of Wight Council.

Isle of Wight SFRA (2009) *Tidal Climate Change Mapping Update Supplementary Technical Note,* Entec UK Ltd for Isle of Wight Council Planning Services.

IPCC (2001) *Climate Change 2001: The Scientific Basis, Contribution of Working Group I to the Third Assessment Report of the Intergovernmental Panel on Climate Change.* Houghton, J.T., Ding, Y., Griggs, D.J., Noguer, M., vand der Linden, P.J., Dai, X., Maskell, K., Johnson, C.A. (eds). Cambridge University Press.

IPCC (2007) *Summary for Policy Makers. In:Climate Change 2007: The Physical Science Basis, Contribution of Working Group I to the Fourth Assessment Report of the Intergovernmental Panel of Climate Change.* Solomon, S., Qin, D., Manning, M., Marquis, M., Averyt, K.B., Tignor, M., and Miller, H.L., (eds). Cambridge University Press, Cambridge, United Kingdom and New York, NY, USA.

IPCC (2013): *Summary for Policy Makers. In: Climate Change 2013: The Physical Science Basis, Contibution of Working Group I to the Fifth Assessment Report of the Intergovernmental Panel of Climate Change,* Stocker, T.F., Qin, D., Plattner, G.-K., Tignor, M., Allen, S.K., Boschung, J., Nauels, A., Xia, Y., Bex, V., Midgley, P.M. (eds). Cambridge University Press, Cambridge, United Kingdom and New York, NY, USA.

Jackson, N.L. and Nordstrom, K.L. (1992) 'Site-Specific Controls on Wind and Wave Processes and Beach Mobility on Estuarine Beaches in New Jersey, USA' *Journal of Coastal Research,* 8, 88-98.

Jackson, N.L., Nordstrom, K.F., Eliot, I., Masselink, G. (2002) 'Low Energy Sandy Beaches in Marine and Estuarine Environments: A Review' *Geomorphology*, 48, 147-162.

Jakobsen, B. (1953) 'Landskabsudviklingen I Skallingmarsken' *Geogr. Tidsskr.* 52, 147-158.

Jenkins, G., Perry, M., Prior, M. (2008) *The Climate of UK and Recent Trends.* Met Office, Hadley Centre, Exeter, UK.

Jenkins, G., Murphy, J., Sexton, D.S., Lowe, J.A., Jones, P., Kilsby, C. (2009) *UK Climate Projections: Briefing Report.* Met Office, Hadley Centre, Exeter, UK.

Jevrejeva, S., Moore, J.C., Grinsted A. (2010) 'How will sea level respond to changes in natural and anthropogenic forcings by 2100?' *Geophysical research Letters*, 27, 5pp.

JNCC (2008) *Information Sheet on Ramsar Welands*, Available from URL: http://www.jncc.gov.uk/pdf/RIS/UK11017.pdf,

Jones, L., Angus, S., Cooper, A., Doody, P., Everard, M., Garbutt, A., Gilchrist, P., Hansom, J., Nicholls, R., Pye, K., Ravenscroft, N., Rees, S., Rhind, P., Whitehouse, A. (2011) 'Coastal Margins' In: *The UK National Ecosystem Assessment Technical Report*, UK National Ecosystem Assessment, UNEP-WCMC, Cambridge.

Kaiser, M.F.M. and Frihy, O.E. (2009) 'Validity of the Equilibrium Beach Profiles:Nice Delta Coastal Zone, Egypt' *Geomorphology*, 107, 25-31.

Kamphuis, J. (1987) 'Recession Rates of Glacial Till Bluffs' *Journal of Waterway, Port, Coastal, and Ocean Engineering*, 113, 60-73.

Kaplin, P.A. and Selivanov, A.O. (1995) 'Recent Coastal Evolution of the Caspian Sea as a Natural Model for Coastal Responses to the Possible Acceleration of Global Sea-Level Rise' *Marine Geology*, 124, 161-175.

Kearny, M.S., Stevenson, J.C. (1991) 'Island Land Loss and Marsh Vertical Accretion Rate: Evidence for Historical Sea Level Changes in Chesapeake bay' *Journal of Coastal Research*, 7, 403-415.

Kirby, R. (1987) 'Sediment Exchanges across the Coastal Margins of N.W. Europe' *Journal of the Geological society*, 144, 121-126.

Kirby, R. (2000) 'Practical Implications of Tidal Flat Shape' *Continental Shelf Research*, 20, 1061-1077.

Kirwan, M.L., and Murray, A.B. (2007) 'A Coupled Geomorphic and Ecological Model of Tidal Marsh Evolution' *Proceedings of the National Academy of Sciences of the United States of America*, *104*(15), 6118-22.

Kirwan, M.L., Guntenspergen, G.R., D'Alpaos, A., Morris, J.T., Mudd, S.M., Temmerman, S. (2010) 'Limits on the Adaptability of Coastal Marshes to Rising Sea Level' *Geophysical Research Letters*,37, L23401.

Klige, R.K. (1982) 'Oceanic Level Fluctuations in the History of the Earth', In *Sea and Oceanic Level Fluctuations for 15,000 years, Acadd.Sc. USSR, Institute of Geography, Moscow, Nauka (in Russian), 11-22.*

Knutson, P.L., Ford, J.C., Inskeep, M.R., Oyler, J. (1981) 'National Survey of Planted Salt Marshes (Vegetative Stabilization and Wave Stress)' *Wetlands, Journal of the Society of Wetland Scientists.*

Komar, P.D. (1999) 'Coastal Change-scales of Processes and Dimensions of Problems' In: Kraus, N.C. and Douglas W.G. (eds) *Coastal Sediments '99: Proceedings of the 4th International Symposiumon Coastal Engineering and Science of Coastal Sediment Transport Processes,* 1, 1-17.

Koppari, K., Karlsson, U., Steivall, O. (1994) 'Airborne Laser Depth Sounding in Sweden' *Proceedings U.S. Hydrographic Conference 1994, The Hydrographic Society Spec.,* 32, 124-133.

Kraus, N.C., Larson, M., Kriebel, D.L. (1991) 'Evaluation of Beach Erosion and Accretion Predictors' *Coastal Sediments'91,* Americal Society of Civil Engineers, Seattle, 527-587.

Kriebel, D.L., Kraus, N.C., Larson, M. (1991) 'Engineering Methods for Predicting Beach Profile Response' *Coastal Sediments '91* American Society Civil Engineers, 557-571.

Krone, R.B. (1987) 'A Method for Simulating Historic Marsh Elevations' In Kraus, N.C. (ed) *Coastal Sediments '87*, Americal Society of Civil Engineers, New York, 316-323.

Lambeck, K. (2002) 'Sea Level Change from mid Holocene to Recent Time: An Australian Example with Global Implications' *Ice Sheets, Sea Level and the Dynamic Earth, Geodynamics Series*, 29, American Geophysical Union, Washington, DC, 33-50.

Larsen, L., Moseman, S., Santor, A., Hopfensperger, K., & Burgin, A. (2010) 'A Complex-systems approach to predicting effects of sea level rise and nitrogen

loading on nitrogen cycling in coastal wetland ecosystems' *Eco-DAS VIII Chapter 5*. American Society of Limnology and Oceanography,Inc, 67-92.

Larson, M. (1991) 'Equilibrium Profile of a Beach with Varying Grain Size' *Coastal Sediments'91*, New York: ASCE, 905-919.

Larson, M., and Kraus, N.C. (1989) *SBEACH: Numerical Model for Simulating Storm Induced Beach Change*, Technical Report, Vicksburg, Mississipi: U.S. Army Corps of Engineers, 256pp.

Larson, M., Kraus, N.C., Hanson, H. (2002) 'Simulation of Regional Longshore Sediment Transport and Coastal Evolution – The Cascade Model' *Proceedings28th Coastal Engineering Conference,* ASCE, 2612-2624.

Laurence, D. (1980) 'Wave Climatology of the UK Continental Shelf' In: Banner, F.T., Collins, M.B., Massie, K.S. (eds) *The North-West European Shelf Seas: The Sea Bed and the Sea in Motion II. Physical and Chemical Oceanography, and Physical Resources,* Elsevier Oceanography Series, chapter 10.

Lawrence, R. (1990) *Southwold River: Georgian Life in the Blyth Valley*, Suffolk Books, Exeter, UK.

Le Hir, P., Roberts, W., Cazaillet, O., Christie, M., Bassoullet, P., Bacher, C. (2000) 'Characterization of Intertidal Flat Hydrodynamics' *Continental Shelf Research,* 20, 12-13.

Leatherman, S.P. (1984) 'Coastal Geomorphic Responses to Sea-Level Rise: Galveston Bay, Texas' In: Bath, M.C., Titus, J.G. (eds) *Greenhouse Effect and Sea Level Rise*, New York: Van Nostrand Reihhold, 151-178.

Leatherman, S.P. (1990) 'Modeling Shore Response to Sea-Level Rise on Sedimentary Coasts' *Progress in Physical Geography*, 14, 447-464.

Leatherman, S.P. (2001) 'Social and Economic Cost of Sea Level Rise' In: Douglas, B.C., Kearney, M.S., Leatherman, S.P. (eds) *Sea Level Rise: History and Consequences*, San Diego: Academic Press, 181-223.

Leatherman, S.P., Zhang, K., Douglas, B.C. (2000) 'Sea Level Rise Shown to Drive Coastal Erosion' *EOS Transactions of the American Geological Union*, 81, 55-56

Lee, J.K., Park, R.A., Mausel, P.W. (1992) 'Application of Geoprocessing and Simulation Modeling to Estimate Impacts of Sea Level Rise on the Northeast Coast of Florida' *Photogrammetric Engineering and Remote Sensing*, 58, 1579-1586.

Lee, J.K., Park R.A., Mausel, P.W., Howe, R.C. (1991) 'GIS-related modelling of Impacts of Sea Level Rise on Coastal Areas' GIS/LIS '91 Conference, Atlanta, Georgia. , 356-367.

Leonard, L.A. (1997) 'Controls of Sediment Transport and Deposition in an Incised Mainland Marsh Basin, Southeastern North Carolina' *Wetlands,* 2, 263-274.

Lesser, G.R., Roelvink, J.A., van Kester, J.A.T.M., Stelling, G.S. (2004) 'Development and Validation of a Three-Dimensional Morphological Model' *Coastal Engineering*, 51, 883-915.

Letzch, W.S., Frey, R.W. (1980) 'Deposition and Erosion in a Holocene Salt Marsh, Sapelo Island, Georgia' *Journal of Sedimentary Research,* 50, 529-542.

Leuliette, E.W., Nerem, R.S., Mitchum, G.T. (2004) 'Calibration of TOPEX/Poseidon and Jason altimeter data to construct a continuous record of mean sea level change' *Marine Geodesy,* 27, 79-94.

Liao, M., Jiang, Y., Wang, Y., Gao. W. (2011) 'Sea Level Affecting Marshes Model and Remotely Sensed and Geo-spatial Datasets for a Large Area' *Annals of GIS,* 17:2, 99-104.

Lillycrop, W.J. and Banic, J.R. (1993) 'Advancements in the U.S. Army Corps of Engineers Hydrographic Survey Capabilities: The SHOALS system' *Marine Geodesy,* 15, 177-185.

Lillycrop, W.J., Parson, L.E., Guenther, G.C. (1993) 'Processing LiDAR returns to Extract Water Depth' *Proceedings International Symposium Spectral Sens. Res. November 1992*, Maui, Hawaii.

Lillycrop, W.J., Irish, J.L.M., Parson, L.E. (1997) 'SHOALS System: Three Years of Operation with Airborne Lidar Bathymetry – Experiences, Capability and Technology Advancements' *Sea Technology*, 38, 17-25.

Lillycrop, W.J., Parson, L.E., Estep, L.L., LaRocque, P.E., Guenther, G.C., Reed, M.D., Truitt, C.L. (1994) 'Field Testing of the U.S. Army Corps of Engineers Airborne Lidar Hydrographic Survey System' *Proceedings U.S. Hydrographic Conference '94, The Hydrographic Society Spec.,* 32, 144-151.

Linhoss, A.C., Kiker, G., Shirley, M, Frank, K. (2015) 'Sea-Level Rise, Inundation, and Marsh Migration: Simulating Impacts on Developed Lands and Environmental Systems' *Journal of Coastal Research*, 31, 36-46.

Linhoss, A.C., Kiker, G.A., Aiello-Lammens, M.E., Chu-Agor, M.L., Convertino, M., Munoz-Carpena, R., Fischer, R., Linkov, I. (2013) 'Decision Analysis for Species preservation under Sea-Level Rise' *Ecological Modelling*, 264-272.

List, J. H., Sallenger, A. H., Hansen, M. E., Jaffe, B. E. (1997) 'Accelerated Relative Sea-level Rise and Rapid Coastal Erosion: Testing a Causal Relationship for the Louisiana Barrier Islands' *Marine Geology*, *140*, 347-365.

Lisitzin, E. (1974) 'Sea Level Changes' *Elsevier*, New York.

Lowe, J., and Gregory, J. (2005) 'The Effects of Climate Change on Storm Surges around the United Kingdom' *Phylosophical Transactions of Mathematical, Physical & Engineering Science, 363*, 1313-28.

Lowe, J., Howard, T., Pardaens, A., Tinker, J., Holt, J., Wakelin, S., Milne, G., Leake, J., Wolf, J., Horsburgh, K., Reeder, T., Jenkins, G., Ridely, J., Dye, S., Bradley, S. (2009) *UK Climate Projections science Report: Marine and Coastal Projections.* Met Office, Hadley Centre, Exeter, UK.

Lozano, I., Devoy R.N.J., May, W., Andersen, U. (2004) 'Storminess and Vulnerability along the the Atlantic Coastlines of Europe: Analysis of Storm Records and of a greenhouse gases induced climate scenario' *Marine Ecology 210:* 205-226.

Lyon, J.G and McCarthy, J. (1995) 'Introduction to Wetland and Environmental Applications of GIS' In: Lyon, J.G and McCarthy, J. (eds), *Wetland and Environmental Applications of GIS,* Lewis Publishers, United States of America, 3-8.

Mah, D.Y.S., Putuhena, F.J., Lai, S.H. (2011) 'Modelling the Flood Vulnerability of Deltaic Kuching City, Malaysia' *Natural Hazard*, 58, 865-875.

Mariotti, G. and Fagherazzi, S. (2013) 'Critical Width of Tidal Flats Triggers Marsh Collapse in the Absence of Sea-Level Rise' *Proceedings of the National Academy of Sciences of the United States of America*, v.110, no 14, 5353-5356.

Maxwell, B.A. and Buddemeier, R.W. (2002) 'Coastal Typology Development with Heterogeneous Data Sets' *Regional Environmental Change*, 3, 77-87.

May, V.J. (2003) 'Coastal assemblage GSR sites, Site: North Norfolk Coast (GCR ID: 2038)' Chapter 11 in: May, V.J. and Hansom, J.D. (eds) *Coastal Geomorphology of Great Britain* Geological Conservation Review Series, No.28, Joint Nature Conservation Committee, Peterborough, pp 754.

May, V.J. and Hansom, J.D. (2003) *Coastal Geomorphology of Great Britain* Geological Conservation Review Series, No.28, Joint Nature Conservation Committee, Peterborough, pp 754.

McCaffery, R.J., Thomson, J. (1980) 'A Record of the Accumulation of Sediment and Trace Metals in a Connecticut Salt Marsh' *Advances in Geophysics*, 22, 165-236.

McCave, I.N. (1987) ‘Fine Sediment Sources and Sinks around the East Anglian Coast’ *Journal of the Geological Society*, 144, 149-152.

MCCIP (2011) *Marine climate change impacts Annual Report Card 2010-2011.*

McKee, K.L., Cahoon, D.R., Feller, I.C. (2007) ‘Caribbean Mangroves adjust to Rising Sea Level Through Biotic Controls on Change in Soil Elevation’ *Global Ecology and Biogeography,* Journal Compilation, Blackwell Publishing Ltd.

McLean, R.F., Tsyban, A.; Burkett, A.; Codignotto, J.O.; Forbes, D.L.; Mimura, N.; Beamish, R.J.; Ittekkot, V. (2001) ‘Coastal zones and marine ecosystems’ *In:* McCarthy, J.J., Canziani, O.F., Leary, N.A., Dokken, D.J., and White, K.S. (eds.), *Climate Change 2001: Impacts, Adaptation and Vulnerability*. Cambridge: Cambridge University Press, pp. 343–380.

Mcleod, E., Poulter, B., Hinkel, J., Reyes, E., Salm, R. (2010) ‘Sea-Level Rise Impact Models and Enviroenmental Conservation: A Review of Models and their Applications’ *Ovean and Coastal Management*, 53, 507-517.

Meadowcroft, I.C., Hall, J.W., Lee, E.M., Milheiro-Oliveira, P. (1999) *Coastal Cliff Recession: Development and Application of Prediction Method,* HR Wallingford Report SR549.

Miller, L. and Douglas, B.C. (2004) ‘Mass and volume contributions to twentieth-century global sea level rise’ *Nature*, 428, 406-409.

Milliman, J.D., and Haq, B.U. (1996) ‘Sea-Level Rise and Coastal Subsidence-Towards Meaningful Strategies’ In: Milliman, J.D., and Haq, B.U. (eds.), *Sea-Level Rise and Coastal Subsidence:Causes, Consequences, and Strategies,* Kluwer Academic Publishers, 1-11.

Mitchell, J.F.B., Johns, T.C., Ingram, W.J., Lowe, J.A. (2000) ‘The Effect of Stabilising Atmospheric Carbon Dioxide Concentrations on Global and Regional Climate Change’ *Geophysical Research Letters*, 27, 2997-3100.

Moller, I. (2006) ‘Quantifying Saltmarsh Vegetation and its Effect on Wave Height Dissipation: Results from a UK East Coast Saltmarsh’ *Estuarine, Coastal and Shelf Science*, 69, 337- 351.

Moller, I., Spencer, T., French, J.R., Leggett, G.J., Dixon, M. (1999) ‘Wave Transormation over Salt Marshes: A Field and Numerical Modelling Studyfrom North Norfolk, England’ *Estuary, Coastal and Shelf Science*, 49, 411-426.

Moore, B.D. (1982) ‘Beach Profile Evolution in Response to Changes in Water Level and Wave Height’ *M.S.Thesis,* University of Delaware, Newark, Delaware, 164p.

Morris, J.T., Sundareshwar, P.V., Nietch, C.T., Kjerfve, B., and Cahoon, D.R. (2002) 'Responses of Coastal Wetlands To Rising Sea Level' *Ecology*, *83*(10), 2869-2877.

Morris, R.K.A., Reach, I.S., Duffy, M.J., Collins, T.S., Leafe, R.N. (2004) 'On the Loss of Saltmarshes in South-East England and the Relationship with Nereis Diversicolor' *Journal of Applied Ecology*, 41, 787-791.

Murray, A.B. (2003) 'Constructing the Goals, Strategies, and Predictions Associated with Simplified Numerical Models and detailed Simulations' In: Iverson, R.M. and Wilcock, P.R. (ed) *Prediction in Geomorphology*, AGU Geophys. Monogr. 151-165.

Murray, A.B. (2007) 'Reducing Model Complexity for Explanation and Prediction' *Geomorphology*, 90, 178-191.

Murray, A.B. and Paola, C. (1994) 'A Cellular Model of Braided Rivers' *Nature*, 371, 54-7.

Nairn, R. (1994) 'Royal Australian Navy Laser Airborne Depth Sounder, The First Year of Operations' *International Hydro. Rev., Monaco*, LXXI(1), 109-119.

Nakiboglou, S.M. and Lambeck, K. (1991) 'Secular sea level change' In:Sabanidi, R., Lambeck, K., Boschi, E. (eds) *Isostasy, Sea-Level and mantle Pheology*, Kluwer Academic, Dordrecht, 237-258.

Nakicenovic, N., Alcamo, J., Davis, G., de Vries, B., Fenhann, J., Gaffin, S., Gregory, K., Grubler, A., Jung, T.Y., Kram, T., La Rovere, E.L., Michaelis, L., Mori, S., Morita, T., Pepper, W., Pitcher, H., Price, L., Riahi, K., Roehrl, A., Rogner, H., Sankovski, A., Schlesinger, M., Shukla, P., Smith, S., Swart, R., van Rooijen, S., Victor, N., Dadi, Z. (2000) 'Emission Scenarios' *A Special Report of IPCC Working Group III*, Intergovermental Panel on Climate Change, Cambridge University Press, Cambridge, UK, 599.

National Research Council (NRC) (1987) *Response to Changes in Sea-Level _Engineering Implications*, Marine Board National Research Council, Washington, DC: National Academic Press, 135p.

National Research Council (NRC) (1990) *Managing Coastal Erosion*, Washington, DC: National Academic Press.

Nguyen, H.N., Vu, K.T., Nguyen, X.N. (2007) 'Flooding in Mekong River Delta, Vietnam' *Human Development Report 2007/2008, Fighting Climate Change: Human Solidarity in a Divided World*, Human Development Report Office Occasional Paper.

Nicholls, R.J. (1995) 'Coastal Megacities and Climate Change' *GeoJournal*, 373, 369-379.

Nicholls, R.J. (2002) 'Rising Sea Levels: Potential Impacts and Responses' In: Hester, R. and Harrison, R.M. (eds) *Global Environmental Change* Issues in Environmental Science and Technology, Royal Society of Chemistry, Cambridge, 17, 83-107.

Nicholls, R.J. (2003) *Case Study on Sea-Level Rise Impacts* Workshop on the Benefits of Climate Policy: Improving Information for Policy Makers, Organisation for Economic Co-operation and Development.

Nicholls, R.J. (2004) 'Coastal Flooding and Wetland Loss in the 21st century: Changes under the SRES Climate and Socio-Economic Scenarios' *Global Environmental Change*, 14, 69-86.

Nicholls, R.J., Leatherman, S.P. (1996) 'Adapting to Sea-Level Rise: Relative Sea Level Trends to 2100 for the USA' *Coastal Management*, 24, 301-324.

Nicholls, R.J., Birkemeier, W.A., Lee, G. (1998) 'Evaluation of Depth of Closure Using Data from Duck, NC, USA' *Marine Geology*, 148, 179-201.

Nicholls, R.J., Hoozemans, F.M.J., Marchand, M. (1999) 'Increasing Flood Risk and Wetland Losses due to Global Sea-Level Rise: Regional and Global Analyses' *Global Environmental Change*, 9, S69-S87.

Nicholls, R.J., Wong, P.P., Burkett, V.R., Codignotto, J.O., Hay, J.E., McLean, R.F., Ragoonaden, S., Woodroffe, C.D. (2007) 'Coastal Systems and Low-lying Areas' In: Parry, M.L., Canzianni, O.F., Palutikof, J.P., Linden, P.J., Hanson, C.E. (eds) *Climate Change 2007: Impacts, Adaptation and Vulnerability*, Cambridge University Press, Cambridge/New York, 315-356.

Nicholls, R.J., Bradbury, A., Burningham, H., Dix, J., Ellis, M., French, J., Hall, J.W., Karunarathna, H.U., Lawn, J., Pan, S., Reeve, D.E., Rogers, B., Souza, A., Stansby, P.K., Sutherland, J., Tarrant, O., Walkden, M., Whitehouse, R. (2012) 'iCOASST – Integrating Coastal Sediment Systems', In: Lynett, P., McKee Smith, J. (eds) *Proceedings of the 33rd International Conference on Coastal Engineering 2012*, Reston, US, Coastal Engineering Research Council, Sediment, 100-15pp.

Nicholls, R.J., French, J.R., Burnhinham, H., Van Maanen, B., Payo, A., Sutherland, J., Walkden, M., Thornhill, G., Brown, J., Luxford, F., Simm, J., Reeve, D.E., Hall, J.W., Souza, A., Stansby, P.K., Amoudry, L.O., Rogers, B.D., Ellis, M., Whitehouse, R., Horrillo-Caraballo, J.M., Karunarathna, H., Pan, S., Plater, A.,

Dix, J., Barnes, J. and Heron, E. (2015) 'Improving decadal coastal geomorphic predictions: an overview of the iCOASST project' *Proceedings Coastal Sediments 2015*, San Diego, USA.

Nicholson, J., Broken, I., Roelvink, J.A., Price, D., Tanguy, J.M., Moreno, L. (1997) 'Intercomparison of Coastal Area Morphodynamic Models' *Coastal Engineering*, 31, 97-123.

Nielsen, N. (1935) 'Eine Methode zur Exakten Sedimentations-messung' *Meddelelser fra Skalling Laboratoriet*, 1.

Nielsen, P. (1992) *Coastal Bottom Boundary Layers and Sediment Transport,* World Scientific, Singapore, 324.

NOAA (2000) *Tidal Datums and Their Applications* NOAA Special Publication NOS CO-OPS 1.

Nordstrom, K.F. and Jackson, N.L. (2012) 'Physical Processes and Landforms on Beaches in Short Fetch ENcironments in Estuaries, Small Lakes and Reservoirs; A Review' *Earth-Science Reviews*, 11, 232-247.

Nunn, P.D. and Mimura, N. (1997) 'Vulnerability of South Pacific Island Nations to Sea-Level Rise' *Journal of Coastal Research Special Issue*, 24: 133-51.

NWF (2006) *An Unfavourable Tide – Global Warming, Coastal Habitats and Sportfishing in Florida*, national Wildlife Federation, Florida, Wildlife Federation, June 2006.

Nyman, J.A. and Delaune, R.D. (1995) 'Organic-Matter Fluxes and Marshes Stability in a Rapidly Submerging Estuarine Marsh' *Estuaries*, 18, 207-218.

Nyman, J.A., Crozier, C.R., Delaune, R.D. (1995) 'Roles and Patterns of Hurricane Sedimentation in an Estuarine Marsh Landscape' *Estuarine Coastal and Shelf Science*, 40, 665-679.

O'Brien, D.J., Whitehouse, R.J.S., Cramp, A. (2000) 'The Cyclic Development of a Macrotidal Mudflat on Varying Timescales', *Continental Shelf Research*, 20, 1593-1619.

Olson, C.E., Jr. (2008) 'Is 80% Accuracy Good Enough?' *Conference Proceedings*, Pecora 17, The Future of Land Imaging… Going Operational, November 18-20, 2008, Denver Colorado.

Orson, R., Panageotou, W., Leatherman, S.P. (1985) 'Response of Tidal Salt Marshes to Rising Sea Levels Along the U.S. Atlantic and Gulf Coasts' *Journal Coastal Research*, 1, 29-37.

Park, R.A. (1991) *Global Climate Change and Greenhouse Emissions*, Washington, DC: Subcommittee on Health and Environment, US House of Representatives, 171-182.

Park, R.A., Armentano, T.V., Cloonan, C.L. (1986) 'Predicting the Effects of Sea Level Rise on Coastal Wetlands' In: Titus, J.G. (ed) *Effects of Changes in Stratospheric Ozone and Global Climate and Sea Level Rise*, U.S. Environmental Protection Agency, Washington, D.C., 129-152.

Park, R.A., Lee, J.K., Canning, D. (1993) 'Potential Effects of Sea Level Rise on Puget Sound Wetlands' *Ceocarto International* , 8, 99-110.

Park, R.A., Cough, J.S., Jones, R., Galbraith, H. (2003) 'Modelling the Impacts of Sea-Level Rise' *Proceedings of the 13th Bienial Coastal Zone Conference*, July 13-17, 2003.

Park, R.A., Lee, J.K., Mausel., P.W., Howe, R.C. (1991) 'Using Remote Sensing for Modelling the Impacts of sea Level Rise'*World Resource Review*, 3, 184-205.

Park, R.A., Trehan, M.S., Mausel, P.W., Howe, R.C. (1989) 'The Effects of Sea Level Rise on U.S. Coastal Wetlands' In: Smith, J.B. and Tirpak, D.A. (eds) *The Potential Effects of Global Climate Change on the United States, Appendix B – Sea Level Rise*, U.S. Environmental Protection Agency, Washington, D.C.

Parkison, R.W., Delaune, R.D., White, G.R. (1994) 'Historical and Geological Mangrove Peat Accretion Rates and Their Use in Sea-Level Rise Forecasting Models', *Journal Coastal Research*, 10.

Pascual, A., and Rodriguez-Lazaro, J. (2006) 'Marsh Development and Sea Level Changes in the Gernika Estuary (Southern Bay of Biscay): Foraminifers as Tidal Indicators' *Scientia Marina*, 70S1, 101-117.

Paul, A. (1993) *Saltmarsh Ecology*, Cambridge University Press.

Peizen, Z., Molnar, P., Downs, W.R. (2001) 'Increased Sedimentation Rates and Grain Sizes 2-4 Myr ago due to Influence of Climate Change on Erosion Rates' *Nature*, 410, 891-897.

Peltier, W.R. and Tushingham, A.M. (1989) 'Global Sea Level Rise and the greenhouse Effect: Might they be Connected?' *Science*, 244, 806-810.

Peltier, W.R. and Tushingham, A.M. (1991) 'Influence of Glacial Isostatic Adjustment on Tide-gauge Measurements of Secular Sea *Level* Change' *Journal of Geophysical Research*, 96, 6779-6796.

Pethick, J. (1980) ‘Salt-marsh Initiation during the Holocene Transgression: The Example of the North Norfolk Marshes, England’ *Journal of Biogeography,* 7, 1-9.

Pethick, J.S. (1981) ‘Long-term Accretion Rates on Tidal Salt Marshes’ *Journal of Sedimentary Petrology, 6*1, 571-577.

Pethick, J.S. (1992) ‘Saltmarsh Geomorphology’ In: Allen, J.R.L. and Pye, K. (eds) *Saltmarshes: Morphodynamics Conservation and Engineering Significance*, Cambridge University Press, Cambridge, 41-62.

Pethick, J.S. (2001) ‘Coastal Management and Sea-Level Rise’ *Catena*, 42, 307-322.

Pethick, J.S. (2002) ‘Estuarine and Tidal Wetland Restoration in the United Kingdom: Policy versus Practice’ *Restoration Ecology*, 10, 431-437.

Pethick, J.S., Legget, D. (1993) ‘The Morphology of the Anglian Coast’ In: Hillen, R., Verhagen, H.D. (eds) *Coastlines of the Southern North Sea*, Americal Society of Civil Engineers, New York, 52-64.

Pethick, J.S., Reed, D. (1987) ‘Coastal Protection in an Area of Saltmarsh Erosion’ In: Krauss, N.C. (ed) *Proceedings Coast Sediments ’87*, New York, Americal Society of Civil Engineers, 1094-1104.

Phillips, J.D. (1986) ‘Coastal Submergence and Marsh Fringe Erosion’ *Journal of Coastal Research, 2, 427-436.*

Phillips, J.D. (2014) ‘State Transitions in Geomorphic Responses to Environmental Change’, *Geomorphology*, 204, 208-216.

Pilkey, O. H., and Cooper, J. A. G. (2004) ‘Society and sea level rise’ *Science (New York, N.Y.), 303*(5665), 1781-2.

Pilkey, O.H. and Davis, T.W. (1987) ‘An Analysis of Coastal Recession Models: North Carolina Coast’ In: Nummedal, D., Pilkey, O.H., Howard, J. (eds) *Sea Level Fluctuations and Coastal Evolution*. Tuscon, Arizona: SEP.M. Special Publication 41, 59-68.

Pilkey, O.H., Young, R.S., Riggs, S.R., Sam Smith, A.W., Wu, H., Pilkey, W.D. (1993) ‘The Concept of Shoreface Profile of Equilibrium: ACritical Review’ *Journal of Coastal Research*, 9, 255-278.

Pilkey, O.H., Young, R.S., Bush, D.M. (2000) ‘Comment on sea level rise by Leatherman et al.’ *EOS*, 81, 436.

Pirazzoli, P.A. (1989) ‘Present and Near-future Global Sea-Level Changes’ *Palaeogeography, Palaeoclimatology, Palaeoecology (Global and Planetary Change Section)*, 75, 241-58.

Planning Policy Statement 25 (PPS25) (2006) *Developement and Flood Risk.*

Polli, S. (1952) 'Gli Attualli Movimenti Verticali Delle Coste Continentali' *Ann. Geofis.*, 5, 597-602.

Pont, D., Day, J., Hensel, P., Franquet, E., Torre, F., Rioual, P., Ibanez, C., Coulet, E. (2002) 'Response Scenarios for the Deltaic Plain of the Rhone in the face of an Acceleration in the Rate of Sea Level Rise, with a Special Attention for Salicornia-type Environments' *Estuaries*, 25, 337-358.

Pontee, N. (2013) 'Defining Coastal Squeeze: A Discussion' *Ocean and Coastal Management*, 84,204 - 207.

Poulos, E.S., Ghionis, G., Maroukian, H. (2009) 'The Consequences of a Future Eustatic Sea-Level Rise on the Deltaic Coasts of Inner Thermaikos Gulf (Aegan Sea) and Kyparissiakos Gulf (Ionian Sea), Greece' *Geomorphology*, 17, 18-24.

PSMSL (2012) *Permanent Service for Mea Sea Level, http://www.psmsl.org.*

Pugh, D.T. (1987) *Tides, Surges and Mean Sea-Level,* John Wiley and Sons Ltd

Pye, K. (2000) 'Saltmarsh Erosion in Southeast England: Mechanisms, Causes and Implications' In: Sherwood, B.R., Gardiner, B.G., Harris, T. *British Saltmarshes*, The Linnean Society of London, London, UK, 360-396.

Pye, K. and Blott, S.J. (2008) 'Past and Future Shoreline Change in Alnmouth Bay' *Internal Research Report IR957, Kenneth Pye Associates Ltd,* Northumberland, UK.

Pye, K. and Blott, S.J. (2008a) *Time, Space and Causality in Coastal Geomorphological Change,* Kenneth Pye Research Associates Ltd, Internal Research Report, No. 905.

Pye, K. and Blott, S. (2008b) *Blyth Estuary Sedimentation Study, Draft Version 1.0*, A Report to Suffolk County Council, Suffolk Coastal District Council, Waveney District Council, Southwold Town Council, Blyth Estuary Group, The Environment Agency.

Pye, K. and French, P.W. (1993) 'Erosion and Accretion Processes on British Saltmarshes' *Database of British Saltmarshes*, Cambridge Environmental Research Consultants Ltd, London, UK.

Rahmstorf, S. (2007) 'A Semi-Empirical Approach to Projecting Future Sea-Level Rise' *Science*,315, 368-370.

Rahmstorf, S. (2010) 'A New Review on Sea Level Rise' *Nature Reports Climate Change.* doi:10.1038/climate.2010.29.

Ranasinghe, R. and Stive, M.J.F. (2009) 'Rising Seas and Retreating Coastlines' *Climatic Change,* 97, 465-468.

Raper, S.C.B, Wigley, T.M.L & Warrick, R.A. (1996) 'Global Sea-Level Rise:Past and Future'. In: Milliman, J.D. and Haq, B.U. (eds.) *Sea-Level Rise and Coastal Subsidence:Causes, Consequences, and Strategies,* Kluwer Academic Publishers, 11-45.

Redfield, A.C. (1972) 'Development of a New England Salt Marsh' *Ecological Monographs, 42*(2), 201-237.

Reed, D. (1988) 'Sediment Dynamics and Deposition in a Retreating Coastal Salt Marsh' *Estuarine, Coastal and Shelf Science,* 26, 67-79.

Reed, D. (1990) 'The Impact of Sea Level Rise on Coastal Salt Marshes' *Progress in Physical Geography 14*, 465-481.

Reed, D. (1995) 'The Response of Coastal Marshes to Sea-Level Rise: Survival or Sumbergence?' *Earth Surface Process. Landforms,* 20, 39-48.

Reed, D., and Foote, A. (1997) 'Effect of Hydrologic Management on Marsh Surface Sediment Deposition in Coastal Luisiana' *Estuaries, 20*(2), 301-311.

Reed, D., Davidson-Arnott, R., Perillo, G.M.E. (2009) 'Estuaries, Coastal marshes, Tidal Flats and Coastal Dunes' In: Slaymaker, O., Spencer, T., Embleton-Hamann, C. (eds) *Geomorphology and Global Environmental Change*, Cammbridge University Press, 130-157.

Reed, D.J., Spencer, T., Murray, A.L., French, J.R., Leonard, L. (1999) 'Marsh Surface Sediment Deposition and the Role of Tidal Creeks: Implications for Created and Managed Coastal Marshes' *Journal of Coastal Conservation*, 5, 81-90.

Restrepo, J.D. (2012) 'Assessing the Effect of Sea-level Change and Human Activities on a Major Delta on the Pacific Coast of Northern South America: The Patia River' *Geomorphology 151-152*, 207-223.

RESPONSE, (2006) 'Coastal Processes and Climate Change Predictions in the Coastal Study Areas' *LIFE Environment Project 2003-2006, LIFE 03 ENV/UK/000611*

Reyes, E. (2009) 'Wetland Landscape Spatial Models' In: Perillo, G.M.E., Wolanski, E., Cahoon, D.R., Brinson, M.M. (ed.) *Coastal Wetlands An Integrated Ecosystem Approach,885-902.*

Richards, K.S. and Lorriman, N.R. (1987) 'Basal Erosion and Mass Movement' In: Anderson, M.G. and Richards, K.S. (eds) *Slope Stability*, New York, 331-357.

Roelvnik, J.A. and Broker, I. (1993) 'Cross-Shore Profile Models' *Coastal Engineering*, 21, 163-191.

Roelvnik, J.A., Reniers, A., van Dongeren, A.R., van Thiel de Vries, J.S.M., McCall, R.. Lescinski, J. (2009) 'Modelling Storm Impacts on Beaches, Dunes and Barrier Islands' *Coastal Engineering*, 56, 1133-1152.

Rodríguez, I., Montoya, I., Sánchez, M., Carreño, F. (2009) 'Geographic Information Systems applied to Integrated Coastal Zone Management' *Geomorphology, 107*, 100-105.

Rosen, P.S. (1978) 'A Regional Test of the Bruun Rule on Shoreline Erosion' *Marine Geology*, 26, M7-M16.

Rossington, S.K., Nicholls, R.J., Knaapen, M.A.F., Wang, Z.B. (2007) 'Morphological Behaviour of UK Estuaries Under Conditions of Accelerating Sea Level Rise' In: Dohmen-Janssen and Hutscher (eds) *River, Coastal and Estuarine Morphodynamics:RCEM 200.*

Roy, P. and Connell, J. (1991) 'Climate Change and the Future of Atoll States' *Journal of Coastal Research*, 7, 1057-1096.

Sallenger, A.H., Morton, R., Fletcher, C., Thieler, R., Howd , P. (2000) 'Comment on Sea Level Rise by Leatherman et al.', *EOS*, 81, 436.

Scavia, D., Field, J.C., Boesch, D.F., Buddemeier, R.W., Burkett, V., Cayan, D.R., Fogarty, M., Harwell, M.A., Howarth, R.W., Mason, C., Reed, D.J., Royer, T.C., Sallenger, A.H., Titus, J.G. (2002) 'Climate Change Impacts on U.S. Coastal and Marine Ecosystems' *Estuaries*, 2, 149-164.

Schuerch, M., Rapaglia, J., Liebetrau, V., Vafeidis, A., Reise, K. (2012) 'Salt Marsh Accretion and Storm Tide Variation: An Example from a Barrier Island in the North Sea', *Estuaries and Coasts*, 35, 486-500.

Schwartz, M.L. (1965) 'Laboratory Study of Sea Level Rise as a Cause of Shore Erosion' *Journal of Geology*, 73, 528-534.

Schwartz, M.L. (1967) 'The Bruun Theory of Sea Level Rise as a Cause of Shore Erosion' *Journal of Geology*, 75, 76-92.

Schwartz, M.L. (1982) *The Encyclopedia of Beaches and Coastal Environments*. Stroudsburg, Hutehinson Ross.

Schwartz, M.L. (1987) 'The Bruun Rule – Twenty Years Later' *Journal of Coastal Research*,3, ii-iv.

Schwimmer, R.A. (2001) 'Rates and Processes of Marsh Shoreline Erosion in Rehoboth Bay, Delaware, U.S.A.' *Journal of Coastal Research*, 17, 672 – 683.

Schwimmer, R.A., Pizzuto, J.E. (2000) 'A Model for the Evolution of Marsh Shorelines' *Journal of Sedimentary Research*, 70, 1026-1035.

SCOPAC (2003) *SCOPAC Sediment Transport Study North West Isle of Wight (Needles to Old Castle Point).*

SCOR Working Group 89 (1991) 'The Response of Beaches to Sea Level changes: A Review of Predictive Models' *Journal of Coastal research, 7,* 895-921.

Scott, D.B. and Greenberg, D.A (1983) 'Relative Sea Level Rise and Tidal Development in the Fundy Tidal Systems' *Canadian Journal of Earth Sciences,* 20, 1554-1564.

Scott, M.J., Csuti, B., Jacobi, J.D., Estes, J.E. (1987) 'Species Richness. A Geographic Approach to Protecting Future Biological Diversity', *BioScience,* 37, 782 – 788.

Scott, T.R. and Mason, D.C. (2007) 'Data assimilation for a coastal area morphodynamic model: Morecambe Bay' *Coastal Engineering,* 54, 91-109.

Selivanov, A.O. (1996) 'Morphological Changes on Russian Coasts under Rapid Sea-Level Changes: Examples from the Holocene History and Implications for the Future' *Journal of Coastal Research,* 12, 823-830.

Sestini, G. (1992) 'Implications of Climatic Changes for the Po Delta and Venice Lagoon' In:Jeftic, L., Milliman, J., Sestini, G. (1992) *Climatic Change and the Mediterranean,* Edward Arnmold, London.

Setter, C. and Willis, R.J. (1994) 'LADS – From Development to Hydrographic Operations' *Proceedings U.S. Hydrographic Conference 1994, The Hydrographic Society Spec.,* 32, 134-139.

Shaw, J., Ceman, J. (1999) 'Salt Marsh Aggradation in Response to Late-Holocene Sea-Level Rise at Amberst Point, Nova Scotia, Canada' *The Holocene*, 9, 439-51.

Shellenbarger Jones, A., Bosch, C, Strange, E. (2009) '*Vulnerable Species: The Effects of Sea-Level Rise on Coatsal Habitats' In:* J.G. Titus, K.E.Anderson, D.R.Cahoon, D.B.Gesch, S.K.Gill, B.T. Gutierrez, E.R.Thieler, and S.J. Williams (ed.) *Coastal Sensitivity to Sea-Level Rise:A Focus on the Mid-Atlantic Region.* A report by the U.S.Climate Change Science Programme and the Subcommittee on Global Change Research, U.S. Environmentan Protection Agency, Washington DC, 1-8.

Shepherd, A. and Wingham, D. (2007) 'Recent Sea-Level Contributions of the Antarctic and Greenland Ice Sheets', *Science,* 315, 1529-1532.

Shennan, I. (1989) 'Holocene Crustal Movements and Sea Level Changes in Great Britain' *Journal of Quaternary Science,* 4, 77-89.

Shennan, I. (1993) 'Sea-Level Changes and the Threat of Coastal Inundation' *The Georaphical Journal*, *159*(2), 148-156

Shennan, I. and Woodworth, P. (1992) 'A Comparison of late Holocene and twentieth-century Sea-Level Trends from the UK and North Sea Region' *Geophysical Journal International,* 109, 96-105.

Sherif, M.M. and Singh, V.P. (1999) 'Effect of Climate Change on Sea Water Intrusion in Coastal Aquifers' *Hydrological Processes,* 13, 1277-1287.

Sherman, R.E., Fahey, T.J., Battles, J.J. (2000) 'Small-scale Distirbance and Regeneration Dynamis in a Neotropical Mangrove Forest' *Journal of Ecology,* 88, 165-178.

Silvestri, S., Defina, A., Marani, M. (2005) 'Tidal Regime, Salinity and Salt Marsh Plant Zonation', *Estuarine, Coastal and Shelf Science,* 62, 119-130.

Simas, T., Nunes, J., and Ferreira, J. (2001) 'Effects of Global Climate Change on Coastal Salt Marshes' *Ecological Modelling, 139,* 1-15.

Sklar, F.H., Costanza, R., Day, Jr., J.W. (1985) 'Dynamic Spatial Simulation Modeling of Coastal Wetland Habitat Succession' *Ecological Modelling, 29, 261-281.*

Sklar, F.H., White, M.L., Costanza, R. (1989) 'The Coastal Ecological Landscape Spatial Simulation (CELSS) Model: Structure and Results for the Atchafalaya/Terrebonne Study Area' *NWRC open file report,* US Fish and Wildlife Service, Washington, DC.

Sklar, F.H., Gopu, K.K., Maxwell, T., Costanza, R. (1994) 'Spatially Explicit and Implicit Dynamic Simulations of Wetland Processes' In: Mitsch, W.J. (ed) *Global Wetlands: Old World and New*, Amsterdam, Elsevier, 537-54.

Slaymaker, O., Spancer, T., Dadson, S. (2009) 'Landscape and landscape-scale Processes as the Unfilled Niche in the Global Environmental Change Debate:An Introduction' In: Slaymaker, O., Spencer, T., Embleton-Hamann, C. (eds) *Geomorphology and Global Environmental Change*, Cammbridge University Press, 1-36.

Smart, G.M., Bind, J., Duncan, M.J. (2009) 'River Bathymatry from Vonventional LiDAR using Water Surface Returns' *18th World IMACS/MODSIM Congrss, Caims, Australia, 13-17 July 2009.*

SMP2 (2010) *North Norfolk SMP2, Appendix C – Baseline Processes.*

SMP7 (2010) *The Suffolk SMP, First Review of Shoreline Management Plan SMP7 (previously Sub-Cell 3C), Lowestoft Ness to Felixstowe Landguard Point – Appendix I: Estuaries Assessment.*

Snoussi, M., Ouchni, T, Khouakhi, A., Niang Diop, I. (2009) 'Impacts of Sea-level Rise on the Moroccan Coastal Zone; Quantifying Coastal Erosion and Flooding in the Tangier Bay' *Geomorphology*, 107, 32-40.

Spencer, T., Brooks, S.M., Moller, I., Evans, B.R. (2014) 'Where Local Matters; Impacts of a Major North Sea Storm Surge', *Eos, Transactions American Geophysical Union*, 95, 30, 269-270.

Stanley, D.J. (1988) 'Subsidence in the Northeastern Nile Delta: Rapid Rates, Possible Causes, and Consequences' *Science*, 240, 497-500.

Steers, J.A. (1946) 'Twelve Years' Measurment of Accretion on Norfolk Salt marshes' *Geological Magazine,* 85, 163 – 166.

Steer, J.A., Stoddart, D.R., Bayliss-Smith, T.P., Spencer, T., Durbidge, P.M. (1979) 'The Storm Surge of 11 January 1978 on the East Coast of England', *The Geographical Journal*, 145, 2, 192-205.

Steinvall, O., Koppari, K., Karlsson, U. (1994) 'Airborne Laser Depth Sounding: System Aspects and Performance' *Proceedings SPIE Ocean Optics XII,* 2258, 392-412.

Stevenson, J., Ward, L., & Kearny, M. (1986) 'Vertical Accretion in Marshes with Varying Rates of Sea-Level Rise' In: Wolfe, D.A. (ed.) *Estuarine Variability*, Orlando:Academic Press, 241-259.

Stive, M.J.F. (2004) 'How Important is Global Warming for Coastal Erosion?' *Climatic Change*, 64, 27-39.

Stive, M.J.F. and Wang, Z.B. (2003) 'Morphodynamic modelling of tidal basins and coastal inlets. In: Lakhan V.C (ed.) *Advances in coastal modeling, Elsevier Oceanography Series*, 67, 367-392. Amsterdam:Elsevier.

Stive, M.J.F., Roelvink, D.J.A., de Vriend, H.J. (1991) 'Large-Scale Coastal evolution Concept' *Proceedings of the 22nd International Conference on Coastal Engineering* Delft, American Society of Civil Engineers, New York, 1962-1974.

Stive, M.J.F., Cowell, P.J., Nicholls, R.J. (2009) 'Beaches, cliffs and deltas'. In: Slaymaker, O., Spencer, T., Embleton-Hamann, C. (eds) *Geomorphology and Global Environmental Change*, Cammbridge University Press, 158-179.

Stive, M.J.F., Capobianco, M., Wang, Z.B., Ruol, P., Buijsman, M.C. (1998) 'Morphodynamics of a Tidal Lagoon and the Adjacent Coast' In: Dronkers, J. and Scheffers, M. (eds) *Physics of Estuaries and Coastal Seas*, Balkema, Rotterdam, Netherlands, 397-407.

Stoddart, D.R., Reed, D.J., French, J.R. (1989) 'Understanding Salt Marsh Accretion, Scolt Head Island, Norfolk, England' *Estuaries*, 12, 228-236.

Storch, H., and Woth, K. (2008) 'Storm surges: Perspectives and Options' *Sustainability Science, 3*, 33-43.

Stumpf, R.P. (1983) 'The Process of Sedimentation on the Surface of a Salt Marsh' *Estuarine, Coastal and Shelf Science*, 17, 494-508.

Sunamura, T. (1988) 'Projection of Future Coastal Cliff Recession Under Sea Level Rise Induced by the Greenhouse Effect: Nii-Jima Island, Japan' *Transactions, Japanese Geomorphological Union*, 9, 17-33.

Sutherland, J., Walstra, D.J.R., Chester, T.J., van Rijin, L.C., Southgate, H.N. (2004) 'Evaluation of Coastal Area Modelling Systmes at an Estuary Mouth' *Coastal Engineering*, 51, 119-142.

Sylvitski, J., Harvey, N., Wolanski, E., Burnett, W., Perillo, G., and Gornits, V. (2005) 'Dynamics of the Coastal zone' In: C. Crossland, H. Kremer, H. Lindeboom, J. Marshall Crossland, and M. Le Tissier (ed.) *Coastal Fluxes in the Anthropocene,* 40-94.

Taylor, J.A., Murdock, A.P., Pontee, N.I. (2004) 'A Macroscale Analysis of Coastal Steepening around the Coast of England and Wales' *Geographical Journal*, 170, 179-188.

Temmerman, S., Govers, G., Meire, P., Wartel, S. (2003) 'Modelling Long-term Marsh Growth under Changing Tidal Conditions and Suspended Sediment Concentrations, Scheldt Estuary, Belgium, *Marine Geology*, 193, 151-169.

Thieler, E.R., Himmelstoss, E.A., Zichichi, J.L., Ergul, Ayhan (2009) *Digital Shoreline Analysis System (DSAS) version 4.0 – An ArcGIS Extension for Calculating Shoreline Change*, U.S. Geological Survey Open-File report 2008-1278.

Thieler, E.R., Brill, A.L., Cleary, W.J., Hobbs III, C.H., Gammisch, R.A. (1995) 'Geology of the Wrightsville Beach, North Carolina Shoreface: Implications for the Concept of the Shoreface Profile of Equilibrium' *Marine Geology*, 126, 271-287.

Thieler, E.R., Pilkey, O.H., Young, R.S., Bush, D.M., Chai, F. (2000) 'The Use of Mathematical Models to Predict Beach Behavior for U.S. Coastal Engineering: A Critical Review' *Journal of Coastal Research, 16*(1), 48-70.

Thomas, R.H. (1986) 'Future Sea Level Rise and its Early Detection by Satellite Remote Sensing' In: Titus, J.G. (Ed) *Effects of Changing Stratospheric Ozone*

and Global Climate, Volume 4: Sea Level Rise, 19- 36, Washington, U.S., Environmental Protection Agency.

Thornhill, G., French, J.R., and Burningham, H. (2015) 'ESTEEM – A new 'Hybrid Complexity' Model for Simulating Estuary Morphological Change at Decadal to Centennial Scales' *Proceedings Coastal Sediments 2015, San Diego, USA*.

Tian, B., Zhang, L., Wang, X., Zhou, Y., Zhang, W. (2010) 'Forecasting the Effects of Sea-Level Rise at Chongming Dongtan Nature Reserve in the Yangtze Delta, Shangai, China' *Ecological Engineering* 36, 1383-1388.

Titus, J.G. (1986) 'Greenhouse Effect, Sea Level Rise and Coastal Zone Management' *Coastal Zone Management*, 14, 147-171.

Titus, J.G. (1990) 'Greenhouse Effect, Sea Level Rise and Land Use' *Land Use Policy*, 7, 138-153.

Titus J.G. (1991) 'Greenhouse Effect and Coastal Wetland Policy: How Americans could abandon an Area the Size of Massachusetts at Minimum Cost. *Environmental Management* , 15, 39-58.

Titus J.G. (2002) 'Does sea-level rise matter to transportation along the Atlantic Coast?*' Potential Impacts of Climate Change on Transportation*., U.S. Department of Transportation, Rep.Washington,DC.

Titus, J.G. and Narrayanan, V. (1996) 'The Risk of Sea Level Rise: Delphic Monte-Carlo Analysis in Which twenty Researchers Specify Subjective Probability Distributions for Model Coefficients within their Respective Areas of Expertise. *Climate Change*, 33, 151-212.

Titus, J.G., Park, R.A., Leatherman, S.P., Weggel, J.R., Greene, M.S., Mausel, P.W., Brown, S., Gaunt, G., Trehan, M., Yohe, G. (1991) 'Greenhouse Effect and Sea Level Rise: The Cost of Holding Back the Sea' *Coastal Management*, 19, 171-204.

Tooley, M.J. and Jelgersma, S. (1992) *Impacts of Sea-Level Rise on European Coastal Lowlands*, Oxford, Blackwell.

Trenhaile, A.S. (2000) 'Modelling the Development of Wave-cut Shore Platforms' *Marine Geology*, 166, 163-178.

Trupin, A. and Wahr, J. (1990) 'Spectroscopic analysis of global tide-gauge sea level data', *Geophysical Journal International* , 100, 441-453.

Twilley, R.R., Rivera-Monroy, V.H., Chen, R., Botero, L. (1999) 'Adapting an Ecological Mangrove Model to Simulate Trajectories in Restoration Ecology' *Marine Pollution Bulletin*, 37, 404-419.

UKCP (2009) http://www.ukcip.org.uk/resources/ukcp09-sea-level-change/

United Kingdom Marine Monitoring and Assessment Strategy (UKMMAS) (2010) *Charting Progress 2 Feeder Report: Ocean Processes* (ed Huthnance, J.). Department fro Environment Food and Rural Affairs on Behalf of UKMMAS, 279pp.

Unal, Y.S., Ghil, M. (1995) 'Interannual and Interdecadal oscillation patterns in Sea Level', *Climate Dynamics*, 11, 255-278.

U.S. Fish and Wildlife Service (1974) *The National Wetlands Inventory (NWI)* http://www.fws.gov/wetlands/NWI/index.html

USAGE (1984) *Shore Protection Manual*, Vicksburg, Mississipi: US Army Corps of Engineers, 2 vols.

Vafeidis, A.T., Nicholls, R.J., McFadden L., Tol, R.S.J., Hinkel, J, Spencer, T., Grashoff, P.S., Boot, G., Klein, R.J.T. (2008) ' A New Global Ciastal Database for Impact and Vulnerability Analysis to Sea-Level Rise' *Journal of Coastal Research*, 24, 917-924.

Valentin, H. (1952) 'Die Kusten der Erde' *Petermans Geographische Mitteilungen, Erganzungsband*, 246.

Van der Wal, D., and Pye, K. (2004) 'Patterns, Rates and Possible Causes of Saltmarsh Erosion in the Greater Thames Area (UK)'*Geomorphology*, 61, 373-391.

Van Dongeren, A.R., de Vriend, H.J. (1994) 'A Model of Morphological Behaviout of Tidal Basins' *Coastal Engineering*, 22, 287-310.

Van Goor, M.A., Zitman, T.J., Wang, Z.B., Stive, M.J.F. (2003) 'Impact of Sea-Level Rise on the Morphological Equilibrium State of Tidal Inlets' *Marine Geology*, 202, 211-227.

Van Koningsveld, M., Davidson, M.A., and Huntley, D.A. (2005) 'Matching Science with Coastal Management Needs: The Search for Appropriate Coastal State Indicators' *Journal of Coastal Research*, 21 (3), 399-411.

Vanderzee, M.P. (1988) 'Changes in Saltmars Vegetation as an Early Indicator of Sea-Level Rise' In: Pearman, G.I. (ed) *Greenhouse: Planning for Climate Change*, Commonwealth Scientific and Industrial Research Organisation, 147-160.

Van Rijn, L.C., Walstra, D.J.R., Grasmeijer, B., Sutherland, J., Pan, S., Sierra, J.P. (2003) 'The Predictability of Cross-Shore bed Evolution of Sandy Beaches at the time scale of Storms and Seasons using Process-based Profile Models' *Coastal Engineering*, 47, 295-327.

Vellinga, P., Leatherman, S.P. (1989) 'Sea Level Rise, Consequences and Policies' *Climatic Change*, 15, 175-189.

Vermeer, M., and Rahmstorf, R. (2009) 'Global Sea Level Linked to Global Temperature', *Proceedings of the National Academy of Sciences of the United States of America, 106,* 21527-32.

Villaret, C., Huybrechts, N., Davies, A.G. (2012) 'A Large Scale Morphodynamic Process-Based Model of the Gironde Estuary' Jubilee Conference Proceedings, NCK-Days 2012, doi: 10.3990/2.172.

Wahls, T, Haigh, I.D., Woodworth, P.L., Albrecht, F., Dillingh, D., Jensen, J., Nicholls, R.J., Weisse, R., Woppelmann, G. (2013) 'Observed Mean Sea Level Changes Around the North Sea Coastline from 1800 to Present' *Earth Science Reviews*, 124, 51-67.

Wahr, J.M. and Trupin, A.S. (1990) 'New Computation of Global Sea Level Rise from 1990 tide-gauge data' *EOS*, 71,1267.

Walkden, M., and Dickson, M. (2008) 'Equilibrium Erosion of Soft Rock Shores with a Shallow or Absent Beach under Increased Sea Level Rise' *Marine Geology*, -251, 75-84.

Walkden, M.J.A. and Hall, J.W. (2005) 'A Predictive Mesoscale Model of the Erosion and profile Development of Soft Rock Shores'*Coastal Engineering*, 52, 535-563.

Walkden, M.J.A. and Hall, J.W. (2011) 'A Mesoscale Predictive Model of the Erosion and Management of a Soft-rock Coast' *Journal of Coastal Research*, 27, 529-543.

Walker, H.J., Coleman, J.M., Roberts, H.H., Tye, R.S. (1987) 'Wetland Loss in Louisiana' *Geografiska Annaler*, 69, 189-200.

Wang, Z.B., Louters, T., DeVriend, H.J. (1995) 'Morphodynamic Modelling for a Tidal Inlet in the Wadden Sea' *Marine Geology*, 126, 289-300.

Wang, H., Zhenming, G., Yuan, L., Zhang, L. (2014) 'Evaluation of the Combined Threat from Sea-Level Rise and Sedimentation Reduction to the Coastal Wetlands in the Yangtze Estuary, China' *Ecological Engineering*, 71, 346-354.

Warner, J.C., Sherwood, C.R., Signell, R.P., Harris, C.K., Arango, H.G. (2008) 'Development of a three-dimensional, Regional, Coupled Wave Current and Sediment Transport Model' *Computer and Geosciences*, 34, 1284-1306.

Warren, I.R, and Bach, H.K. (1992) 'MIKE21: A Moastal Waters and Seas' *Environmental Software*, 7, 4, 229e240.

Warren Pinnacle Consulting Inc (2011a) *SLAMM Analysis of Grand Bay NERR and Environs*, Prepared for The nature Conservancy, Gulf of Mexico Initiative.

Warren Pinnacle Consulting Inc (2011b) *SLAMM Analysis of Southern Jefferson County, TX*, Prepared for Gulf of Mexico Alliance.

Warren Pinnacle Consulting Inc (2011c) *Application of the Sea-Level Affecting Marshes Model (SLAMM 6) to Cape May NWR*, Prepared for U.S. Fish and Wildlife Service National Wildlife Refuge System.

Warrick, R.H. and Oerlemans, J. (1990) 'Sea Level Rise' In: Houghton, J.T., Jenkins, G.J., Ephraums (eds) *Climate Change – the IPCC Scientific Assessment.* Cambridge, Cambridge University Press, 257-81.

Warrick, R.H., LeProvost, C., Meir, M. Oerlemans, J., Woodworth, P.L. (1996) 'Changes in Sea Level' In: Houghton, J.T., Meira Filho, L.G., Calander, B.A., Harris, N., Kattenberg, A., Maskell, K. (eds) *Climate Change 1995: The Science of Climate Change*, Cambridge, cambridge University Press, 358-405.

WASA GROUP (1998) 'Changing Waves and Storms in The Northeast Atlantic?' *Bulletin of the Americal Meteorological Society, 79*, 741-760.

Weggel, R.J. (1979) *A Method for Estimating Long-Term Erosion Rates from a Long-Term Rise in Water Level* USAGE-WES Coastal Engineering Technical Aid 79-2.

Weiss, J.L., Overpeck, J.T., Strauss, B. (2010) 'Implications of Recent Sea Level Rise Science for Low-Elevation Areas in Coastal Cities of the Conterminous U.S.A' *Climatic Change*, 105, 635-645.

Werner, A.D. and Simmons, C.T. (2009) 'Impact od Sea-Level Rise on Sea Water Intrusion in Coastal Aquifers' *Ground Water*, 47, 197-204.

Whitehouse, R., Balson, P., Beech, N., Brampton, A., Blott, S., Burningham, H., Cooper, N., French, J., Guthrie, G., Hanson, S., Nicholls, R., Pearson, S., Pye, K., Rossington, K., Sutherland, J., Walkden, M. (2009) *Characterisation and Prediction of large-scale, long-term Change of Coastal Geomorphological Behaviours: Final Science Report.* Science Report SC060074/SR1. Environment Agency.

Wiedenman, R.E. (2010) *Adaptive Response Planning for Sea-Level Rise and Saltwater Intrusion in Miami-Data County*, Department of Urban and Regional Planning Florida State University.

Wigley, T.M.L. (1995) 'Global Mean Temperature and Sea-Level Consequences of Greenhouse Stabilization' *Geophysical Research Letters, 22* (1), 45-48.

Wigley, T.M.L. and Raper, S.C.B. (1992) 'Implications for Climate and Sea Levels of Revised IPCC emissions scenarios, *Nature*, 357, 293-300.

Wigley, T.M.L. and Raper, S.C.B. (1993) 'Future Changes in Global Mean Temperature and Sea Level' In: Warrick, R.A., Barrow, E.M., Wigley, T.M.L. (eds) *Climate and Sea Level Change: Observations, Projections and Implementation*, Cambridge University Press, 111-113.

Wolanski, E., Brinson, M.M., Cahoon, D.R., Perillo, G.M.E (2009) 'Coastal Wetlands:A Synthesis' In: Perillo, G.M.E., Wolanski, E., Cahoon, D.R., Brinson, M.M. (ed.) *Coastal Wetlands An Integrated Ecosystem Approach, 1-57.*

Wolf, J., Leake, J., Lowe, J. (2009) 'Wave Climate Changes on the NW European shelf from Ensemble Climate Model Downscaling' *Proudman Oceanographic Laboratory, Royal Society Sea Level Meeting*, 2-3 November 2009.

Wolters, M., Bakker, J.P., Bertness, M.D., Jefferies, R.L., Moller, I. (2005) 'Saltmarsh Erosion and Restoration in south-east England:Squeezing the Evidence requires realignment' *Journal of Applied Ecology*, 42, 844-851.

Woodroffe, C.D. (1993) 'Sea Level' *Progress in Physical Geography*, 17, 359-368.

Woodworth, P., Tsimplis, M., Flather, R., Shennan, I. (1999) 'A Review of the Trends observed in British Isles Mean Sea Level Data Measured by Tide Gauges' *Geophysical Journal International, 136*, 651-670.

Woodworth, P.L., Teferle, F.N., Bingley, R.M., Shennan, I., Williams, S.D.P. (2009) 'Trends in UK Mean Sea Level Revisited' *Geophysical Journal International*, 176, 19-30.

Wright, L.D. (1995) *Morphodynamics of Inner Continental Shelves*, Boca Raton, Florida: CRC Press, 241p.

Wright, L.D., Boon, J.D., Kim, S.C., List, J.H. (1991) 'Modes of Cross-Shore Sediemnt Transport on the Shoreface of the Middle Atlantic Bight' *Marine Geology*, 96, 19-51.

WWF (2009) *Mega-Stress for Mega-Cities: A Climate Vulnerability Ranking of Major Coastal Cities in Asia*

Zhang, K., Douglas, B.C., Leatherman, S.P. (2004) 'Global Warming and Coastal Erosion' *Climatic Change*, 64, 41-58.

Zsamboky, M., Fernandez-Bilbao, A., Smith, D.E., Knight, J., Allen, J. (2011) *Impacts of Climate Change on Disadvantaged UK Coastal Communities* Joseph Rowntree Foundation, www.jrf.org.uk.

APPENDIX

transfer.inc

```
    BEGIN
  IF ERODING Then Exit;                  //Inundaion of Dryland
650
  IF not ProtectAll Then
   Begin
     With Cell^ DO
      If FALSE {(CatSums[RockyIntertidal] > CatSums[LowerMarsh]) {Rocky Intertidal Assumption Removed}
       Then Convert(Cell,FromCat,RockyIntertidal,-99)
       Else
        Begin
         If (AdjOcean) and ((not IncludeDikes) or (not Cell.ProtDikes))
           Then Begin
                  If OceanNearer then Convert(Cell,FromCat,OceanBeach,LowerBound(FromCat,Subsite))
                                  else Convert(Cell,FromCat,TransMarsh,LowerBound(FromCat,Subsite))      //mod

                End
           Else
            If (AdjWater and (Erosion > None)) and ((not IncludeDikes) or (not Cell.ProtDikes))
              Then Convert(Cell, FromCat, TransMarsh,LowerBound(FromCat,Subsite))                      //mod
              Else
                Begin
                  IF (Tropical AND NearWater)
                    Then Convert(Cell,FromCat,Mangrove,LowerBound(FromCat,Subsite))
                    else If (FromCat <> Backshore) then Convert(Cell,FromCat,TransMarsh,LowerBound(FromCat,Subsite))    //mod
                                                        {else Convert(Cell,FromCat,TransMarsh,LowerBound(FromCat,Subsite))};
                End; {else not exposed and erosion not heavy}
        End; {not rocky}
    End; {not ProtAll}
END; {INUNDATE}
(*****************************************************************************)
      If not ERODING then
       If (LowBound > CatElev(Cell,Wetland)) then   { Inundation Model }
        BEGIN           {erosion & inundation}
         CalcFracLostBySlope(Cell,Wetland,LowBound);

        { simple inundation}
          Case Wetland of
            VegTidalFlat, TidalFlat:  Convert(Cell,Wetland,EstuarineSubtidal,LowBound);
            EstuarineBeach: Convert(Cell,Wetland,EstuarineSubtidal,LowBound);
            OceanFlat:    Convert(Cell,Wetland,OpenOcean,LowBound);
            LowerMarsh:    Convert(Cell,Wetland,TidalFlat,LowBound);
            UpperMarsh:     Begin
                                      If Tropical
                                        then Convert(Cell,Wetland,Mangrove,LowBound)
                                        else Convert(Cell,Wetland,LowerMarsh,LowBound);
                                    End;
            TransMarsh:  Begin
                                      If Tropical
                                        then Convert(Cell,Wetland,Mangrove,LowBound)
                                        else Convert(Cell,Wetland,UpperMarsh,LowBound);  //mod
                                    End;
            Mangrove:     Convert(Cell,Wetland,EstuarineSubtidal,LowBound);
            end;

          SetCatElev(Cell,Wetland,LowBound);
        END;  {erosion/inundation}

  End; {with Cell}
End; {ConvertWetland}
```

Figure A- 0.1: Procedure for inundation.

SiteEdits

```
procedure TSiteEditForm.TSGridExit(Sender: TObject);
Const NUMRowsOrig = 24;
      NUMRowsAccr = 12;
      NUMRowsOverwash = 6;

Var AM, R, C: Integer;
    V: String;
    TSS: TSubSite;
-------------------------------------------------------------------------------
  If v='' then exit;
  With TSS do
    Try
      Case R of
        1: Description := V;
        2: NWI_Photo_Date := Trunc(StrToFloat(V));
        3: DEM_Date := Trunc(StrToFloat(V));
        4: Begin
             V := Lowercase(V);
             If v='' then exit;
             If V[1] = 's' then Direction_OffShore := Southerly
                else if Pos('n',V) > 0 then Direction_OffShore := Northerly
                else if Pos('w',V) > 0 then Direction_OffShore := Westerly
                else Direction_OffShore := Easterly;
           End;
        5: Historic_Trend := StrToFloat(V);
        6: NAVD88MTL_Correction := StrToFloat(V);
        7: GTideRange := StrToFloat(V);
        8: SaltElev := StrToFloat(V);
        9: HAT := StrToFloat(V);          //mod
        10: MHWS := StrToFloat(V);        //mod
        11: MHW := StrToFloat(V);         //mod
        12: MHWN := StrToFloat(V);         //mod
        13: LAT := StrToFloat(V);          //mod
        14: MarshErosion := StrToFloat(V);
        15: SwampErosion := StrToFloat(V);
        16: TFlatErosion := StrToFloat(V);
        17: FixedLowerMarshAccr  := StrToFloat(V);
        18: FixedUpperMarshAccr  := StrToFloat(V);
        19: FixedTideFreshAccr  := StrToFloat(V);
        20: Fixed_TF_Beach_Sed := StrToFloat(V);
        21: Freq_BigStorm := Trunc(StrToFloat(V));
        22: UK_GLobal_slr := StrToFloat(V);         //mod
        23: Begin
              v := Lowercase(v);
              If (v[1]='f') or (v[1] = '0')
                then Use_Preprocessor:= False
                else Use_Preprocessor:= True;
            End;
        24: OW_Width_Adj:=StrToFloat(V);    //mod adjasent to ocean

      End; {Case}
```

Figure A- 0.2: Format of each parameter.

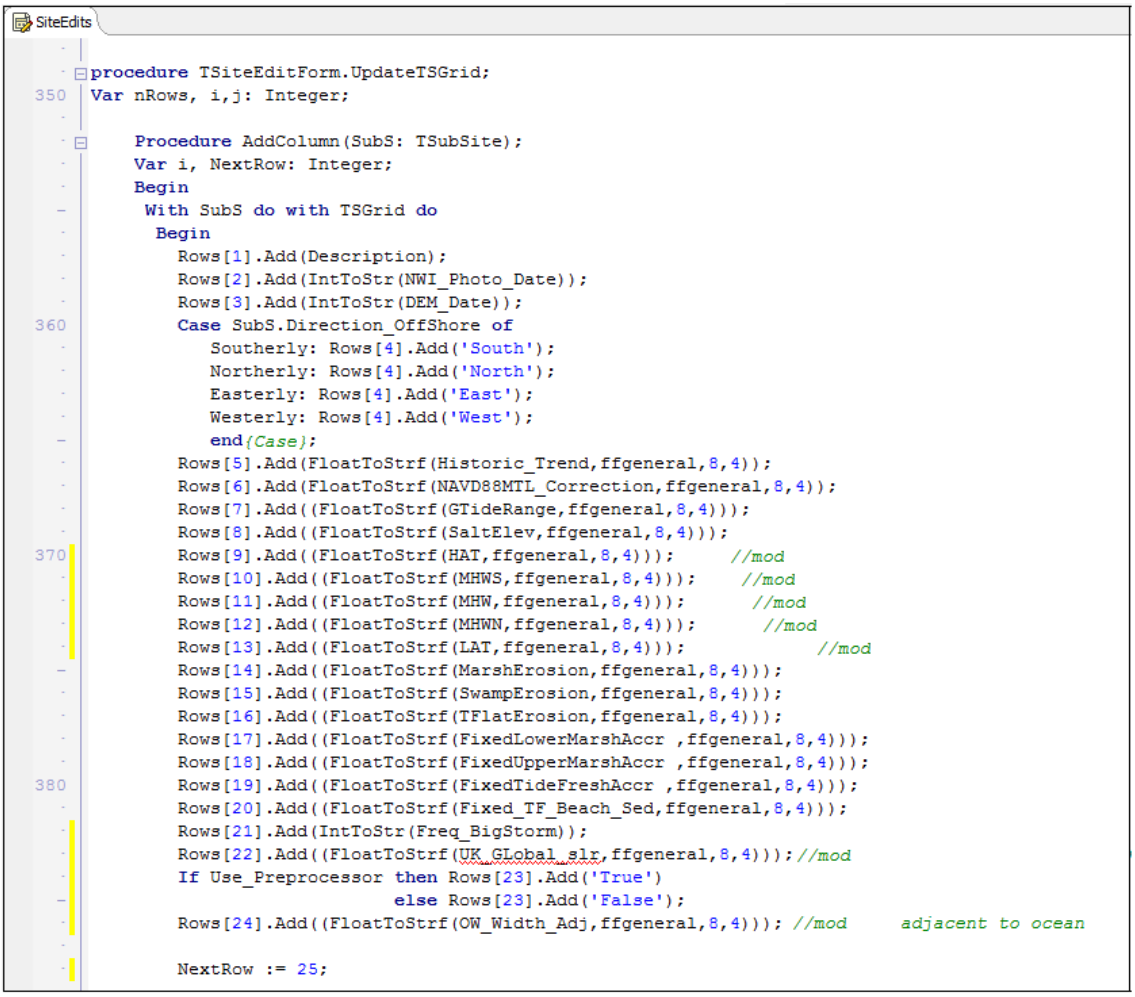

Figure A-0.3: Create lines for each parameter at the site parameter table.

SiteEdits

```
begin
  With TSGrid do
    Begin
      If ShowOverwash.Checked then NRows := 31                //
                              else NRows := 24;               //
      If ShowAccr.Checked then NRows := NRows + 12 * N_ACCR_MODELS;
      RowCount := NRows+1;  {plus header}
      ColCount := TS.NSubSites + 2;  {plus header and global site}

      ColWidths[0]:=205;
//      ColWidths[ColCount-1]:=130;

      For i := 0 to RowCount-1 do
        Rows[i].Clear;

      Rows[0].Add('Parameter');
      Rows[0].Add('Global');

      For i := 1 to TS.NSubSites do
        Rows[0].Add('SubSite '+IntToStr(i));

      Rows[1].Add('Description');
      Rows[2].Add('NWI Photo Date (YYYY)');
      Rows[3].Add('DEM Date (YYYY)');
      Rows[4].Add('Direction Offshore [n,s,e,w]');
      Rows[5].Add('Historic Trend (mm/yr)');
      Rows[6].Add('MTL-NAVD88 (m)');
      Rows[7].Add('GT Great Diurnal Tide Range (m)');
      Rows[8].Add('Salt Elev. (m above MTL)');
      Rows[9].Add('HAT (m)');                          //mod
      Rows[10].Add('MHWS (m)');                        //mod
      Rows[11].Add('MHW (m)');                         //mod
      Rows[12].Add('MHWN (m)');                         //mod
      Rows[13].Add('LAT(m)');                           //mod
      Rows[14].Add('Marsh Erosion (horz. m /yr)');
      Rows[15].Add('Swamp Erosion (horz. m /yr)');
      Rows[16].Add('T.Flat Erosion (horz. m /yr)');
      Rows[17].Add('Lower Marsh Accr (mm/yr)');
      Rows[18].Add('Upper Marsh Accr (mm/yr)');
      Rows[19].Add('Tidal Fresh Marsh Accr (mm/yr)');
      Rows[20].Add('Beach Sed. Rate (mm/yr)');
      Rows[21].Add('Freq. Overwash (years)');
      Rows[22].Add('UK/Global slr(mm/yr)');//mod
      Rows[23].Add('Use Elev Pre-processor [True,False]');
      Rows[24].Add('Adj. Ocean (m)');                  //mod
```

Figure A-0.4: Add labels for each parameter at the site parameter table.

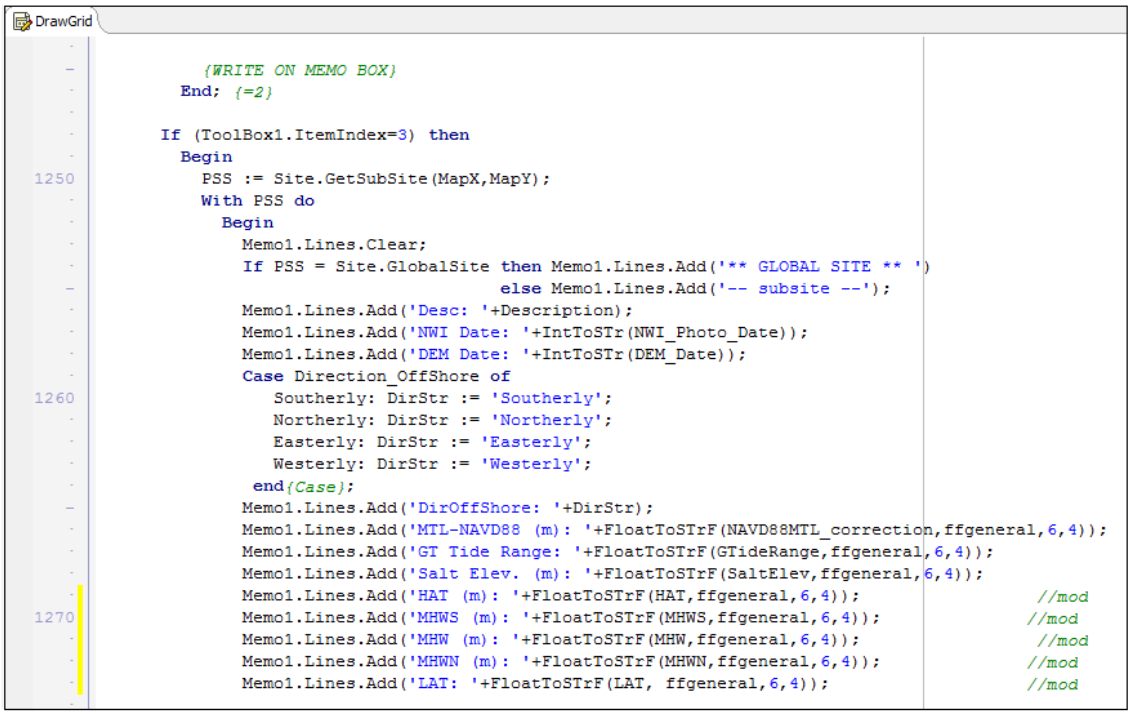

Figure A-0.5: Add legend and type of value of each parameter at the site parameters table.

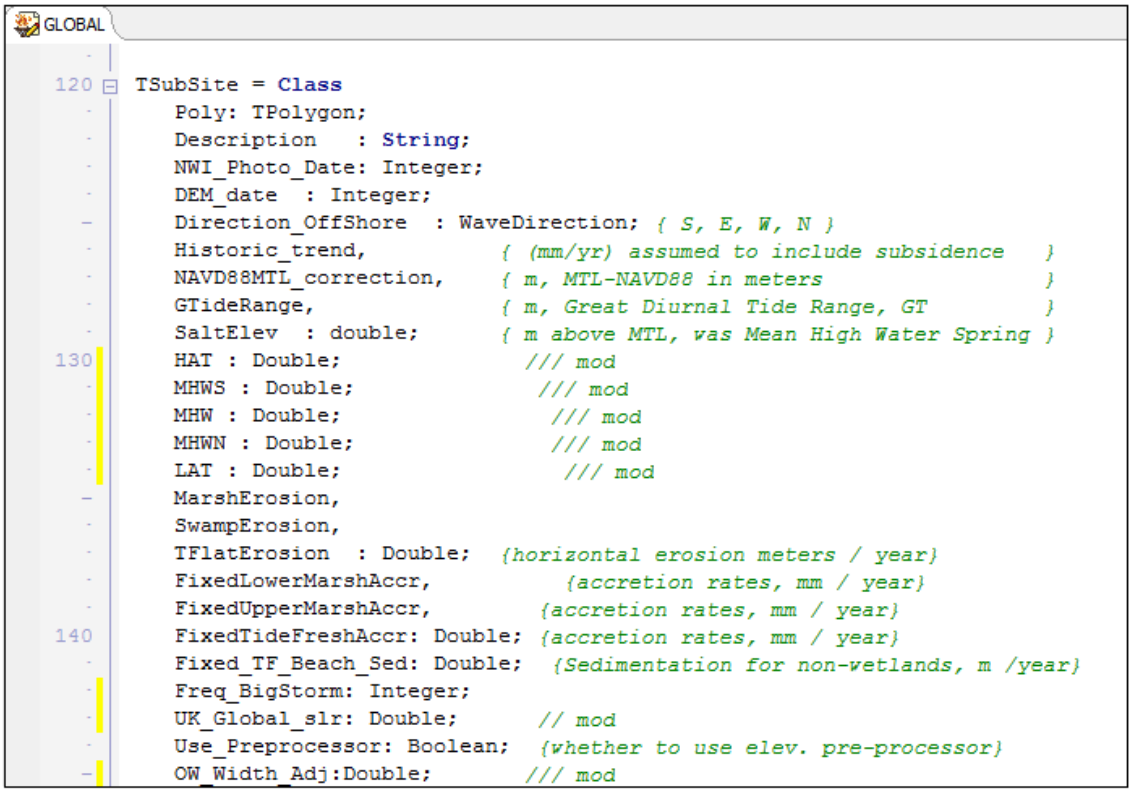

Figure A-0.6: Declare variables of site parameter table.

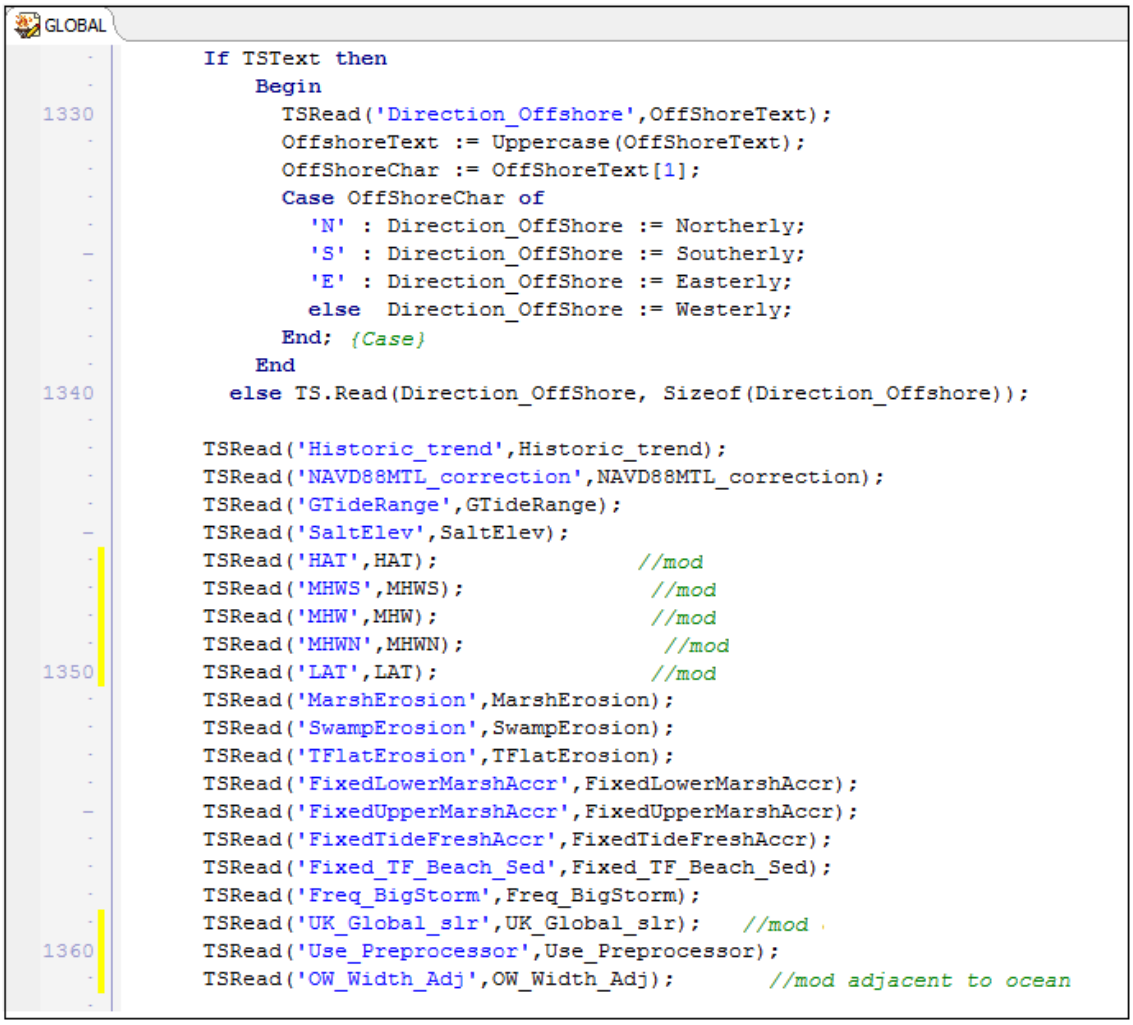

Figure A-0.7: Read the labels of the parameters from the text file.

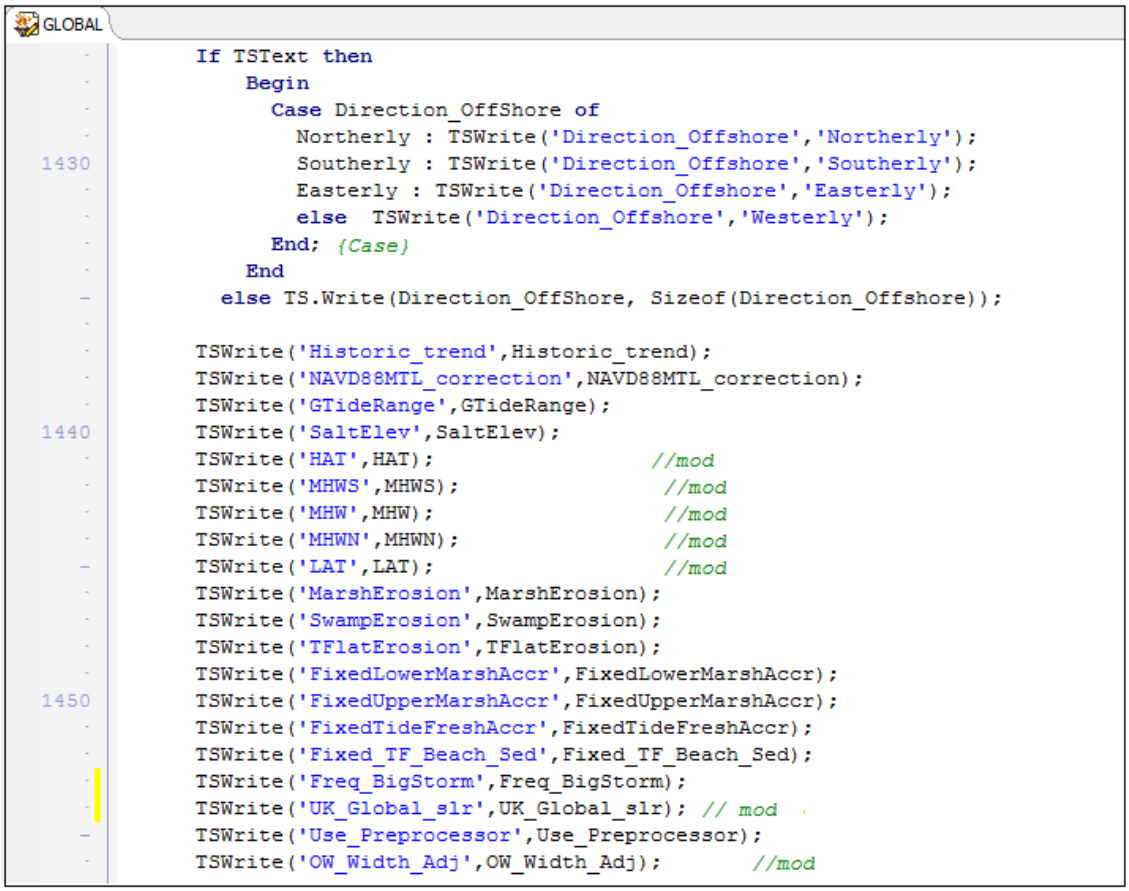

Figure A-0.8: Write the labels of the parameters to the text file

GLOBAL

```
      Readln(ReadFile,GTideRange);
      GetToComma;
      Readln(ReadFile,SaltElev);
      GetToComma;
      Readln(ReadFile,HAT);              //mod
      GetToComma;
      Readln(ReadFile,MHWS);             //mod
      GetToComma;
      Readln(ReadFile,MHW);               //mod
      GetToComma;
      Readln(ReadFile,MHWN);             //mod
      GetToComma;
      Readln(ReadFile,LAT);              //mod

      Readln(ReadFile,ReadStr);
      If Pos('erosion',Lowercase(ReadStr)) > 0
        then MarshErosion := FloatAfterComma(ReadStr)
         else
          Begin
            Junk := FloatAfterComma(ReadStr);
            GetToComma;
            Readln(ReadFile,MarshErosion);     {horz meters/year}
          End;

      GetToComma;
      Readln(ReadFile,SwampErosion); {horz meters/year}
      GetToComma;
      Readln(ReadFile,TFlatErosion); {horz meters/year}

      GetToComma;
      Readln(ReadFile,FixedLowerMarshAccr); {mm/year}
      GetToComma;
      Readln(ReadFile,FixedUpperMarshAccr); {mm/year}
      GetToComma;
      Readln(ReadFile,FixedTideFreshAccr); {mm/year}
      GetToComma;
      Readln(ReadFile,Fixed_TF_Beach_Sed); {mm/year}
      GetToComma;
      Readln(ReadFile,Freq_BigStorm); {years}
      GetToComma;
      Readln(ReadFile,UK_Global_slr); {mm/years}   //mod
      GetToComma;
      Readln(ReadFile,ReadStr); {Boolean, whether to use elev pre processor}
      Use_PreProcessor := pos('true',lowercase(ReadStr))>0;
      GetToComma;
      Readln(ReadFile,OW Width Adj);            //mod    adjacent to ocean
```

Figure A-0.9: Read the values of the parameters from the text file.

```
GLOBAL
constructor TSubSite.CreateWith(TSS: TSubSite);
begin
    Poly := TPolygon.Create;
    Description    := TSS.Description;
    NWI_Photo_Date := TSS.NWI_Photo_Date;
    DEM_date       := TSS.DEM_date;
    Direction_OffShore   := TSS.Direction_OffShore;
    Historic_trend       := TSS.Historic_trend;
    NAVD88MTL_correction := TSS.NAVD88MTL_correction;
    GTideRange  := TSS.GTideRange;
    SaltElev    := TSS.SaltElev;
    HAT    := TSS.HAT;                  //mod
    MHWS    := TSS.MHWS;                //mod
    MHW    := TSS.MHW;                  //mod
    MHWN    := TSS.MHWN;                //mod
    LAT   := TSS.LAT;                   //mod
    MarshErosion := TSS.MarshErosion;
    SwampErosion := TSS.SwampErosion;
    TFlatErosion   := TSS.TFlatErosion;
    FixedLowerMarshAccr := TSS.FixedLowerMarshAccr;
    FixedUpperMarshAccr := TSS.FixedUpperMarshAccr;
    FixedTideFreshAccr := TSS.FixedTideFreshAccr;
    Fixed_TF_Beach_Sed := TSS.Fixed_TF_Beach_Sed;
    Freq_BigStorm := TSS.Freq_BigStorm;
    UK_Global_slr := TSS.UK_Global_slr; //mod
    Use_Preprocessor := TSS.Use_Preprocessor;
    OW_Width_Adj := TSS.OW_Width_Adj;          //mod  adjacent to ocean
    OW_Max_Width_Overwash := TSS.OW_Max_Width_Overwash;
    OW_Beach_to_Ocean := TSS.OW_Beach_to_Ocean;
    OW_Dryland_to_Beach := TSS.OW_Dryland_to_Beach;
    OW_Est_to_Beach := TSS.OW_Est_to_Beach;
    OW_Marsh_Pct_Loss := TSS.OW_Marsh_Pct_Loss;
    OW_Mang_Pct_Loss := TSS.OW_Mang_Pct_Loss;
    UseAccrModel := TSS.UseAccrModel;
    MaxAccr := TSS.MaxAccr;
    MinAccr := TSS.MinAccr;
    AccrA := TSS.AccrA;
    AccrB := TSS.AccrB;
    AccrC := TSS.AccrC;
    DistEffectMax := TSS.DistEffectMax;
    Dmin := TSS.Dmin;
    SalinityTMax := TSS.SalinityTMax;
```

Figure A-0.10: Create parameters for sub-sites.

```
Welcome Page | main | GLOBAL
70
TYPE

  ElevUnit = (HalfTide, SaltBound, Meters, zHATBound, yBound, MHWBound, nMHWNBound, LATBound);

  ClassElev = packed Record
      MinUnit : ElevUnit;
      MinElev : Double;
      MaxUnit : ElevUnit;
      MaxElev : Double;
80  End; {Record}
```

Figure A-0.11: Determine different wetland elevation units.

```
GLOBAL
Procedure LoadElevRangesFromText(Var TCA: TClassElevArray);
Var Cat: Category;
   UnitStr: String;

   Function Str2Unit(UStr: String): ElevUnit;
   Begin
     UStr := Lowercase(UStr);
     If Pos(UStr,'halftide')>0 then Result := HalfTide
        else If Pos(UStr,'saltbound')>0 then Result := SaltBound
        else If Pos(UStr,'zhatbound')>0 then Result := zHATBound        //mod
        else If Pos(UStr,'ybound')>0 then Result := yBound               //mod
        else If Pos(UStr,'mhwbound')>0 then Result := MHWBound           //mod
        else If Pos(UStr,'nmhwnbound')>0 then Result := nMHWNBound       //mod
        else if Pos(UStr,'latbound')>0 then Result := LATBound          //mod

        else Result := Meters;
   End;

Begin
  For Cat := FirstCategory to LastCategory do
    Begin
      TSRead(TitleCat[Cat]+' MinElev',TCA[Cat].MinElev);
      TSRead(TitleCat[Cat]+' MinUnit',UnitStr);
      TCA[Cat].MinUnit := Str2Unit(UnitStr);

      TSRead(TitleCat[Cat]+' MaxElev',TCA[Cat].MaxElev);
      TSRead(TitleCat[Cat]+' MaxUnit',UnitStr);
      TCA[Cat].MaxUnit := Str2Unit(UnitStr);
    End;
End;
{-------------------------------------------------------------------------------}

Procedure SaveElevRangesToText(TCA: TClassElevArray);
Var Cat: Category;
   UnitStr: String;

   Function Unit2Str(EU:ElevUnit): String;
   Begin
     Case EU of
       HalfTide: Result :='HalfTide';
       SaltBound: Result := 'SaltBound';
       zHATBound: Result := 'zHATBound';                        //mod
       yBound: Result := 'yBound';     //MHWSBound             //mod
       MHWBound: Result := 'MHWBound';                          //mod
       nMHWNBound: Result := 'nMHWNBound';                       //mod
       LATBound: Result := 'LATBound';                          //mod
```

Figure A-0.12: Load and save elevation units from the text file.

Elev_Analysis

```
Try
 Case C of
   1: SS.ElevRanges[EditCat].MinElev := StrToFloat(V);
   3: SS.ElevRanges[EditCat].MaxElev := StrToFloat(V);
   2,4: Begin
         V := Lowercase(V);
         If V[1]='n' then UType := HaltTide
         else if V[1]='s' then Utype := SaltBound
         else if V[1]='h' then Utype := zHATBound                    //mod
         else if V[1]='x' then Utype := yBound    //MHWSBound        //mod
         else if V[1]='y' then Utype := MHWBound                     //mod
         else if V[1]='z' then Utype := nMHWNBound                   //mod
         else if V[1]='l' then Utype := LATBound                     //mod
         else UType := Meters;
         If C=2 then SS.ElevRanges[EditCat].MinUnit := UType
                else SS.ElevRanges[EditCat].MaxUnit := UType;
        End;
 End; {Case}
```

Figure A-0.13: Create columns at the Elevation Input and Analysis Table.

Elev_Analysis

```
procedure TElevAnalysisForm.UpdateTSGrid;
Var nRows, i: Integer;

    Function UnitStr(InUnit: ElevUnit): String;
    Begin
      Case InUnit of
        HalfTide: Result := 'HTU';
        SaltBound: Result := 'Salt Elev.';
        zHATBound: Result := 'HAT';            //mod
        yBound: Result := 'MHWS';               //mod
        MHWBound: Result := 'MHW';             //mod
        nMHWNBound: Result := 'MHWN';          //mod
        LATBound: Result := 'LAT';            //mod
        else Result := 'Meters';
      End; {case}
    End;
```

Figure A-0.14: Write elevation units at the Elevation Input and Analysis Table.

Initx.Inc

```
PROCEDURE TSLAMM_Simulation.SetDefaultCategoryVariables;  {Set default min-max t
Var Cat: Category;
Begin
  For Cat := FirstCategory to LastCategory do
    With ElevRanges[Cat] do
      Case Cat of
        BackShore, Dryland,UndDryLand,Swamp..InlandFreshMarsh,TidalFreshMarsh,
        TidalSwamp, InlandOpenWater, RiverineTidal,TidalCreek :
                              Begin
                                MinUnit := zHATBound;
                                MinElev := 1.0;
                                MaxUnit := Meters;
                                MaxElev := 3.048;  {assumes 10 foot contour}
                              End;
        UpperMarsh:           Begin
                                MinUnit := MHWBound;                    //mod
                                MinElev := 1.0;
                                MaxUnit := yBound;                      //mod
                                MaxElev := 1.0;
                              End;
        TransMarsh:           Begin
                                MinUnit := yBound;                      //mod
                                MinElev := 1.0;
                                MaxUnit := zHATBound;                   //mod
                                MaxElev := 1.0;
                              End;
        LowerMarsh:           Begin
                                MinUnit := nMHWNBound;                  //mod
                                MinElev := 1.0;
                                MaxUnit := MHWBound;                    //mod
                                MaxElev := 1.0;
                              End;
        Mangrove:             Begin
                                MinUnit := Meters;
                                MinElev := 1.0;
                                MaxUnit := SaltBound;
                                MaxElev := 1.0;
                              End;
        InlandShore,OceanBeach,EstuarineBeach,OceanFlat:
                              Begin
                                MinUnit := LATBound;                    //mod
                                MinElev := 1.0;
                                MaxUnit := zHATBound;                   //mod
                                MaxElev := 1.0;
        VegTidalFlat, Tidalflat: Begin
                                   MinUnit := LATBound;                 //mod
                                   MinElev := 1.0;
                                   MaxUnit := nMHWNBound;               //mod
                                   MaxElev := 1.0;
                                 End;
        RockyIntertidal:      Begin
                                MinUnit := HalfTide;
                                MinElev := -1.0;
                                MaxUnit := SaltBound;
                                MaxElev := 1.0;
                              End;
        else {OpenOcean,EstuarineSubtidal, blank}
                              Begin
                                MinUnit := Meters;
                                MinElev := -5;
                                MaxUnit := LATBound;
                                MaxElev := 1.0;  {Not really relevant}
                              End;
```

Figure A-0.15: Set default elevation ranges for each wetland category.

```
Initx.Inc
FUNCTION TSLAMM_Simulation.LowerBound(Cat: Category; Var SS: TSubSite): Double;
Begin
  With SS do With ElevRanges[Cat] do
     Case MinUnit of
       SaltBound: Result  := MinElev * SaltElev;
       HalfTide: Result := MinElev * MHHW;
       zHATBound: Result := MinElev * HAT;          //mod
       yBound: Result := MinElev * MHWS;            //mod
       MHWBound: Result := MinElev * MHW;           //mod
       nMHWNBound: Result := MinElev * MHWN;        //mod
       LATBound: Result := MinElev * LAT;           //mod
       else {Meters:} Result := MinElev;
     End; {Case}
End;

FUNCTION TSLAMM_Simulation.UpperBound(Cat: Category; Var SS: TSubSite): Double;
Begin
  With SS do With ElevRanges[Cat] do
     Case MaxUnit of
       SaltBound: Result  := MaxElev * SaltElev;
       HalfTide: Result := MaxElev * MHHW;
       zHATBound: Result := MaxElev * HAT;              //mod
       yBound: Result := MaxElev * MHWS;                //mod
       MHWBound: Result := MaxElev * MHW;               //mod
       nMHWNBound: Result := MaxElev * MHWN;            //mod
       LATBound: Result := MaxElev * LAT;               //mod
       else {Meters:} Result := MaxElev;
     End; {Case}
End;
```

Figure A-0.16: Define upper and lower boundaries of the wetland categories.

```
GLOBAL
Type
  IPCCScenarios  = (Scen_A1B,Scen_A1T,Scen_A1F1,Scen_A2,Scen_B1,Scen_B2,Scen_SE,Scen_SW,Scen_NE,Scen_NW);
  IPCCEstimates  = (Est_Min,Est_Mean,Est_Max);
  ProtScenario   = (NoProtect, ProtDeveloped, ProtAll);
  ESlammError    = Exception;
```

Figure A-0.17: Incorporate UKCP09 type scenarios into the IPCC ones.

```
GLOBAL

Const

  LabelProtect: Array[NoProtect..ProtAll] of String [31] =
            ('No Protect','Protect Dry','Protect All');

  LabelIPCC : Array[Scen_A1B..Scen_NW] of String [31] =
              ('Scenario A1B','Scenario A1T','Scenario A1F1','Scenario A2',...*
  *'Scenario B1','Scenario B2','Scenario SE','Scenario SW','Scenario NE','Scenario NW');//mod
   LabelIPCCEst : Array[Est_Min..Est_Max] of String [8] =
              ('Minimum','Mean','Maximum');

  LabelFixed: Array[1..3] of String[31] = ('1 meter','1.5 meter','2 meter');
```

Figure A-0.18: Define labels for each scenario.

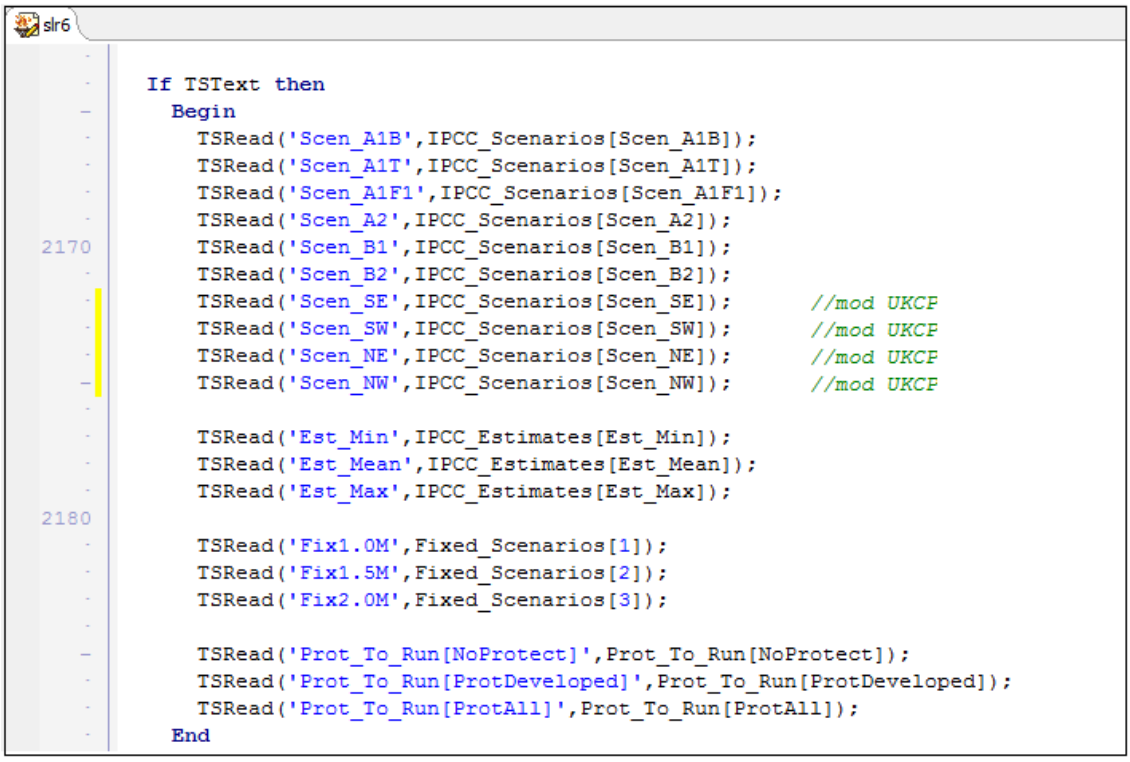

Figure A-0.19: Read each sea-level rise scenario.

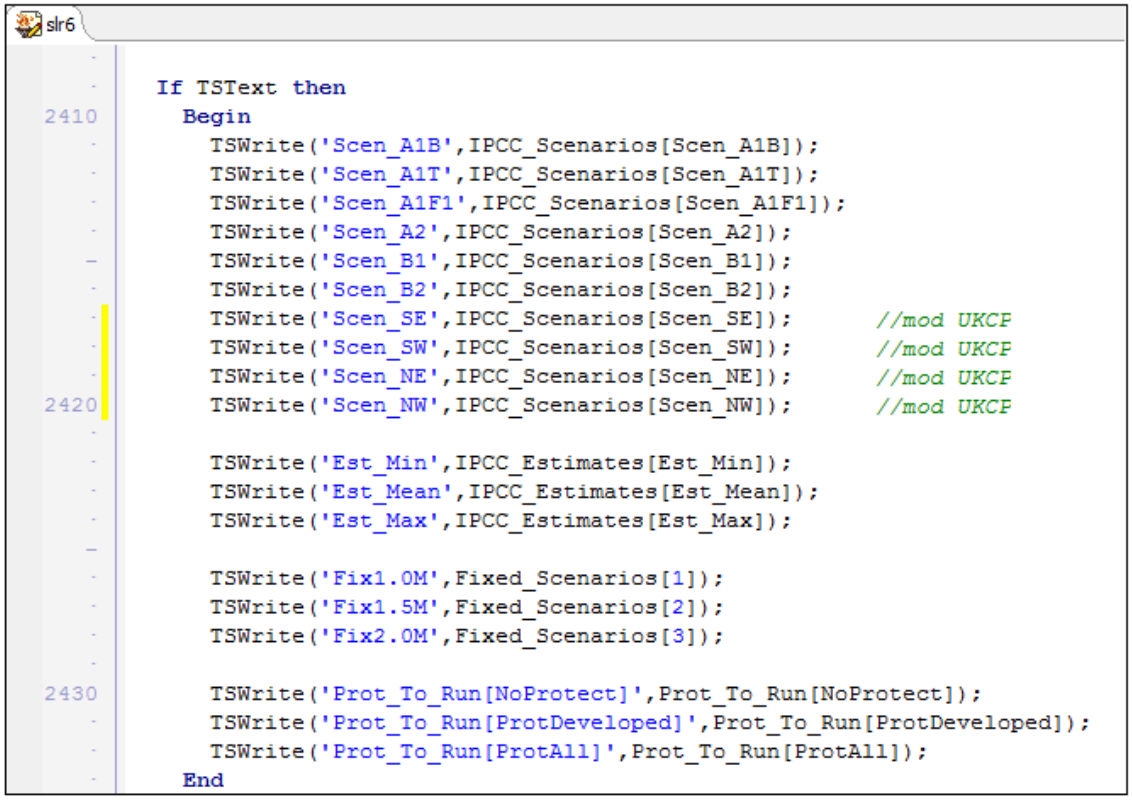

Figure A-0.20: Write each sea-level rise scenario.

```
Execute
type
  TExecuteOptionForm = class(TForm)
    SLRPanel: TPanel;
    Label4: TLabel;
    TabControl1: TTabControl;
    HistoricBox: TCheckBox;
    FiftyBox: TCheckBox;
    NinetyFiveBox: TCheckBox;
    NinetyNineBox: TCheckBox;
    IPCCPanel: TPanel;
    Label6: TLabel;
    Label7: TLabel;
    Label10: TLabel;
    A1B: TCheckBox;
    A1T: TCheckBox;
    A1F1: TCheckBox;
    A2: TCheckBox;
    B1: TCheckBox;
    B2: TCheckBox;
    SE: TCheckBox;          //mod UKCP
    SW: TCheckBox;          //mod UKCP
    NE: TCheckBox;          //mod UKCP
    NW: TCheckBox;          //mod UKCP
    Min: TCheckBox;
    Mean: TCheckBox;
    Max: TCheckBox;
    fix1: TCheckBox;
    fix15: TCheckBox;
    fix2: TCheckBox;
    Panel3: TPanel;
    ProtectionPanel: TLabel;
    ProtectAllBox: TCheckBox;
    ProtectDevBox: TCheckBox;
    DontProtectBox: TCheckBox;
    Panel4: TPanel;
    RunNWI: TCheckBox;
    Panel7: TPanel;
    DikeBox: TCheckBox;
```

Figure A-0.21: Create checkboxes at the interface.

```
Execute
procedure TExecuteOptionForm.A1BClick(Sender: TObject);
begin
  If Updating then Exit;
  LSS.IPCC_Scenarios[Scen_A1B] := A1B.checked;
  LSS.IPCC_Scenarios[Scen_A1T] := A1T.checked;
  LSS.IPCC_Scenarios[Scen_A1F1] := A1F1.checked;
  LSS.IPCC_Scenarios[Scen_A2] := A2.checked;
  LSS.IPCC_Scenarios[Scen_B1] := B1.checked;
  LSS.IPCC_Scenarios[Scen_B2] := B2.checked;
  LSS.IPCC_Scenarios[Scen_SE] := SE.checked;    //mod UKCP
  LSS.IPCC_Scenarios[Scen_SW] := SW.checked;    //mod UKCP
  LSS.IPCC_Scenarios[Scen_NE] := NE.checked;    //mod UKCP
  LSS.IPCC_Scenarios[Scen_NW] := NW.checked;     //mod UKCP
  LSS.IPCC_Estimates[Est_Min] := Min.checked;
  LSS.IPCC_Estimates[Est_Mean] := Mean.checked;
  LSS.IPCC_Estimates[Est_Max] := Max.checked;
```

Figure A-0.22: Assign each scenario to the relevant checkbox.

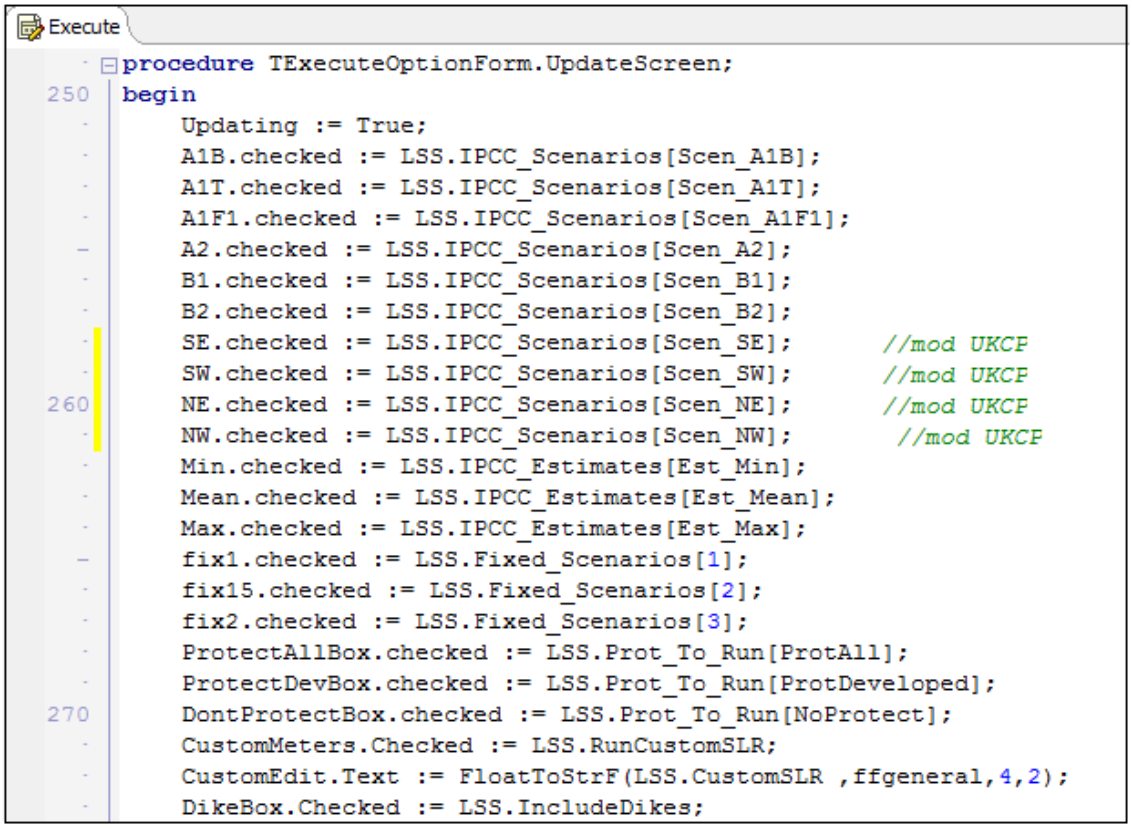

Figure A-0.23: Each checkbox reads the relevant scenario.

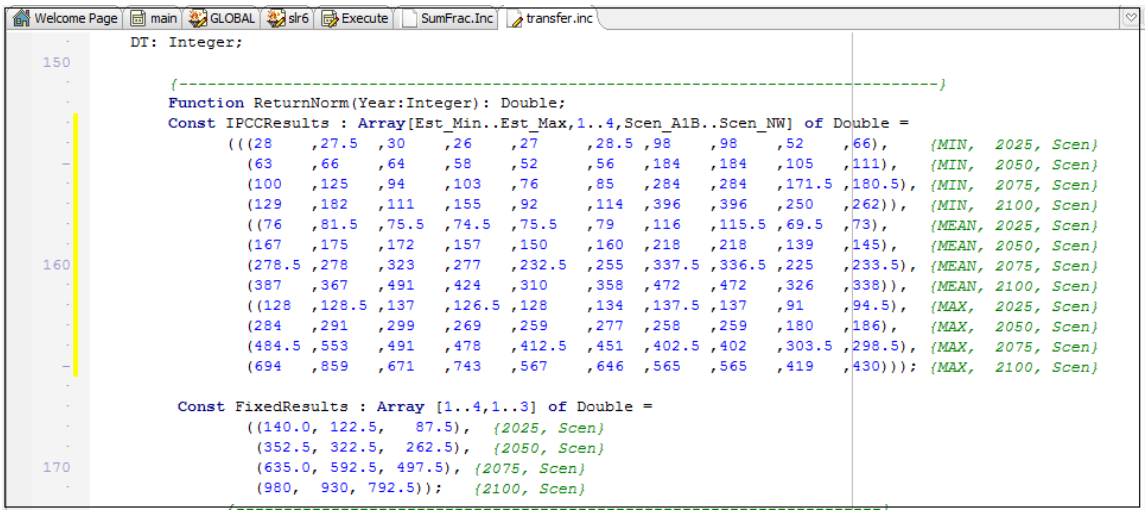

Figure A-0.24: Determine sea-level rise for each scenario (in mm).

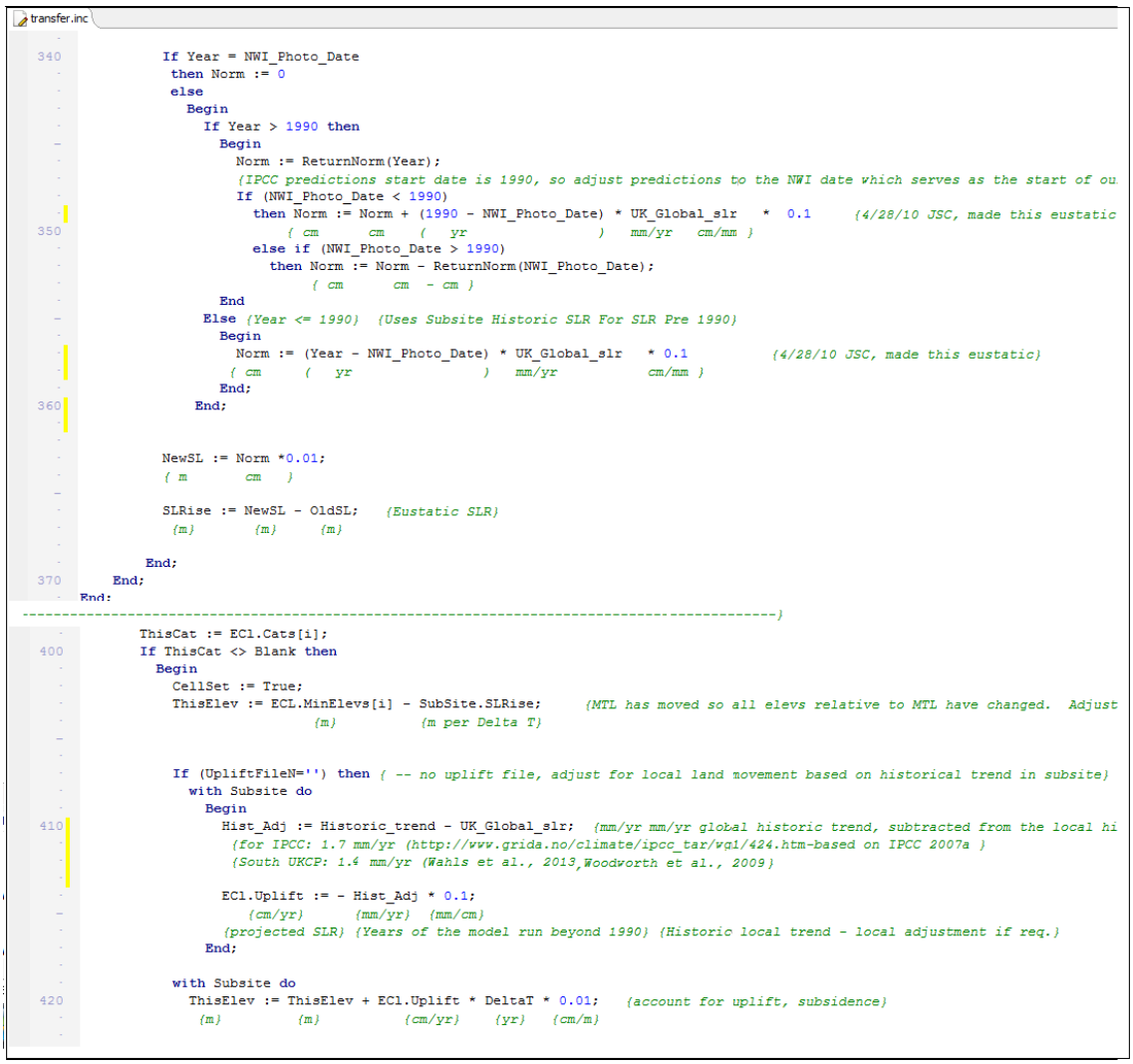

```
transfer.inc
340          If Year = NWI_Photo_Date
              then Norm := 0
              else
                Begin
                  If Year > 1990 then
                    Begin
                      Norm := ReturnNorm(Year);
                      {IPCC predictions start date is 1990, so adjust predictions to the NWI date which serves as the start of ou
                      If (NWI_Photo_Date < 1990)
                        then Norm := Norm + (1990 - NWI_Photo_Date) * UK_Global_slr   *  0.1     {4/28/10 JSC, made this eustatic
350                          { cm       cm      (   yr                )   mm/yr    cm/mm }
                        else if (NWI_Photo_Date > 1990)
                          then Norm := Norm - ReturnNorm(NWI_Photo_Date);
                               { cm       cm   - cm }
                    End
                  Else {Year <= 1990}  {Uses Subsite Historic SLR For SLR Pre 1990}
                    Begin
                      Norm := (Year - NWI_Photo_Date) * UK_Global_slr    * 0.1          {4/28/10 JSC, made this eustatic}
                     { cm      (   yr                 )   mm/yr           cm/mm }
                    End;
360               End;


              NewSL := Norm *0.01;
              { m        cm    }

              SLRise := NewSL - OldSL;   {Eustatic SLR}
               {m}        {m}     {m}

            End;
370       End;
        End;
-------------------------------------------------------------------------------------}
            ThisCat := ECl.Cats[i];
400         If ThisCat <> Blank then
              Begin
                CellSet := True;
                ThisElev := ECL.MinElevs[i] - SubSite.SLRise;     {MTL has moved so all elevs relative to MTL have changed.  Adjust
                                {m}          {m per Delta T}


                If (UpliftFileN='') then { -- no uplift file, adjust for local land movement based on historical trend in subsite}
                  with Subsite do
                    Begin
410                   Hist_Adj := Historic_trend - UK_Global_slr;  {mm/yr mm/yr global historic trend, subtracted from the local hi
                       {for IPCC: 1.7 mm/yr (http://www.grida.no/climate/ipcc_tar/wg1/424.htm-based on IPCC 2007a }
                       {South UKCP: 1.4 mm/yr (Wahls et al., 2013,Woodworth et al., 2009)}

                      ECl.Uplift := - Hist_Adj * 0.1;
                         {cm/yr}      {mm/yr}  {mm/cm}
                      {projected SLR} {Years of the model run beyond 1990} {Historic local trend - local adjustment if req.}
                    End;

                with Subsite do
                  ThisElev := ThisElev + ECl.Uplift * DeltaT * 0.01;   {account for uplift, subsidence}
420                {m}         {m}          {cm/yr}     {yr}   {cm/m}
```

Figure 0.25: Calculation of sea-level rise.

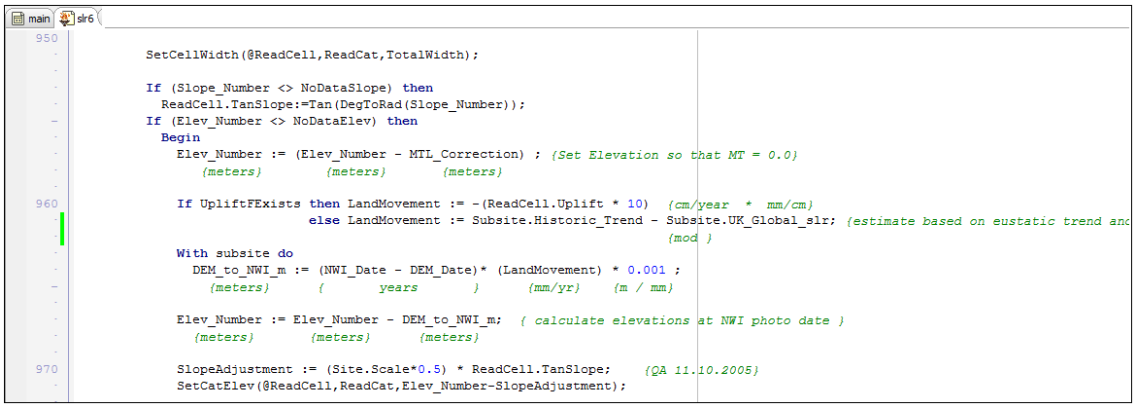

```
main  slr6
950          SetCellWidth(@ReadCell,ReadCat,TotalWidth);

             If (Slope_Number <> NoDataSlope) then
               ReadCell.TanSlope:=Tan(DegToRad(Slope_Number));
             If (Elev_Number <> NoDataElev) then
               Begin
                 Elev_Number := (Elev_Number - MTL_Correction) ; {Set Elevation so that MT = 0.0}
                    {meters}        {meters}       {meters}

                 If UpliftFExists then LandMovement := -(ReadCell.Uplift * 10)  {cm/year  *  mm/cm}
960                              else LandMovement := Subsite.Historic_Trend - Subsite.UK_Global_slr; {estimate based on eustatic trend and
                                                                                {mod }
                 With subsite do
                   DEM_to_NWI_m := (NWI_Date - DEM_Date)* (LandMovement) * 0.001 ;
                     {meters}      {       years       }      {mm/yr}    {m / mm}

                 Elev_Number := Elev_Number - DEM_to_NWI_m;  { calculate elevations at NWI photo date }
                   {meters}       {meters}      {meters}

                 SlopeAdjustment := (Site.Scale*0.5) * ReadCell.TanSlope;    {QA 11.10.2005}
970              SetCatElev(@ReadCell,ReadCat,Elev_Number-SlopeAdjustment);
```

Figure A-0.26: Adjustment of elevation when different dates on DEM and Land cover map are used.

transfer.inc

```
      PROCEDURE CALCULATE_AGGRADATION;
      Var ToCat: Category;
      BEGIN
       With Cell^ do
        BEGIN
         MaxElev :=  CatElev(Cell,Wetland) + TanSlope * CellWidth(Cell,Wetland);
1090     UpBound := UpperBound(Wetland,SubSite);
         //mod assumes same accretion rate within cell
         If MaxElev > UpBound then
           Begin
             If TanSlope = 0 then FracLost[Wetland] := 1
                else If TanSlope < 0 then FracLost[Wetland] := 0
                else FracLost[Wetland] := ((MaxElev - UpBound) / TanSlope) / CellWidth(Cell,Wetland);
             {frac. of cat to conv.}         {m}      {m}        {unitless}      {m}

             ToCat := UndDryLand;
1100         If Tropical
               Then Case Wetland of
                      TidalFlat:    ToCat := Mangrove;
                      LowerMarsh:  ToCat := Mangrove;
                      TransMarsh, UpperMarsh,
                      EstuarineBeach: ToCat := UndDryland;
                      Mangrove:     ToCat := UndDryland;
                    end {case}
              Else Case Wetland of {Not Tropical}
                      TidalFlat:    ToCat := LowerMarsh;
1110                  LowerMarsh:  ToCat := UpperMarsh;
                      UpperMarsh:  ToCat := TransMarsh;
                      TransMarsh, EstuarineBeach: ToCat := Dryland;
                     end; {Case}

             Convert(Cell,Wetland,ToCat,-99);
             SetCatElev(Cell,ToCat,UpBound);
           End; {MaxElev > UpperBound}
        END;  {with}
       END;  {aggradation}
1120   {-------------------------------------------------------------}

Begin
 With Cell^ do
  Begin
   //FracLost[Wetland] := 0.0; {initialization}

   With subsite do
 {   IF ((DeltaT * Accrete) > LocalSLRise) and (NOT ERODING) THEN  {aggradation  mod jsc Dec '05}
{     Calculate_Aggradation; }
1130     If FracLost[Wetland]>0 then Calculate_Aggradation;           //mod
```

Figure A- 0.27: Procedure of aggradation.

transfer.inc

```
1750  RetA(ER, EC, CWC);
      With CWC Do With subsite do
        Begin
          If (CellWidth(@CWC,OpenOcean)/Site.Scale > 0.5)
              Then SetBit(ExposedWater,ER,EC,True)
              Else SetBit(ExposedWater,ER,EC,False);

          IF ((CellWidth(@CWC,OpenOcean) + CellWidth(@CWC,EstuarineSubtidal)
               + CellWidth(@CWC,TidalFlat))/Site.Scale) > 0.9              //mod
              Then SetBit(MostlyWater,ER,EC,TRUE)
1760          Else SetBit(MostlyWater,ER,EC,FALSE);

          If (CellWidth(@CWC,Mangrove) + CellWidth(@CWC,LowerMarsh) + CellWidth(@CWC,TransMarsh) +
             + CellWidth(@CWC,EstuarineBeach)+CellWidth(@CWC,TidalFlat)+CellWidth(@CWC,OceanBeach)+
             + CellWidth(@CWC,UpperMarsh)+CellWidth(@CWC,OceanFlat)+CellWidth(@CWC,OpenOcean))/Site.Scale > 0.1
             Then SetBit(Saltwater,ER,EC,TRUE) {saltwetlands occur or salt water}
             Else SetBit(Saltwater,ER,EC,FALSE);
```

Figure A-0.28: High tide is included into the fetch calculation.

transfer.inc

```
(*******************************)
(* obtain qual. est. of erosion *)
(*******************************)
Procedure Erode(Cell: PCompressedCell; Var Erosion: ErosionScale);

BEGIN
 With Cell^ DO
  Begin
   IF (AdjMaxFetch <= 0.5) THEN Erosion := None;
   IF (AdjMaxFetch > 0.5)  AND (AdjMaxFetch <= 3) {km}  THEN Erosion := Little;
   IF (AdjMaxFetch > 3)  AND (AdjMaxFetch <= 9)  THEN Erosion := Moderate;
   IF (AdjMaxFetch > 9)  AND (AdjMaxFetch <= 20) THEN Erosion := Heavy;
   IF (AdjMaxFetch > 20) THEN Erosion := Severe;
  End; {with}
END; {Erosion}
(*******************************)     (*******************************)
      If ERODING then
        Begin
          If Wetland = TidalFlat then ErodeTFlat(Cell,Wetland)
          else If ((Erosion > None) AND (AdjOcean OR AdjWater)) Then // mod
           Case Wetland of
              VegTidalFlat,
                EstuarineBeach:  ErodeTFlat(Cell,Wetland);
              LowerMarsh,
                UpperMarsh,
                TransMarsh:    ErodeMarsh(Cell,Wetland);
              Mangrove:        ErodeSwamp(Cell,Wetland);
             end
        End;
```

Figure A-0.29: Fetch threshold.

transfer.inc

```
            If ERODING and (not diked) then
              Begin
                IF ((Erosion > None) AND (AdjOcean OR AdjWater))  // mod
                      Then ErodeMarsh(Cell,Dryland)
              End;
```

Figure A- 0.30: Procedure of dryland erosion.

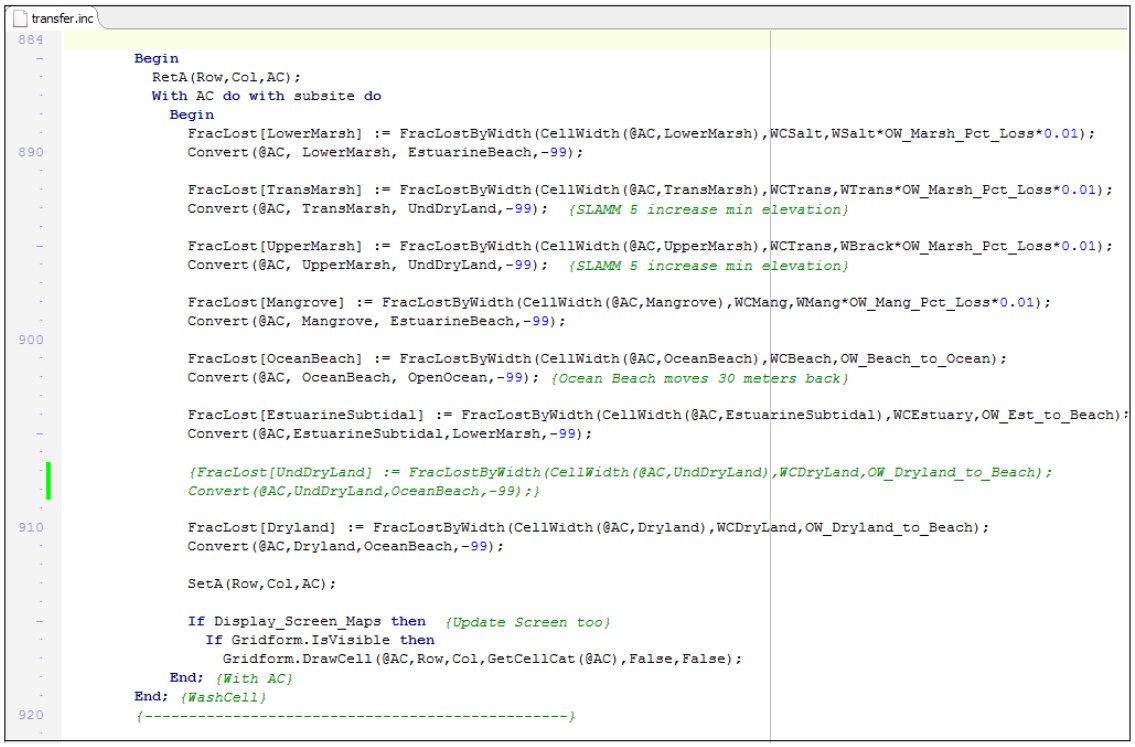

Figure A- 0.31: Procedure of overwash.

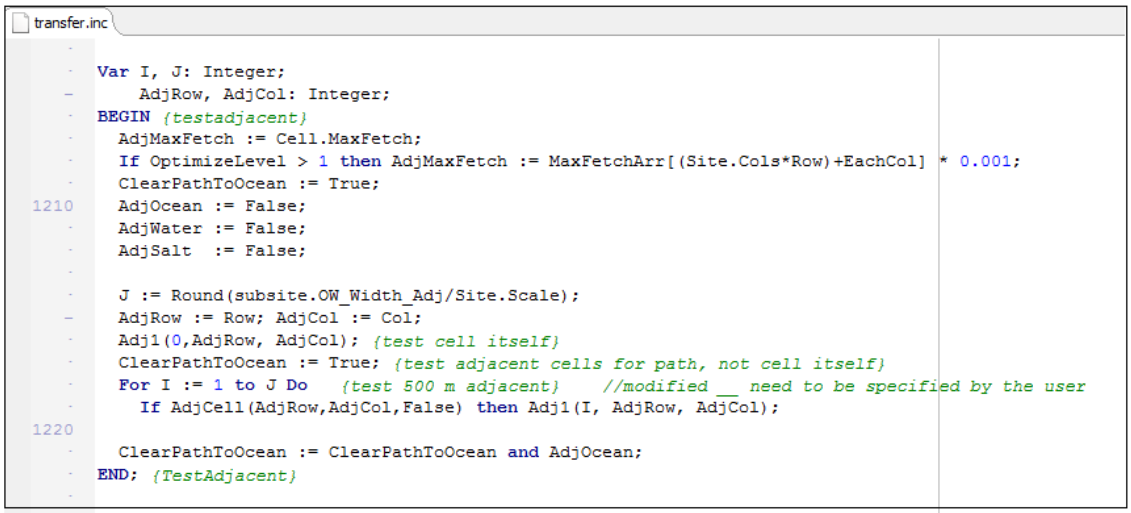

Figure A- 0.32: Test adjacent to the ocean.